UNIVERSIDADE D
COIMBRA

Pedro Daniel Geadas Farias

New bacterial strategies for Tellurium bioleaching and high value nanoparticles production

Tese no âmbito do doutoramento em Biociências, área de especialização em Microbiologia, orientada pela Professora Doutora Paula Maria de Melim Vasconcelos de Vitorino Morais, Professor Doutor Søren Johannes Sørensen e pelo Doutor Romeu Miranda Francisco e apresentada ao Departamento de Ciências da Vida da Faculdade de Ciências e Tecnologia da Universidade de Coimbra.

Dezembro de 2021

Faculdade de Ciências e Tecnologia
da Universidade de Coimbra

New bacterial strategies for Tellurium bioleaching and high value nanoparticles production

Pedro Daniel Geadas Farias

Dissertação de Doutoramento na área científica de Biociências orientada pela Professora Doutora Doutora Paula Maria de Melim Vasconcelos de Vitorino Morais, pelo Professor Doutor Søren Johannes Sørensen e pelo Doutor Romeu Miranda Francisco e apresentada ao Departamento de Ciências da Vida da Faculdade de Ciências e Tecnologia da Universidade de Coimbra.

Dezembro de 2021

The work that led to the present thesis was carried out in Centro de Engenharia Mecânica Materiais e Processos, University of Coimbra, Coimbra, Portugal and in Section of Microbiology, Department of Biology, University of Copenhagen.

This research was funded by the Portuguese Foundation for Science and Technology (FCT) through national funds and the co-funding by COMPETE in the framework of the projects PTW PTDC/AAGREC/3839/2014 and UIBD/0285/2020; the project ERA-MIN/0002/2015 BioCriticalMetals, through the program for International Cooperation ERA-NET, supported by ERA-MIN (2011-2015) funded under the EU 7th Framework Program FP7-NMP and the project Biorecover under grant agreement nº 821096, funded by the European Union Horizon 2020.

Pedro Daniel Geadas Farias received finantial support through the Ph.D. grant SFRH/BD/12491/2016 by FCT funded by Programa Operacional Potencial Humano (POPH) - Quadro de Referência Estratégico Nacional (QREN) cofunded by Fundo social Europeu (FSE) and national funds by Ministério da Educação e Ciência (MEC).

Agradecimentos/ Aknowledgements

Ao concluir esta Tese reflito em todos os que ajudaram a construí-la e todos os que me apoiaram e ajudaram a crescer enquanto pessoa e investigador. Se o meu percurso foi educativo, construtivo e até alegre foi graças a todos vós.

À Professora Doutora Paula Morais um especial agradecimento por ter ajudado a conceber este trabalho, por ter sido uma guia nos momentos altos e baixos, por acreditar no trabalho mesmo quando eu tinha dúvidas e por ter estado sempre presente na sua execução, do início ao fim. A sua orientação foi um pilar na minha formação científica e a sua amizade importante no meu crescimento como indivíduo e como membro de um grupo.

Ao Doutor Romeu Francisco agradeço pela sua disponibilidade e paciência para resolver as minhas dúvidas, das mais mundanas às mais complexas. Pelos serões de discussão de resultados e protocolos que me ajudaram a tornar-me critico e autónomo. E pela sua amizade que perdurará bem para além desta Tese.

To Professor Doctor Søren Sørensen for accepting my invitation as co-supervisor, we were strangers at the beginning, but you welcomed me, unreservedlye, and became a collaborator and a friend. Thank you for expanding my horizon, for showing me new and different ways of working and to incentivize me to collaborate and take risks in the unfamiliar.

A todos no laboratório de Microbiologia em Coimbra, os que estão e os que passaram, foram todos peças importantes na minha vida. Ao Cristophe e à Susana por me terem guiado na introdução à microbiologia. Às minhas colegas Ana Paula e Rita pela ajuda no tratamento de dados e em implementação de metodologias tão importantes à minha tese. À Catarina por ter estado sempre presente desde o mestrado, às bolsas, ao doutoramento.

A todos os meus restantes colegas no laboratório, Diogo, Igor, Catarina, Pedro, Filipa, Tânia, Gabriel, Joana, Beatriz, e tantos mais, foram todos importantes no meu percurso científico. Um sincero obrigado.

To all my friends in the Section of Microbiology, Biology Department – University of Copenhagen thank you for receiving me, for all the support and good times. To Lorrie Macarrio, Jakob Hershend and Joseph Nesme for your patience and guidance.

A todos os que colaboraram na construção da minha Tese um especial agradecimento. À Professora Doutora Ana Paula Piedade por me abrir portas e guiar em todas as técnicas que tão fundamentais a este projeto. Ao Professor Doutor José Paixão pela disponibilidade e acesso a uma plataforma que me foi tão importante na execução da minha Tese.

A todas as instituições que me acolheram: o Centro de Engenharia Mecãnica Materiais e Processos, a Universidade de Coimbra e a Universidade de Copenhaga um especial obrigado pelo apoio. Um agradecimento às instituições externas com quem colaborei: Universidade de Arrus, Universidade Técnica da Dinamarca e Centro de Materiais da Universidade do Porto, foram uma parte importante na minha formação e no desenvolvimento da minha Tese. E um agradecimento à Empresa do Desenvolvimento Mineiro, na pessoa do Eng. Carlos Rosa, por lançar o tema que germinou nesta tese.

Aos meus amigos novos e de longa data Sara, Paulo, Carlos, Denis, André, Samuel, Márcio, Cláudia e tantos mais, pelos momentos de escape da vida académica e da investigação. Covosco vivi alguns dos momentos mais decisivos na minha vida, um grande obrigado por estarem presentes.

À Carina Coimbra por teres entrado na minha vida. Os momentos que partilhámos até agora estão entre os mais especiais que já vivi e os que ainda temos reservados no nosso futuro entre os que mais anseio. Obrigado pela nossa nova vida.

Finalmente, e com um carinho especial, um agradecimento à minha família pelos anos que me formaram e me moldaram na pessoa que sou. À minha mãe pelo seu otimismo e por dar sempre alento ao meu pai pelo apoio e dedicação, à minha irmã por me ensinar dedicação e inspirar diariamente e à minha avó pela alegria que traz sempre em qualquer momento.

Table of Contents

List of Figures

List of Tables

Abbreviations

ACN – Acetonitrile

cDNA – Complementary Deoxyribonucleic acid

CDS – Coding sequences

DDTC – Diethyl-di-thiocarbamate

DMDTe – di-methyl di-tellurium

DMTe – di-methyl-tellurium

DNA – Deoxyribonucleic acid

FA – Formic acid

FDR – False discovery rate

H_2DCFDA – 2,7-dichlorofluorescein-diacetate

HEPES – 4-(2-hydroxyethyl)-1-piperazineethanesulfonic acid

ICP-MS – Inductively coupled plasma mass spectrometry

IPTG – Isopropyl-β-D-thiogalactoside

IR – Infra-red

LB – Luria Bertani

LC-MS/MS – Liquid chromatography tandem mass spectrometry

MTT – 3-(4,5-dimethylthiazol-2-yl)-2,5-diphenyl tetrazolium bromide

NP – Nanoparticle

OD – Optical density

PBS – Saline phosphate buffer

PCR – Polymerase chain reaction

q RT-PCR – Quantitative real time-polymerase chain reaction

R2A – Reasoners 2A

Re – reduction efficiency

RFU – relative fluorescent units

RNA – Ribonucleic acid

ROS – Reactive oxygen species

Rr – Reduction rate

RU – Relative units

SCA – Significant change in abundance

SDS-PAGE – Denaturing, by sodium dodecyl sulphate, polyacrylamide gel electrophoresis

Se (IV) – Selenite

SEM-EDS – Scanning electron microscopy with coupled energy-dispersive X-ray spectroscopy

STB – Saccharose-Tris buffer

Te (0) – Metallic tellurium

Te (IV) – Tellurite

Te (VI) – Tellurate

TeNP – Tellurium containing nanoparticle

Te^r – Tellurite resistance

TeRed – Tellurite reduction

TFA – Tri-fluoroacetic acid

UV – Ultra-violet

XRD – X-Ray diffraction

Abstract

The biochemical importance of a given natural element does not always align with the significance it has for human activity. This is the case of tellurium, a metalloid with increasing importance for society but with limited known roles in biology. The studies of Te interaction with living organisms is old but it focused mainly on the toxicity of the natural forms of Te and the resistance developed by living beings to its toxic effects. This has led to a focus on clinical related research in the first years of Te related bioresearch. Nowadays, the interest in Te bioresearch is broader, with the focus shifting to Te mobilization and bioreduction of soluble ionic forms of the metalloid. This recent change in research topics is mainly the result of interest in Te mining and the production of Te containing nanostructures for the industry. Te abundance in Nature is a par with that of rare earth elements, its demand is increasing, therefore, every alternative for Te recuperation from discarded materials, and low Te grade ores (resulting residues from mining of other elements) is enticing. Bioleaching and microbial assisted selective mobilization are techniques that have proven effectiveness in low grade ore mining and are of interest in Te mining since most sources of Te worldwide are also low grade and thus commercially challenging.

The industry demand for Te containing products is impacted, positively, by the growing tech sectors. Incorporation of Te in photovoltaic products, fluorescent probes for diagnostic and overall nanoparticles demands new materials and often new fabrication processes. Production of nanoparticles by living organisms, or products of living organisms, is changing the manufacturing industry introducing new products or “green” production methodologies, that align with the current agenda of sustainable development. In this work, an initial screening of mining sediments revealed the existence of bacterial strains with high Te mobilization activity, that when acting in a *consortium*, improve the bioleaching

performed by a natural microbial community. The same method of screening for bacteria, originated from metal impacted discarded material, revealed an high number of Te (IV) resistant strains with different Te (IV) reducing abilities, able to produce Te containing structures and with varying Te (IV) resistance potential. Detailed analysis of the genetic potential for Te (IV) resistance and reduction in the strains *Paenibacillus pabuli* ALJ109b and *Bacillus altitudinis* 3W19, as well as the metabolic variation demonstrated by differential proteomic, reveals different strategies of dealing with the metabolic impact and oxidative stress resulting from Te (IV) exposure. Differences can be observed on the expression of metabolic pathways, in most part, unique for each bacteria and only partially overlapping to what is seen for other metals. Detailed interpretation of specific protein expression demonstrated common strategies between the two strains, such as the activation of the *psp* determinants for redox control. Nevertheless, each bacterial strain activates specific response mechanisms, such as the Te (IV) resistance determinants *ter* overexpressed by *B. altitudinis* 3W19. The Te (IV) reducing ability, explored in detail in *P. pabuli* ALJ109b, revealed the involvement of the protein flagellin in the production of Te nanostructure. This protein activity is better than what is observed for most explored proteins with Te (IV) reducing ability, with optimal activity observed at pH 9 and room temperature. This thesis expands the collection of known organisms with Te (IV) resistance and reduction ability and reveal this characteristic for the first time in some genus. Moreover, the metabolic response to Te (IV) in *Bacillus* and *Paenibacillus* strains is, for the first time, revealed by a multi technique approach. This allowed the comparison of specific metabolisms and link individual proteins and genetic clusters to phenotypical observable effects of Te (IV) exposure. Finally, the characterization of *P. pabuli* ALJ109b flagellin ability to reduce Te (IV) reveals the potential of a bio-based approach of Te nanoparticle production. In overall, this thesis contributed to the growing know-how on Te

biochemistry and offers biological tools to be explored and optimized in Te mobilization and nanoparticle production.

Keywords: Te (IV) resistance, Te (IV) reduction, Te mobilization, bacterial metabolism, nanoparticles.

Resumo

A relevância bioquímica de um determinado elemento natural nem sempre está alinhada com a importância que o mesmo tem para a atividade humana. É o caso do telúrio, metaloide com crescente importância para a sociedade, mas com um papel considerado irrelevante na biologia. Os estudos da interação de Te com organismos vivos são antigos, e focam principalmente a toxicidade das formas naturais de Te e a resistência desenvolvida pelos seres vivos aos seus efeitos tóxicos. Isto levou a um foco na investigação relacionada com a clínica nos primeiros anos da bio-investigação em Te. Atualmente, o interesse na bio-investigação em Te é mais amplo, com foco mudando para a mobilização de Te e a bioredução das formas iónicas solúveis do metaloide. Esta mudança recente nos temas de investigação é, sobretudo, resultado do interesse na mineração de Te e na produção de nanoestruturas contendo Te para a indústria. A abundância natural do Te é equivalente à dos elementos de terras raras e sua procura está a aumentar, portanto, todas as alternativas para a recuperação de Te de materiais descartados e minérios de baixo teor (resídos resultantes da exploração de outros elementos) de Te são apelativas. A biolixiviação e a mobilização seletiva assistida por micróbios são técnicas que se mostraram eficazes na mineração de minérios com baixo teor e são de interesse para a indústria mineira, uma vez que a maioria das fontes de Te globalmente também são de baixo teor e, portanto, um desafio comercial.

A procura da indústria por produtos que contenham Te aumenta com o crescimento dos setores. A incorporação de Te em produtos fotovoltaicos, sondas fluorescentes para diagnóstico e nanopartículas em geral exige novos materiais assim como novos processos de fabricação. A produção de nanopartículas por organismos vivos ou produtos de organismos vivos está a afetar a indústria transformadora, introduzindo novos produtos ou metodologias de produção "verdes", alinhados com a agenda atual de desenvolvimento

sustentável. Neste trabalho, uma triagem inicial de sedimentos de mineração revelou a existência de estirpes bacterianas com elevada atividade de mobilização de Te, que ao atuar em consórcio melhoram a biolixiviação realizada por uma comunidade microbiana nativa. O mesmo método de triagem para bactérias originárias de material descartado rico em metais revelou a presença de um elevado número de estirpes resistentes a Te (IV) com diferentes capacidades de redução de Te (IV), capazes de produzir estruturas contendo Te, e com potencial de resistência a Te (IV) variável. A análise detalhada dos elementos no genoma conferentes de resistência e redução de Te (IV) nas estirpes *Paenibacillus pabuli* ALJ109b e *Bacillus altitudinis* 3W19, bem como a variação metabólica, demonstrada por proteómica diferencial, revelou diferentes estratégias de resposta ao impacto metabólico e stress oxidativo resultantes da exposição a Te (IV). Podem ser observadas diferenças na expressão das vias metabólicas, na sua maioria únicas para cada bactéria, e apenas com sobreposição parcial ao que é observado para outros metais. A interpretação detalhada da expressão de proteínas específicas demonstrou estratégias comuns entre as duas estirpes, como a ativação dos determinantes *psp* para o controlo redox. No entanto, cada estirpe bacteriana ativa mecanismos de resposta específicos, como os determinantes de resistência a Te (IV), *ter*, que foram sobreexpressos por *B. altitudinis* 3W19. A capacidade de redução de Te (IV), explorada em detalhe em *P. pabuli* ALJ109b, revelou o envolvimento da proteína flagelina na produção de nano estruturas contendo Te. A atividade desta proteína é superior à observada para a maioria das proteínas estudadas com capacidade de redução de Te (IV), demonstrando atividade ótima a pH 9 e temperatura ambiente. Esta tese expande a coleção de organismos conhecidos com resistência e capacidade de redução de Te (IV), revelando esta característica pela primeira vez em alguns géneros. Além disso, a resposta metabólica ao Te (IV) em estirpes de *Bacillus* e *Paenibacillus* é, pela primeira vez, revelada por uma

abordagem usando múltiplas técnicas. Isto permitiu a comparação de metabolismos específicos e a associação de proteínas individualmente assim como agrupamentos genéticos com os efeitos fenotípicos observados pela exposição ao Te (IV). Finalmente, a caracterização da capacidade da flagelina de *P. pabuli* ALJ109b reduzir Te (IV) revela o potencial de uma abordagem de base biológica para a produção de nanopartículas de Te. No geral, esta tese contribuiu para o crescente conhecimento sobre a bioquímica de Te e oferece ferramentas biológicas a serem exploradas e otimizadas na mobilização e produção de nanopartículas de Te.

Palavras-chave: Resistência a Te (IV), redução de Te (IV), mobilização de Te, metabolismo bacteriano, nanopartículas.

Chapter I: General Introduction

Tellurium in nature and importance in human activity

Tellurium (Te) was discovered by Franz Joseph Müller von Reichensteinin in 1782 (Dittmer, 2003) not by a determination of a new element but as an exclusion of other alternatives, the last being proof that the element, which Müller had isolated from a Transylvanian gold ore, was not antimony. Tellurium, along with oxygen, sulfur, selenium, and, to lesser extent germanium, antimony and arsenic, are collectively referred to as chalcogens (Fischer, 2001).

Tellurium is one of the rarest elements in both the Earth's crust (0.4– 10 ppb) (Govett, 1983; Levinson, 1974) and in seawater (up to 0.00 ppb) (Andreae, 1984). The prevailing theory for Te scarcity in the crust relates to the element strong siderophile character at high pressure, which led to most of primeval Te being sequestered into the core, (Wang & Becker, 2014).

The distribution of Te is uneven in the globe with the higher concentration found in oceanic sediments of Fe-Mn crusts, abyssal iron-manganese nodules and chlorite chondrites (Hein et al., 2003). These mineral formations are known for being enriched in elements with an atomic number over 40. A particular case is Te enriched more than any other element (up to about 50,000 times from Earth's crustal mean of 1 ppb), compared with 250 times for the next most enriched element (Hein et al., 2003).

In nature, when not bound in mineral forms, Te can be found mostly in the form of oxyanions and, as is characteristic of most of the metalloids, tellurium's oxyanions are relatively stable. There are four more common oxidation states, positive VI, IV, II and negative II. Environmentally, tellurite [Te (IV)] is the most abundant form, since it is the most thermodynamically favored form in water (Rouxel et al., 2004), followed by the oxyanion tellurate [Te (VI)], the second most abundant form with natural occurrence.

Similarly, to its occurrence in the earth, in water, Te concentrations are highly variable. Studies have reported seawater Te concentration never exceeding 0.002 ppb, with the possible dominance of Te (VI) over Te (IV) (Belzile & Chen, 2015), Figure 1.1. It is also more often found in higher concentrations in surface waters than in dept, which follows the opposite trend of nutrient-like elements, such as calcium, iron and manganese (Filella et al., 2019), that are remineralized by natural organic matter. The very high affinity of Te for ferromanganese oxides, common in benthic environments, also plays in favor of low concentrations in marine systems (Belzile & Chen, 2015; Hein et al., 2003). This element increases in coastal (up to 0.0054 ppb) and fresh waters (0.0033 ppb) (Andreae, 1984), possibly as a result of weathering or anthropogenic sources. The concentrations of Te in rainwater and snow are usually found with values between 0.002 and 0.025 ppb (Andreae, 1984), Figure 1.1.

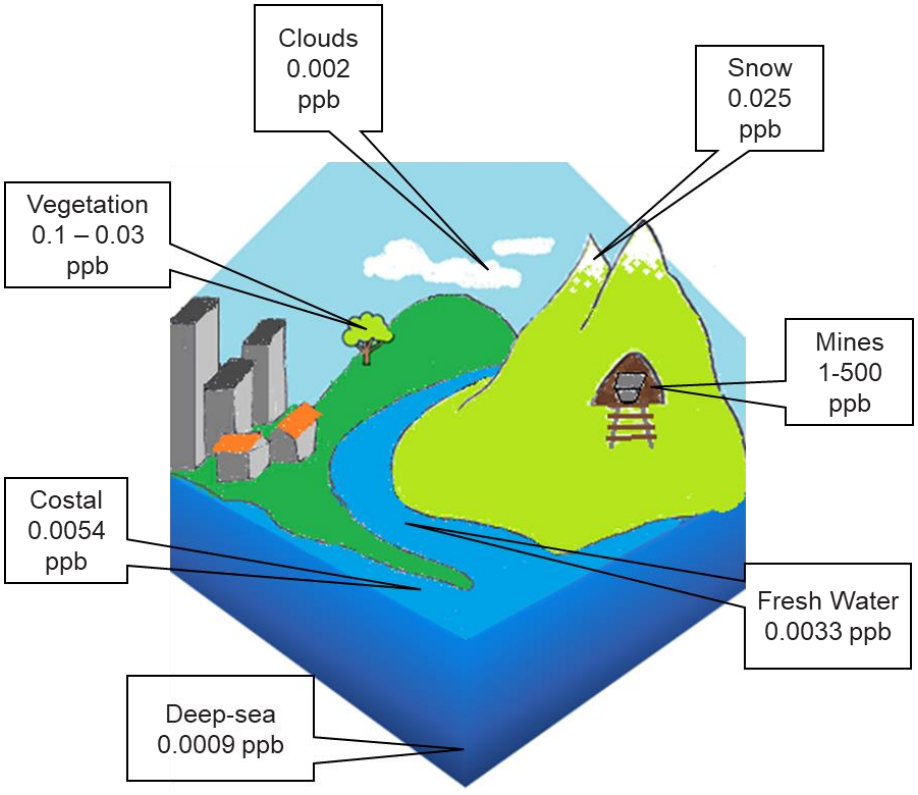

Figure 1.1. Natural occurrence of tellurium in the environment. Tellurium abundances represent average values based on literary references.

To this date, Te was found and explored in mineral formations mostly from gold and silver ores such as calaverite ($AuTe_2$), sylvanite ($AgAuTe_4$), and krennerite [$(Au_{1-x},Ag_x)Te_2$] (Zhao & Pring, 2019), but it is also commonly found associated with copper- and sulfur-bearing ores (Whiteley & Murray, 2005). Such ores are dispersed in localized pockets around the world, and their Te content is variable. It is from these ores that Te is most commonly mined, averaging 220 tons per year (Belzile & Chen, 2015; Nuss, 2019). The largest, primary Te, mining operations occurrs in Sweden, were one mine accounts for nearly 10 % of world Te production (Voigt & Bradley, 2020), followed by Canada, with the exploration of recently discovered Te containing copper reserves in British Columbia. The next are in China with two mines in Dashuigou, Sichuan province and in Shimian, Majiagou, where Te is the primary commodity of economic interest (Godfarb et al., 2017). Apart from these Te focused operations the mining industry mainly recovers this metal as a byproduct of copper refining (Anderson, 2021; Dittmer, 2003).

Apart from the elemental and ionic states measured in environmental samples, Te is often reported in the environment in volatile molecules. These compounds, most in the form of alkyl tellurides; di-methyl-tellurium (DMTe) and di-methyl di-tellurium (DMDTe), have been detected in sewage and landfill gases (Feldmann & Hirner, 1995), in geothermal gases and waters (Hirner et al., 1998), in compost samples (Kösters et al., 2003) and sediments of river and harbours, (Krupp et al., 1996).

For most of the industrial age, Te was primarily used in copper alloys and stainless steel, making these easier to machine and mill. Tellurium has also been added to lead to increase its strength and resistance to sulfuric acid. Other common uses were to colour glass and ceramics, in the vulcanization of rubber and it is one of the primary ingredients in blasting caps (Rouxel et al., 2004). Interestingly this metalloid has seen a radical shift in its uses in manufacturing, while in 1999 the estimated use of Te, globally, followed: iron and steel

products, 50 %; catalysts and chemicals, 25 %; additives to non-ferrous alloys, 10 %; photoreceptors and thermoelectric devices, 8 %; and other uses, 7 % (Anderson, 2021), this has since changed, Figure 1.2. During the last two decades, Te has been associated with the development of new materials from emerging technologies like photovoltaic products, fluorescent CdTe probes, and other compounds used in nanotechnology such as solar panels (Ba et al., 2010). In 2021, the global consumption estimates of Te by end use are solar, 40%; thermoelectric production, 30%; metallurgy, 15%; rubber applications, 5%; and other, 10% (Anderson, 2021), Figure 1.2.

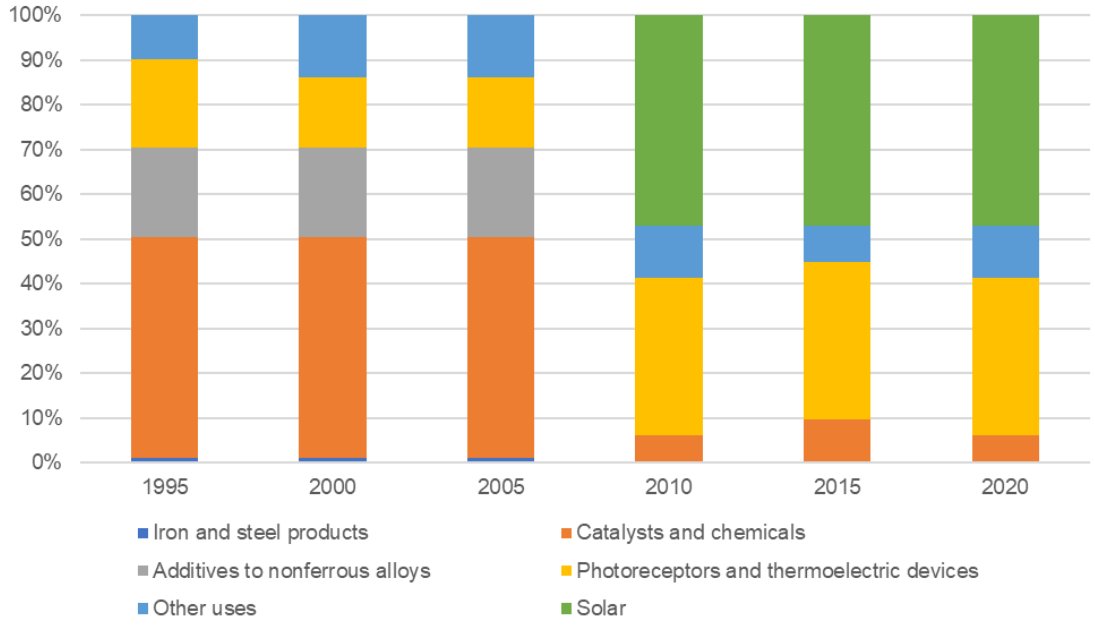

Figure 1.2. Evolution of tellurium usage in several industries and materials. Variation in percentage of tellurium utilization by applycations from the period 1995 to 2020. Adapted from (Anderson, 2021).

Since the demand in traditional uses, alloy production and catalysts and chemicals, are not expected to decrease and the surge in emerging technologies, such as solar photovoltaics, will continue to increase demand, it is expected that Te will be ever more present in human activity.

Other uses, that required lesser amounts of Te, have historically maintained its demand and some are expected to increase. Te and Te containing compounds have been used in medical and therapeutical applications such as for treatments of bacterial infections and diseases such as tuberculosis, leprosy, cystitis and severe eye infections (Zare et al., 2012). More recently, these molecules have been studied in the inhibition of cytokine production by T cells, immunomodulatory activities and anti-sickling (Sredni et al., 2007). These applications are of biotechnological interest because of their antibacterial properties, which are equal to or greater than silver nanoparticles. Apart for these uses, in clinical field, Te containing molecules have been used to manufacture nitric oxide (Tamura et al., 2007) and chlorine sensors (Arenas-Salinas et al., 2016; Sen et al., 2009), because of their improved reactivity.

Microbial interaction with tellurium in nature

Why are so few studies demonstrating the importance of Te to biological functions? The largest amount of Te focused biological studies are in the field of medicine where Te oxyanions and organotellurium compounds were tested for their toxicity to humans (Nogueira et al., 2004; Yarema, 2005) and were employed as selecting agents for bacterial growth (Kellogg & Wende, 1946; Moore & Parsons, 1958). Unlike its relative selenium (Se), Te is not an essential biological trace element in most organism (Ba et al., 2010), this comparison is even more distinct when comparing to other group XVI elements, oxygen and sulfur.

Is possible that the main reason for Te to be disregarded by living organisms as an integral part of their function and structure are its low abundance and the fact that it is mostly found in pockets of localized ore formations, as either native Te or more often found as combined with other metals.

Despite having an unknown biological function, Te was found incorporated in some types of proteins and detected as tellurocysteine, telluro-cystine, telluro-methionine, and serine in a Te-tolerant fungus (Ramadan et al., 1989). In 2000, Franzle and Markert postulated that Te could be an essential nutrient according to certain criteria based on the Biological System of the Elements model (Fränzle & Markert, 2000). Factors considered included the potential essentiality of an element to its redox state and other speciation, loss pathways, and the multiplicity with which it fulfils its possible function *in vivo* and *ex vivo*, in addition to its availability (Belzile & Chen, 2015; Chasteen et al., 2009).

Moreover, when considering the basic thermodynamic for the dissimilatory electron transport, anaerobic respiration is more favorable using the TeO_3^{2-}/Te redox couple than the SO_4^{2-}/HS^- redox couple, utilized by sulfate reducers (Lloyd et al., 2001). Finnaly, Te oxyanions are extremely versatile ions in structure forming. The known structures of Te oxycompounds reveals extraordinary diversity due to a combination of factors, namely: Te (IV) and Te (VI) are of comparable stability under atmospheric conditions, so compounds also occur with both oxidation states coexisting. Te (VI) is almost invariably octahedrally coordinated by oxygen with the Te (VI)O_6 group strongly bound, while Te (IV) may adopt a wide range of geometries (Christy et al., 2016). Nevertheless, Te continues to be one of the few elements in the Periodic Table almost entirely ignored by biochemists.

For those organisms that incorporate Te in its structure of fucnctions it needs to be mobilized from the environment. Scavenging for essential elements to maintain cell' structure and metabolism is a function all bacteria perform. While in rich environments microbial cells can simply uptake the existing elements from its surrounding, in poorer environments additional strategies are needed. Such strategies can range from the production and release of organic acids to mobilize essential macro-micro nutrients from

nearby solid matrixes, ores, soils, and others (Freitas & Nascimento, 2017), to the production of specific molecules, such as siderophores that sequester iron from the environment and retrieve it to the cell (Faraldo-Gómez & Sansom, 2003). Siderophores are included in a broader range of molecules, recently named metallophores, that have varying metal(loid) affinity. One study concluded that, in a collection of environmental aerobic anoxygenic phototrophs, the siderophores produced placed Te as the fourth preferential binding element, by strong production or significant interaction, after iron, zinc and vanadium (Kuzyk et al., 2021), Figure 1.3.

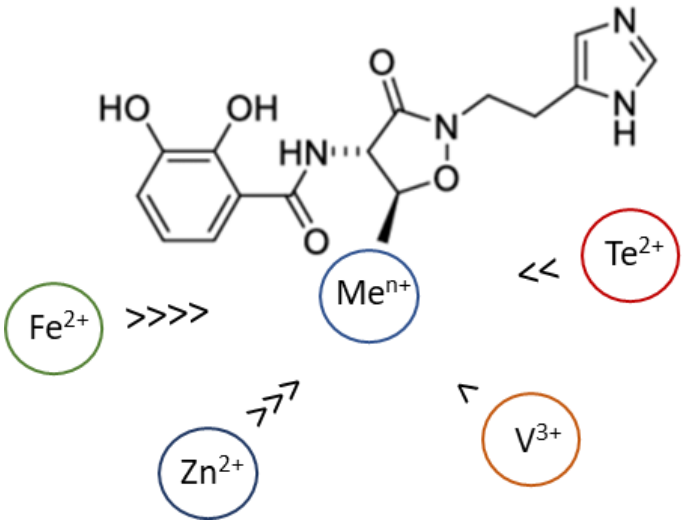

Figure 1.3. Binding preference of the mettalophore acinetobactin for cations. Schematic illustration of binding preference of likely produced methalophore (acinetobactin) for Fe, Zn, Te and V, order of preference from highest >>>>, to lowest >. Based on results from Kuzyc, Hughes and Yurkov 2001 (Kuzyk et al., 2021).

These bacterial features have been commercially explored for the retrieval of metals/ metalloids of interest in the mining industry, through a process named bioleaching.

Studies focused on Te bioleaching have been performed on ores (Guo et al., 2012; Ningfei & Hongguan, 2011) and e-wastes, (Ramos-Ruiz et al., 2017).

Tellurium toxicity and resistance in Bacteria and metabolic response

Tellurium toxicity is well detailed in reviews from Chasteen and colleagues, 2009; Ba, Mandy & Jamier 2010; Turner, Borghese & Zannoni, 2012 and Maltmand and Yurkov, 2019 (Ba et al., 2010; Chasteen et al., 2009; Maltman & Yurkov, 2019; Turner et al., 2012). Here, it is important to summarize the key aspects of Te toxicity, and new data only added to clarify the previously described resistance mechanisms with an update to what was known about resistance and toxicity.

Te (IV) is more toxic than Te (VI) which in turn is more toxic than Te (0) (Chasteen et al., 2009), this is the case in prokaryotes and humans alike. When comparing different ionic forms and molecules of/ with Te it is reported that organotellurium compounds, those containing a C –Te chemical bond, are generally considered as less toxic compared to inorganic Te compounds, such as Te (VI) and Te (IV) (Ba et al., 2010). The toxicity of the oxyanion Te (IV) can occur at concentrations as low as 1µg.mL^{-1} in *Escherichia coli*, (Turner et al., 2012).

The toxicity of Te (IV)/ Te (VI), in prokariotes, although not well described, may be mostly related to the metalloid interactions and substitution with sulfur containing residues, in thiol containing enzymes, or the competition with selenium in vital roles (Ba et al., 2010). Another hypothesis comes from Te (IV) and Te (VI) strong oxidizing ability. When in the cytoplasm, if not reduced by a specific mechanism, Te (IV) (mainly) will be reduced by unspecific molecules such as glutathione, in Gram negative bacteria and/or other reduced thiols, like cysteinyl glycine or cysteine, in both Gram positive and negative bacteria. Superoxide dismutase then acts on the resulting oxygen anion. All this process leads to an exhaustion of the oxidative stress protection mechanism (Taylor, 1999).

The exposure to Te oxyanions, similarly to other metal/ metalloid exposure, induces a cell response that is observable at the metabolic level. A strategy to determine the impact

on metabolism is to evaluate the differential proteomic response to a specific stress, comparing the control and post-stress induction protein production (Djoko et al., 2017; Herschend et al., 2017). The proteomic response to the chalcogenides Te (IV) and Se (IV) was evaluated in a study that followed the growth, physiology, and proteome of *Halomonas sp*. strain MAM. The proteomic response, determined by two-dimensional total protein electrophoresis, concluded that a total of 208 proteins were found differentially expressed in either condition, showing for the first time an overall analysis of the metabolic cell response to growth in the presence of Te (IV) and Se (IV). In this organism stress-related proteins were found over-expressed, as expected. Moreover, the impact of Te (IV) and Se (IV) in metabolic response was visible on the pathways of energy production, fatty acid synthesis, cell transport, oxidative stress detoxification, DNA replication, transcription and translation (Kabiri et al., 2009).

The process by which bacteria tolerate or resist Te ions has been thoroughly analyzed and reviewed by Taylor, 1999 (Taylor, 1999), Chasteen and colleagues, 2009, (Chasteen et al., 2009) and by Maltaman and Yurkov, 2019, (Maltman & Yurkov, 2019). In recent years, Te oxyanions resistance was reviewed, with a prevalent focus on Te (IV) and Te (VI) reduction. The most recent review focusing on Te oxyanions reduction was performed in 2019, by Presentato and colleagues, where they researched microbial Te (IV) reduction (TeRed) focusing on the formation of nanostructures (Presentato et al., 2019). To this date, several studies identified Te (VI) detoxification mechanisms such as alkylation and volatilization (Rouxel et al., 2004) as well as iron-, (Kim et al., 2013), protein-, (Etezad et al., 2009; Sabaty et al., 2001; Theisen et al., 2013; Valdivia-González et al., 2018) or culture-mediated precipitation, (Gharieb et al., 1999). Another strategy observed of Te (IV) resistance (Te^r) was the reduced efflux demonstrated on *Rhodobacter capsulatus*, (Borghese & Zannoni, 2010; Borsetti et al., 2003), a process dependent on

ΔpH and acetate. Unlike the case of many metals and metalloids, efflux is generally not considered a method of Te^r, (Chasteen et al., 2009). Precipitation to Te (0) is, as appears, the preferred Te (IV)/ Te (VI) detoxification mechanisms in bacteria. The process of reduction of Te oxyanions to its elemental form presents, phenotypically, as a black coloring of cells and colonies due to the optical properties of Te (0) deposits.

Figure 1.4. Visual demonstration of tellurite reduction by bacteria. Bacterial reduction of Te (IV) displayed by blackening of colonies in solid media, left image, and by blackening of inoculated medium, right image.

Molecular mechanisms of transport, resistance and reduction to tellurium ions in Bacteria

Tellurite transport

Te (IV) toxic effects are observed once it is inside the cell, for this reason it is important to determine which mechanisms are involved in the transport of Te (IV) through the cell wall/ membrane. These mechanisms may not represent the resistances mechanisms since these may be independent of transport or may even occur without the necessity for uptake. Several studies indicate different mechanisms and/or transporters implicated in Te (IV) transport. As early as 1986, the work of Tomás and Kay proposed that a phosphate

transport system would be involved in Te (IV) uptake (Tomás & Kay, 1986). This was later confirmed in *Escherichia coli* where over-expression of the phosphate transporter *pitA* led to the increase of intracellular Te (IV) (Elias et al., 2012). Another mechanism that involved in Te uptake was described in the organism *Rhodobacter capsulatus*, by determining Te (IV) uptake dependence on pH and its complete inhibition by carbonyl cyanide p-trifluoromethoxy-phenylhydrazone and the K+/H+ exchanger nigericin (Borsetti et al., 2003). More recently, in the same bacteria, it was reported that, intracellular Te (IV) accumulation was mediated by a monocarboxylate transporter since it could be inhibited by monocarboxylates as pyruvate, lactate, or acetate (Borghese et al., 2008). The same author later demonstrated that acetate permease, ActP, was the monocarboxylate transporter responsible for Te (IV) transport in *R. capsulatus* (Borghese & Zannoni, 2010). The same transporter, ActP, was also identified in *E. coli* as a Te (IV) transporter (Elías et al., 2015). Another study determined that expression of the *E. coli* gene *gutS* is induced by Se (IV) or Te (IV) (Guzzo & Dubow, 2000), inting at a new Te (IV) transport mechanism, later this gene was renamed *tsgA* and identified as the hypothetical transporter TsgA.

Regarding Te (VI), studies have reported the of the ionic form internalization via the SulT-type sulfate transporter CysPUWA in *E. coli* strain K-12 (Goff & Yee, 2017).

Molecular resistance to tellurium ions

Molecular mechanisms of resistance to Te oxides have been researched for at least three decades. Over time, several genes and proteins, involved in Te oxyanions resistance/ tolerance, were identified. Of these, some were subject to deepened exploration than others. The *kil* loci, from broad-host range plasmid RK2 (IncP), consisting of genes *klaA*/ *klaB*/ *klaC* in *Escherichia coli* demonstrated to be essential for Te^r (Goncharoff et al., 1991). An homologous Te^r determinant was identified, in the same year, in the RK2

variant RP4, composed of genes *kilA*/ *telA*/ *telB* (Walter et al., 1991). None of these studies produced a conclusive mechanism of action for this Te^r systems. Few attention was given to this system ever since with studies conducted in 1994, (Turner et al., 1994) and 1995, (Turner et al., 1995). The later work performed compared the requirements of the kilA Te^r with the *tehAtehB* Te^r operon. Experimental determination of the Te^r of the *tehAtehB* operon was demonstrated previously to the *kilA* locus (Walter & Taylor, 1989). More studies demonstrated the Te^r of the *tehAtehB* operon in the following years (Turner et al., 1994; Walter et al., 1991). Further characterization of the Te^r conferred by *tehB* was done leading to conclude that, in *E. coli*, the protein TehB requires S-adenosylmethionine as a cofactor to mediate Te^r (Liu et al., 2000), in a process observed similarly to Se (IV) reduction to methyl-Se, therefore TehB is involved in Te^r by volatilization. This was later validated by Choudhury and colleagues that confirmed the protein structure and hypothesised Te (IV)-TehB binding (Choudhury et al., 2011) and by identifying key aminoacids residues, cysteines, that were responsible for Te (IV) coordination (Dyllick-Brenzinger et al., 2000). The importance of cysteine residues for high-level Te^r has been observed early on and was validated by the identification of another Te^r determinant, the *trgABcysK* locus. Following on a work that demonstrated that exogenous cysteine addition to the growth of *Rhodobacter sepharoids* reduced Te^r (Moore & Kaplan, 1992), O'Gara and colleagues demonstrated that, in *R. sepharoids* and *Paracoccus denitrificans*, the *trgB* and *cysK* genes were essential for Te^r (O'Gara et al., 1997), highlighting the importance of cysteines in Te^r. For this genetic system the mechanism of resistance is still unclear. In *E. coli* it was also demonstrated the ArsC protein, from the anion-translocating ATPase, conferred moderate levels of resistance to Te (IV) by decreasing Te (IV) uptake, at least 55 %, comparing to control strains, (Turner et al., 1992). A particularly interesting specific Te^r is the mechanism encoded by the gene

cluster *terZABCDEF*. The core *ter* operon, as described so far, contains genes that encode for three main protein families, the TerD family that includes the paralogous proteins TerD, TerA, TerE, TerF and TerZ, the TerB family, and the TerC family. From these protein families *terB, terC, terD* and *terE* have been identified as directly responsible for conferring a resistance up to 1024 $g.L^{-1}$ of Te (IV) (Turner et al., 1994). This operon also appears to control the resistance to infection by various bacteriophages, known as phage inhibition (Phi), and is involved in the resistance to pore-forming colicins (Taylor, 1999). Originally discovered in the IncHI-2 plasmid pMER610 of *E. coli*, this Te^r mechanism has received great interest over the years. The first reported case focused on the gene cluster *terABCDE* demonstrated the essentiality of *terA* gene for Te^r, by knockout mutagenisis, without determining a specific function (Hill et al., 1993). This result was latter confirmed by Blake and colleagues 2003, (Blake et al., 2003). Later, in 1995, Whelan and colleagues focused on the *terZABCDEF* gene cluster, identified in plasmids IncHI2 and R478 from in *E. coli*, and determine that *terZ*, *terC* and *terD* were all essential for Te^r, but not *terA* (Whelan et al., 1995). Studies on the abundance and diversity of the *ter* operon in *E. coli* remain of interest to this day. In 2007, Orth and colleagues demonstrated that a large collection of serotypes of Shiga toxin-producing *E. coli*, from various sources including humans, animals, and food, harboured the *ter* operon and that positively correlated with Te^r (Orth et al., 2007). More recently, the diversity of *ter* operon was observed in *E. coli*, demonstrating the existence of four main groups, based on sequence and genetic arrangement, amongst the species (Nguyen et al., 2021). Apart from *E. coli*, functional *ter* operon and gene cluster were identified in *Yersinia pestis* (Ponnusamy et al., 2011), *Streptomyces coelicolor* (Sanssouci et al., 2011) and in *Proteus mirabilis* (Toptchieva et al., 2003). In a later work, the authors demonstrated that, in the strain, the *ter* operon is inducible by Te (IV). Regulation of *ter* operon was only observed

in *E. coli*, conferred by gene *terW*, that binds the *ter* promoter regulating the transcription of the *terZABCDE* genes, not the *terF* (Valkovicova et al., 2011).

Table 1.1. Genes involved in tellurite resistance in bacteria. Compilation of genes, with experimentaly confirmed tellurite resistance activity in bacteria, from publications between 1993 and 2021.

Gene symbol	Organisms	References
arsABC	*E. coli*	Review by (Chasteen et al., 2009)
aceE, aceF	*E. coli*	
csdB	*E. coli*	
cysM	*E. coli*	
cysK	*E. coli, Rhodobacter sepharoides, Geobacillus stearothermophilus*	
iscS	*E. coli*	
katA	*Staphylococcus epidermis*	
katG	*E. coli*	
kilA, telA, telB - kla operon	*E. coli*	
lpdA	*Aeromonas caviae*	
narGHIJ	*E. coli*	
phoB	*E. coli*	
sodAB	*E. coli*	
soxS	*E. coli*	
tehA, tehB	*E. coli*	
terBCDE	*E. coli*	
terC	*Proteus mirabilis*	
tmp	*Pseudomonas syringae*	
trgAB	*R. sepharoides*	
ubiE	*G. stearothermophilus*	
yqhD	*E. coli*	
terBCDE	*Alcaligenes sp.*	(Kormutakova et al., 2000)
terA	*Alcaligenes sp.*	(Blake et al., 2003; Hill et al., 1993)
actP	*R. capsulatus*	(Borghese & Zannoni, 2010)
terWZ	*Serratia marcescens*	(Valkovicova et al., 2011)
icdA	*E. coli*	(Reinoso et al., 2013)
gdhA	*E. coli*	
yceGH	*Bacillus anthracis*	(Franks et al., 2014)
pitA	*E. coli*	(Elías et al., 2015)
zwf	*E. coli*	(Sandoval et al., 2015)

The *ter* operon has been identified in multiple organisms and presents in several arrangements, this was extensively reviewed by Anantharaman, Iyer, and Aravind in 2014 (Anantharaman et al., 2014) and more recently by Munoz-Villagrán and colleagues in 2018 (Muñoz-Villagrán et al., 2018). One such example is the *ter* gene cluster analogue found in *Bacillus* sp., the *yceBCDEFGH* gene cluster, Figure 1.5. The amino acid sequences of YceC, YceD, YceE and YceF showed considerable similarity to TerZ (37.6 % identity), TerD (57%), TerE (53.6 %) and TerC (22.6 %), respectively. YceD and YcdE were also quite similar to TerE (51 %) and TerD (52.9 %), respectively (Kumano et al., 1997). Additionally, the protein YceH showed homology with previously reported TelA resistance protein and together with YceG they are involved in Te^r (Franks et al., 2014; Kumano et al., 1997).

Despite extensive studies on the *ter* operon and its homologue structures, few information exists on the actual resistance mechanism. Te^r resulting from *ter* genes is most likely due to a reduction process since the only directly observed effect of the action of these Te^r determinants has been the deposition of Te crystals in the vicinity of the membrane, with reduced deposition of the metal inside cells (Burian et al., 1998).

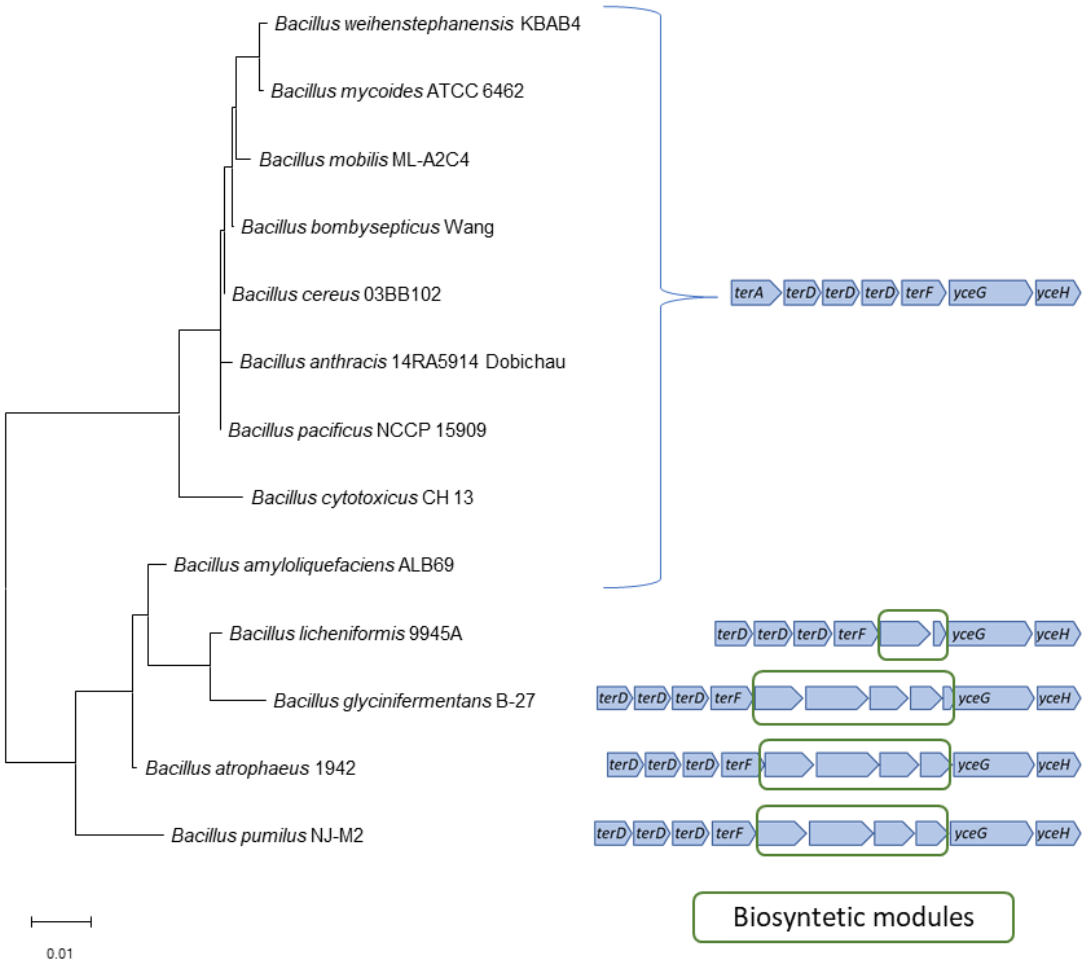

Figure 1.5. Organization of the ter gene cluster/ operon in *Bacillus* sp. strains. Bacterial strains are grouped in a 16S rRNA based phylogenetic tree (MEGAX), gene cluster were obtained by blast search and neighbourhood clustering in deposited *Bacillus sp.* genomes (IMG/JGI).

Non Te-specific resistance mechanisms were also identified in studies comparing several metals and mettaloids, including Te (IV). In this case resistance was observed by induced expression of DNA repair mechanisms. Mutated cells of *Pseudomonas aeruginosa* strain PAO1, with impaired expression of the *ruvB* and *recG* genes, showed a clearly increased sensitivity to both Te (IV) and Se (IV) (Miranda et al., 2005), a response similar to what is observed for other metals (Morais et al., 2011).

Molecular reduction of tellurium ions

Reduction is a wildly broad metabolic trait in bacteria, serving many functions from anabolism, catabolism, resistance and others. For these mechanisms there are a large number of associated genetic mechanisms, those that act specifically to one target, others with a broader range of substrates. Although most Te (IV) reducing enzymes were identified as nonspecific for this reaction, the exception is a Te (IV) specific reductase, that prefers Te (IV) to any other substrate tested, found in a *Bacillus* sp. STG-83. This protein is also thought to be involved in respiratory processes (Etezad et al., 2009).

Nitrate reductases are among the most well characterized non-specific Te (IV) reducing molecules. The enzymatic activity of nitrate reductases to catalyze Te (IV) reduction has been demonstrated, multiple times (Avazéri et al., 1997; Sabaty et al., 2001). It was proven that the nitrate reductase enzymes of *E. coli* act to reduce Te (IV) and Se (VI) and that this activity is necessary for the basal resistance, of the species, to Te (IV) (O'Gara et al., 1997). A single study demonstrated unspecific Te (IV) reducing activity from the known proteins thioredoxin reductase (EC 1.8.1.9), the alkyl hydroperoxide reductase (EC 1.11.1.26), the mercury reductase (EC 1.16.1.1), the flavorubredoxin reductase (EC 1.7.2.5) and the putative pyridine nucleotide-disulfide oxidoreductase YkgC (Arenas-Salinas et al., 2016). Other studies focused on specific proteins, such as, the dihydrolipoamide dehydrogenase (EC 1.8.1.4), (Arenas et al., 2014) or the FAD-dependent oxireductase (EC 1.4.3.3) (Pugin et al., 2014). In other cases, only putative Te (IV) reducing activity was observed, as for catalase (EC 1.11.1.6) (Calderón et al., 2006), 6-phosphogluconate dehydrogenase (EC 1.1.1.44) (Sandoval et al., 2015) or type II - NADH dehydrogenase (EC 1.6.99.3) (Díaz-Vásquez et al., 2015). A recent study also demonstrated the involvement of the HflKC complex, a proteolytic mechanism, in TeRed (Chien et al., 2011).

Regarding the specific TeRed, a common feature, of some reducing proteins identified, was the existence of a molybdopterin-containing motif, the case of nitrate reductases, formate dehydrogenases and other enzymes. A study from 2013 demonstrated that, in *E. coli*, a mutation in the molybdate uptake *modABC*, genes *modB* and *modC*, and molybdopterin biosynthesis gene *moaE*, removed the ability of the cells to reduce Te (VI) (Theisen et al., 2013). These authors further demonstrated that multiple different molybdoenzymes can catalyze Te (VI) reduction and that deletion of a single molybdoenzyme gene does not abolish all Te (VI) reducing activity. Therefore, Te (VI) reduction could be a secondary activity of a molybdoenzyme for which the primary function is the reduction of another substrate (Theisen et al., 2013).

In other cases, it has been reported the importance of the electron transport chain for TeRed. Klonowska and colleagues, 2005, demonstrated that *Shewanella oneidensis* MR-1 was able to use elements of the electron transport chain to reduce Te (IV) (Klonowska & Heulin, 2005). These authors demonstrated that, in *S. oneidensis* MR-1, Se (IV) and Te (IV) were both used as electron acceptors by distinct processes, determined by the difference in molecules able to inhibit reduction of each metalloid (Klonowska & Heulin, 2005). Later work, also in *S. oneidensis* MR-1, postulated that the cellular components, CymA, MtrA, MtrB, MtrC, and OmcA, which are related to electron transfer reactions, play important roles in TeRed (Kim et al., 2012). Over the years, the use of the respiratory process in TeRed was described in other organisms such as *Bacillus selenitireducens* and *Sulfurospirillum barnesii*, with the ability to grow using Te (IV) and Te (VI), respectively, as their electron acceptors (Baesman et al., 2007), or in *E. coli* where the *ndh* gene, coding for type II NADH dehydrogenase (NDH-II), is induced in Te (IV)-exposed cells. In this organism, NDH-II catalyzes the NADH-dependent TeRed while generating superoxide *in vitro* (Díaz-Vásquez et al., 2015).

Tabel 1.2. Proteins with demonstrated tellurite reducing activity. Literary review, from 2000 to 2021, of non dedicated proteins with demonstrated tellurite reducing ability.

Protein	Reference
Nitrate reductase EC 1.7.99.4	(Sabaty et al., 2001)
Thioredoxin reductase EC 1.8.1.9	(Arenas-Salinas et al., 2016)
Alkyl hydroperoxide reductase EC 1.11.1.26	
Flavorubredoxin reductase EC 1.7.2.5	
Mercuric reductase EC 1.16.1.1	
Putative pyridine nucleotide-disulfide oxidoreductase YkgC	
Dihydrolipoamide dehydrogenase EC 1.8.1.4	(Arenas et al., 2014)
FAD-dependent oxireductase EC 1.4.3.3 similar to Glutatione reductase	(Pugin et al., 2014)
6-phosphogluconate dehydrogenase EC 1.1.1.44	(Sandoval et al., 2015)
Isocitrate dehydrogenase EC 1.1.1.42	(Reinoso et al., 2013)
Tipe II - NADH dehydrogenase EC 1.6.99.3	(Díaz-Vásquez et al., 2014)
Catalase EC 1.11.1.6	(Calderón et al., 2006)

Growing interest in tellurium reducing Bacteria

In recent years the search for Te (IV) reducing bacteria is evermore a matter of interest, not for diagnostic purposes, but mainly due to the lack of well characterized, environmental, tellurite-tolerant and Te^r bacteria in culture collection (Arenas et al., 2014). Tellurite resistant/ tolerant bacteria from diverse environments may also reveal new resistance and reduction mechanisms of interest for scientific, clinical and biotechnological purposes (Maltman & Yurkov, 2019). Considering the toxicity effect resulting from Te (IV) exposure, increased oxidative stress, the search for organisms that may have good reactive oxygen species (ROS) protection mechanisms, led researchers to

target Antarctica to recover tellurite-resistant bacteria from an extreme environment, impacted by high UV radiation and desiccation (Arenas et al., 2014; Plaza et al., 2016). Moreover, many organisms recovered from mines and metal-polluted sites are being tested for their ability to tolerate or resist Te (IV). These environments have characteristically high concentration of metals/ metalloids, namely Te, which makes them valuable search places for microorganisms with metal resistance. From the central gold mine in Nopiming Provincial Park, Manitoba Canada a high Te (IV)-resistant *Pseudomonas reactans* strain CM-3 was recovered and characterized (Maltman et al., 2015). Similarly, in the heavily polluted Er-Jen River in the Tainan County, Taiwan, researchers targeted isolation of Te resistant bacteria leading to the recovery of a highly Te (IV) resistant *Paenibacillus* sp. strain TeW (Chien & Han, 2009) and later a *Pseudomonas* sp. strain TeU (Chien et al., 2011). Furthermore, bacteria from Te enrich sediments from the Fe-Mn crust in deep-sea trenches, were recovered with the specific aim of increasing the collection of reducers of group XVI metalloids, such as Te, (Rouxel et al., 2004) or from deep sea hydrothermal vent (Csotonyi et al., 2006).

Production of nanostructures by Bacteria

Nanoparticles: properties and production

Nanoparticles (NPs) have characteristic properties that set them apart from bulk materials of the same composition. Unique physical, chemical, optoelectronic and, at times, electrical, mechanical, magnetic, thermal, dielectric, and biological properties are determined by NPs surface plasmon resonance, enhanced Rayleigh scattering and surface enhanced Raman scattering (Narayanan & Sakthivel, 2010). Ultimately, NPs definition lies in being a material under 100 nm in dimension in, at least, one axis (Vert et al., 2012). The great potential of nanoparticles, derived from their properties, gave new tools to

applications in the fields of biology, medicine and environmental remediation (Tugarova & Kamnev, 2017).

There are three main methodologies to produce Te nanostructures: a bottoms-up, a top-down and a template based approach. The bottom-up processes are based on chemical interactions between a metalloid precursor and a suitable reducing/oxidizing agent. As for top-down methods, the formation of nanostructures is achieved by a hot solvent-mediated dissociation of a Te precursor upon UV/laser irradiation. Finally, the template-based approaches, in which metalloid-nanomaterials are formed in template structures with the aid of growth-directing agents. This last methodology is used to generate of desired features, mostly specific shapes (Piacenza et al., 2018).

Investment on the formation of Te containing NPs (TeNPs) is attributed both to the inherent properties of said NPs and to those of the element itself (Christy et al., 2016).

Biogenic reduction of tellurium ions and assembly of tellurium nanoparticles

Most studies that focus on the biogenic formation of Te-containing nanoparticles reference a bottoms-up fabrication approach (Piacenza et al., 2018). The resulting structures obtained from the biogenic reduction of Te ions are limited in shape and form from the physical characteristics of the ions and the resulting element. Te (0) tendency to form one dimensional nanostructures relies on the high thermodynamic stability of trigonal tellurium (t-Te), which is responsible for the anisotropic growth of Te-nano crystallinities along one axis (Piacenza et al., 2018; Presentato et al., 2018). Over the past few years, the biosynthesis of Te nanostructures such as TeNPs, Te nanorods and Te nanocrystals has been reported (Mirjani et al., 2015). Without specification of cellular location many organisms produce mono or polydisperse TeNPs. Since the polydispersity is the major concern for some applications, it is important to optimize the conditions for monodispersity in a biological process (Nayak et al., 2011). In case of intracellular

production, the accumulated particles are of specific dimension and with less polydispersity (Narayanan & Sakthivel, 2010).

Studies exploring the nanostructures formed by Te anions could be traced back to 1995 when the *Pseudomonas putida* strain BS228 was reported to produce long crystal-like structures that grew at a tangent to the cell surface, even at low concentrations of potassium tellurite (about 2-5 $\mu g.mL^{-1}$) (Suzina et al., 1995). The ability to reduce Te oxyanions into nanoparticles have been reported in *Bacillus selenireducens* and *Sulforospirillum barnesii* that use Te (IV) and Te (VI) as electron acceptors in respiration (Baesman et al., 2007). *B. selenireducens*, was able to form nanorods of ~10 nm in diameter and 200 nm in length that were clustered together to form larger rosettes of ~1000 nm, while *S. barnesii* formed small irregularly shaped extracellular nanospheres of diameter ~50 nm. *Rhodobacter capsulatus* strain B100 was extensively studied in its capacity to reduce Te (IV) to form nanoparticles (Borghese et al., 2014, 2017, 2020). The strain *Pseudomonas pseudoalcaligenes* strain Te was able to synthesize rod shaped TeNPs with ~22 nm in diameter and 58–220 nm in length (Forootanfar et al., 2015).

Microbial synthesis of metal nanoparticles depends up on the localization of the reductive components of the cell. When the cell wall reductive enzymes or soluble secreted enzymes are involved in the reductive process of metal ions then it is expected to find the metal nanoparticles extracellularly (Narayanan & Sakthivel, 2010).

Intracellular precipitation of Te (IV) was observed on the inner membrane of bacteria and on the inner surface of mitochondria involving oxidative chain processes in the reduction to Te (0) (Pontieri et al., 2015). The intracellular production of rod shaped TeNPs has the most reported cases studied so far. *Bacillus* sp. strain BZ can produce Te nanorods with nearly 180 nm in length and widths less than 20 nm (Zare et al., 2012). *Lactobacillus plantarum* strain ATCC 8014, was used to biosynthesize intracellular spherical Te

nanoparticles with an average size of 45.7 nm (Mirjani et al., 2015). Recently, the ability to reduce Te (IV) into nanoparticles was demonstrated in *Ochrobactrum sp* strain MPV1, reporting the involvement of intracellular NADH-dependent oxiredutases (Zonaro et al., 2017). Evenly distributed long electron-dense rods, representing most probably Te nanostructures were observed in *Acinetobacter schindleri* strain MF09, exposed to Te (IV) (Figueroa et al., 2018).

Less polydisperse, intracellular nanostructures, are of interest in manufacturing of uniform products (Narayanan & Sakthivel, 2010). In contrast, since optoelectronic and physicochemical properties of nanoscale matter are size- and shape-dependent, for optoelectronics, electronics, bioimaging and sensor technology, it is relevant to produce polydisperse materials (He et al., 2007). For this, extracellular Te nanostructures production is more relevant. Examples of extracellular produced TeNPs include the, aforementioned, irregularly shaped extracellular nanospheres from *S. barnesii* or the Te nanorods produce by *Shewanella oneidensis* strain MR-1 (Kim et al., 2015). More recent studies also investigated alternative biogenic Te nanostructure fabrication methods. In *Magnetospirillum magneticum* strain AMB-1, grown in the presence of Te (IV) the metalloid competes with other metals for the use of the magnetosome construction machinery (Tanaka et al., 2010).

Studies continue to improve on the knowledge of TeRed focusing on the factors affecting different Te nanostructure formation in the same strain. *S. oneidensis* MR-1 produced uniform metallic Te nanorods extracellularly in the presence of Fe (III), in anaerobic conditions both Te (IV) and Fe (III) function as electron acceptors in the respiration process. Te nanorods are 240 nm in length and 25 nm in width. Nevertheless, the same strain produced intracellular Te nanorods, with lengths of 100–200 nm and widths of ∼10 nm, as the result of a synthetic pathway in the absence of Fe (III). The intracellular Te

rods are anticipated to attain better electrical contact through the direct carbonization of the organic bacterial cell (Kim et al., 2015). Recently, it was demonstrated that *Rhodococcus aetherivorans* strain BCP1 was able to generate intracellular Te-nanostructures in the form of ribbon like nanoparticles or nanorods with sizes varying depending on growth conditions (Presentato et al., 2016, 2018).

Despite all research performed on biogenic production of Te nanostructures, no descriptions of fisiologic functions of such structures were found to this date.

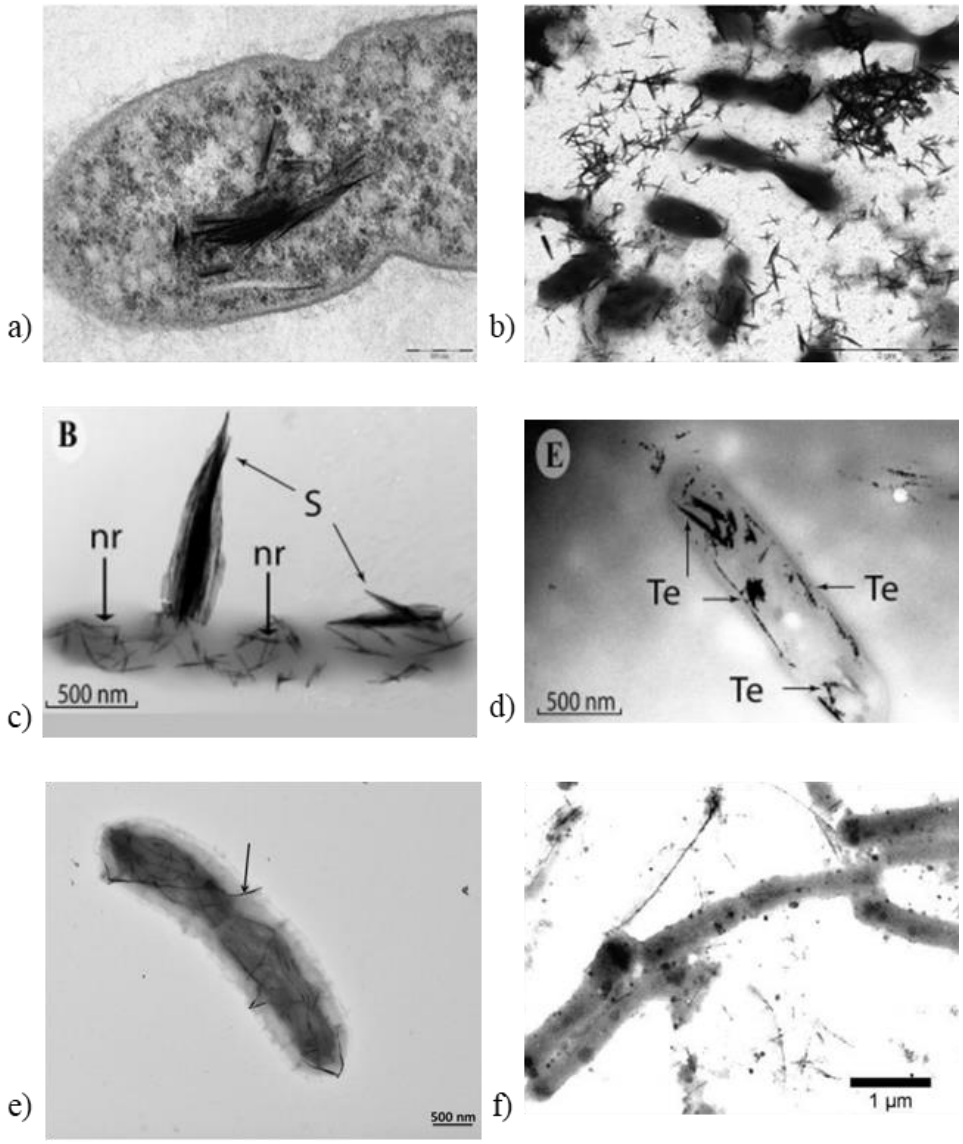

Figure 1.6. Biotic production of tellurium containing nanostructures. Compilation fo TEM images of Te nanostructure in bacteria. Te containing nanoshards produced by *Rhodobacter capsulatus* a) intracellularly, b) extracellularly. Adapted from Borghese and colleagues, 2014 (Borghese et al., 2014) Production of multiple Te containing nanostructures by *Bacillus selenireducens* c) polydisperse nanorods (nr) and shards (S), d) intracelular nanorods (Te). Adapted from Baesman and colleagues, 2007 (Baesman et al., 2007). Production of enlongated Te nanorods by *Rhodococcus aetherivoran.* Adapted from presentato and colleagues, 2018 (Presentato et al., 2018). Te nanoparticles produced by *Lactobacillus plantarum*. Adapted from Mirjani and colleagues, 2015 (Mirjani et al., 2015).

Advantages, disadvantages and applications of biological production of tellurium nanoparticles

The main chemical production of TeNPs, using current manufacturing technologies, is hydrothermal synthesis, a bottom-up methodology, (Byrappa & Adschiri, 2007; Cao et al., 2011; Piacenza et al., 2018). This is used to generate 1D Te-nanomaterials in a process based on the use of high pressures and temperatures to favor heterogeneous reactions in aqueous solvents (Byrappa & Adschiri, 2007). All TeNPs biogenic formation strategies described thus far are, by definition, template based or bottom-up approaches. By comparing to the hydrothermal synthesis approach, the biogenic techniques offer less extreme conditions of nanofabrication, near atmospheric pressures and mild temperatures.

The current chemical procedures to produce Te-nanomaterials are effective and advantageous in different ways. Nevertheless, the major drawback of any approaches is the generation of Te-nanostructures with various size (Piacenza et al., 2018). Consensually, there are still two challenges that researchers face using current fabrication methods, the high production costs, and the obtainment of Te-nanostructure mixtures with homogenous size and morphology, to assure their uniformity for application purposes. The uniformity, in shape and size, is also a difficulty in biogenically produced Te-nanostructures since most organisms produce either polydisperse structures or monodisperse structures of great variety in size (Borghese et al., 2014, 2017; Kim et al., 2015; Mirjani et al., 2015). Nevertheless, the use of living organisms offers great potential in cost reduction since most organisms are reaction catalysts, they can, in some cases, regenerate by continuing growth, extruding NPs, during the fabrication process. Moreover, the general cost of biosynthesis using mesophilic organisms is not demanding, for reagents and apparatus. Finally, biogenic synthesis offers the possibility of formation

of structures that are difficult to obtain by chemical synthesis (Singh et al., 2015; Wang et al., 2018).

TeNPs range of applications extend from industrial to biomedical. In the form of nanoparticles Te is characterized by its semi conductive abilities and for improving thermal, optical and electric characteristics in alloys. In applications, such as new rechargeable batteries or fluorescent probes, refered as quantum dots if they can be light activated, (Srivastava et al., 2015; Turner et al., 2012) Te is needed in single-element nanoparticles or multi-element nanoparticles, CdTe/ZnTe. Also, in the field of therapeutics, it was demonstrated that the biogenically produced Te nanorods, by S. *oneidensis*, could effectively inhibit the production of pioverdine, one of the main virulence factors in *P. aeruginosa* (Mohanty et al., 2014).

Due to the electrochemical characteristics of Te ions it is very interesting to consider Te as a scaffold for new structures and applications (Dodson et al., 2015). Outside the clinical field, some applications have been proposed for biogenic TeNPs such as a new energy conversion and storage material, incorporated in electrodes of lithium batteries (Kim et al., 2015). Biosynthesized TeNPs, produced by *Shewanella baltica*, act as stable photo-catalysts to bioremediate methylene blue dye, a contaminant in the effluents of textile industries (Vaigankar et al., 2018). Ultimately, all the bacteria described above that are Te (IV)/ Te (VI) uptakers and that form intracellular Te structures offer potential strategies in bioremediation of Te ions contaminated sites by biofiltration.

Current and future research in TeNPs is expected to reveal several applications were biogenically produced TeNPs are of interest and can compete and/ or outperform with their chemically produced counterparts.

Objectives and thesis outline

New techniques for Te mining and retrieval from secondary sources are necessary for efficient resource utilization. Bio-based leaching, bioleaching, can be a suitable alternative or complementary technique for current mining of Te. Furthermore, new materials and fabrication techniques are in high demand. The use of bacterial reduction and precipitation for the metalloid tellurium could provide an alternative solution for the current industrial fabrication of Te nanostructures. Current studies proved that Te nanostructures bacterial formation is highly variable, in size, form and polydispersity, and could lead to products with high commercial value. Uncovering the molecular mechanisms responsible for Te ions reduction is essential to understand and optimize this process.

Considering the information above, this thesis aims to describe new, bacterial-based, biological strategies to mobilize Te from complex substrates and to produce Te nanoparticles. To fulfil this main goal, the specific aims that guided the development of this thesis are the following. To determine the Te bioleaching potential, using single strain and bacterial *consortia*, from complex substrates. To evaluate environmental samples for their biological activity in Te (IV) resistance, leaching and precipitation. To assess, by genomic and proteomic approach, the metabolic variation induced by growth in the presence of Te (IV), in highly Te (IV) resistant bacteria. To evaluate, in Te (IV) reductive bacterial strains, the nanostructures of tellurium formed and their ability to be used as a biotecnological tool.

The thesis is divided into general introduction (Chapter I), results from original research (Chapters II – V) and concluding remarks (Chapter VI). The detailed outline of Chapters II – V is as follow:

In Chapter II, Te (IV) resistant strains were selected from mining sediments to be tested in mobilization of Te. These strains were selected from an inoculum with a mine sediment, subjected to incremental spiking with Te (IV). For Te mobilization secondary sources of the mining industry were used as substrate after an initial determination of metal conten, namely Te. To determine the effect of a controlled/ known microbial community vs a native unknown microbial community, bio-mobilization assays were performed separately with isolated strains, microbial communities and with bacterial *consortia* bioaugmentation. Abiotic controls were performed in paralel, when applicable. The experiments conducted discriminate between bioleaching activity and biological immobilization, accumulation and/ or biosorption.

In Chapter III, the designed experiments focused on screening a large bacterial collection for characteristics that identified the strains with higher Te (IV) resistance, higher Te (IV) reduction ability and the ability to produce visible Te containing nanostructures. Moreover, to determine Te (IV) resistance potential, by screening selected resistance genes. Bacterial strains were isolated from mining environments and added to the collection of strains pre-selected in Chapter II. All bacterial isolates were screened for Te (IV) resistance, in solid and liquid media, with increasing Te (IV) concentrations. Strains displaying high Te (IV) resistance were selected for evaluation of Te (IV) reduction. Factors for selection of the best Te (IV) reducers included reduction efficiency, Te per biomass, and reduction rate, Te per biomass per time. A selection of strains, from all three sites, with high reduction efficiency an/ or high reduction rate were screened for the formation of Te precipitates. Furthermore, a selection of strains, preselected from the first screening technique, were also screened for genetic traits of resistance based on previously demonstrated Te (IV) resistance mechanisms.

In Chapter IV, two strains, *Paenibacillus pabuli* ALJ109b and *Bacillus altitudinis* 3W19, selected in Chapter II and Chapter III, were grown in the presence of Te (IV) to evaluate the metabolic impact of the metalloid in each strain. Determination of Te (IV) impact on each strain grown was performed by following bacterial growth in increasing concentrations of Te (IV) as well as determining production of reactive oxygen species and variation in metabolic activity. Each strain genome was sequenced by next generation genome sequencing for the purpose of genome mining of genes and regulatory elements of interest and for the construction of a reference proteome. Variations in the proteome expressed, determined by high throughput proteomics, provided a detailed description of metabolic impact of growth in the presence of Te (IV). Additionally, the expression levels of Te resistance genes was determined by quantitative real time.

In Chapter V, the search of Te containing nanoparticles led to the exploration of the strain *P. pabuli* ALJ109b and its protein flagellin. Physical characteristics of the nanoparticles produced by strain ALJ109b were determined by scattering electron microscopy, UV-Visible spectrometry and X-ray diffraction. Proteomic profiling, detailed in Chapter IV, was used to screen potential Te (IV) reduction proteins, but it was a one dimensional, total protein profile that revealed the over expression of flagellin responsible for Te (IV) reduction. The Te (IV) reducing activity of this protein was characterized in this section, by determining optimal protein-Te (IV) ratio, pH and temperature.

List of publications:

This thesis is based on the published or drafted manuscripts:

Farias P, Francisco R, Maccario L, Herschend J, Piedade AP, Sørensen S, Morais PV. Impact of Tellurite on the Metabolism of *Paenibacillus pabuli* AL109b With Flagellin Production Explaining High Reduction Capacity. Front Microbiol. 2021 Sep 7; 12:718963. doi: 10.3389/fmicb.2021.718963

Farias P, Francisco R, Morais P V. Potential of tellurite resistance in heterotrophic bacteria from mining environments. (Draft).

Farias P, Francisco R, Maccario L, Herschend J, Sørensen S, Morais PV. Metabolic versatility of tellurium resistant and reducing *Bacillus altitudinis* strain 3W19 subjected to metalloid stress. (Draft)

Chapter II: Tellurium mobilization and bioleaching:

strains vs consortia

Abstract

Scarce critical metals are in high demand due to the growing tech sectors. This is pushing for ever more extensive mining and for exploitation of alternative sources. Recovering of metals from mining residues is not often cost effective by traditional mining methodologies and require alternative solutions such as bioleaching. This methodology can offer a solution to the problems associated with mining runoffs and leachates while, selectively, retrieve high value metals. The main objective of this work is to evaluate the ability of bacterial strains, isolated from mine tailings, to mobilize Te using as substrate secondary sources of the mining industry. Mobilization assays were conducted using *Paenibacillus pabuli* ALJ109b, *Bacillus mycoides* ALJ98a *and Paenibacillus taichungensis* ALJ98b, and followed the appearance of Te in leachates, Te bioleaching, in cells, Te accumulation or in both, Te removal. These strains are mesophilic and highly resistant to Te (IV). Each bacterium is effective in Te mobilization, with most of Te removed found in leachates. In experiments conducted with a microbial community from a mining residue, bioleaching was as high as 17.84 %. The effect of bioaugmentation, adding a bacterial *consortium*, of highly Te (IV) resistant bacteria, to a microbial community with under-performing Te mobilization activity is positive, resulting in a 12.18 % increase in Te mobilized.

Bioleaching is a viable alternative for the recovery of low concentration metals and other elements of interest from discarded mining material. Although it is a under-explored technology, in Te focused application, it shows potential in Te mobilization from discarded residues, transforming them into secondary raw materials. By using environmental, heterotrophic bacteria the process of Te mining can be achieved in mesophilic conditions in a sustainable approach that complements existing mining methodologies.

Introduction

Tellurium is a strategic element in today's industry incorporating in technologies such as solar cells, special alloys, semiconductors, glass colorants, catalysts, and fabric hardeners (Choi et al., 2018) and its increasing demand fuels its increasing value. Historically, Te was extracted in mining activities as a byproduct of other mining activities, this is mainly due to the low abundance of this metal, its scattered occurrence, and historical low demand (Dittmer, 2003). The recovery of Te, in most cases around the world, is dependent on ores with low Te content and it is, therefore, non profitable and/ or requires environmental impactable mining methodologies for its recovery. New technologies, such as bioleaching, can provide an answer to the recovery of high value elements of low abundance from low-grade ores, waste ores and even e-wastes (Ningfei & Hongguan, 2011). Bioleaching is a technology that has proven tests in some mining industries, such as copper, cobalt, manganese and lithium (Demergasso et al., 2005; Moazzam et al., 2021; Naseri et al., 2019) and it stands out from alternative technologies for its economic, energy-efficient, pollution-free process and low capital requirements. Increasing interest in Te bioleaching has been observed in the last decade with works performed in sulfide ores (Guo et al., 2012; Ningfei & Hongguan, 2011) and gold concentrates (Choi et al., 2018; Climo et al., 2000). Nevertheless, all bioleaching experiments conducted focus on acidophilic bacteria for the selective or non-selective recovery of Te from ores. The use on acidophilic bacteria such as *Thiobacillus ferroxidans, Acidithiobacillus ferrooxidans* or *Acidithiobacillus thiooxidans* proves effective in solubilizing metals and metalloids, such as Te, from sulfur bearing ores but requires very low pH conditions for optimal bacterial activity (Choi et al., 2018). This process results in a drainage solution, with very low pH, acid mine water, particularly in sulphidic ores (Feng et al., 2000). Acid mine waters are an undesirable by product of a minig operation, mainly due to their pH.

Therefore, this strategy is not sustainable for in situ applications and an alternative must be developed to ensure an eco-friendlier solution. Mining environments are rich ecological niche with diverse bacterial communities (Chung et al., 2019; Liu et al., 2021; Lopes et al., 2020), including several non-acidophilic organisms. The bacteria found in these environments are metabolically diverse and are often characterized by high metal resistance (Chung et al., 2019), a trait of interest in bioleaching experiments. Among the bacteria taxa commonly found in these niches whose characteristics are of interest in bioleaching, *Bacillus* and *Paenibacillus* could serve as bioleaching alternatives to acidophiles. Such examples were demonstrated with the use of *Bacillus mucilaginosus* in vanadium bioleaching from stone coal (Dong et al., 2019), *Bacillus subtilis* used for nickel bioleaching from laterite ore (Giese et al., 2019) and *Paenibacillus mucilaginosus* in silicon bioleaching from electrolytic manganese residue (Lv et al., 2020). Further studies are needed in the evaluation of bioleaching of mining sludges, tailings and other discarded material that are byproducts of previous mining activities and can, with appropriate methodologies, bu used as secondary raw materials.

The objective of this work was to evaluate, in selected strains, the ability to mobilize Te from mining and industrial secondary sources. This work focus on heavy metal resistant bacterial strains, isolated from mining environments, that demonstrate high Te resistance. The variability in Te leaching will be determined by comparing individual strains and the mine residues microbial community along with the effect of bioagmentation.

Materials & Methods

Tellurium containing sediments

Sediments were provided by EDM – Empresa para o Desenvolvimento Mineiro, from the Aljustrel copper mining site, (37°52'07.3"N 8°09'24.7"W), in southern Portugal. ALJ

sediments were collected from an abandoned mine site, by digging a superficial mine discarded basin, less than 1 m. Sediments were divided in two batches: first, for bacterial isolation and for autochthonous microbial community bioleaching assays, biologically active sediments – ALJ98, ALJ109 and ALJ121, second, to serve as substrate for leaching assays, sediment ALJ. Each biologically active sediment was divided in two batches: first, preserved with addition of 15 % glycerol at -80 °C, for bacterial isolation and the second preserved at 4 °C for authoctonous community bioleaching assays. The ALJ sediment was sterilized three times, by autoclave, dried in an oven, for total water removal, and resulted in a fine dust, this was preserved in a low moisture environment.

Bacterial strains isolation and purification

Biologically active sediments ALJ98, ALJ109 and ALJ121 from Aljustrel mining site were suspended in 50 % diluted Luria Bertani (LB) medium (Sigma). These suspensions were incubated at 25°C for 7 days in an orbital shaker. Timely increments of sodium tellurite (Sigma Aldrich) were added to the cultures, increasing from 5×10^{-4} M, 1×10^{-3} M, 3×10^{-3} M, 5×10^{-3} M up to 1×10^{-2} M. Prior to each Te (IV) enrichment an aliquot of the suspension was plated in 50 % diluted LB agar for selection of isolates. Plates were incubated at 25 ºC for up to one month. Pure isolates were obtained from repeated streaking of a selection of all colonies with different morphology and preserved at -80 ºC in growth media containing 15% glycerol.

DNA extraction and 16S rRNA gene amplification and identification

DNA from each isolate was obtained using standard freeze-thaw method (Nielsen et al., 1995). Amplification of the near full-length 16S rRNA gene sequence was performed by PCR with universal primers (Rainey et al., 1996). PCR amplicons were observed on a 1 % agarose electrophoresis and purified using a gel purification kit (EZNA, VWR),

according to manufacturer instructions. The resulting amplicons, sequenced by Sanger method (Stabvida) were matched with the existing sequences using a nBlast search against the reference type strain database on the EzTaxon portal (Kanz et al., 2005; Rutherford et al., 2000)

Individual strain tellurium mobilization assay

Each bacterial strain, *Paenibacillus pabuli* ALJ109b, *Bacillus mycoides* ALJ98a and *Paenibacillus taichungensis* ALJ98b, was inoculated. Individualy, in in 50 mL of LB media, diluted 1:10, with 1 g of ALJ sediment added. Bioleaching assays were performed in a rotating shaker, 140 rpm, for 30 days at room temperature. Full suspension was collected at day 30, decanted, and 1 mL was collected for differential centrifugation, to determine Te content in cells and sediment. Differential centrifugation was performed at 4 °C, 3220 rpm, for 30 min, on a 10 mL volume of increasing concentrations of saccharose, 30 %, 45 %, 70%, top to bottom. After centrifugation the resulting phases and interphases were collected and weigh prior to additional centrifugation to further separate soluble and insoluble phases. The latter were washed twice in PBS, partitioned for protein content determination and to Te determination and all fractions were stored at 4 °C.

Community and bioaugmentation tellurium mobilization assays

Mobilization of elemental Te from sediments was determined in biologically active sediments. These assays were performed by mixing 1 g of ALJ sediment with 1 g of biologically active ALJ98, ALJ109 or ALJ121, forming three composite substrates, in 50 mL of LB media, diluted 1:10. For mobilization of Te from biologically active sediments with bioaugmentation, a mixture was prepared with 1 g of ALJ sediment, 1 g of biologically active ALJ121, and a consortia of the isolates *P. pabuli* ALJ109b, *B. mycoides* ALJ98a and *P. taichungensis* ALJ98b, final O.D. of 0.1 each, in 50 mL of LB

media, diluted 1:10. All assays were performed in a rotating shaker, 140 rpm, for 30 days at room temperature. Full suspension was collected at day 30, was decanted, and 1 mL was collected for differential centrifugation, as described in the section Individual strain Te mobilization assay.

Total protein determination

Total protein was determined in recovered and washed pellets from differential centrifugation interphases described before. Bradford assay was used to determine mass of protein using a calibration curve constructed with a bovine serum albumin calibration (Bradford, 1976).

Tellurium removal determination

Evaluation of Te removal was performed by determining elemental composition by ICP-MS, in liquid phase. Pre-recovered pellets, from single strain, authoctonous microbial community and bioagmentation Te mobilization experiments, were subjected to acid treatment, 5 % nitric acid, 30 min, at 50 °C and resulting liquid phase was recuperated. A mix of either liquid phases, from differential centrifugation, and acid treated pellets was prepared with 2 % nitric acid for ICP-MS.

Results

Bacterial isolates and secondary sources for leaching

The isolation of strains by enrichment of live sediments resulted in two identified bacterial species from sediment ALJ98, *Bacillus mycoides* ALJ98a and *Paenibacillus taichungensis* ALJ98b and one strain from sediment ALJ109, *Paenibacillus pabuli* ALJ109b. No bacterial isolate was recovered from sediment ALJ121.

For Te leaching/ mobilization efficiency determination the initial concentration of Te in each sediment was determined by ICP-MS. Sediments tested contained Te in similar concentrations, with the lowest concentration in the dried, abiotic, sediment of 0.418 ± 0.033 ppm. Biologically active sediments varied, on average, between 0.42 ± 0.029 ppm and 0.473 ± 0.058 ppm, Table 2.1.

Table 2.1. Quantification of tellurium in mining sediments. Tellurium was quantified in sediments from Aljustrel mine by ICP-MS.

	ALJ	**ALJ98**	**ALJ109**	**ALJ121**
Te concentration (ppm)	0.418	0.443	0.423	0.473
SD (±)	0.033	0.083	0.029	0.058

Tellurium mobilization by individual strains

Tellurium mobilization was determined for individual strains using sediment ALJ containing 0.418 ± 0.033 ppm of Te. All strains mobilized Te from the sediments, with *B. mycoides* ALJ98a mobilizing, as much as, 54 % of initial Te, 73 % for *P. taichungensis* ALJ98b and 76 % for *P. altitudinis* ALJ109b. Leaching was also similar between *Paenibacillus* strains, with approximately 9 µg of Te in solution, after 30 days, higher than *B. mycoides* ALJ98a with 6.34 µg of Te in solution. Leaching amounts were higher than accumulated amounts for any strain tested, Figure 2.1.

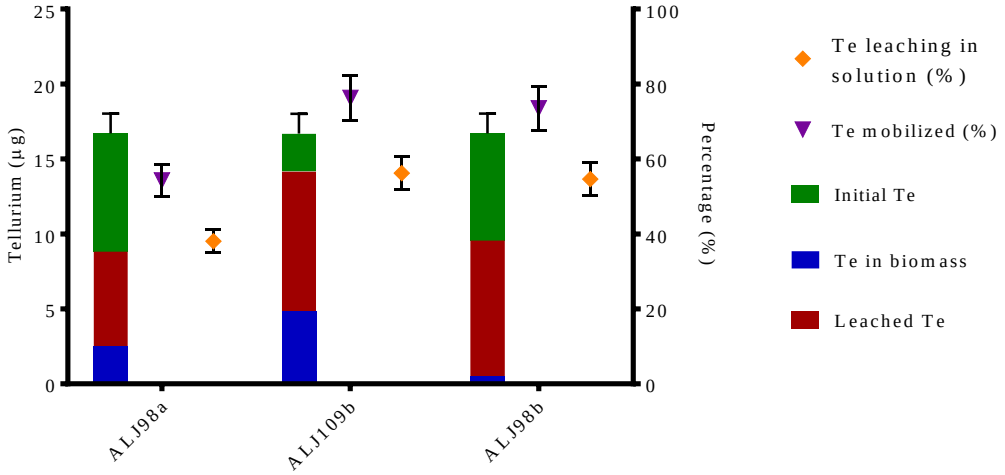

Figure 2.1. Mobilization of tellutium from secondary sources by environmental bacteria from *Bacillus* and *Paenibacillus*. Tellurium mobilization by *Bacillus mycoides* ALJ98a, *Paenibacillus pabuli* ALJ109b and *Paenibacillus taichungensis* ALJ98b from secondary source ALJ. Bars represent mass of Te in each fraction (green) initial, (blue) accumulated and (red) leached. Symbols represent the percentage of Te mobilized for each organism from the initial sediment, (inverted triangle) total Te mobilized, (diamond) Te leached into solution.

Community and bioagmentation tellurium mobilization

The evaluation of Te leaching and overall Te mobilization using the sediments native microbial community was tested with the same parameters selected for individual strains. Initial amounts of Te were similar between composite substrates (sterilized secondary source and biologically active sediment), ranging from 34.44 ± 2.1 µg (ALJ + ALJ98), 33.64 ± 2.3 µg (ALJ + ALJ109) to 35.64 ± 1.94 µg (ALJ + ALJ121). The amount of Te in biomass was determined in all differential centrifugation phases and interphases with positive amounts of protein. The amount of Te leached was determined, from the decanted leachate and from differential centrifugation phases and interphases without quantifiable protein. The most effective microbial community in Te mobilization from the composite substrates was from ALJ98 with the highest Te mobilization and Te leaching percentages of 42.23 % and 17.84 %, Figure 2.2. Microbial communities from ALJ109 and ALJ121

performed similarly, removing 23.62 % and 21.11 % of Te with 4.88 and 6.39 % of the metalloid being leached to the medium, respectively, Figure 2.2. The bioaugmented assay, with microbial community from ALJ121 and the three strain consortium, increased by 12.17 % the Te mobilized when compared to the action of the microbial community alone, Te leaching to the medium and remaining in solution did not increase in this condition, Figure 2.2. The increment of Te mobilization by bioaugmentation was the result of higher amounts of Te in biomass, Figure 2.3.

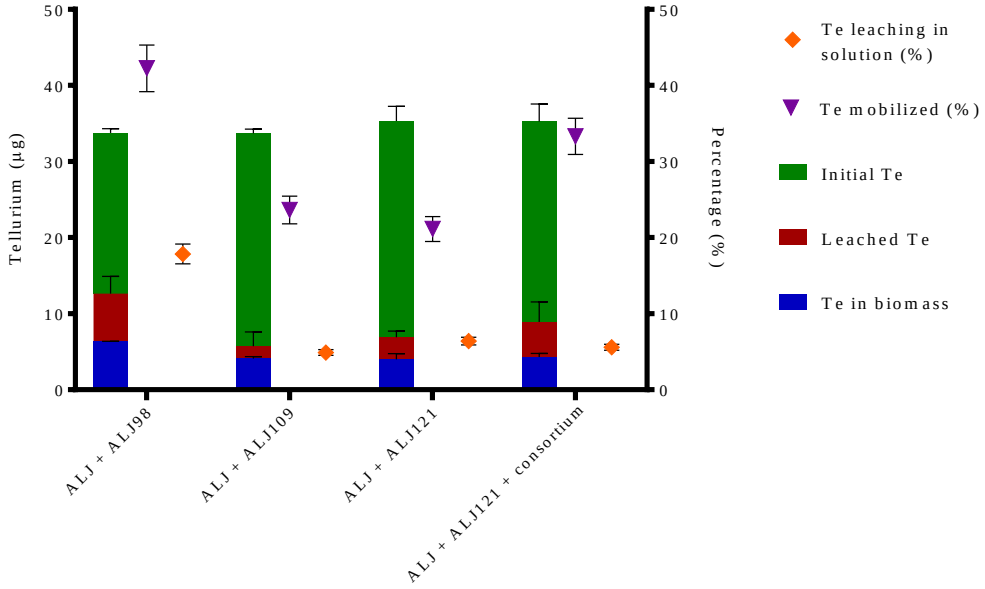

Figure 2.2. Mobilization of tellutium from secondary sources by autochtonous microbial community and by a consortium of environmental bacteria. Bioleaching using live sediments ALJ98, ALJ109 and ALJ121 and with bioaugmentation. Bars representing the amount (µg) of initial Te in sediment (green), leachate (red) and in a cell containing fraction (blue). Symbols represent the percentage of Te mobilized for each organism from the initial sediment, (inverted triangle) total Te mobilized, (diamond) Te leached into solution.

An opposing trend was observed in Te imobilization, measured as Te per biomass, with higher amounts, 6.36 µg.mg^{-1}, observed for the ALJ121 microbial community followed by 2.33 µg.mg^{-1}, for the ALJ109b microbial community, Figure 2.3. The experiment with

the lowest Te accumulation was the ALJ121 community with the *consortium* at 0.35 µg.mg^{-1}.

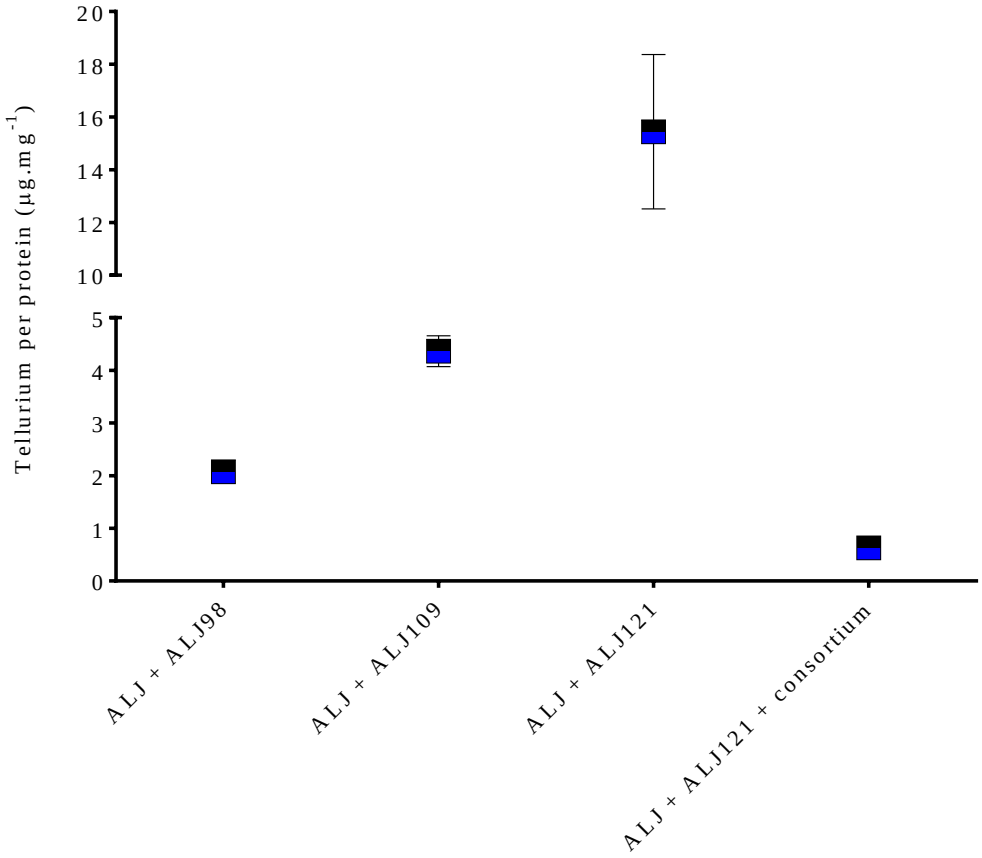

Figure 2.3. Tellurium bio-imobilization. Tellurium immobilization, accumulation/ biosorption, by an autochtonous microbial community and by a *consortium* of environmental bacteria. Values represented in tellurium per biomass, µg.mg^{-1}.

Discussion

Bioleaching is a technique with demonstrated potential in assisting mining technologies and may be in several cases the only viable eco-friendly alternative to chemical reduction techniques (Rasoulnia et al., 2021). Moreover, leaching technologies allow for the convertion of discarded material in secondary sources by increasing relative abundance

of some elements with initial concentrations too low to be considered for mining (Ningfei & Hongguan, 2011; Rasoulnia et al., 2021).

In this work bacterial strains, isolated from mining sediments, are capable of performing Te mobilization in the same sediments they originated from. This work presents the first account of Te bioleaching using *Paenibacillus* and *Bacillus* strains, with *Paenibacillus* performing marginally better than *Bacillus* when acting solely. B. *mycoides* ALJ98a, *P. taichungensis* ALJ98b and *P. altitudinis* ALJ109b are efficient Te bioleachers, achieving Te mobilization percentages comparable to what is observed by *Acidithiobacillus ferrooxidans* W18 and *Acidithiobacillus thiooxidans* PD2, between 54 % and 76 % (Ningfei & Hongguan, 2011). Depending on the authochtonous microbial community present different Te leaching and Te mobilization is seen. The authochtonous microbial community that performed better at Te leaching and mobilization was the one present in sediment ALJ98. It was from this sediment that the strains *P. taichungensis* ALJ98b and *B. mycoides* ALJ98a were isolated. Moreover, the bioaugmentation of the less effective biologically active sediment, ALJ121, with a consortium of bacteria with Te removal ability, led to an increase in Te leaching and recovery, 6.95 % to 12.03 %. This result supports previous findings were bacteria enriched and adapted in Cu containing media increased multiple metal mobilization when compared to non-enriched/ non-adapted bacterial strains (Choi et al., 2018). Nevertheless, the higher Te per biomass values were observed for the action of the ALJ121 authochtonous microbial community, 6.26 $\mu g.mg^{-1}$, with a 2.7 fold increase compared to the second best ALJ109, 2.33 $\mu g.mg^{-1}$. This result suggest the presence of microorganisms with high Te accumulation/ sorption ability. This work reveals for the first time the positive synergistic effect of a authochtonous sediment microbial community in Te recovery from secondary sources. Further work will explore

the improvement of the present bacteria in Te mobilization and determine its action in secondary sources with higher Te content.

Chapter III: Tellurite resistance and reduction in environmental isolates

Abstract

Tellurium is a metalloid with raising economic importance but remains to be fully understood in terms of its interaction with living organisms. The untreated mining wastes and the improper disposal of high-tech devices leads to increased presence of bioavailable metalloids, which become a source of environmental contamination, exerting stress on autochthonous microbial populations. However, this selective pressure can be viewed as an opportunity to study microorganism adaptation to the presence of increasing concentrations of metalloids, such as Te, and use this knowledge to solve contemporary problems. The objectives of this study were to determine the ability of aerobic heterotrophic bacteria isolated from high metal content mining residues to resist to Te (IV) and reduce Te (IV). In bacteria with high Te (IV) reduction ability to evaluate the formation of metallic Te. Morover, to determine the presence of confirmed Te (IV) resistance genetic determinants in resistant strains. From a total of 87 identified bacteria, isolated from mining sediments, over 50 were able to grow in presence of 3×10^{-3} M of Te (IV) and were considered resistant. From this group, eight strains showed capacity to reduce Te (IV) to Te (0) at different rates, with the concomitant production of Te (0) insoluble deposits, verified by the formation of Te insoluble particles. Most Te (IV) resistance genes were found in strains belonging to the order Bacillales, with a higher prevalence of genes of the *ter* operon. In conclusion, bacterial isolates originating from an environment, with a persistent selective pressure by heavy metals and metalloids, showed an ubiquitous ability to resist to low concentrations of Te (IV) and over 50 % could be described as highly resistant. Moreover, the response to the presence of Te (IV) was organism-specific, as demonstrated by different reduction efficiencies. The presence of genes associated to Te (IV) resistance varied among genera and families of bacteria, with higher prevalence of *ter* genes found in *Bacillus* than another genus.

Introduction

Although being rare in Earth's crust, Te is highly sought after in the field of nanotechnology (Mayers & Xia, 2002) due the combination of useful properties such as photoconductivity, nonlinear optical response and relevant thermoelectric capacity. Among the five most common oxidation states Te exists in nature mostly as Te (IV) or Te (VI). These forms are the most biologically relevant since both are soluble in water and therefore bioavailable, with Te (VI) being less soluble and less toxic than Te (IV) (Ollivier et al., 2011). Most studies have focused on toxicity and resistance of the most soluble and toxic Te oxyanion, Te (IV), while the toxicity of the elemental form is yet to be determined. The increasing demand for Te is a result of the production of components containing this metalloid which, by reaching their end-of-life, will result in high-tech waste disposal. Improper disposal practices and poor waste management will create the conditions for Te leaching in the form of Te (IV) and Te (VI), which will seep into the surrounding environment, creating contaminated zones with niches subjected to high selective pressure by this metalloid (Kyle et al., 2011). The bactericidal activity of this metalloid was recognized prior to the use of antibiotics (Arenas et al., 2014), with a toxicity of the oxyanion tellurite occurring at concentrations as low as 1 $\mu g.mL^{-1}$ in *Escherichia coli* (Turner et al., 2012).

Biological Te^r is not ubiquitous and occurs mainly by reduction of the anionic form to a less toxic form. To this date, two reduction mechanisms have been described: the generation of the volatile DMTe or the direct conversion to Te (0). The resistance by reduction of Te (IV) to Te (0) can be mediated by several genetic mechanisms. Some are unspecific, such as nitrate-reductases, (Sabaty et al., 2001) or other molybdopterin-containing enzymes (Theisen et al., 2013), and others are specific/ semi-specific mechanisms.

To this date, although possessing unclear mechanisms of resistance, a few genetic determinants have been linked to Te^r. An example of Te^r by methylation, is mediated by the *tehAB* genetic system (Dyllick-Brenzinger et al., 2000), which confers moderate levels of resistance in *E. coli* K12, 128 $\mu g.mL^{-1}$. In this system, the TehB protein has been identified as a methyltransferase. Te^r by reduction has been thoroughly explored in a *Rhodobacter sp*. possessing the *trgAB*/ *cysK* determinants (Borghese et al., 2014, 2017). However, the genetic determinant conferring the highest Te^r is the *ter* operon. The *ter* operon was initially detected in plasmid pMER610 and in plasmid R478, both from *E. coli*, and contains seven genes (*terZABCDEF*). Within the core *ter* operon, the genes present encode for three main protein families, the TerD, the TerB, and the TerC family. From the three family proteins *terB*, *terC*, *terD* and *terE*, the last two encoding protein in the TerD family, have been shown to be directly involved in Te^r (Turner et al., 1994). Several genetic arrangements of the *ter* operon have been identified among Actinobacteria, Firmicutes and Gammaproteobacteria lineages (Anantharaman et al., 2014). In some of these genetic organizations, additional genes for Te^r are present, such as the genes encoding protein TelA and homologues (Franks et al., 2014). The only directly observable effect of the presence of Te^r determinants in the genome has been the extracellular deposition of Te-containing crystals on the vicinity of the outer membrane, with reduced intracellular Te bioaccumulation (Burian et al., 1998; Kormutakova et al., 2000).

As verified for other metals, bioreduction leads to the formation of Te-containing intra-/extra-cellular nanostructures. A diversity of microorganisms has shown the capacity to form these nanostructures, such as *Enterobacter cloacae* (Contreras et al., 2018), *Ochrobactrum* sp. (Zonaro et al., 2017), Shewanella *baltica* (Vaigankar et al., 2018), and *Rhodobacter capsulatus* (Borghese et al., 2014, 2017). An increasing interest in

understanding the formation of these structures is the result of the growing potential range of applications for bio-produced nanoparticles covering fields such as optical imaging (Plaza et al., 2016) or novel battery technology (Kim et al., 2015). Consequently, there is a gain in importance for the isolation and characterization of organisms with potential in Te ions reduction from a large number of different environments, such as sea sediments (Csotonyi et al., 2006; Ollivier et al., 2008), fouled waters (Chien & Han, 2009), Antarctic/ Arctic samples (Arenas et al., 2014; Plaza et al., 2016), mine tailings (Maltman et al., 2015), among others. One environment of interest, for the isolation of target organisms, is mines and long lasting mine tailings where the continuous selective pressure of multiple metals is present on the ecosystem. In our study two mining sites were used to isolate microorganisms. Panasqueira site is an active tungsten mine and the tailings where bacteria were isolated from are either old, over 50 years, and still with high content of tungsten, or recent and with less concentration of target elements for mining (Grangeia et al., 2011). Jales site is an exploratory test gallery in a region of gold deposits (Martins et al., 2019). Samples collected are superficial and mostly undisturbed by either human or environmental activity. In the previous chapter, isolates were obtained from Aljustrel, a site of a decommissioned copper mine where sediments were collected from superficial tailings (Silva et al., 2020). These tailings were unaffected by human activity for many years but were subjected to environmental pressures.

The aim of this study is to reveal the diversity of Te^r responses of environmental strains, isolated from different mining sites, where the continuous presence of metals exerts selective pressure on the autochthonous microbial community. The tellurite reduction capacity of metabolically active isolates was determined by following Te (IV) depletion and by visualization of the resulting Te insoluble particles. Genetic determinants

conferring resistance to Te (IV) were confirmed by targeted polymerase chain reaction (PCR).

Materials & Methods

Sample collection

Sediment samples were collected from one mining site the Panasqueira tungsten mine (40°07'32.71"N, 7°42'51.18"W), in central Portugal, as well as from a test gallery for gold mining, in Jales north Portugal (41°28'13.1"N 7°34'38.1"W). This chapter also explores the organisms isolated from the Aljustrel mining site, described in Chapter II. Samples from Panasqueira were collected at 2 and 4 m from boreholes, using a dynamic geotool probe and a 50 mm poly-vinyl carbonate sampler with a diameter of 50 mm. Between each core sampling (B2S2, B2S3, B1S4 and B1S5) the sampler was decontaminated using 70 % ethanol. Jales disturbed samples were collected from the walls of the gallery. All sites and samples have unique characteristics, Table 3.1. All samples were collected and transported into sterile containers. Sediment samples were broken apart, homogenized and partitioned for further studies.

Table 3.1. Sampled mines and samples general characteristics. Description of sampled sites sediments, Aljustrel and Panasqueira mines and Jales gallery. General description of sediments collected.

	Site Characteristics			**Sediments Characteristics**	
	Location	**Activity state**	**Main product of mining activity**	**Moisture content**	**Dept**
Aljustrel	37°52'07.3"N 8°09'24.7"W	Inactive	Copper	Slightly hidrated	2 to 4 m
Jales	40°07'32.71"N 7°42'51.18"W	Test galery	Gold	Mixed (dry/wet)	surface
Panasqueira	41°28'13.1"N 7°34'38.1"W	Active	Tungsten	Mostly hidrated /water samples	till 1 m

Bacterial strains and growth media

The bacterial isolation protocol targeted aerobic heterotrophic bacterial strains from sediments from all isolation sites. Aliquots from sediment samples, Panasqueira and Jales mining sites, were collected and seriate dilutions were prepared, with saline solution (NaCl 0.85 %) for inoculation of Reasoner 2A (R2A) agar (NZYTech, Portugal). Plates were incubated at 25 ºC for up to one month. Pure isolates were obtained from repeated streaking of a selection of all colonies with different morphology and preserved at -80 ºC in growth media containing 15% glycerol.

DNA extraction and 16S rRNA gene amplification and identification

DNA from each isolate was obtained using standard freeze-thaw method (Nielsen et al., 1995). Amplification of the near full-length 16S rRNA gene sequence was performed by PCR with universal primers (Rainey et al., 1996). PCR amplicons were observed on a 1 % agarose electrophoresis and purified using a gel purification kit (EZNA, VWR), according to manufacturer instructions. The resulting amplicons, sequenced by Sanger method (Stabvida) were matched with the existing sequences using a nBlast search against the reference type strain database on the EzTaxon portal (Kanz et al., 2005; Rutherford et al., 2000).

Isolates heavy-metal resistance determination and growth

Metalloid resistance of the isolates was determined by mininmal inhibitory concentration (MIC). For this assay growth was performed, in Reasoners 2A (R2A) agar (Jales and Panasqueira isolates) and LB agar (Aljustrel isolates) with increasing concentrations of Te (IV), 5×10^{-4} M, 1×10^{-3} M and 3×10^{-3} M. All bacterial growth was performed with incubation at 25 ºC for 24 to 48 h.

For determination of specific growth rates each isolate was grown in increasing concentrations of Te (IV), 1×10^{-4} M, 2.5×10^{-4} M and 5×10^{-4} M in LB (Aljustrel isolates) and R2A broth (Panasqueira and Jales isolates), while comparing against growth in the absence of Te (IV). Growth kinetics were determined by evaluation of optical density (OD) variation (Abs 600 nm) of bacterial strains grown at 25 ºC, 100 rpm.

Tellurite bio-reduction from liquid media

Tellurite reduction was evaluated in R2A for Jales and Panasqueira isolates and LB for Aljustrel isolates, at the concentrations of 1×10^{-4} M, 2.5×10^{-4} M, 5×10^{-4} M. Aliquots for TeRed testing were recovered at four points, lag/early exponential, mid exponential, late exponential and late stationary growth phase. After growth, cells were centrifuged 20 min at 4000 g, the pellets were preserved for further tests and the supernatant was stored for evaluation of TeRed. Quantitative depletion of Te (IV) was evaluated using a chromophore Diethyl-di-thiocarbamate (DDTC), method adapted from Turner and colleagues (Turner et al., 1992b). The reagent mixture was prepared with 1 mM DDTC, Tris-HCl pH7 buffer and each sample was incubated for no more than 15 min prior to absorbance reading at 340 nm. Quantitative data was obtained from a minimum of three experimental replicates.

The efficiency of Te (IV) depletion, Reduction efficiency (Re), was determined as the ratio of the absolute variation of Te (IV) in grams, from time 0 (T0) to late exponential growth (Tf), per growth, expressed as a variation on optical density, Tf – T0. Reduction rate (Rr) was determined as reason of the Re per time at Tf, as demonstrated in the equation.

$$Re = \frac{|\Delta Te|}{\Delta \mathrm{DO(Tf-T0)}} \qquad Rr = Re/t(Tf)$$

Tellurium aggregates production

Demonstration of Te precipitation was performed by scanning electron microscopy with coupled energy-dispersive X-ray spectroscopy (SEM-EDS) on preparations of cells recovered from a late exponential phase in the presence of 5×10^{-4} M of sodium tellurite. Cell pellets from cultures were collected by centrifugation at 4000 g, washed twice in cold saline phosphate buffer (PBS) and resuspended in 0.1 mL the same buffer. Droplets of cell concentrate ≈30 μL were dried in a 5×5 mm stainless steel plate, at room temperature, followed by two-step fixation with 2.5 % glutaraldehyde followed by desiccation with increasing ethanol concentration, 70/80/90/95%. SEM micrographs were obtained on a FEI Quanta 400FEG ESEM and EDS analysis was performed on an Oxford INCA Energy 350 equipped with the SAMX IDIFIX software, with an accelerating voltage of 15 kV and a beam current of 20 nÅ.

Screening for tellurite resistance genes

DNA from each isolate was obtained using standard freeze-thaw method (Nielsen et al., 1995). Targeted genes for screening were selected based on experimental confirmation of Te^r (Pal et al., 2014), with preference given to genes conferring resistance with absolute or narrow specificity to Te ions. Oligonucleotide design was conducted considering, at least, inter-genus genetic homology between selected strains, to reduce degeneracy, Table 3.2. Amplification of *terD* gene using primers terD_F and terD_R with annealing 45 s, 50 °C; elongation 1 min, 72 °C; *terZ* gene using primers yceD_F and yceD_R with annealing 1 min, 58 °C; elongation 1 min, 72 °C; *terC* gene using primers yceF_F and yceF_R with annealing 1 min, 54 °C; elongation 1 min, 72 °C and *telA/ yceH* gene using primers yceH_F and yceH_R with annealing 1 min, 57 °C; elongation 1 min, 72 °C; *tehA* gene using primers tehA_F and tehA_R with annealing 1 min, 50 °C; elongation 1 min,

72 °C; see detailed primer and PCR condition in Table 3.2. Polimerase chain reaction (PCR) amplicons were observed on a 1 % agarose electrophoresis and purified using a gel purification kit (EZNA, VWR), according to manufacturer instructions. The resulting amplicons, sequenced by Sanger method (Stabvida) were matched with the existing sequences using a nBlast search.

Table 3.2. Tellurite resistance genes in bacterial isolates. Genes screened in this study detailing the amplicon name, PCD conditions and oligonucleotide s sequences.

Amplicon	PCR conditions	Sequence
tehA	94 °C for 60 s 50 °C for 45 s 72 °C for 60 s	tehA_F: 5'-GARAAACATAACACNAAA tehA_R: 5'-AATNARGTTATANCCNC
terD	94 °C for 45 s 50 °C for 45 s 72 °C for 60 s	terD_F: 5'-ATGCCTATTATTTTAGAAAAAGG terD_R: 5'-TAACGTGATACAATCTCACTTAA
terC	94 °C for 60 s 54 °C for 60 s 72 °C for 60 s	yceF_F: 5'-TTGGACATTTTGAAACATATGTTG yceF_R: 5'-CTATTCTTCTTTTGAAGCCGC
yceH/telA	94 °C for 45 s 57 °C for 60 s 72 °C for 60 s	yceH_F: 5'-ATGACAAATACAAACGGAAATGAC yceH_R: 5'-TCAAGCATACGTTTTGTTCCG
terZ	94 °C for 45 s 58 °C for 60 s 72 °C for 60 s	terZ_F: 5'-CTAGTTGGACTTGGCTGGGAC terZ_R: 5'-CGGCAAGCTTCGCATCGTTTG
terZ - terC 1	94 °C for 45 s 58°C for 60 s 72 °C for 90 s	terZ_F: 5'-CTAGTTGGACTTGGCTGGGAC yceF_R: 5'-CTATTCTTCTTTTGAAGCCGC
terZ - terC 2	94 °C for 60 s 67-60 °C, <0.5 °C/ cycle for 60 s 72 °C for 90 s	terZ_F: 5'-CTAGTTGGACTTGGCTGGGAC yceF_F: 5'-TTGGACATTTTGAAACATATGTTG
terZ - terC 3	94 °C for 60 s 58 °C for 60 s 72 °C for 90 s	terZ_R: 5'-CGGCAAGCTTCGCATCGTTTG yceF_F: 5'-TTGGACATTTTGAAACATATGTTG
terZ - terC 4	94 °C for 60 s 67-60 °C, <0.5 °C/ cycle for 60 s 72 °C for 90 s	terZ_R: 5'-CGGCAAGCTTCGCATCGTTTG yceF_R: 5'-CTATTCTTCTTTTGAAGCCGC
terC - telA 1	94 °C for 45 s 56 °C for 60 s 72 °C for 90 s	yceF_R: 5'-CTATTCTTCTTTTGAAGCCGC yceH_F: 5'-ATGACAAATACAAACGGAAATGAC
terC - telA 2	94 °C for 45 s 55 °C for 60 s 72 °C for 90 s	yceF_F: 5'-TTGGACATTTTGAAACATATGTTG yceH_F: 5'-ATGACAAATACAAACGGAAATGAC
terC - telA 3	94 °C for 45 s 56 °C for 90 s 72 °C for 90 s	yceF_F: 5'-TTGGACATTTTGAAACATATGTTG yceH_R: 5'-TCAAGCATACGTTTTGTTCCG
terC - telA 4	94 °C for 45 s 57 °C for 60 s 72 °C for 90 s	yceF_R: 5'-CTATTCTTCTTTTGAAGCCGC yceH_R: 5'-TCAAGCATACGTTTTGTTCCG

Genetic organization of *ter* system

Organization of the Te^r determinants from the *ter* system was determined by PCR for the *Bacillus* strains 5W24, 3W19, ALJ98a and 10W7. Sets of primers for genes *terZ* and *terC* were designed based on the known sequences of *terZ* and *terC* genes from *B. altitudinis* 3W19. Combinations of forward reverse primers were designed to generate four sets of amplicons with primers from *terZ* and *terC*: terZ_F + terC_R, terZ_F + terC_F, terZ_R + terC_F and terZ_R + terC_R. The same combinations were performed with primers from *terC* and *telA*: telA_F + terC_R, telA_F + terC_F, telA_R + terC_F and telA_R + terC_R. Full list of PCR conditions can be seen in, Table 3.2

Phylogenetic reconstruction and statistical analysis

Alignment of PCR amplified *ter* genes and closely related reference genes, obtained by PSI-Blast, was performed with ClustalW and the phylogenetic reconstruction was performed using Mega10 software package. All data presented in graphs presented is calculated with statistic based on three biological replicates and statistical significance is calculated using one-way ANOVA, when applicable, using Prism GraphPad10 software. Statistical significance is represented as $*p \leq 0.05$, $**p \leq 0.01$.

Results

Isolation, identification and screening for tellurite resistant bacteria

A total of 144 different isolates were collected from the three sites sampled. From Panasqueira mine, 95 different isolates were recovered in R2A agar, 83 from cores of the tailings basins, 12 from the tailings surface waters. From the entire collection of Panasqueira microorganisms, 47 were resistant to 1×10^{-3} M Te (IV) and of these, 27 were resistant to the concentration of, at least, 3×10^{-3} M Te (IV), Supplementary Table 1/ Table 3.3. From Aljustrel the enrichment yielded three strains, all able to grow in solid media

spiked with concentrations of up to 5×10^{-3} M Te (IV). From Jales samples, a total of 44 organism were isolated in R2A agar, with 24 isolates being resistant to concentrations of 1×10^{-3} M Te (IV) and 9 to 3×10^{-3} M Te (IV), Supplementary Table 1/Table 3.4.

Strains with MIC higher than 5×10^{-4} M Te (IV) were identified based on 16S rRNA gene sequence and phylogenetic relatedness with type strains from NCBI database. The identification results grouped the strains recovered in those belonging to the Phylum *Actinobacteria* (44.7 %), *Firmicutes* (34.2 %) and *Proteobacteria* (21.1 %) phyla. The identified bacteria with MIC over 1×10^{-3} M Te (IV) were tested for increasing Te (IV) concentrations in liquid media. The most representative resistant organisms, MIC of 5 $\times10^{-4}$ M Te (IV), belonged to the genera *Bacillus, Paenibacillus, Cellulomonas* and *Mezorhizobium*, Table 3.3/ Table 3.4.

Table 3.3. Tellurite resistance in bacterial isolates from Panasqueira mine. Minimal Inhibitory Concentrations in solid and liquid R2A media, in the presence of Te (IV) of identified bacterial isolates from Panasqueira. Only represented bacteria with growth in ≥ 3 mM Te (IV) in solid media and/ or ≥ 0.5 mM Te (IV) in liquid media. Mathematical signals indicate growth compared to control situation: + - higher than control, ± - comparable to control and − - lesser than control.

Mine	Sample	Strain	Species	Solid media				Liquid media		
				Te (IV) mM				Te (IV) mM		
				0	0.5	1	3	0	0.5	3
Panasqueira mine	Basin 1 core sediments	B1.S5.4.2 5W23	*Bacillus zhangzhouensis*	+	+	+	+	+	−	−
		B1.S4.2.2 10W10	*Paenibacillus etheri*	+	+	+	+	+	−	−
		B1.S5.3.2 10W1	*Bacillus zhangzhouensis*	+	+	+	+	−	−	−
		B1.S5.4.2 10W15	*Paenibacillus amylolyticus*	+	+	+	±	+	−	−
		B1.S5.4.2 10W28	*Paenibacillus xylanexedens*	+	+	+	+	+	−	−
		B1.S5.4.2 5W10	*Cellulomonas fimi*	+	+	+	+	+	−	−
		B1.S4.2.2 2As4	*Cellulomonas cellasea*	+	±	±	±	+	+	−
		B1.S5.4.2 5W29	*Paenibacillus xylanexedens*	+	+	+	+	−	−	−
		B1.S5.4.2 5W33	*Paenibacillus sp.*	+	±	±	±	+	−	−
		B1.S5.3.2 10W7	*Paenibacillus sp.*	+	+	+	+	+	+	-
		B1.S5.4.2 10W7	*Bacillus safensis*	+	+	+	+	+	+	+
		B1.S5.4.2 3W19	*Bacillus altitudinis*	+	+	+	+	+	+	+
Panasqueira mine	Basin 2 core sediments	B2.S2.2.2 5W24	*Bacillus zhangzhouensis*	+	+	+	+	+	+	−
		B2.S2.3.2 10W3	*Actinotalea ferrariae*	+	+	+	+	+	−	−
		B2.S3.2.2 10W11	*Cellulomonas cellasea*	+	±	±	±	+	−	−
		B2.S2.2.2 10W19	*Mesorhizobium qingshengii*	+	+	+	+	+	−	−
		B2.S2.2.2 2As20	*Cellulomonas cellasea*	+	±	±	±	+	−	−
		B2.S2.2.2 5W10	*Cellulomonas marina*	+	±	±	−	+	+	−
		B2.S3.2.2 2As13	*Cellulomonas cellasea*	+	±	±	±	+	−	−
		B2.S2.4.2 3W3	*Mesorhizobium qingshengii*	+	±	±	±	+	−	−
		B2.S2.3.2 3W12	*Rhodococcus corynebacterioides*	+	+	+	±	+	−	−
		B2.S2.2.2 2As1	*Cellulomonas cellasea*	+	+	+	±	+	+	−
		B2.S3.4.2 2As5	*Bacillus altitudinis*	+	+	+	+	+	+	−
		B2.S3.2.2 2As8	*Flavihumibacter stibioxidans*	+	±	−	−	+	+	−
		B2.S3.3.2 3W8	*Nocardioides pakistanensis*	+	±	±	±	+	−	−
		B2.S3.2.2 2As7	*Cellulomonas cellasea*	+	−	±	±	−	−	−
		B2.S3.2.2 3W3	*Bacillus zhangzhouensis*	+	+	+	+	−	−	−
		B2.S2.2.2 2As2	*Rhizobium selenitireducens*	+	±	±	±	+	−	−
		B2.S3.2.2 5W2	*Cellulomonas cellasea*	+	±	±	±	+	+	−
		B2.S3.2.2 3W14	*Cellulomonas cellasea*	+	±	±	±	+	−	−
	Water	B2.A1 In2	*Rhodanobacter glycinis*	+	±	+	±	+	−	−
		B2.A2 W2	*Diaphorobacter polyhydroxybutyrativorans*	+	+	+	−	+	+	−
		B2.A1 Ga1	*Serratia glossinae*	+	+	+	±	+	−	−
		B2.A2 0.5Te1	*Tsukamurella strandjordii*	+	+	+	+	+	−	−

Table 3.4. Tellurite resistance in bacterial isolates from Aljustrel mine and Jales gallery. Minimal Inhibitory Concentrations in solid and liquid R2A media, in the presence of Te (IV) of identified bacterial isolates from Aljustrel and Jales. Only represented bacteria with growth in ≥ 3 mM Te (IV) in solid media and/ or ≥ 0.5 mM Te (IV) in liquid media. Mathematical signals indicate growth compared to control situation: + - higher than control, ± - comparable to control and − - lesser than control.

Mine	Sample	Strain	Species	Solid media				Liquid media		
				Te (IV) mM				Te (IV) mM		
				0	0.5	1	3	0	0.5	3
Aljustrel mine	Sediments	ALJ98a	*Bacillus mycoides*	+	+	+	+	+	+	+
		ALJ98b	*Paenibacillus tundrae*	+	+	+	+	+	+	+
		ALJ109b	*Paenibacillus sp.*	+	+	+	+	+	+	+
Jales galery	Sediments	Jales Ga15	*Mesorhizobium qingshengii*	+	+	+	±	+	+	−
		Jales 19	*Mesorhizobium qingshengii*	+	+	+	±	+	−	−
		Jales As34	*Mycobacterium montmartrense*	+	+	+	±	+	−	−
		Jales As35	*Mycobacterium montmartrense*	+	+	±	±	+	−	−
		Jales W10	*Curtobacterium flaccumfaciens*	+	+	−	±	+	+	−
		Jales W48	*Mycobacterium gilvum*	+	+	±	±	+	−	−
		Jales 20	*Mesorhizobium qingshengii*	+	+	±	±	+	−	−
		Jales 27	*Mesorhizobium qingshengii*	+	+	±	±	+	−	−
		Jales As13	*Curtobacterium flaccumfaciens*	+	+	−	±	+	−	−
		Jales As8	*Sphingobium aromaticiconvertens*	+	±	±	±	+	−	−
		Jales Te58	*Mesorhizobium qingshengii*	+	+	+	−	+	+	−
		Jales 44	*Okibacterium fritillariae*	+	±	±	±	+	−	−
		Jales 54	*Mesorhizobium huakuii*	+	+	±	±	+	−	−
		Jales 62	*Sphingobium sp.*	+	+	+	±	+	−	−
		Jales 21	*Mycobacterium fortuitum*	+	+	+	±	+	−	−
		Jales Ga6	*Curtobacterium flaccumfaciens*	+	±	−	±	+	+	−
		Jales Te55	*Mesorhizobium qingshengii*	+	+	±	±	+	+	+
		Jales W3	*Bradyrhizobium cajani*	+	+	±	±	+	−	−
		Jales Te59	*Mesorhizobium qingshengii*	+	+	+	−	+	+	−

Growth kinetics in the presence of tellurite and tellurite reduction

The strains resistant to 5×10^{-4} M Te (IV) in liquid growth, Table 3.3/ Table 3.4, were selected for evaluation of TeRed. Twelve strains did not show ability to remove Te (IV) from the growth medium, as the same or marginally different values of Te (IV), in solution, were detected throughout their growth. The eight remaining strains had their growth affected by Te (IV), Figure 3.1. The specific growth rates of cells grown in $5\times10^{-}$

^{4} M Te (IV) were lower than the control culture, without Te (IV), for all eight strains, Figure 3.1. Strains *P. pabuli* ALJ109b, *B. mycoides* ALJ98a, *P. taichungensis* ALJ98b and *C. marina* strain 5W10 maintained a growth rate similar to the control condition in concentrations up to 2.5×10^{-4} M Te (IV). *B. safensis* strain 10W7 increased its growth rate till 2.5×10^{-4} M of Te (IV), decreasing at the highest concentrations.

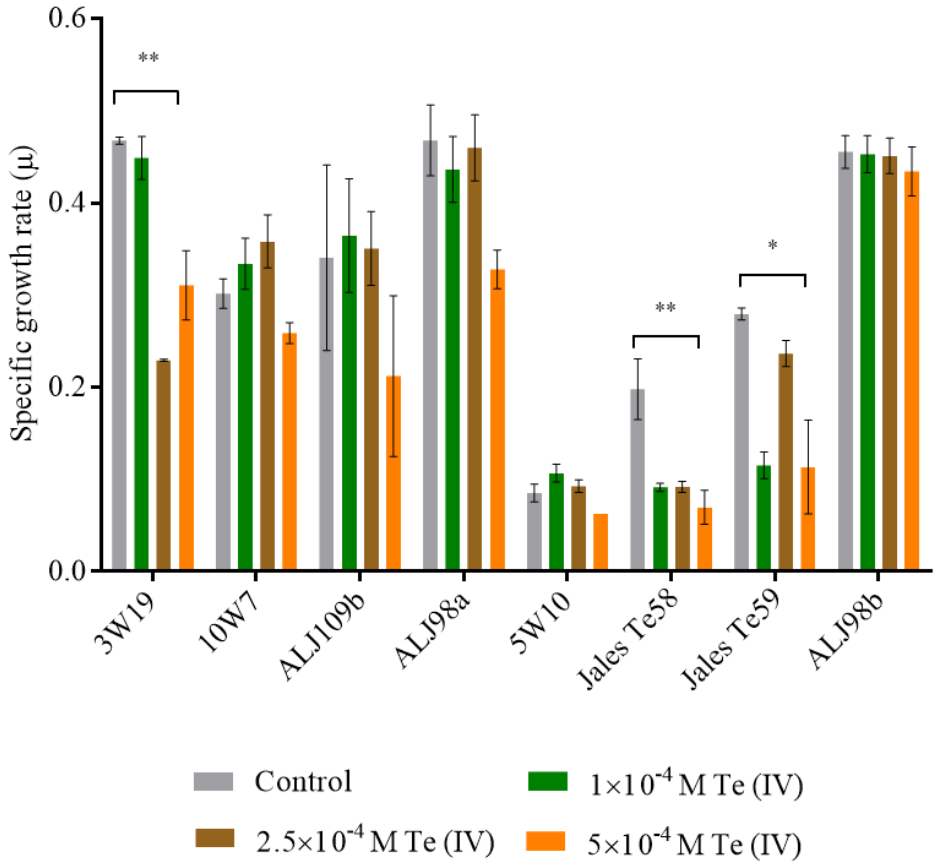

Figure 3.1. Impact of increasing concentrations of tellurite in bacterial growth. Specific growth rates calculated for strains (left to right): *Bacillus altitudinis* 3W19, *Bacillus safensis* 10W7, *Paenibacillus pabuli* ALJ109b, *Bacilus mycoides* ALJ98a, *Cellulomonas marina* 5W10, I Te58, *Mesorhizobium qingshengii* Te59 and *Paenibacillus tundrae* ALJ98b. Comparison of growth in selected concentration of Te (IV), Control (no Te (IV), 1×10^{-4} M Te (IV), 2.5×10^{-4} M Te (IV) and 5×10^{-4} M Te (IV). All experiments conducted in triplicate and statistical significance indicated $*p \leq 0.05$, $**p \leq 0.01$.

The strains that performed better at removing Te (IV) from liquid media were Panasqueira isolates *B. altitudinis* 3W19, *B. safensis* 10W7 and *C. marina* 5W10, Figure 2.2, with Re values ranging from 6.03 to 4.39 $\Delta mg.DO^{-1}$, Table 2.5. The isolates from Aljezur *B. mycoides* ALJ98a, *P. taichungensis* ALJ98b and *P. pabuli* ALJ109b showed moderate depletion efficiencies, with values ranging from 3.35 to 1.08 $\Delta mg.DO^{-1}$. Finally, the two Jales isolates *M. qingshengii* jales Te59 and *M. qingshengii* jales Te58 had the lowest Te (IV) depletion efficiencies, with reduction rates in the mid hundreds of $\Delta \mu g.DO^{-1}$. The time required for each different strain to reach late exponential phase was very distinct, ranging from 8 to 48 h. When considered, *B. altitudinis* 3W19 remained the highest performer with a reduction rate of 0.75 $\Delta mg.DO^{-1}.h^{-1}$, clearly higher than the second-best performer *B. safensis* 10W7, with a Rr of 0.23 $\Delta mg.DO^{-1}.h^{-1}$, Table 3.5.

Table 3.5. Reduction efficiency (Re) and reduction rate (Rr) for selected organism from three different mining sites. Determinantion of Re and Rr for a slection of eight high tellurite resistant strains. For Re calculation tellurite was determined by DDTC assay and growth determination using OD. For Rr calculation the Re value was calculated at late exponential phase for each strain.

Organism	**Origin**	**Re (Δmg/DO)**	**Rr (mg/DO/h)**
Bacillus mycoides ALJ98a	Aljezur	3.35	0.17
Paenibacillus tundrae ALJ98b		1.08	0.05
Paenibacillus pabuli ALJ109b		1.26	0.06
Bacillus altitudinis 3W19	Panasqueira	6.03	0.75
Bacillus safensis 10W7		5.49	0.23
Cellulomonas marina 5W10		4.39	0.09
Mesorhizobium qingshengii Jales Te59	Jales	0.52	0.02
Mesorhizobium qingshengii Jales Te58		0.88	0.04

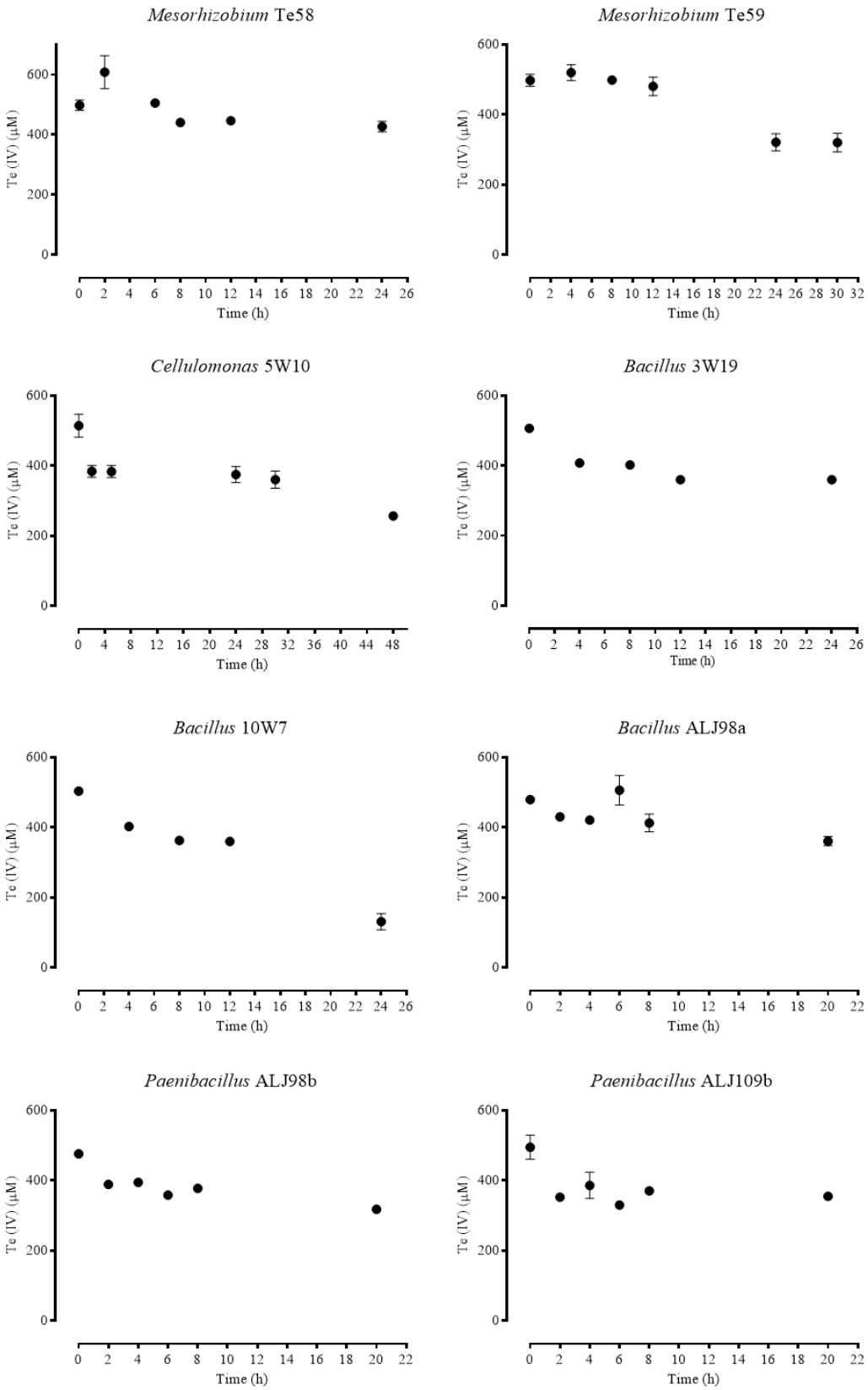

Figure 3.2. Bacteria-mediated tellurite reduction. Tellurite depletion from liquid media, over time, for strains able to grow in liquid media with 5×10^{-4} M Te (IV), determined by DDTC assay. Values presented with abiotic subtraction.

Tellurium aggregates production

Visual identification of Te containing aggregates was performed by SEM with identification of Te by coupled EDS for the six strains showing Re over 1 mg.DO^{-1} and Rr over 0.05 (Re.h^{-1}). These were prepared for SEM-EDS imaging as described in the methods section. Cell pellets of all strains revealed the presence of high-density deposits that by EDS were confirmed to have Te in varying abundances, Figure 3.3.

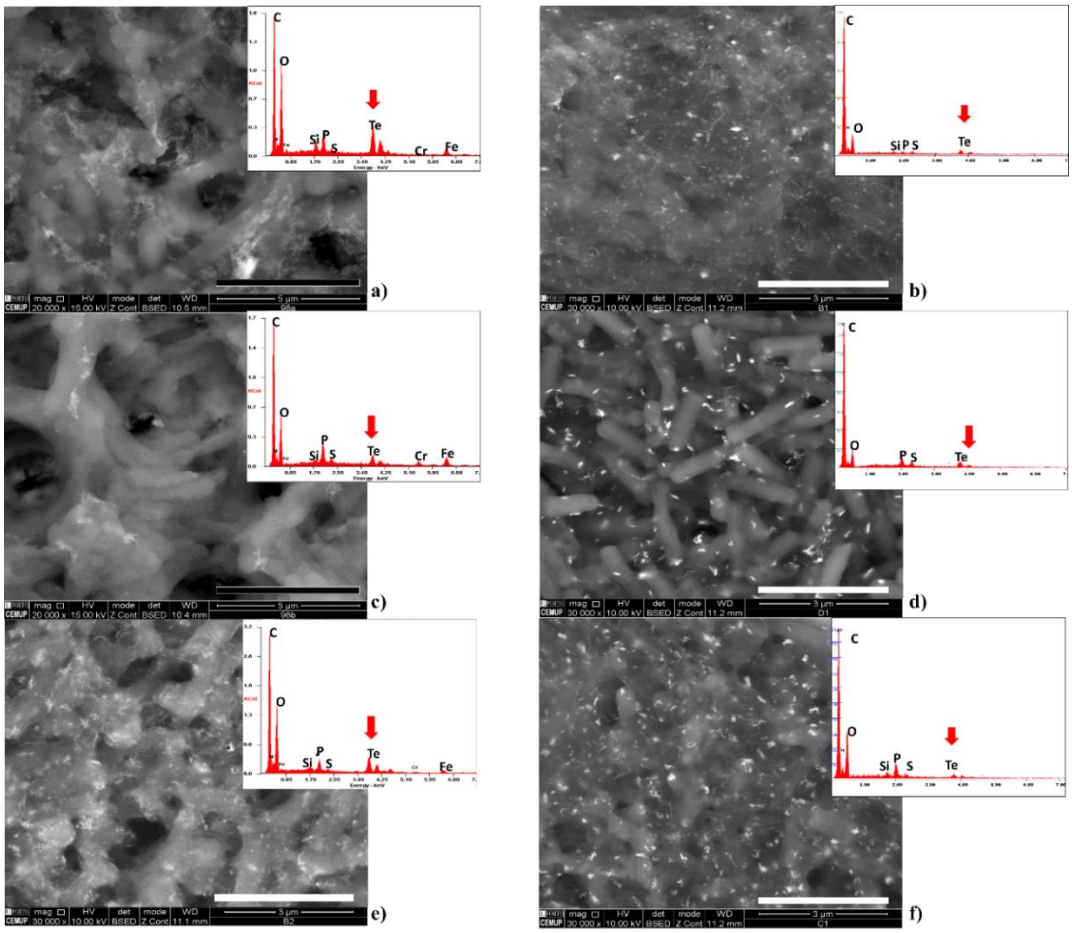

Figure 3.3. Biological production of tellurium containing nanostructures. SEM micrographs of tellurite reducing cells fixated in stainless steel surfaces. **a)** *Bacilus mycoides* ALJ98a, **b)** *Bacillus safensis* 10W7, **c)** *Paenibacillus tundrae* ALJ98b, **d)** *Bacillus altitudinis* 3W19, **e)** *Cellulomonas marina* 5W10 and **f)** *Paenibacillus pabuli* ALJ109b. For images **a)**, **c)** bar (black) = 5 µm; for images **b)**, **d)**, **e)** and **f)** bar (white) = 3 µm. High density metal deposits are represented in white. EDS spectra are obtained from reads at randomly selected white segments and red arrows highlight Te detection in spectra.

B. safensis 10W7, *B. altitudinis* 3W19 and *C. marina* 5W10 formed shard or string like Te-containing particles, all other strains revealed Te-containing nanostructures with unclear geometries, Figure 3.3.

Screening for tellurite resistance genes

Resistance genes for Te (IV) were found in nine strains mostly belonging to the *Bacillus* genus. Gene *terZ* from the TerD family is the most represented, of all genes screened, in the strains tested being present in nine strains, Supplementary Figure 1, *Bacillus altitudinis* 3W19, *Bacillus safensis* 10W7, *Paenibacillus pabuli* ALJ 109b, *Bacillus mycoides* ALJ 98a, *Mesorhizobium qingshengii* Jales Te55, *Cellulomonas marina* 5W10, *Flavihumibacter stibioxidans* 2As8 and *Fictibacillus enclensis* 5W6.

Gene *telA* was present in four strains, *B. altitudinis* 3W19, *B. safensis* 10W7, *F. stibioxidans* 2As8 and *Bacillus zhanghouensis* 5W24. Both *terC* and *terD* were present in three strains each. Gene *terC* was found in *B. altitudinis* B1. S5. 4.2 3W19, *B. safensis* 10W7 and *B. zhanghouensis* 5W24 and gene *terD* was found in *B. mycoides* ALJ 98a, *P. pabuli* ALJ 109b and *B. altitudinis* 3W19. Only one *terB* was found, in *B. altitudinis* 3W19. The strains with the highest number of resistance genes found were *B. altitudinis* 3W19 with *terD, terZ, terC* and *telA,* followed by *B. safensis* B1. S5. 4.2 10w7 and *B. zhangouensis* 5W24 with *terZ, terC* and *telA.* No positive amplicons were detected for the gene *tehA* in mining isolates.

Organization of the *ter* genetic determinants

Bacillus strains possessing more than one element of the *ter* gene cluster were considered for the determination of the arrangement of the constituting *ter* genes. From the eight combinations selected for *ter* genes arrangement only two produced amplicons. All amplicons produced, from the two combinations of gene arrangements in four strains,

were sequenced and an identification of the amplified region was presented for all the identifiable regions. The four strains tested had amplicons from *terZ* forward to *terC* reverse, contrarily only *B. subtilis* ALJ98a had an amplicon from *terC* forward to *telA* reverse, Figure 3.4/ Table 3.6. Fragment sizes from amplicon terZ – terC ranged from 1.4 kb to 2.9 kb, approximately, with amplicons in each strain varying in number and in size. In *B. mycoides* ALJ98a and *B. safensis* 10W7 only one amplicon resulted from the fragment *terZ – terC* PCR, of approximately 2.9 kb. PSI-Blast identified, in *B. safensis* 10W7, from 5' to 3', two TerD family protein/stress response protein (Id = 99.48 %/ Id = 99.49 %) and one TerC family protein (Id = 98.98 %). In *B. mycoides* ALJ98a, from 5' to 3', one TerD family protein (Id = 99.23 %) and one TerC family protein (Id = 99 %), Figure 3.4/ Table 3.6. Both *B. altitudinis* 3W19 and *B. zhangouensis* 5W24 produced multiple fragments in terZ – terC PCR. Strain 3W19 produce a fragment of approximately 2.7 kb with, from 5' to 3', two TerD family protein (Id = 100 %/ Id = 99.23 %) and one TerC family protein (Id = 99.45 %). The smaller amplicon from strain 3W19 that was possible to sequence was 1.4 kb and were identified, from 5' to 3', one TerD family protein (Id = 100 %) and one TerC (Id = 99.16 %). Strain 5W24 produce a fragment of approximately 2.7 kb with, from 5' to 3', one VWA domain-containing protein (ID=99.76 %), one tellurium resistance protein TerD (Id = 100 %) and one TerC/Alx family metal homeostasis membrane protein (Id = 100). The smaller amplicon from strain 5W24 that was possible to sequence was 2.1 kb and were identified, from 5' to 3', one tellurium resistance protein TerD (Id = 100 %), one TerD family protein (Id = 99.35 %) and one TerC/Alx family metal homeostasis membrane protein (Id = 100 %), Figure 3.4/ Table 3.6. The terC – telA amplicon obtained in strain ALJ98a was 2.9 kb in size and were identified, from 5' to 3', one TerC family protein (Id = 99.35 %) and one toxic anion resistance protein (Id = 99.09), Figure 3.4/ Table 3.6.

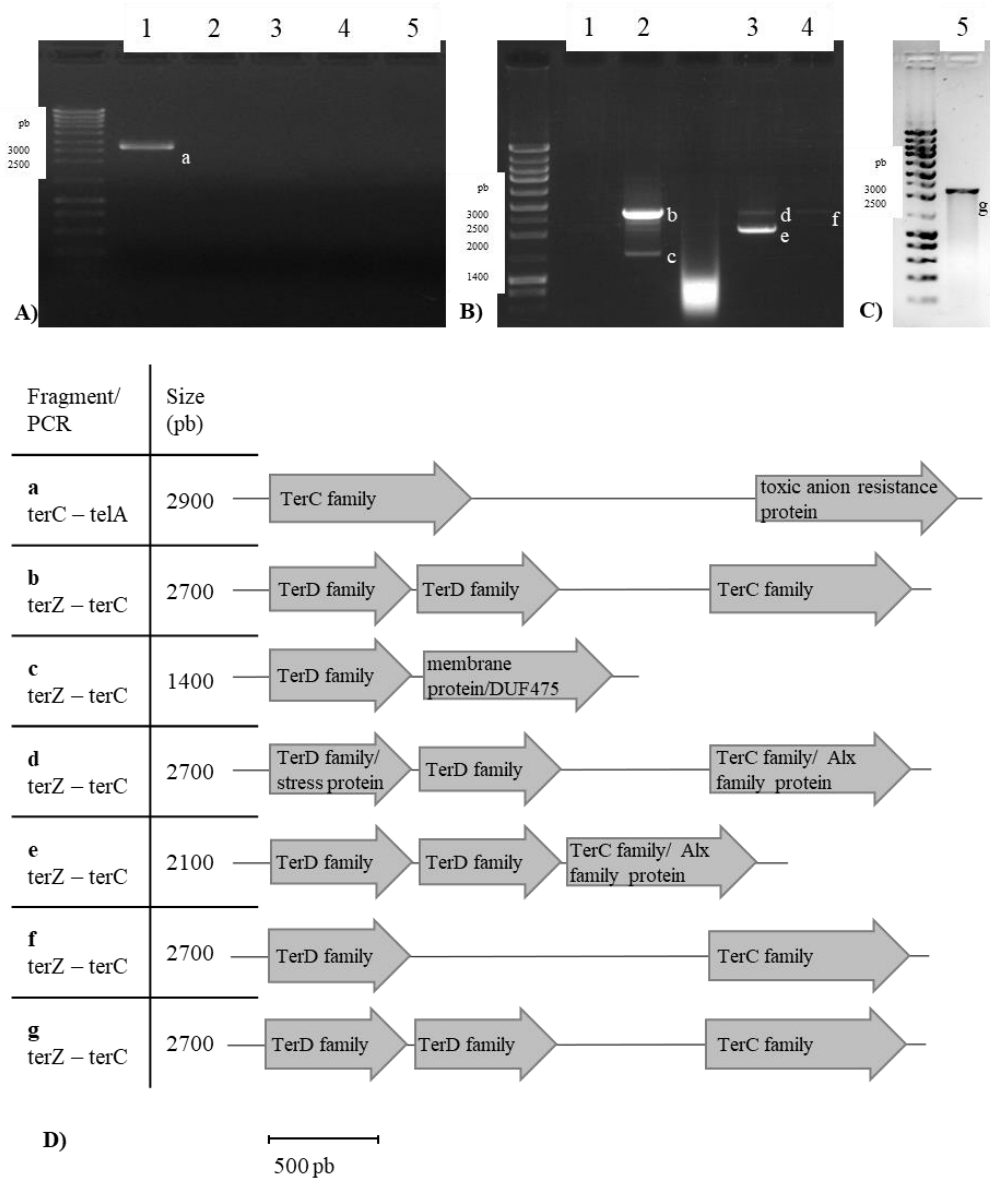

Figure 3.4. PCR screening for *ter* genes, identification of amplification products and putative genetic arrangements. PCR **A)** of fragment *terC – telA*, 1. *Bacillus mycoydes* ALJ98a, 2. *Bacillus zhangouensis* 5W24, 3. *Bacillus safensis* 10W7, 4. *Bacillus altitudinis* 3W19 and 5. Negative control. PCR **B/C)** of fragment *terZ – terC*: 1. Negative control, 2. *Bacillus altitudinis* 3W19, 3. *Bacillus zhangouensis* 5W24, 4. *Bacillus mycoides* ALJ98a and 5. *Bacillus safensis* 10W7. Diagram representation **D)** of genetic arrangement based on sequenced and identified amplicons a to g, size indication based on amplicon positioning on the gel.

Table 3.6. Identification of amplification products and putative genetic arrangements for amplicons of ter gene cluster elements. Identification obtained by

Blastn of fragments indicated on Figure 3.4/ bottom image, left to right. All identified fragments with coverage E ≤ 0.01.

Amplicon	Blastx Identification	Assession number	Identity (%)
a	TerC family protein	WP_153252914.1	99.4
	toxic anion resistance protein	WP_098333049.1	99.1
b	TerD family protein	WP_007498343.1	100
	TerD family protein	WP_008342133.1	99.2
	TerC family protein	WP_007498342.1	99.5
c	TerD family protein	WP_039166394.1	100
	TerC family protein	WP_144556175.1	99.2
d	VWA domain-containing protein	WP_202671625.1	99.8
	Tellurium resistance protein TerD	WP_071681669.1	100
	TerC/Alx family metal homeostasis membrane protein	WP_024485071.1	100
e	Tellurium resistance protein TerD	WP_071681669.1	100
	TerD family protein	WP_141130909.1	99.4
	TerC/Alx family metal homeostasis membrane protein	WP_024485071.1	100
f	TerD family protein	WP_007498343.1	99.2
	TerC family protein	WP_144556175.1	99
g	Stress response protein SCP2	SDD49373.1	99.5
	TerD family protein	WP_025751616.1	99.5
	TerC family protein	WP_153252914.1	99

Discussion

The mining environments have characteristic elements that shape microbiome including pH, metal concentration/content, temperature, dissolved oxygen, and total organic carbon (Liu et al. 2014; Chung et al. 2019; Sibanda et al. 2019). The continuous exposure to a high concentration of different metals and low carbon selects for distinct microorganisms able to deal with such environments (Liu et al. 2019; Chung et al. 2019). All three sampled mining sites in this study had different features; in none of these Te was a target element for mining, Figure 2.1. Since Te was not the metal extracted, discarded residues are

expected to have this metalloid in relative higher concentrations than non-mined environmental samples.

The overall diversity of Te (IV) resistant bacteria was large with four different Phyla recovered from all three sampling sites, *Actinobacteria*, *Proteobacteria*, *Firmicutes* and *Bacteroidetes*. The results indicate that *Mesorhizobium*, *Cellulomonas*, *Bacillus* and *Paenibacillus*, may be prevalent genera with high tolerance to the presence of Te (IV).

Tellurium ions resistance in *Bacillus* is usually related to their ability to reduce Te (IV), the oxyanion toxic form, to Te (0) (Franks et al., 2014). In *Paenibacillus*, although there are no publicly available reports concerning Te^r mechanisms. Considering the phylogenetic proximity of the two taxa, likely resistant strains of *Paenibacillus* were also able to reduce Te (IV). This work presents for the first time strains from the genera *Cellulomonas* and *Mesorhizobium*, as resistant to Te (IV). This opens a new possibility of study in Te^r mechanisms and genes.

The Te (IV) reduction capacity of metabolically active isolates was determined by following Te (IV) depletion and by visualization of the resulting Te insoluble particles. In this work, bacterial strains demonstrated varied and/or high performance, either calculating by cell mass or time, allowing different manufacturing protocols. Isolates from Panasqueira mine *B. altitudinis* 3W19, *B. safensis* 10W7 and *C. marina* 5W10 performed better than isolates from Aljustrel and Jales in reduction efficiency, mostly for the highest depletion values of Te (IV) in liquid media. Reduction rate was also higher for strains *B. altitudinis* 3W19 and *B. safensis* 10W7 as well as for *B. mycoides* ALJ98a, all these strains have high specific growth rates with small variation in growth, with 5×10^{-4} M Te (IV), compared to most other strains. *Bacillus* strains are from an application perspective the best reducers, having highest Te (IV) depletion, with less cell mass in

shorter times. The use of reduction efficiencies and reduction rates allows an efficient strategy to select strains able to manufacture Te structures.

Moreover, formation of Te precipitates was observed for selected strains. Most show clear indication of the formation of Te (0) aggregates with different levels of structural organization. The formation of different structures of aggregates is indicative of different metabolic mechanisms involved in the formation of those structures, as is observed in previous works (Wang et al., 2018).

Most of the Te^r genes identified in the strains tested belonged to the TerD family, nine *terZ* and three *terD* according to our identification, despite PSI-Blast identification available only identified most genes as belonging to TerD family. Some genes from this family, *terD* paralogues, *terE* and *terZ* are highly conserved among Firmicutes lineage (Anantharaman et al., 2014), hence the higher abundance in the strains tested, mostly from the *Bacillus* and *Paenibacillus* genera. The TerC family is also represented in the strains tested but the TerB family was not found. Considering that, it seems that in the strains tested, Te (IV) resistance involve the *ter* operon, this result is contrary to what is seen in the literature for several strains, namely *Escherichia coli* O157:H17, where it was demonstrated that for Te^r, the genes *terB*, *terC*, *terD* and *terE* were required (Taylor et al., 2002). This result may suggest the presence of new genetic mechanisms of Te^r.

The study of the arrangement of genes from the *ter* operon in the strains possessing more than one gene revealed two possible organizations. *B. mycoides* ALJ98a seems to have a structure similar to the *yceC* operon in *Bacillus subtilis* strain trpC2 attSPβ, with two terD family genes, a *terC* and a *telA*, only lacking the *yceG* upstream to *telA*. Contrarily, *B. altitudinis* 3W19, *B. safensis* 10W7 and *B. zahngouensis* 5W24 only share the initial structure with two/ three terD family genes and a *terC*. Considering that *telA* was also present in these three strains, the genetic arrangement present seems more related to that

of *Chitinophaga pinensis* DSM 2588 where the *terC* – *telA* region is interrupted by a biosynthetic module (Anantharaman et al., 2014). In this work, we demonstrated that an organized cluster of *ter* determinants was present in strains with resistance to Te (IV) and demonstrated Te (IV) high reducing ability, except for the slow reducer *C. marina* 5W10. The relation between Te (IV) reduction and the existence of Te^r genetic determinants is visible in the *Bacillus* genera in mining isolates. The organization, as well as the components present in the *ter* gene cluster, are worthy of study to understand better why many variations of this gene cluster exist and how it affects Te^r.

Chapter IV: Tellurite impact on metabolism and resistance in *Bacillus* and *Paenibacillus* – an omics approach

Abstract

Resistance to metals and metalloids is a field of research with a long-lasting interest. The impact of metalloids, such as Te, on bacterial structure and metabolism continues to improve with the use of new modern methodologies that complement existing characterization methods. Omics based technologies give a holistic view of a strain metal resistance potential and metal resistance response that allows a broader exploration of a stress response. Considering that new isolates can be a source of not yet known genetic and metabolic strategies that are selected on organisms colonizing new contaminated environments it is of interest to explore such environments for novel bacterial strains.

The objective of this study was to evaluate the metabolic response of a *Paenibacillus* and a *Bacillus* strain to grow in the presence of Te (IV). This was performed by evaluating oxidative stress, by ROS production, overall metabolic increase/ decrease by MTT assay, genomic potential of Te (IV) response by genome mining and differential proteomic response by LC-MS/MS to the growth in the presence of Te (IV). Growth in the presence of the metalloid ion showed that each strain decreased metabolism and increased production of ROS. Cultivation in the presence of Te (IV), lead to the overexpression in *B. altitudinis* 3W19 of the proteins from *ter* and the *ars* operons, and *ter* system has a characteristic gene organization. The overrepresentation of aminoacids metabolism and membrane transport pathways coupled with under representation of carbohydrate metabolism showed some similarity with previously described proteomics analysis to other metal ions. The quantification of cell ROS and metabolic activity by MTT supported the proteomic results. The work shows the importance of environmental dynamism on the diversity of genomes, and the existence of different genetic rearrangements resulting in diverse metabolic pathways in microorganisms living under metal stress.

Introduction

Amongst the known bacterial taxa Bacillale, particularly *Bacillus* and *Paenibacillus*, are of great interest for biotechnological purposes. These genera are found ubiquitously in the environment, are highly resistant to environmental and man-made stress and produce important substances for clinical, industrial and agricultural fields (Sansinenea, 2012). Certain strains from the *Bacillus* genera are some of the best-studied bacteria, such as *Bacillus subtilis*, a model organism, or the pathogenic *Bacillus cereus* and *Bacillus anthracis*. Several enzymes with important commercial value are obtained nowadays from *Bacillus* strains, alpha amylase for starch hydrolysis or the protease subtilisin used in detergents. Recently several studies have demonstrated interest in using *Bacillus* strains in recovering metal from solution by some form of accumulation, i.e.: for chromium, copper, lead and nickel using *Bacillus thuringiensis* strain OSM29 (Oves et al., 2013) or for chromium using *Bacillus sp.* strain MH778713 (Ramírez et al., 2019). Among the Bacillales, growing attention has been given to *Paenibacillus* spp. for its potential in biotechnological applications (Du et al., 2021; Jimoh & Lin, 2019). To this date, some studies on the interactions of *Paenibacillus* strains with metals have been produced (Knuutinen et al., 2019; Ogunyemi et al., 2020) but only a few concerning Te (Chien & Han, 2009). Strains of *Paenibacillus* have been characterized for their biochemistry and proteomic, and considered of interest in rhizostabilization of cadmium (Kumari & Thakur, 2018) for their high metal resistance, siderophore production, biocontrol activities, and xenobiotic degradation. Additionally, *Paenibacillus* is also known to produce extracellular polysaccharides with high metal ions uptake ability (Prado Acosta et al., 2005).

Resistance to Te ions in *Bacillus* was observed at the genetic level in *Bacillus subtilis* chromosomes with the identification of homologues of the *ter* operon. Four gene

products, YceC, YceD, YceE and YceF, show significant identity with the R478 proteins, from Inc2 plasmid, TerZ (37.6 %), TerD (57 %), TerE (53.6 %) and TerC (22.6 %), respectively (Taylor, 1999). These genes have been identified in other *Bacillus* strains with different arrangements and have been classified as *yceC* operon. In this genetic arrangement, additional genes have been linked to Te^r *yceH* and *yceG*, with no homologous sequences in the original R478 proteins (Franks et al., 2014). For *Paenibacillus* several elements of the *tehAB* or *ter* operons have been reported or are recoverable from deposited genomes of *Paenibacillus* strains, nevertheless, there are no experimentally confirmed involvement of any genes in Te^r.

Observing the bacterial metabolic response to the exposure to toxic elements is a way to identify potential molecules involved in their detoxification and, therefore, uncover how bacteria copes with toxic metals. This approach has been wildly used in clinical microbiology (Cash, 2009), industrial microbiology (Manso et al., 2005) and response to environmental stresses (Moreno & Rojo, 2013). The differential proteomics resulting from exposure to metals, a factor of environmental stress, has been observed for multiple organisms, namely *Pseudomonas putida san ai* in studies involving the response to cadmium (Izrael-Živković et al., 2018) and nickel (Cheng et al., 2009) and *Lactobacillus* sp. in response to cadmium (Zhai et al., 2017). To this date, the study of the effect of Te by a protein analysis has been only performed on moderately halophilic bacterium, (Kabiri et al., 2009) using two-dimensional gel electrophoresis. This technique, despite being valuable for the identification of differences in protein expression, is limited in resolution, as it results from the analyses of only a fraction of the total protein content. The proteomic approach by liquid chromatography tandem mass spectrometry (LC-MS/MS) broadens the spectrum of protein coverage resulting in a better description of the bacteria metabolic response.

The aim of this study is to determine, in the Te (IV) resistant bacteria, *Bacillus altitudinis* 3W19 and *Paenibacillus pabuli* ALJ109b, the metabolic impact of growth in the presence of Te (IV). For this purpose, we evaluated stress response and determined the metabolism associated with Te (IV) stress using differential proteomics in the two Te (IV) resistant strains grown in the presence and absence of the metalloid. The resulting expressed proteins were identified using the genome based *in silico* proteome. Furthermore, the effect of growth in the presence of Te (IV) on the protein profile, and therefore metabolism, was analyzed by differential proteomic. Furthermore, genome mining was used in combination with differential proteomic analysis to determine which genetic elements may be linked to Te^r.

Materials & Methods

Growth of *Paenibacillus* strain ALJ109b and *Bacillus* strain 3W19 in the presence of tellurite

Growth in liquid media for strains *P. pabuli* ALJ109b and *B. altitudinis* 3W19 was performed in LB and R2A media, respectively, at 25 °C, in aerated conditions and in and rotating shaker at 140 rpm. Cells were always streaked from a single colony for planktonic growth. Timely reads of optical density OD_{600} were used to determine bacterial growth and identify growth phases.

Tellurite induced stress response

Stress response was determined, for selected strains, by tracking the regulation of metabolic activity using 3-(4,5-dimethylthiazol-2-yl)-2,5-diphenyl tetrazolium bromide (MTT) assay, (Caldeira et al., 2020) and by determining the formation of ROS by using 2,7-dichlorofluorescein-diacetate (H_2DCFDA) assay (Jakubowski, 2000). For both

assays, cells were grown in R2A broth in Te (IV) at 5×10^{-4} M, 1×10^{-3} M and control without metal. For MTT assay, cell cultures were incubated for 6 h and collected by centrifugation of 1mL, 13.300 g 10 min and washed twice in growth media. Dilutions with growth media were prepared to obtain cell suspensions with OD 0.2. For formazan crystals formation 200 µL of cell suspension were mixed with 20 µL of MTT solution and incubated for 1 h at 25 ºC. Crystals were retrieved by centrifugation at 13300 g 2 min, these were then resuspended in 2.5 mL of di-methyl sulfoxide and incubated 1 h at room temperature. Absorbance of the mix solution was determined at 550 nm. For ROS determination cultures were incubated up till an OD of 0.3, 3 h for *B. altitudinis* 3W19 and 6 h for *P. pumilus* ALJ109b. Cells were washed twice with PBS, incubated in 25 µM H_2DCFDA for 30 min at 25 ºC and cells were retrieved and again washed twice with PBS. After centrifugation, supernatants were collected and fluorescence (λem = 527 nm and λex = 495 nm) was read hourly for 15 h. For both the MTT and ROS assays the values presented show the ration between the values in the test condition (with metal) and the value in the control situation (without metal). All assays were conducted in triplicates.

Genome sequencing, annotation and strain identification

Cells, from strains *P. pabuli* AlJ109b and *B. altitudinis* 3W19 were collected, in late exponential phase, and DNA was extracted using a DNeasy PowerSoil Kit (Quiagen), according to manufacturer instructions. Libraries of total genomic DNA were prepared using Nextera XT preparation kit (Illumina) following the manufacturer's instructions. Libraries were purified using beads HighPrep PCR Clean Up (MagBio Genomics. Inc). Fragment analyzer 5200 (Agilent - NGS Fragment 1-6000 pb methods) was used to check the fragment size distribution and molarity of each library. Nine pM libraries were sequenced on an Illumina MiSeq System based at the Section of Microbiology in the Department of Biology - Copenhagen University, with 2 × 300 bp chemistry (MiSeq

Reagent Kit v3). Pairing, trimming and assembly based on Bruijn graphs were performed using CLC genomics workbench v9.5.4 (Qiagen) using default parameters. Resulting contigs were submitted to GhostKOALA (KEGG Orthology And Links Annotation) annotated genomes as reference proteomes (Kanehisa et al., 2016). In GhostKOALA, Kegg identifiers (K numbers) were assigned to the sequences data by GHOSTX searches, against a non-redundant set of KEGG GENES. Additionally, genomes were submitted to de online repository RAST using the platform RAST-tk algorithm for an alternative annotation (Aziz et al., 2008; Brettin et al., 2015).

Genome phylogeny was determined by using rMLST (Jolley et al., 2012) and phylophlan, (Segata et al., 2013) analyses and similarity results were calculated by average nucleotide identity, using ANI calculator, Kostas software, (Goris et al., 2007).

To determine genes of interest were under the control of one or more promoters, the promoter prediction tools Prom Predict algorithm (Rangannan & Bansal, 2010) and the online program BPROM (Solovyev & Salamov, 2010) were used on specific contigs where genes of interest were found. Both results were jointly analysed.

Protein extraction and digestion

Total protein content was extracted from exponential phase grown cultures, at the same growth phase, of both *P. pabuli* ALJ109b and *B. altitudinis* 3W19 strains grown in Te (IV) treated or un-treated condition. Log grown cells were centrifuged at 4000 g for four min and washed twice in cold PBS. Cells were lysed, by resuspension in lysis buffer (guanidinium hydrochloride 6 M, tris(2-carboxyethyl) phosphine 10 mM, 2-chloroacetamide 40 mM, HEPES 50 mM pH 8.5), vortexed and boiled at 95 °C for 5 min. Additionally, samples were subjected to sonication with continued on/off cycles of 10 s with a Q500 sonicator (Qsonica, Newtown, USA) for 4 min, on an ice-water mixture. The sonicated samples were centrifuged at 10000 g before proceeding for digestion. Prior to

trypsin digestion, protein concentration was measured in all samples using Bradford (BioRad) according to manufactures description. Thirty µg protein material was used for digestion. The samples were four-fold diluted in digestion buffer (acetonitrile (ACN) 10%, HEPES 50 mM pH8.5) and then incubated 4 h with trypsin (1:100 trypsin-to-protein ratio) (Sigma T6567) at room temperature with horizontal shaking at 500 rpm. Inactivation of trypsin was achieved by adding tri-fluoroacetic acid (TFA) to 2 % and debris were removed by centrifugation (10000 g, 10 min). The tryptic peptides were fractionated using a Stage tip protocol as described by Rappsilber (Rappsilber et al., 2007). A total of three C18 plugs were gently punched out from the filter disk with the help of the sampling tool syringe. Plugs were placed at the tip of a 200 µL pipette tip with a plunger and activated with 30 µL methanol by centrifugation at 1000 g for 2 min., followed by 30 µL 100 % ACN, and finally 2x 30 µL of 3 % ACN with 1 % TFA. Peptides were loaded onto the filter unit by centrifugation at 1000g. Bound peptides were washed twice using 30 µL of 0.1 % formic acid (FA). Peptides were eluted using two rounds of 30 µL 60 % ACN in 0.1% FA, with centrifugation between each round. Liquid was evaporated and peptides were re-dissolved in 2 % ACN with 1 % TFA. Peptide concentration in the samples was estimated with NanoDrop, and 1.5 µg peptide was loaded for analysis on a Q-Exactive (Thermo Scientific).

Mass spectrometry

The samples were analysed by liquid chromatography tandem mass spectrometry LC-MS/MS) and data were recorded in a data-dependent manner, automatically switching between MS and MS/MS acquisition, on a Q-Exactive (Thermo Scientific). An EASY nLC-1000 liquid chromatography system (Thermo Scientific) was coupled to the mass spectrometer through an EASY spray source and peptide separation was performed on 15 cm EASY-spray columns (Thermo Scientific) with a 2 µm size C18 particles and the

inner diameter of 75 µm. The mobile phase consisted of solvents A (0.1 % FA) and B (80 % ACN in 0.1 % FA). The initial concentration of solvent B was 6%, and hereafter gradients were applied to reach the following concentrations: 14 % B in 18.5 min, 25 % B in 19 min, 38 % B in 11.5 min, 60 % B in 10 min, 95 % B in 3 min and 95 % B for 7 min. The total length of the gradient was 70 min. The full scans were acquired in the Orbitrap with a resolution of 120000 and a maximum injection time of 50 ms was applied. For the full scans, the range was adjusted to 350-1500 $m.z^{-1}$. The top ten most abundant ions from the full scan were sequentially selected for fragmentation with an isolation window of 1.6 $m.z^{-1}$ (Kelstrup et al., 2012), and excluded from re-selection for a 60 s time period. For the MS/MS scans, the resolution was adjusted to 120000 and maximum injection time of 80 ms. Ions were fragmented in a higher-energy collision dissociation cell with a normalized collision energy of 32 % and analysed in the Orbitrap.

Protein annotation and statistical analysis

The acquired raw data were analysed using MaxQuant version 1.5.5.155, using the standard settings. Oxidation (M) and Acetyl (Protein N-term) was set as variable modifications and Carbamidomethyl (C) was set as fixed modification. To enhance protein identification in the simple experimental setup, the Match-Between-Runs function was applied. The label-free quantification algorithm was applied for quantification with a LFQ min ratio count of 2 (Cox et al., 2014) a maximum of 2 missed tryptic cleavages were permitted. A minimum length of seven amino acids per peptide was required. The standard mass tolerance settings for the Orbitrap was used. A target-decoy search approach with the default MaxQuant setting of 1 % false discovery rate (FDR) was applied for identification at both peptide and protein levels using the built-in Andromeda peptide search engine (Cox et al., 2011; Cox et al., 2014) and GhostKOALA annotated genomes as reference proteome. Differential abundance analysis was performed using a

Welsh t-test, with S0 = 1, while only including proteins observed in 3 out of the 5 biological replicates in both groups. P-values were adjusted for multiple hypothesis testing by FDR correction, with $q < 0.05$ as significance cut-off. Regulated pathways were identified using Fishers exact test and Storey FDR correction (Storey, 2002) was used for correcting for multiple hypothesis testing. The comparative analyses of the metabolism were constructed with the annotated proteins, with K numbers attributed, assigned to all 3 KEGG Metabolic Pathway levels.

Ribonucleic acid purification and quantitative real time-polymerase chain reaction

Total ribonucleic acid (RNA) extractions from log grown cells ($OD_{600} \approx 0.5$) of Control (no Te (IV)) and Treated (5×10^{-4} M) were carried out using the GeneJet RNA Purification kit (Thermo Scientific) according to the manufacturer's protocol and stored at −80 °C until further use. The purity and integrity of total RNA isolated were analysed both by agarose gel electrophoresis and Nanodrop spectrophotometer (Thermo Scientific). The presence of any DNA contamination in isolated total RNA was removed by using RNase free-DNase (Invitrogen, Thermo Fisher Scientific). First-strand cDNAs were synthesized from 5 µg of DNAse treated RNA with the SuperScript™ II RT cDNA Synthesis Kit (Invitrogen, Thermo Fisher Scientific) using oligo dT primer (NZYTech), as per the recommended protocol. Transcription of Te^r *terD* paralogues was analysed by quantitative real time-polymerase chain reaction (q RT-PCR). For each treatment, three different complementary DNA (cDNA) samples were considered, and each sample included three technical triplicates. Specific primers for *terD* - Ba_CDS_3823, *terD* - Ba_CDS_3824 and *terD* - Ba_CDS_3825 and the housekeeping gene (16s rRNA), designed on the nucleotide sequences previously obtained with genome sequencing, were used, Table 4.1. Validation of primer amplification efficiency was visualised by PCR and confirmed on a 1 % agarose gel (results not shown). Quantitative RT-PCR was performed

on 10 µL-volume of SYBR Green Master mix (Biotool^{TM}) containing 50 ng of complementary DNA, using the Bio-Rad CFX96^{TM} Real-Time PCR System, with the following cycling parameters: 95 °C for 2 min (denaturation), 38 cycles at 95 °C for 20 s and 60 °C for 1 min (annealing), and the last phase at 95 °C for 15 s, 60 °C for 1 min, 95 °C for 15 s and 60 °C for 15 s (extension). No genomic contamination was detected by the dissociation curve. Relative quantification values were obtained using the Pfaffl mathematical model ($2^{-\Delta\Delta Ct}$ calculation) (Pfaffl, 2001), where values obtained for treated samples were compared with those obtained for untreated samples. The amounts of expression level were normalized with respect to the housekeeping gene, in order to compensate for variations in the amounts of cDNA.

Table 4.1. Conditions for quantitative real-time amplification of *ter* genes from *Bacillus altitudinis* 3W19. Oligonucleotides used in this study with description of annealing temperatures used in q RT-PCR and sequences.

Amplicon	Annealing temperature	Primer sequence
16S rRNA	58 /59 °C	357F: 5'-TACGGGAGGCAGCAG 534R: 5'-ATTACCGCGGCTGCTGG
terD - Ba_CDS_3823	58 °C	qyceC_F: 5'-TGGTAACTTGAAAAGCAAATGCGG qyceC_R: 5'-ATTCTTGATTGTTTGAACGGT
terD - Ba_CDS_3824	58 °C	qyceD_F: 5'-GCGGAAGTATCGTACATACAG qyceD_R 5'-TGAGCTCTTCATTTGATGCCG
terD - Ba_CDS_3825	59 °C	qyceE_F: 5'-AATCTGCAGCATCCAAGCGGC qyceE_R: 5'-TCAATTCTTCCCCGCCCTCTTC

Results

Tellurite induced stress response

The response to metal-induced stress, in *B. altitudinis* 3W19 and *P. pabuli* ALJ109b, was demonstrated by determining loss in metabolic activity, using MTT assay, and by evaluating the production of ROS. ROS formation in *B. altitudinis* 3W19 and *P. pabuli* ALJ109b, mostly at a lower concentration of 5×10^{-4} M of Te (IV), increased 2.1 and 2.3 fold respectively, when compared to the control. Continuous tracking of ROS formation revealed the ability of strains grown in the presence of either concentration of Te (IV) to equalize or even decrease their intracellular ROS levels compared to the control situation, Figure 4.1.

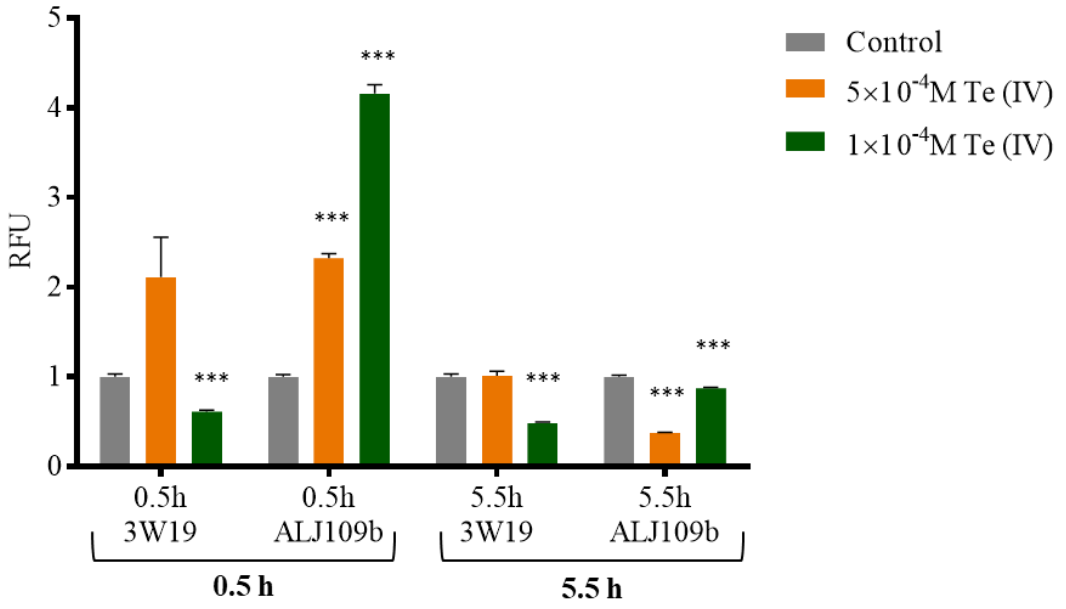

Figure 4.1. Tellurite induced oxidative stress response in *Bacillus* and *Paenibacillus*. ROS assay of strains *Bacillus altitudinis* 3W19 and *Paenibacillus pabuli* ALJ109b, showing two incubation periods with H_2DCFDA. Data shown are the mean values (± standard deviations) obtained from three independent experiments. Significantly different from the value of Control, ***$p < 0.001$, respectively. Relative Units (RFU) means the ratio between the fluorescence of the sample (test) and the fluorescence of the control experiment.

The exposure to Te (IV) resulted in a decrease in cellular metabolic activity in both organisms. In the presence of 1×10^{-3} M of Te (IV) *P. pabuli* ALJ109b dropped its metabolic activity by 31 % when compared to the control situation, Figure 4.2.

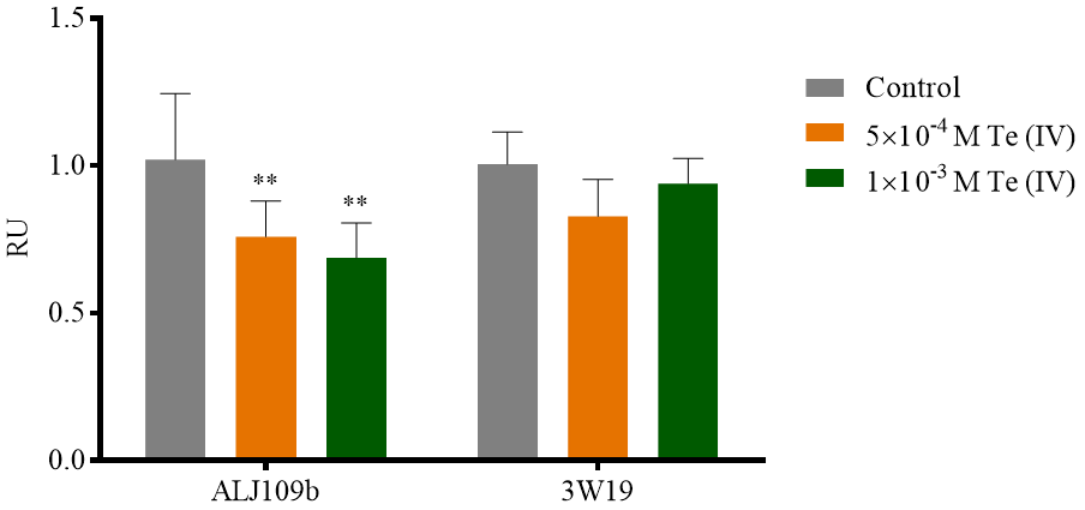

Figure 4.2. Tellurite induced metabolic response in *Bacillus* and *Paenibacillus*. MTT assay of strains *B. altitudinis* 3W19 and *P. pabuli* ALJ109b. Data shown are the mean values (± standard deviations) obtained from three independent experiments. Significantly different from the value of Control, $^{**}p < 0.01$, respectively. Relative Units (RU) means the ratio between the absorbance of the sample (test) and the absorbance of the control experiment.

Genome sequencing and genetic functional annotation

Draft genomes of *P. pabuli* ALJ109b and *B. altitudinis* 3W19 were obtained from Illumina sequencing. *B. altitudinis* 3W19 has a genome of 3.7 Mb, assembled into 54 contigs. *P. pabuli* ALJ109b has a 6.8 Mb genome, assembled into 46 contigs. *B. altitudinis* 3W19 genome annotation yielded a total of 3719 identified CDS regions, 3782 genes, 1 tmRNA, 59 tRNAs and 3 repeat regions. In *P. pabuli* ALJ109b a total of 6105 identified CDS regions, 6210 genes, 7 rRNAs, 1 tmRNA and 97 tRNAs were identified, Table 4.2.

Table 4.2. Genomes of *Paenibacillus pabuli* ALJ109b and *Bacillus altitudinis* 3W19. Summary of data generated from genome sequencing and annotation of *Bacillus altitudinis* strain 3W19 and *Paenibacillus pabuli* strain ALJ109b.

	Genome size	**Coverage**	**Contigs**	**Genes***			**RNA***	
				Total	Coding sequences	tmRNA	tRNA	rRNA
Paenibacillus pabuli ALJ109b	6.8 Mb	99.3	46	6210	6105	1	59	-
P. pabuli (reference genomes)	7.1 Mb¥							
Bacillus altitudinis 3W19	3.7 Mb	28.1	54	3782	3719	1	97	7
B. altitudinis (reference genomes)	3.8 Mb£							

*Data from annotation using RASTtk pipeline; ¥Average of 4 draft genomes of *P. pabuli* from NCBI database; £Average of 17 complete genomes of *B. altitudinis* from NCBI database

The analysis of the genome annotation from *B. altitudinis* 3W19 revealed some genetic potential to Te^r and TeRed. Regarding the potential for Te (IV) uptake an acetate transporter encoding gene (*actP)* was identified. This transporter is involved in the uptake of Te (IV) in *Rodobacter capsulatus* (Borghese & Zannoni, 2010).

Some of the genes known up to date, that are experimentally confirmed to be implicated in Te^r, can be found in this strain. Elements from the *ter* operon, *terA/B/C/D/E/Z*, and the regulatory *terW*, which some genes are described to be involved in Te^r, can be found in *B. altitudinis* 3W19. In this organism, the *ter* operon is structured with a *terB* Ba_CDS_3821, antisense, 3 *terD* paralog genes Ba_CDS_3822/3823/3824 and one *terC* gene Ba_CDS_3825 in an operon like arrangement. In this organized structure, two additional genes are found the Ba_CDS_3830 and Ba_CDS_3831. These are also identified as encoding proteins involved in Te^r and are positioned downstream of the remaining *ter* genes following four genes not related to Te^r. The Ba_CDS_3830 encoding the YceG (Blastp identity of 59 %, E=0.0), and the Ba_CDS_3831 encoding the YceH/TelA (Blastp identity of 83 %, E=0.0) are two proteins described to confer Te^r in *Bacilus antraxis* (Franks et al., 2014). The structure found, or the *ter* system, resembles that found in *Chitinophaga pinensis* (Anantharaman et al., 2014) in which the genes identified as *ter* components are interrupted by a biosynthetic module. This genetic arrangement is also visible in other *Bacillus* strains with deposited genomes in public databases. Additionally, the expression of all *ter* genes in *B. altitudinis* 3W19 seems to be regulated by individual promoters (PromPredict and BPROM analyses), suggesting that they are organized as a gene cluster rather than as an operon.

In *P. pabuli* ALJ109b the genomic analysis did not reveal many Te related determinants. One *terC* gene was found, without any other *ter* operon components nearby. Two putative *terD* genes were found Pp_CDS_1763 (Blastp identity of 26 %, E=0.4) and

Pp_CDS_2410 (Blastp identity of 41 %, E=0.48). Neither of these genes was nearby any other Te^r.

Apart from the Te (IV) dedicated resistance-conferring genetic determinants other relevant genetic elements were found in both strains. Copies of the genes *ruvB* and *recG* were found, these genes are involved in DNA repair and are activated as a result of multiple stresses, including the presence of metals (Morais et al., 2011), or metalloids such as Te (IV) (Decorosi et al., 2009).

Protein profiles

A reference proteome was constructed, for *B. altitudinis* 3W19 and *P. pabuli* ALJ109b, based on the annotated CDS genes from the genome of each strain. The proteome resulting from growth of both *B. altitudinis* 3W19 and *P. pabuli* ALJ109b, with and without Te (IV), reveals differences in the metabolic profile between species and between presence/absence of Te (IV). A total of 1151 proteins were identified in *B. altitudinis* 3W19 after LC-MS/MS analysis, with 370 being exclusively found to either condition, Figure 4.3. In *P. pabuli* ALJ109b, the LC-MS/MS analysis produced 1835 identifiable proteins with 204 being exclusively found to either condition, Figure 4.3. In *B. altitudinis* 3W19, nine proteins were present solely when grown in the presence of Te (IV) while 65 proteins had a positive significant change in abundance (SCA) in growth in the absence of Te (IV). A total of 361 proteins were not found in the presence of Te (IV) with an additional 97 with negative SCA, Figure 4.3. In *P. pabuli* ALJ109b, 164 proteins are exclusively found in the presence of tellurite and 68 others with positive SCA. In the absence of tellurite, 40 proteins are exclusively found with 75 more with negative SCA, Figure 4.3. A full list of exclusive and SCA proteins can be found in supplementary material, Supplementary Tables 2-5.

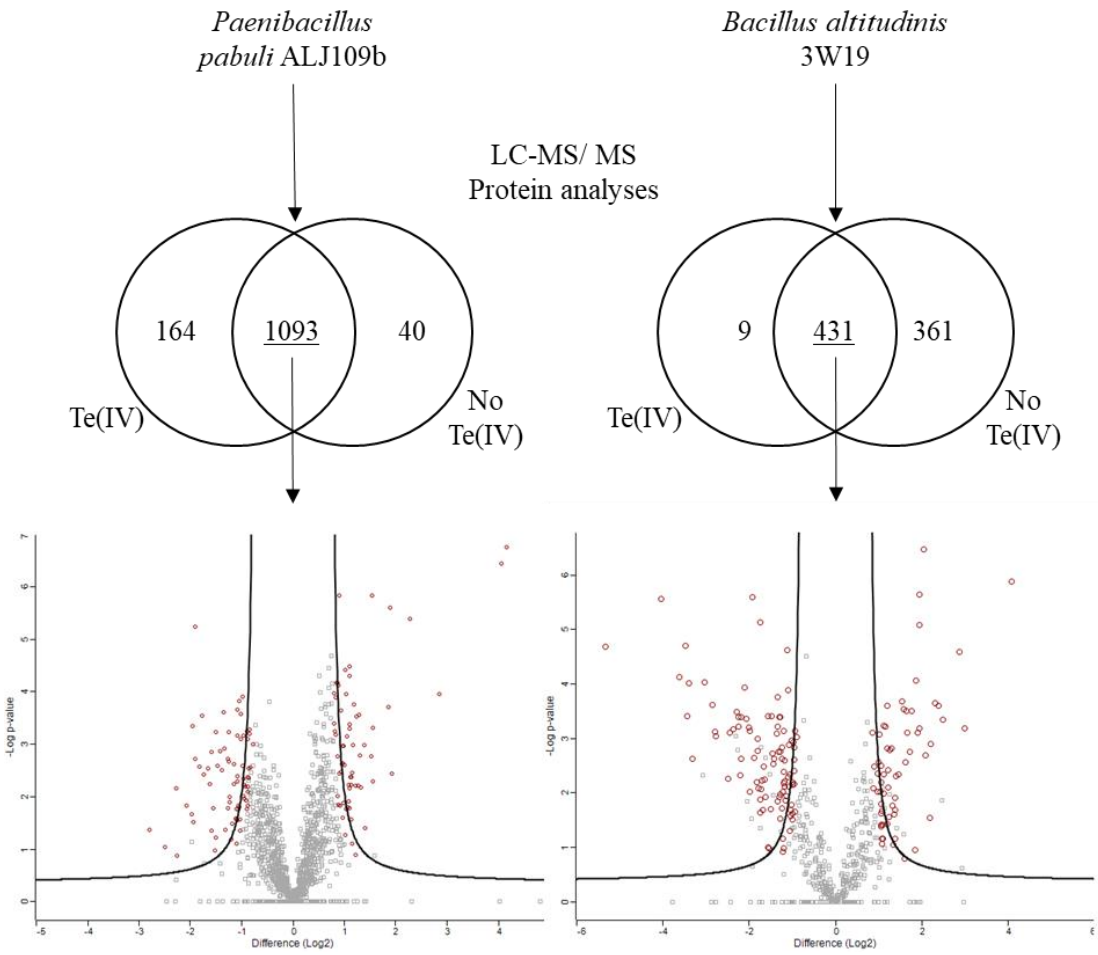

Figure 4.3. Differential proteomics in *Paenibacillus pabuli* ALJ109b and *Bacillus altitudinis* 3W19. Schematic representation of SCA proteins obtained in growth of *Paenibacillus pabuli* ALJ109b and *Bacillus altitudinis* 3W19 in two test conditions, Wild – without Te (IV) and Te – with 5×10^{-4} M of Te (IV). Each test condition was performed in triplicate. Venn diagrams representing the total proteins obtained, exclusive to each test. Each volcano plot indicates total shared proteins between tests (Welsh t.test; FDR-0.05; S0>1), those with SCA indicated by large red circles.

For each bacterial strain, a comparison of the reference proteome to the proteins obtained, in both Te (IV) treated and no treated condition was determined. *B. altitudinis* 3W19 showed 51 % (1988) of the total CDS regions of its reference proteome detected and identified (with K numbers), with 80 % of these annotated sequences (1600) being assigned to, at least, one functional pathway. For *P. pabuli* ALJ109b, 44 % (2828) of the

total CDS regions of its reference proteome were detected and identified, with 59 % of these annotated sequences (1667) assigned to, at least, one functional pathway.

Metabolic variation determined by proteomic profiling

The detected and identified proteins, with SCA and exclusive, assigned to a functional pathway, were used to determine the activation or inactivation of the metabolic pathways they were a part of. The significance of the activation/ inactivation of each pathway was calculated based on the number of proteins detected in relation to the size of the pathway (number of proteins in the pathway present in the reference proteome). Growth of *B. altitudinis* 3W19 in the presence of Te (IV) was associated with a positive SCA of proteins from metabolic pathways (level 2) of translation, cell growth and death, cell motility and metabolism of other aminoacids, Figure 4.4a.

In *B. altitudinis* 3W19 is observed an over-representation of the translation metabolic pathway defined by the negative SCA in nine ribosomal proteins, Supplementary Table 2. Proteins contributing for the over-representation of cell growth and death metabolic functions are Ba_CDS_1903 clpP; ATP-dependent Clp protease, protease subunit [EC:3.4.21.92] and Ba_CDS_3295 murG; UDP-N-acetylglucosamine--N-acetylmuramyl-(pentapeptide) pyrophosphoryl-undecaprenol N-acetylglucosamine transferase [EC:2.4.1.227], Supplementary Tables 2/ 3. The over-representation in the metabolism of cellular motility is conferred by the positive SCA in flagellar assembly protein. Finally, the over-representation of metabolism of other amino acids is conferred by the positive SCA in glutathione and selenocompound metabolism proteins, respectively Ba_CDS_280 CARP; leucyl aminopeptidase [EC:3.4.11.1] and Ba_CDS_1920 trxB; thioredoxin reductase (NADPH) [EC:1.8.1.9], Supplementary Table 2.

Only the metabolism of transcription is significantly down-represented in the presence of Te (IV), Figure 4.4b. This metabolic pathway is defined by the negative SCA in eleven protein Supplementary Table 2.

In *P. pabuli* ALJ109b we observed a significant increase in representation of the metabolic pathways (level 2) of folding, sorting and degradation and biosynthesis of secondary metabolites, Figure 4.4c. In this organism only xenobiotic biodegradation is found with decreased representation, Figure 4.4d.

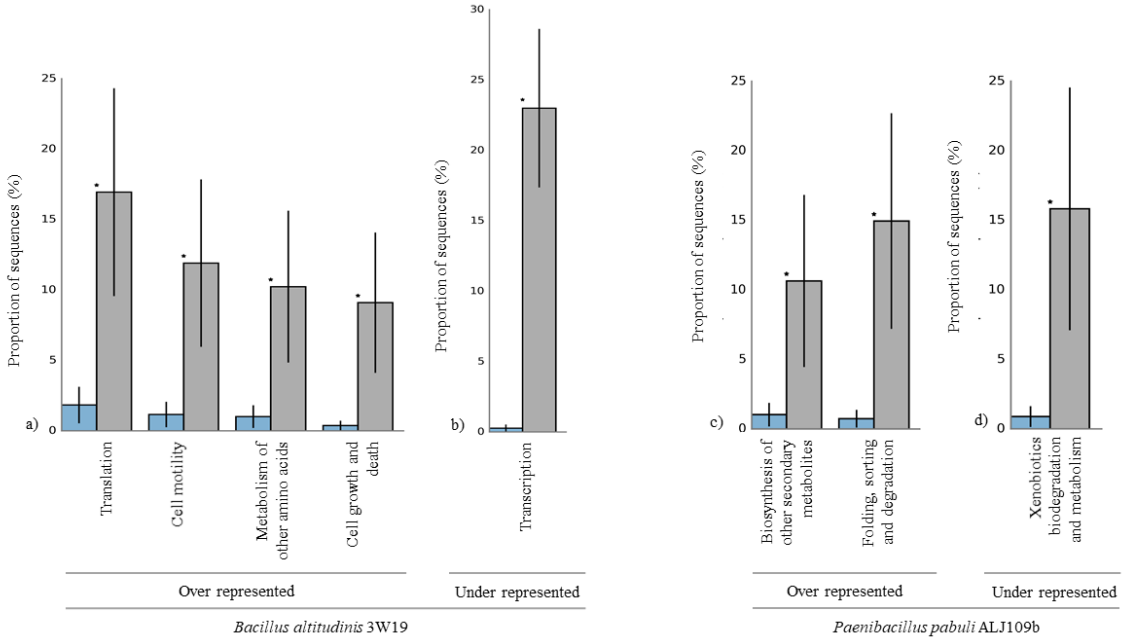

Figure 4.4. Tellurite impact on metabolic pathways representation in *Paenibacillus pabuli* ALJ109b and *Bacillus altitudinis* 3W19. Pathways **a)** over-represented and **b)** down-represented from *Bacillus altitudinis* 3W19 and **c)** over-represented and **d)** down-represented from *Paenibacillus pabuli* ALJ109b showing the metabolic change in the presence of Te (IV). SCA proteins were mapped with subsystems classifications from KEGG. Level 2 KEGG pathway were analyzed for regulation using a Fisher's exact test. FDR adjusted p-values are presented for each pathway, p-values equal or under 0.05 were considered for determining significant pathways. Blue bars display pathway size compared to the size of the reference proteome, which can be grouped in pathways. Grey bars display the ratio of SCA proteins in the pathway compared to the total amount of SCA proteins in pathways. Statistical significance calculated by Fisher exact test and with a Storey FDR correction, * $q < 0.05$.

Detailed analysis of all proteins, either over or down expressed and exclusive to control or Te (IV) conditions, that are co-located in the genome, highlights other pathways that are over or down-represented in *B. altitudinis* 3W19 and in *P. pabuli* ALJ109b. In *B. altitudinis* 3W19 only two clusters of proteins are overexpressed, first comprising two, apparently, unrelated proteins: Ba_CDS_1920 – trxB, thioredoxin reductase (NADPH) [EC:1.8.1.9] and Ba_CDS_1921 – peptidade C40 (BlastX – ID < 50%); second the Ba_CDS_3822/ 3823/ 3824 – Te (IV) resistance determinants. In this strain, several cell functions are decreased/ absent in the presence of Te (IV) such as RNA processing and translation and flagella construction, Supplementary Figure 2. In *P. pabuli* ALJ109b several clusters of amino acids biosynthesis are over-represented/ exclusive in the presence of Te (IV), such as Pp_CDS_700 /701 – lysine biosynthesis; Pp_CDS_724/ 726/ 730 – methionine salvage; Pp_CDS_2315/ 2316 – methionine synthesis and Pp_CDS_3451 - 3453 – threonine and homoserine synthesis. Two other pathways are over-represented/ exclusive, the *lia* operon and the *ars* operon. Other over-represented pathways remain with unknown functions, Supplementary Figure 3. Fewer examples are observed of decreased or absent cell functions in the presence of Te (IV), one example is Pp_CDS_5085 – 5087 – mixed acid fermentation, Supplementary Figure 3.

Protein of interest with significant variation impacted by tellurite

Apart from altering the expression of complete metabolic pathways, the presence of Te (IV) induced a SCA of proteins of interest as is the case of thioredoxin reductase (EC 1.8.1.9) involved in defense against oxidative damage and significantly over-regulated in both *B. altitudinis* 3W19 and *P. pabuli* ALJ109b. In *B. altitudinis* 3W19 the proteins with highest over regulation were Ba_CDS_2106 - *arsC2*, arsenate reductase (thioredoxin) [EC:1.20.4.4] and the Ba_CDS_3823 – *terD*, tellurium resistance protein TerD; with increases of $\log_2$ 3.002 and $\log_2$ 2.872-fold, respectively, Figure 4.7a/ Supplementary

Table 2. On the opposite spectrum, there was a significant down regulation in Ba_CDS_939 – *oppA*, oligopeptide transport system substrate-binding protein (log_2 -5.339); Ba_CDS_3377 - SRP54 signal recognition particle subunit SRP54 [EC:3.6.5.4] (log_2 -4.036); Ba_CDS_2533 – *mhqR*, MarR family transcriptional regulator, 2-MHQ and catechol-resistance regulon repressor (log_2 -3.616); Ba_CDS_1219 – *ackA*, acetate kinase [EC:2.7.2.1] (log_2 -3.442); Ba_CDS_1996 – *degU*, two-component system, NarL family, response regulator (log_2 -3.391) and in Ba_CDS_3453 – *pnp*, polyribonucleotide nucleotidyltransferase [EC:2.7.7.8] (log_2 -3.318), Figure 4.7a/ Supplementary Table 2. In *P. pabuli* ALJ109b, the proteins with highest over regulation were Pp_CDS_3307 – *pspA*, phage shock protein A and the Pp_CDS_865 – FLOT, flotillin; with increases of log_2 4.051 and log_2 2.848 times, respectively, Figure 4.7b/ Supplementary Table 4. Contrarily, there was a significant down regulation in Pp_CDS_5086 - formate C-acetyltransferase [EC:2.3.1.54] (log_2 -2.793); Pp_CDS_5085 – *pflA*, pyruvate formate lyase activating enzyme [EC:1.97.1.4] (-2.493); Pp_CDS_773 – *fldA*, flavodoxin I (log_2 -2,274) and Pp_CDS_5087 – *adhE*, acetaldehyde dehydrogenase/ alcohol dehydrogenase [EC:1.2.1.10 1.1.1.1] (-2.265), Figure 4.7b/ Supplementary Table 4.

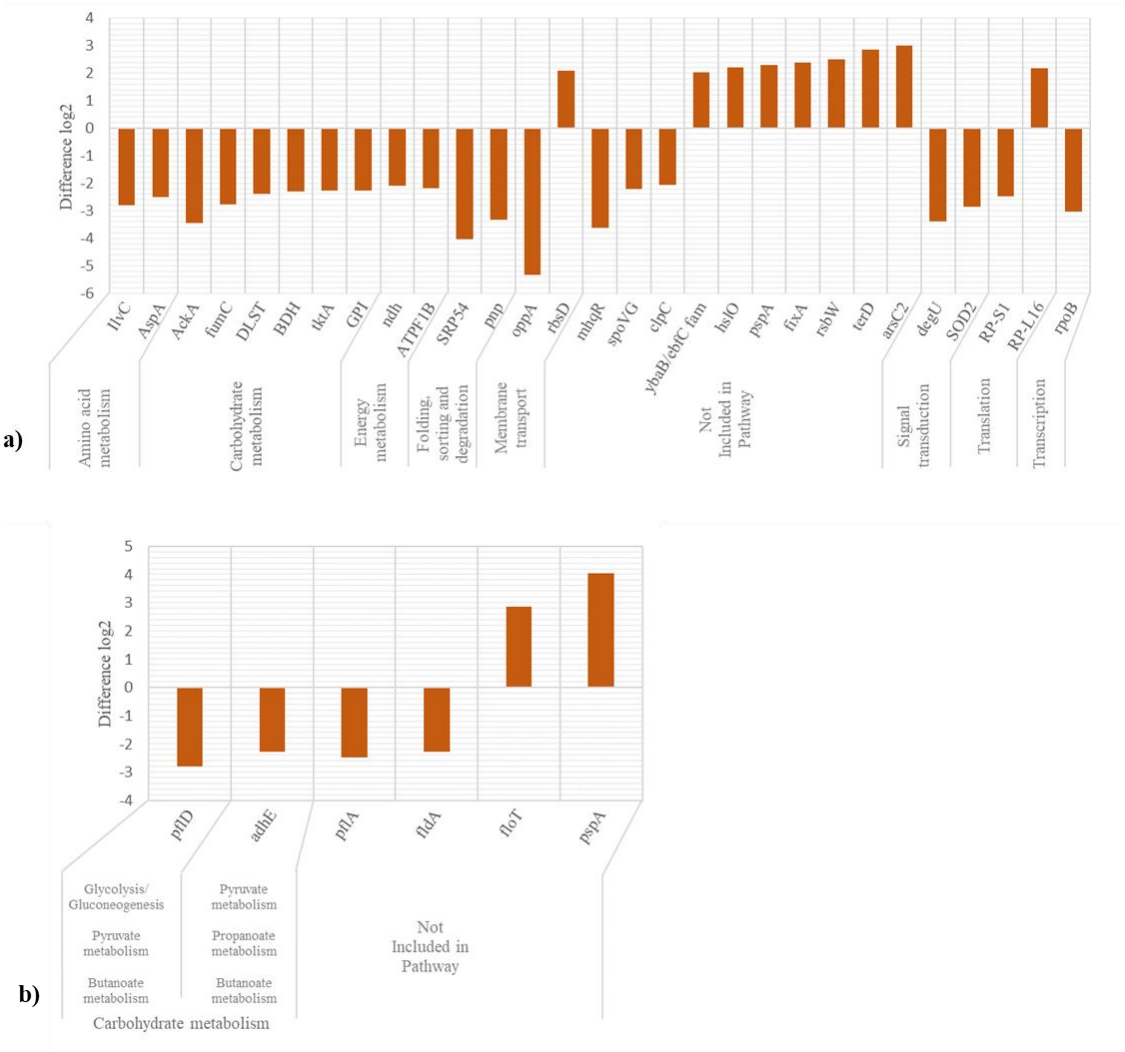

Figure 4.7. Proteins with highest significant change in abundance integrated with metabolic function. Representation of proteins with higher than $\log_2$ 2.0 (absolute value) in both strains of **a)** *Bacillus altitudinis* 3W19 and **b)** *Paenibacillus pabuli* ALJ109b. Protein were grouped according to metabolic function, KEGG functional level 2 for *B. altitudinis* and levels 2 and 3 for *P. pabuli*. Protein identification, in horizontal axis, is summarized and can be linked to full identification in Supplementary Tables 2 and 4.

The proteomes were also analyzed considering the proteins which have previously been experimentally demonstrated to be relevant for Te^r (Pal et al., 2014). Contrarily to *P. pabuli* ALJ109b, in *B. altitudinis* 3W19 proteins with Ter ability were found over expressed in the presence of Te (IV). These proteins include the Ba_CDS_2106 - arsenate

reductase ArsC, and Te^r proteins TerD, Ba_CDS_3823, Ba_CDS_3824 and the exclusive Ba_CDS_3825.

The overexpression of genes encoding the experimentally confirmed Te^r genes, in the *ter* operon, was validated by q RT-PCR. Genes encoding proteins Ba_CDS_3823 – TerD, Ba_CDS_3824 – TerD and Ba_CDS_3825 – TerD were all increased in the presence of 5×10^{-4} M of Te (IV) with ratios of 2.25, 1.95 and 1.91 for each gene respectively, Table 4.3.

In both organisms, with higher prevalence in *P. pabuli* ALJ109b, a significant number of proteins identified remain hypothetical or with unrecognized function.

Table 4.3. Induced expression of *terD* genes from *Bacillus altitudinis* 3W19. Expression levels of genes *terD*, Ba_CDS_3823/ 3824/ 3825 in the presence of 5×10^{-4} M of tellurite. Values calculated by Pfaffl method using housekeeping (16S rRNA) gene as control.

	terD Ba_CDS_3823		*terD* Ba_CDS_3824		*terD* Ba_CDS_3825	
	Average	SD	Average	SD	Average	SD
Bacillus altitudinis 3W19 5×10^{-4} Te (IV)	2.25	0.45	1.95	0.36	1.91	1.02

Discussion

The impact of Te (IV) on cell function of *Paenibacillus pabuli* ALJ109b and *Bacillus altitudinis* 3W19 is firstly observed by increased production of ROS. Both strains display the typical response of ROS production to the metalloid stress, but it is also clear that both strains employ mechanisms to decrease ROS levels over time.

To explore the metabolic changes in response to the presence of Te (IV) of both *Paenibacillus* and *Bacillus* strains, the proteomic profiles were examined, by LC-MS/MS, comparing Te (IV) exposure against a control without metalloid. The observed

differential protein profiles revealed that each strain displays a unique and complex network of biological processes. For either strain significant metabolic changes were seen in carbohydrate and amino acids metabolism, membrane transport and signal transduction. Metabolic analysis reveals that in *B. altitudinis* 3W19 there is a significant over-representation of translation metabolic pathway, with positive SCA in nine ribosomal proteins contributing to this metabolic change. Nevertheless, this result omits the five ribosomal proteins down expressed along with the down regulation of Ba_CDS_756 – RpoA and Ba_CDS_720 – RpoB, -1.5 and -3 $\log_2$ change respectively, significant proteins in the translation process. Co-location analysis also demonstrated that RNA processing and translation are represented in two clusters with most proteins absent and/ or decreased. This result is also demonstrated with the increase, solely, on the metabolism of other amino acids, with the positive SCA in glutathione and selenocompound metabolism proteins, respectively, CARP; leucyl aminopeptidase [EC:3.4.11.1] and trxB; thioredoxin reductase (NADPH) [EC:1.8.1.9].

B. altitudinis 3W19 demonstrated a clear overall metabolic shutdown when considering, the significantly down representation of transcription metabolism, defined by the negative SCA in eleven Aminoacyl-tRNA biosynthesis proteins, demonstrated a lower cellular replication and by a down representation of flagellar assembly, as a function, most likely as an energy preservation strategy. Co-location analysis also demonstrated that the number of down-represented or absent proteins and clusters in the presence of Te (IV) far exceed the over-represented and exclusive proteins and clusters in the presence of Te (IV).

Additionally, cell growth and death metabolism was also over-represented by two specific mechanisms. First, the Ba_CDS_1903, ClpP proteolytic complex subunit. Clp proteolytic complexes are responsible for adaptation to multiple stresses by degrading accumulated

and misfolded proteins (Michel et al., 2006). Secondly, the Ba_CDS_3295 MurG is a known protein involved in pathway peptidoglycan biosynthesis. In *S. oneidensis* MR-1 the gene murG was found to be induced by continuous exposure to chromium (VI) (Chourey et al., 2006). Moreover, *B. altitudinis* 3W19 additionally displays the common metabolic changes linked to the exposure to different metals already described in the literature, increased aminoacids metabolism and decreased carbohydrate metabolism, with a large percentage of negative SCA in proteins for each metabolic pathway.

In *P. pabuli* ALJ109b, the Te (IV) proteomic response was different from that of *B. altitudinis* 3W19, this is apparent in the over and down-representation of specific mechanisms instead of an overall cellular shutdown. The metabolisms significantly over-represented in *P. pabuli* ALJ109b were folding, sorting and degradation and biosynthesis of secondary metabolites. Folding, sorting and degradation metabolism has also been seen upregulated in *Lactobacillus* sp. in response to selenium nanoparticles (Gómez-Gómez et al., 2019) while biosynthesis of secondary metabolites was reporter to be increased in the presence of copper in *E. coli* strains (Nandakumar et al., 2011). These mechanisms are clearly linked to metal-induced stress. Contrarily, there is a down representation in xenobiotic degradation and metabolism. This result has never been linked to metal-induced stress and is most likely a misinterpretation since only two isolated proteins characterize the decreased regulation of this metabolic function, Pp_CDS_5087 – *adhE* and Pp_CDS_ 5365 – *cdd*, and these are also part of other pathways. In *P. pabuli* ALJ109b, Pp_CDS_5087 – *adhE* [EC:1.2.1.10] is among the proteins with the highest absolute down regulation, with a -2.265 change in fold. Co-location analysis of protein and clusters expression was also significantly different from that of *B. altitudinis* 3W19 since in *P. pabuli* ALJ109b there was a higher number of over expressed and exclusive proteins in the presence of Te (IV) as opposed to down expressed and absent proteins in

the presence of Te (IV). The clusters observed are specific to stress different responses, the *ars* and *lia* operons, and to specific amino acid biosynthesis. Metabolism of amino acids has an important role in stress response for its role in improved energy production, synthesis of new building blocks, and the generation of amino acids with metal-binding ability, such as cysteine, and anti-oxidant molecules (Izrael-Živković et al., 2018).

The very high significant change in abundance in the specific proteins, Pp_CDS_3307/ Ba_CDS_2843 - PspA, Ba_CDS_3823 -TerD, Ba_CDS_2106 - ArsC and Ba_CDS_2214 – HslO indicates that Te (IV) induces cell stress response, activating Te and non-Te specific systems. The proteins TerD and ArsC are directly linked to Te^r, (Turner et al., 1992; Turner et al., 1994). The protein PspA is often recognized, in differential proteomic profiling as a marker protein for stress response, acting by maintaining cytoplasmic membrane integrity and/or the proton-motive force (Tsai et al., 2015; Wenzel et al., 2012). In both *P. pumilus* ALJ109b and *B. altitudinis* 3W19 the PspA protein is encoded by a gene organized in an operon-like structure as a part of the *lia* operon, a genetic mechanism involved in cell envelope stress response (Suntharalingam et al., 2009). In *B. altitudinis* 3W19 the overexpression of HslO (log_2 2.21), a chaperone that protects both thermally unfolding and oxidative damaged proteins is a clear indicator of the strain response to the oxidative stress observed by ROS assay. Contrary to what was found in *B. aerophylus* 3W19, where Ba_CDS_3823/ 2824/ 2825 - TerD, proteins directly involved in Te^r, were significantly overregulated and displayed features of a regulated gene cluster, in *P. pabuli* AlJ109b there was no indication of significant overregulation by a specific protein or cluster with recognized function in Te^r. The double confirmation, by LC-MS/M/M and q RT-PCR, of Te^r determinants induction by Te (IV) reveals that for *B. altitudinis* 3W19 all three TerD paralogs are necessary for Te^r. This result indicates a

new strategy of Te^r that may be common in nature, considering the high number of deposited genomes with genetic arrangement displayed by *B. altitudinis* 3W19.

Chapter V: Fllagelin of *Paenibacillus* for the production of high value Te nanoparticles

Abstract

In recent years the genus *Paenibacillus* has been thoroughly explored for its potential in biotechnological applications. Studies on the interactions of *Paenibacillus* strains with metals have demonstrated that these microorganism are important in metal uptake or cadmium stabilization but only one study focuses on the interaction of *Paenibacillus* with Te. Recent studies on bacterial interaction with metals focus on the end products generated by the cells' response to each element, one example is the bioproduction of single or multi-metal nanoparticles. Several studies characterize the Te nanoparticles formed by strains of *Enterobacter, Shewanella, Ochrobactrum* and *Rhodobacter capsulatus*, among others. Nevertheless, this process is still to be described in *Paenibacillus*. Most of the literature focused on molecular Te (IV) reduction is focused on the enzymatic processes of molybdopterin containing protein that convert Te (IV) to Te (0) with scarce information on specific molecular processes.

The objective of this study was to determine the ability of the high metal resistant *Paenibacillus pabuli* strain ALJ109b, isolated from high metal content mining residues, to reduce Te (IV), and to evaluate the formation of metallic Te by cellular reduction and by purified flagellin. *P. pabuli* ALJ109b can efficiently remove soluble Te (IV) from solution, over 20 % in 8 h of growth, and reduce it to elemental Te, forming monodisperse nanostructures, verified by scattering electron microscopy and X-Ray diffraction. Flagellin from *P. pabuli* ALJ109b demonstrated high Te (0) forming activity in neutral to basic conditions in a range of temperatures from 20 to 37 °C. In conclusion, the first characterization of a strain of *P. pabuli* Te (IV) reducing ability reveals that the cell and its flagellin, display all the features of potential tools for Te nanoparticle production.

Introduction

The study of Te-bacteria interaction has been mainly focused on resistance to soluble Te ions, particularly the reduction of Te (IV) and Te (VI) to Te (0). This characteristic resulted in a growing interest in isolation and characterization of new organisms with potential in Te ions reduction from a large number of different environments, such as sea sediments (Csotonyi et al., 2006; Ollivier et al., 2008), mine tailings (Maltman et al., 2015) and fouled waters (Chien & Han, 2009). These environments may provide organisms with novel genes and processes to deal with toxic Te (IV), different from those identified in most bacterial strains studied so far, mainly from clinical settings. Tellurite resistance by reduction targets the Te oxyanions, and to this date, few mechanisms have been identified as TeRed. Several works describe mechanisms of Te^r by unspecific intracellular reduction of Te ions, implicating reducing agents such as nitrate reductases or elements of the respiratory chain (Alavi et al., 2014; Chasteen et al., 2009; Sabaty et al., 2001; Theisen et al., 2013). Bioreduction of Te occurs when cells interact with soluble and toxic forms of Te (IV) and Te (VI) and convert the oxyanions to an inert and insoluble form. Bioreduction to Te can lead to the formation of nanostructures (Baesman et al., 2007; Presentato et al., 2016; Wang et al., 2018; Zare et al., 2012). As verified for other metals, the formation of Te -containing intra-/extra-cellular nanostructures can be monitored by following the bioreduction process. A diversity of microorganisms has shown the capacity to form these nanostructures, such as *Enterobacter cloacae* (Contreras et al., 2018), *Shewanella* sp. (Vaigankar et al., 2018), *Ochrobactrum* sp. (Zonaro et al., 2017), and extensive work performed on *Rhodobacter capsulatus* (Borghese et al., 2014, 2017). An increasing interest in understanding the formation of these structures is the result of the growing potential range of applications for bio-produced nanoparticles covering fields such as optical imaging (Plaza et al., 2016) or novel battery technology

(Kim et al., 2015). Growing attention has been given to *Paenibacillus* spp. for its characteristics, such as their high metal resistance, siderophore production and xenobiotic degradation (Kumari & Thakur, 2018). To this date, some studies on the interactions of *Paenibacillus* strains with metals/ metalloids have been produced (Chien & Han, 2009; Knuutinen et al., 2019; Ogunyemi et al., 2020), revealing the potential use of strains from this genera in Te-bacteria studies.

In this work, we aimed to describe the ability of *Paenibacillus pabuli* strain ALJ109b to resist and to reduce Te (IV) to elemental Te. The resulting Te structures were characterized and revealed an organized structure at the nanoscale size. In *P. pabuli* ALJ109b, flagellin was identified as part of the TeRed process. The protein was cloned in a recombinant system and its ability to reduce Te (IV) was demonstrated. Moreover, the genome and proteome analysis performed to describe the *P. pabuli* ALJ109b response to Te (IV) revealed was instrumental in determining alternative pathways of TeRed in *P. pabuli* ALJ109b

The current study offers new insights on TeRed by *Paenibacillus* strain and identifies the mechanisms by which this strain, using flagellin effectively produce TeNPs. Flagellin demonstrated potential application in Te (IV) decontamination and in the fabrication of Te nanoparticles.

Materials & Methods

Characterization of *Paenibacillus pabuli* ALJ109b tellurium aggregates

To characterize the TeNPs produced by *P. pabuli* ALJ109b, growth and TeRed of Te (IV) by the strain was performed as described in Chapter II, with the determination of Re and Rr over time. Demonstration of Te precipitation was performed by SEM-EDS, as described in Chapter II, and by X-ray diffraction (XRD) in a Bruker APEX II

diffractometer, on preparations of cells recovered from a late exponential phase in the presence of 5×10^{-4} M of sodium tellurite. For XRD cell pellets from cultures were collected by centrifugation at 4000 g, washed twice in PBS and resuspended in (0.1 mL) the same buffer. Droplets of cell concentrate ≈30 μL were dried and ground to a fine powder prior to analysis.

For evaluation of the optical properties of bacterial produced NPs, the strain was grown in the presence of 5×10^{-4} M of Te (IV) (test) and without Te (IV) (control), till an OD of 0.5, centrifuged 4000 g and the cell mass washed 3 times in ultrapure water. Decimal serial dilutions of the cell suspension were prepared to 10^{-4}. The suspensions were dried on a glass plate and preserved in a dry environment. Evaluation of the absorbance spectrum, 300 – 1100 nm, was performed in a spectrophotometer Jasco model V530, Japan. Absorbance reads were obtained in 2 nm intervals with a shift in emission source from visible to UV light at 340 nm.

Comparative methodologies for differential proteomic

To determine the impact of Te (IV) in total protein expression *P. pabuli* ALJ109b was grown in LB broth containing Te (IV), 5×10^{-4} M, 1×10^{-3} M and without metal (control). Upon reaching late exponential growth phase cells were collected by centrifugation and washed twice in PBS.

For the comparison of differential proteomics using denaturing polyacrylamide gel electrophoresis (SDS-PAGE) the cell pellet was resuspend in 0.9 mL Protein extraction Saccharose-Tris Buffer (STB) solution (0.075 $g.L^{-1}$ Tris, 0.345 $mL.L^{-1}$ HCl (1,72 N), 0.5 $mL.L^{-1}$ β-mercaptoethanol and 0.5 $g.L^{-1}$ saccharose) and mixed after adding 0.1 mL of SDS 20 %. Cell suspension was sonicated with continued on/off cycles of 10 s for 4 min, on an ice water mixture, heated at 95 °C for 10 min and cooled on ice. Lastly, the suspension was centrifuge, 14000 rpm for 10 min, and the supernatant harvested. Total

protein obtained was quantified by using Bradford reagent (Biorad®) and 12 µg of total protein were aliquoted by mixing with 7 µL of loading buffer (Morris formulation) and boiled 10 min before loading on a denaturing gel. Protein separation was obtained in a 12 % acrylamide/ bisacrylamide denaturing gel (SDS 0.1%). Electrophoresis was performed at room temperature for 1h at 120 V. The molecular marker, Low Molecular Weight Protein Marker (NZYTech), was used for size reference (kDa). Visualization of proteins was performed by staining with coomassie blue followed by de-staining with a methanol/ acetic acid solution. From the visual analysis and densitogram comparison (QuantityOne, Biorad) selected fragments were excised and stored in ultrapure water for MS/MS identification.

Construction and purification of a recombinant *P. pabuli* ALJ109b flagellin

With the information provided by the genome of *P. pabuli* ALJ109b a set of cloning oligonucleotides were designed, containing recognition sites for endocnucleases EcoRI (sense) and SalI (antisense), for the insertion of *flaA* gene in plasmid pET 30A, EcoRI_flaA (sense) 5' CCG GAA TTC ATG ATT ATC AAT CAC AAC TTA CCA, and SalI_flaA_R (antisense) 5' ACG GCG TCG ACT TAA CGA AGC AAG GAC AA. Amplification of the target sequence was performed using above mentioned oligonucleotides in a PCR reaction, for a final volume of 50 µL, using 2 U Platinum™ Taq DNA Polymerase (Invitrogen), 0.2 mM of each dNTP, PCR Buffer (1X), 1.5 mM $MgCl_2$, 0.4 µM primers, and 2 ng DNA template. The PCR program involved initial denaturation at 94 °C (5 min), followed by 30 cycles of 94 °C (1 min), 61 °C (1 min) and 72 °C (45 s). The PCR-amplified DNA fragments with approximately 700 bp, as well as the plasmid pET 30A, were digested with the restriction enzymes EcoRI and SalI. The digested amplified fragments were purified and ligated into pET 30A expression vector for 1 h at room temperature using 0.5 U of T4 DNA ligase (Thermo Scientific). The

resulting plasmid pET 30A::flaA, was transformed into competent *E. coli* BL21 cells. The correct construction was confirmed by sequencing the complete DNA fragments cloned into the plasmid (Stabvida). *E. coli* BL21 bacterial cells, containing the plasmid pET 30A::flaA were grown in LB broth containing Kanamycin (50 µg.mL^{-1}), at 37 °C 140 rpm. Inducing agent Isopropyl-β-D-thiogalactoside (IPTG) (Sigma Aldrich) was added (5×10^{-2} M) at an OD of 0.5 (Abs 600 nm) and cells resumed growth for 5 h. Cells were harvested by centrifugation at 4000 g for 15 min, resuspended in STB solution and lysed by mechanical sheering in an Emulsiflex® - C3 High-Pressure Homogenizer (Avestin), 2 cycles at 1500-2000 psi. The lysis product was centrifuged 10000 g, 20 min, the supernatant harvested and stored, and the resulting pellet subjected to a Guanidine-HCl (6 M) treatment for 1 h at 30 °C. Finally, a soluble fraction was obtained by centrifugation at 10000 g, 20 min, aliquoted and stored at 4 °C in the presence of a proteinase inhibitor Complete, EDTA-Free (Roche). Confirmation of the recombinant protein FlaA was performed in denaturing gel electrophoresis as described above using as a size (kDa) reference the NZYColour Protein Marker II (NZYTech).

Demonstration of *in vitro* tellurite reduction ability by flagellin

Demonstration of Te (IV) reducing ability by FlaA was determined by incubating the purified enzyme with increasing concentrations of soluble Te (IV) and tracking the formation of elemental Te spectrophotometrically, by measuring the absorbance at 500 nm. The protocol was adapted from Figueroa and colleagues, 2018 (Figueroa et al., 2018) where all tests were performed in a final volume of 200 µL with 1 µg of purified FlaA, in a buffer mixture containing Tris-HCl pH8 50 mM, $K_2H_2PO_4$/$KHPO_4$ (1:1) 50 mM, β-mercaptoethanol 1 mM. Determination of optimal Te (IV) reducing activity by FlaA was tested with variations in initial Te (IV) concentration from 5×10^{-5} M to 2×10^{-4} M (5×10^{-5} M increments), variation in pH 5, 7 and 9 and temperature 4, 20, 25, 30 and 37 °C.

Results are expressed in units of Te (0) formation activity (U) with U=1 equivalent to an increase of 0.001 in absorbance (500 nm) per minute per volume of reaction. Specific activity was calculated as U per mg of protein. All tests were conducted in triplicate.

Results

Tellurite reduction by *Paenibacillus pabuli* ALJ109b and resulting tellurium nanoparticles characteristics

At a concentration of 5×10^{-4} M Te (IV) *P. pabuli* ALJ109b showed Te (IV) depletion efficiencies in the order of 1.25 $\Delta mg.DO^{-1}$ and a reduction rate at 8 h of 0.06 $\Delta mg.DO^{-1}.h^{-1}$, Table 5.1. This reduction rate allowed for the removal of 20.66 % of initial Te (IV) within 8 h, reaching 33.17 % in later stationary phase (20 h). Both Re and Rr decrease over time with the highest values recorded at initial 2 h, Table 5.1.

Table 5.1. Variation of reduction efficenty and rate of tellurite by *Paenibacillus pabuli* ALJ109b. Tellurite **r**eduction efficiencies and reduction rates determined along the growth of *Paenibacillus pabuli* ALJ109b in the presence of 5×10^{-4} M of Te (IV).

Time (h)	**2**	**4**	**6**	**8**	**20**
Re ($\Delta mg.DO^{-1}$)	28.89	21.71	16.53	4.14	3.19
SD (±)	0.17	0.28	0.18	0.12	0.07
Rr ($\Delta mg.DO^{-1}.h^{-1}$)	14.45	5.43	2.75	0.52	0.16
SD (±)	0.08	0.07	0.03	0.02	0.00

Visual demonstration of Te (IV) reduction was observed in SEM imaging of *P. pabuli* ALJ109b with 5×10^{-4} M Te (IV), confirming the presence of Te by EDS analysis. Te-containing nanoparticles are visualised in electron-dense aggregates of structures with clear spheroid organization, Figure 5.1. The observed spheroid structures are sized at the nanometer scale, <100 nm, therefore can be classified as nanoparticles.

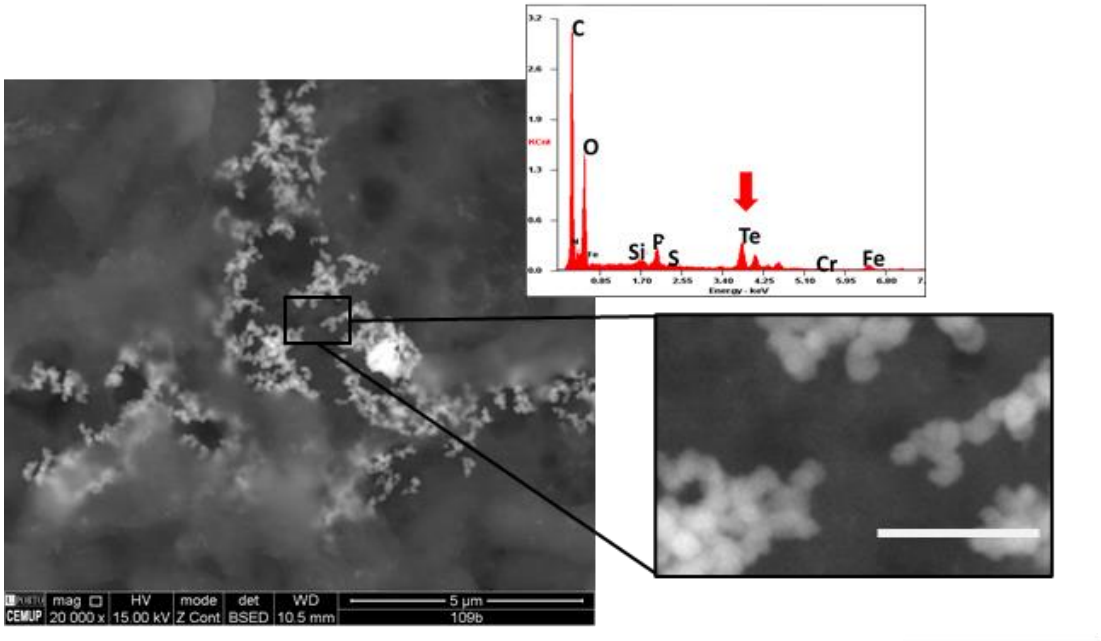

Figure 5.1. Production of Te containing nanoparticles by *Paenibacillus pabuli* ALJ109b. SEM micrographs of Te nanostructures produced with *P. pabuli* ALJ109b cells grown in presence of 5×10^{-4} M Te (IV). A magnification is present for clarification of nanostructure shape and size, white bar – 500 nm. High-density metal deposits are represented in white. EDS spectrum was obtained from reads in an electrodense area. The red arrow highlights Te detection in the spectrum.

The production of Te in metallic form, Te (0), was confirmed by XRD diffraction peaks at $2\theta = 27.5°$, 38.2°, 40.4°, 49.6°, 56.9°, and 62.8°, which are attributable to the (011), (102), (110), (201), (022), and (113) planes of hexagonal Te (PDF#79-0736), Figure 5.2.

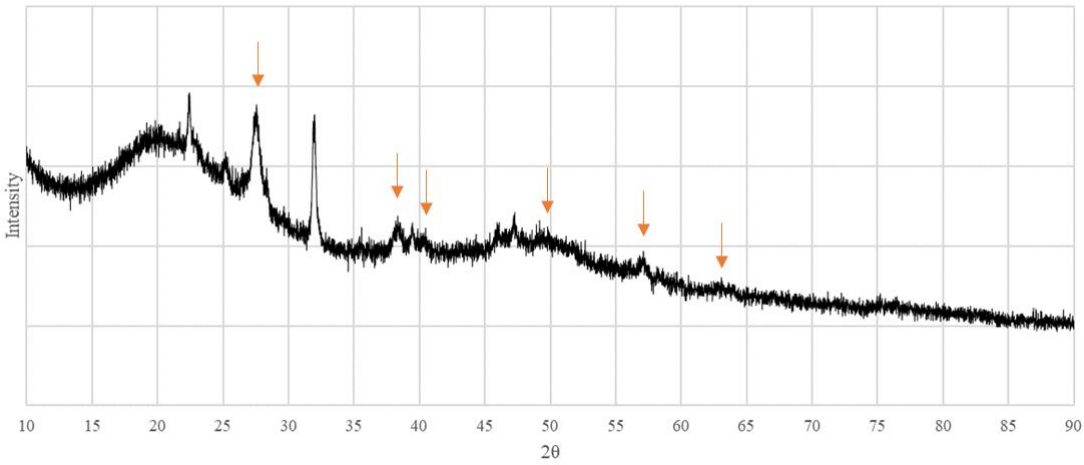

Figure 5.2. Structure of tellurium nanoparticles of *Paenibacillus pabuli* ALJ109b. Diffractogram of Te containing cells. Orange inlets indicating hexagonal Te characteristic diffraction peaks.

The absorbance spectra obtained demonstrated a constant positive variation in absorbance in the sample containing Te from 310 to 1100 nm. The visible spectra neither reveals a pattern variation attributed to the presence of Te (0), appearance/ disappearance of a peak, nor a shift to UV or infra-red (IR) of any peak present in the control without metal, Figure 5.3.

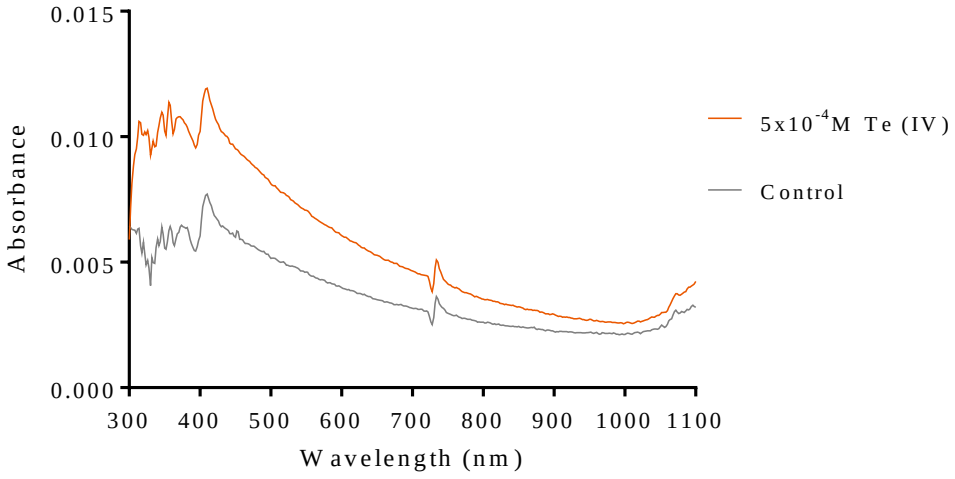

Figure 5.3. Optical properties of tellurium nanoparticles of *Paenibacillus pabuli* ALJ109b. Absorbance spectra of *P. pabuli* ALJ109b (Control) and *P. pabuli* ALJ109b cells grown in presence of 5×10^{-4} M Te (IV) (Te (IV)), dilution 10^{-2}.

Proteins of interest in Te (IV) reduction

A detailed analysis of *P. pabuli* ALJ109b genome allowed the identification of proteins with either demonstrated or putative Te (IV) reducing activity, described in Chapter IV. The analysis also allowed the identification of proteins with demonstrated Te (IV) reducing activity i.e.: Nitrate reductase EC 1.7.99.4 (Sabaty et al., 2001), Thioredoxin reductase EC 1.8.1.9, Alkyl hydroperoxide reductase EC 1.11.1.26 (Arenas-Salinas et al., 2016), Dihydrolipoamide dehydrogenase EC 1.8.1.4 (Arenas et al., 2014), Isocitrate dehydrogenase EC 1.1.1.42 (Reinoso et al., 2013) and FAD-dependent oxireductase EC 1.4.3.3 (Pugin et al., 2014). Some proteins with putative Te (IV) reducing activity were also identified i.e.: Catalase EC 1.11.1.6 (Calderón et al., 2006), 6-phosphogluconate dehydrogenase EC 1.1.1.44 (Sandoval et al., 2015) or Type II - NADH dehydrogenase EC 1.6.99.3 (Díaz-Vásquez et al., 2015). All proteins with a molybdopterin containing motif found in *P. pabuli* ALJ109b genome were included in the group of proteins with hypothetical Te (IV) reducing activity: Oxidoreductase molybdopterin-binding (superfamily) (Pp_CDS_1271); Uncharacterized molybdopterin-containing oxidoreductase YuiH (Pp_CDS_1962) and CTP:molybdopterin cytidylyltransferase EC 2.7.7.76 (Pp_CDS_4487). All the proteins identified were recovered in the high throughput proteomic analysis except for Mercury reductase (EC 1.16.1.1); Flavorubredoxin reductase (EC 1.7.2.5) and the Putative pyridine nucleotide-disulfide oxidoreductase YkgC. None of the proteins enumerated displayed a SCA in the presence of Te (IV), Table 5.2. In the case of Flavorubredoxin this is due to the protein only being required in anaerobioses.

Table 5.2. Screening for proteins with potential tellurite rection ability in *Paenibacillus pabuli* ALJ109b. Identification of know proteins with Te (IV) reducing ability and proteins with putative Te (IV) reducing ability in *Paenibacillus pabuli* ALJ109b reference proteome with abundance change (SCA) when strain ALJ109b grows in the presence of 5×10^{-4} M of Te (IV).

Protein	Reference Proteome ID	log2 difference
Nitrate reductase EC 1.7.99.4	Pp_CDS_1648	No SCA
Thioredoxin reductase EC 1.8.1.9	Pp_CDS_151	No SCA
Alkyl hydroperoxide reductase EC 1.11.1.26	Pp_CDS_2353	No SCA
Flavorubredoxin reductase EC 1.7.2.5	Not found	-
Mercuric reductase EC 1.16.1.1	Not found	-
Putative pyridine nucleotide-disulfide oxidoreductase YkgC	Not found	-
Dihydrolipoamide dehydrogenase EC 1.8.1.4	Pp_CDS_558	No SCA
	Pp_CDS_2587	
	Pp_CDS_4841	
FAD-dependent oxireductase EC 1.4.3.3 similar to Glutatione reductase	Pp_CDS_234	No SCA
Tipe II - NADH dehydrogenase EC 1.6.99.3	Pp_CDS_1274	No SCA
	Pp_CDS_1275	
	Pp_CDS_3377	
	Pp_CDS_3392	
	Pp_CDS_4316	
	Pp_CDS_5529	
Catalase EC 1.11.1.6	Pp_CDS_117	No SCA
	Pp_CDS_197	
	Pp_CDS_1308	
	Pp_CDS_2224	
	Pp_CDS_5110	
	Pp_CDS_5236	
6-phosphogluconate dehydrogenase EC 1.1.1.44	Pp_CDS_2448	No SCA
	Pp_CDS_3328	
	Pp_CDS_5214	
Isocitrate dehydrogenase EC 1.1.1.42	Pp_CDS_1977	
Oxidoreductase molybdopterin-binding (superfamily)	Pp_CDS_1271	No SCA
Uncharacterized molybdopterin-containing oxidoreductase YuiH	Pp_CDS_1962	
CTP:molybdopterin cytidylyltransferase EC 2.7.7.76	Pp_CDS_4487	

In contrast, the protein profile analysis, obtained by SDS-PAGE, revealed two proteins with clear overexpression in the presence of 5×10^{-4} M Te (IV), enolase and flagellin, Figure 5.4, Table 5.3. Analysing the LC-MS/MS results no enolase or phosphopyruvate hydratase homologue is also found exclusively or overexpressed in the presence of 5×10^{-4} M Te (IV). This result is therefore not clear.

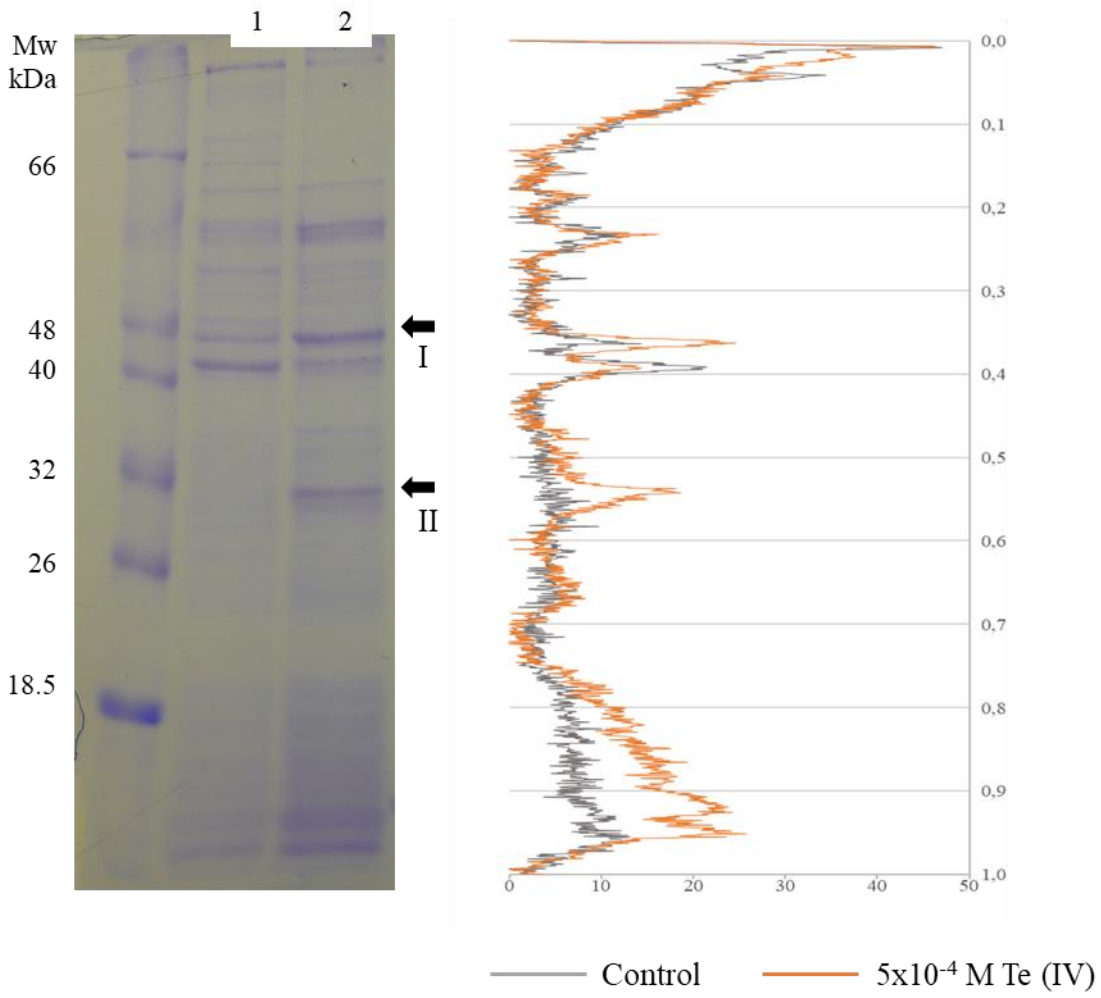

Figure 5.4. Differential expression of total proteins from *Paenibacillus pabuli* ALJ109b. (Right) Denaturing gel comparing total protein from 1) Control (without metal), 2) 5×10^{-4}M Te (IV). Fragments indicated in lane 2 (arrows), were excised purified and identified by MS/MS, resulting in identification in Table 5.3. (Left) Lane comparison of band intensities, densitogram, from control and metal treatment.

Table 5.3. Tellurite induced protein overexpression in *Paenibacillus pabuli* ALJ109b. Identification by MS of fragments purified from denaturing 2D gel electrophoresis, Figure 5.3.

ID	Description	Coverage (%)	Peptides	AAs	MW (kDa)
I	Enolase OS=Bacillus sp. FJAT-27264 OX=1850362 GN=eno PE=3 SV=1	44	17	428	45.7
II	Flagellin OS=Bacillus filamentosus OX=1402861 GN=B1B01_04555 PE=3 SV=1	5	2	286	31

Characterization of tellurite reducing ability of flagellin

The cloning of *P. pabuli* AL109b flagellin gene (*flaA*) in *E. coli* BL21 produced a 37 kDa protein that was used for Te (IV) reducing assays, Figure 5.5. As described by most literature, heterologous flagellin often produced inclusion bodies during protein extraction protocols. This was resolved with incubation in Guanidine HCl that resolubilized the protein, Figure 5.5.

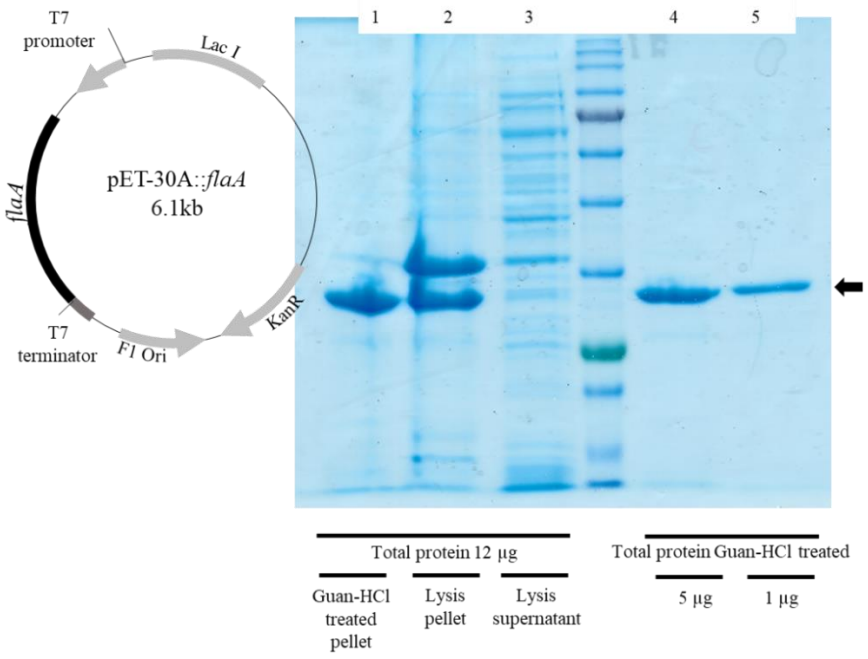

Figure 5.5. FlaA expression and purification in *Escherichia coli* BL21. Graphical representation (Right) of recombinant plasmid pET-30A::*flaA*. Denaturing electrophoresis (Left) with the demonstration of *flaA* expression (black arrow). Lane 1 – Post Lysis Guanidine–HCl treated fraction; lane 2 - the post lysis insoluble fraction; lane 3 - post lysis soluble fraction; all samples loaded are normalized with 12 µg of total protein. In lanes 4 and 5 are, respectively, 5 µg and 2 µg of total protein, post-Guanidine-HCl treatment.

Te (IV) reducing assays demonstrated that flagellin is effective in reducing Te (IV) to its elemental form Te (0), Figure 5.6a. Levels of Te (0) formation were variable depending on pH, temperature, and Te (IV) concentration. Higher pH increased Te (0) formation with peak activity of 24,450 $U.mg^{-1}$ at pH 9, in 1×10^{-3} M Te (IV), Figure 5.6b. An increase in temperature was mostly followed by an increase in Te (0) formation with peak reducing activity increasing from 567 to 23,100 $U.mg^{-1}$ from 20 to 37 °C, in 1×10^{-3} M Te (IV), Figure 5.6c. Results obtained, in higher pH and temperature conditions were more reproducible. The rate of Te (0) formation, in all test conditions, increased with the increase in initial Te (IV) concentration from 5×10^{-4} M to 1×10^{-3} M of Te (IV), Figure 5.5b/c.

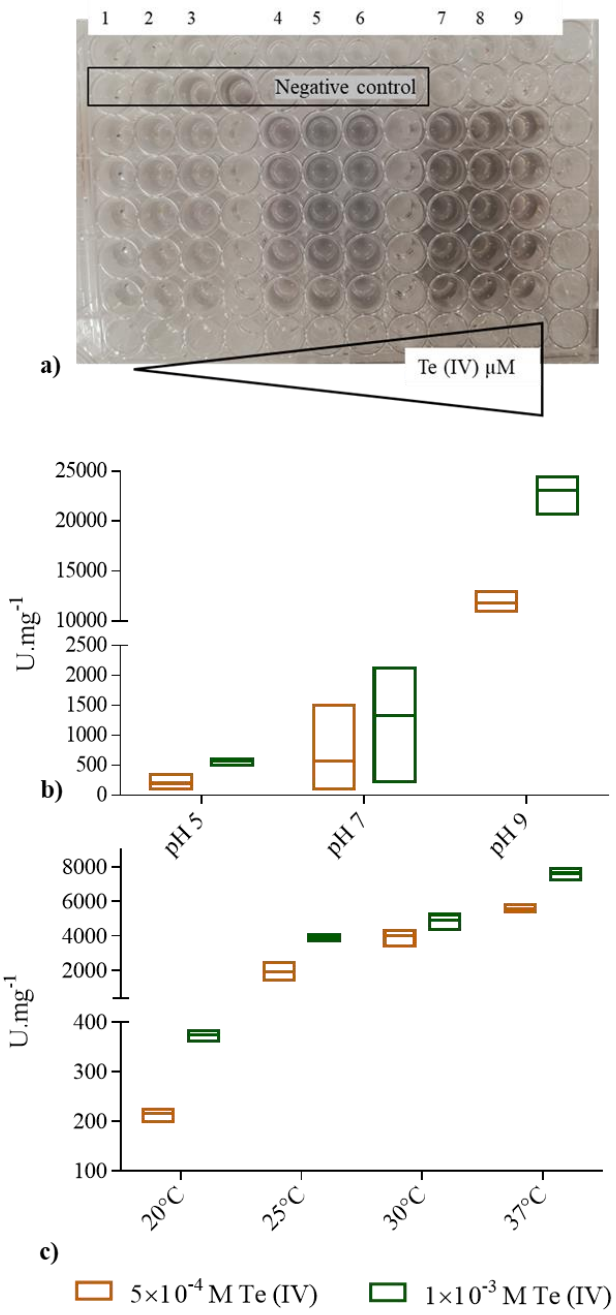

Figure 5.6. Te (0) formation by FlaA. Optimal pH **a)** and temperature **b)** of Te (0) forming activity for 1µg FlaA with two Te (IV) concentrations, 5×10^{-4} M Te (IV) and 1×10^{-3} M Te (IV). Boxes indicate mean and higher/ lower values from three independent replicates. Te (0) formation **c)** visible by the appearance of black precipitates in each reaction mixture (individual wells). Test conditions represented: Control – columns 1, 2, 3; 5×10^{-4} M Te (IV) – columns 4, 5, 6 and 1×10^{-3} M Te (IV) – columns 7, 8, 9.

Analysis of the *P. pabuli* ALJ109b FlaA sequence showed a 256 amino acid protein, it is included in the group of flagellins with the shortest length therefore one with a short, exposed domain D2/D3 (≈136 – 169). Comparison with closely related FlaA sequences from *P. pabulis* strains revealed that N and C terminal D0 domains remain conserved with higher sequence variations observed in N terminal D1a/b domains and D2 D3 domains. Overall FlaA (Pp_CDS_1131) contains a more positive net charge and contains a higher number of long R groups.

Discussion

P. pabuli ALJ109b reduced 20.7 % of Te (IV) in 8 h from a solution at a concentration of 5×10^{-4} M. By reporting Te (IV) reduction efficiency and reduction rates this way, limits comparison but allows for determination of the efficiency of processes that rely on biomass limitations and have specific timeframes. Nevertheless, the rate of Te (IV) reduction is, to our understanding, high. Still, the analysis of the strain genome showed that the reduction ability was not related to known specific Te (IV) reduction mechanisms. The residue formed by the Te reduced was composed of spheroid structures of less than 100 nm, classifying them as nanoparticles. All the structures observed present the same shape indicating a monodisperse synthesis unlike what is seen for *Bacillus selenireducens* that form nanorods, shards, and rosettes (Baesman et al., 2007) or the membrane fractions of *Lysinibacillus sp.* ZYM-1 that form various shapes of Te plates (Zhang et al., 2010). Instead, the monodisperse synthesis of Te nanostructures by *P. pabuli* ALJ109b resembles that of *Rhodococcus aetherivorans* BCP1 (Presentato et al., 2018) or *Bacillus sp.* BZ (Zare et al., 2012). A monodisperse bioproduction of spheroid shaped nanoparticles represents a promising new process in nanoparticle production. The presence of Te in a crystalline form was confirmed by the X-ray diffractogram. The presence of Te (0) in the cells was validated by the increased absorbance in the 310-1100

nm range, corresponding to the increment of light absorbance given by Te, but does not reveal any distinct absorbance peak attributed to Te (0), in the range tested confirming what was observed by previous authors (Forootanfar et al., 2015; Zare et al., 2012). The genomic and proteomic analysis of the genome revealed the existence of several proteins with demonstrated or putative Te (IV) reducing activity, Table 5.2, but none were significantly increased in the presence of Te (IV). At this point, these results suggested that an undescribed mechanism must be responsible for Te (IV) reduction in *P. pabuli* ALJ109b. The 2D denaturing electrophoresis was used also to obtain a differential protein expression and the results differed from LC-MS/MS analysis. Enolase and flagellin, detected by SDS-PAGE, were not detected overexpressed in LC-MS/MS results. Detection of flagellin by LC-MS/MS may be limited for being bonded to Te. As is the case for metallothionines, a flagellin-Te molecule may be resistant to the proteolytic activity of trypsin (Wang et al., 2007). Metal-binding to exposed aminoacids residues impedes the binding of trypsin to lysine and/ or arginine residues and its proteolytic activity. Enolase, like the above-mentioned proteins, has not an expected enzymatic activity commonly associated with a Te (IV) reducer. Alternatively, the overexpression observed for flagellin may be a direct response to the presence of Te (IV). Other studies already demonstrated the ability of flagellin monomers of binding several metals such as silver, gold, copper, cobalt, lead and cadmium (Chen et al., 2019; Gopinathan et al., 2013; Kumara et al., 2007) to surface-exposed amino acids residues. Flagellin has been associated with TeNPs production in *Rhodobacter capsulatus* (Borghese et al., 2020) without being determined its function, if any, in the TeNP assembly. The heterologous produced flagellin was used to evaluate the Te (IV) binding to flagellin and reduction to its elemental form Te (0). *P. pabuli* ALJ109 flagellin showed higher reducing activity at 4 ºC and in a temperature of 37ºC. When comparing to previous results, FlaA

demonstrates a Te (0) formation activity, at similar pH and temperature, higher than the flavoproteins from *E. coli* NorW and YkgC, ~660 and 870 $U.mg^{-1}$ protein, respectively, and lower than *E. coli* flavoprotein GorA, ~30,000 U/mg protein (Arenas-Salinas et al., 2016). When comparing Te (0) formation activity with crude cell extracts from multiple strains (Figueroa et al., 2018), FlaA outperforms all extracts in an average of 10-fold higher activity. To this date, Te (IV) reduction have been reported for several proteins, Table 5.2, but for most proteins, their involvement in further nanoparticle formation has not been described. Further characterization of flagellin from *P. pabuli* ALJ109b could add to knowledge in biobased strategies to Te (IV) reduction and/or TeNP formation.

Chapter V: Concluding remarks

General conclusions

This work focused on the relation of environmental isolates with the element Te and with the toxic anion Te (IV) and in the application of that knowledge in the biotechnological production of NPs. For the first time, it was demonstrated that Te mobilization is a process that can be potentiated by bacteria. Mesophilic and neutrophilic strains, enriched from a mining sediment, were good Te leachers and in a *consortium*, they were able to ehnhance leaching. Moreover, it was determined that resistance to Te (IV) is a common trait in environmental bacteria isolated form mining environments. A selection of Te (IV) resistant bacteria could reduce Te (IV) at different rates and generate different Te (0) structures. These same strains possess the genetic traits associated with Te^r. Genomic analysis of two highly Te (IV) resistant strains showed that different organisms demonstrate different potential for Te (IV) resistance, as demonstrated by the unique genetic information provided by their genome. This results in varied phenotypic and molecular responses to Te (IV). Finally, a flagellin purified from a highly Te (IV) resistant and Te (IV) reducing *Paenibacillus* strain demonstrateed high TeR ability.

Each chapter presents a more detailed set of conclusions:

From this study the results presented in **Chapter II** demonstrate that the bioleaching of Te is achievable using bacteria isolated from mining sediments. *Paenibacillus pabuli*, ALJ109b, *Paenibacillus taichungensis* ALJ98b and *Bacillus mycoides* ALJ98a are all able to leach Te from a mining discarded mining residue. Moreover, Te mobilization is also achievable using the authochothonous microbial community from a mine tailing sediment. The efficiency of Te mobilization is dependent on the community used with the highest Te mobilization observed by microbial communities from sediment ALJ98. This process can be enhanced with the use of bioaugmentation, using a consortium of the three strains mentioned, ALJ98a, ALJ98b and ALJ109b.

The results from **Chapter III** demonstrate that Te^r and TeRed are widespread characteristics that can be observed in several organisms. The genera that included strains with the highest Te^r were *Mesorhizobium*, *Cellulomonas*, *Bacillus* and *Paenibacillus*, and in most strains tested from this group TeRed was high. Nonetheless, the use of TeRed capacity, to obtain Te particles with practical application is still underexplored. In this work, the bottom-up approach to select organisms with Te^r and able to produce metallic Te compounds revealed several types of nanostructures formed. This result indicates a rich diversity in metabolic induced TeRed. The estimation of reduction efficiencies and reduction rates allows for an optimization of biomanufacturing of Te nanostructures. Bacterial strains demonstratied varied and/or high performance in Re and Rr, this variability allowed different biomanufacturing protocols that could consider reaction time and cell density factors. The strains *B. altitudinis* 3W19, *B. safensis* 10W7 and *C. marina* 5W10, isolated from Panasquerira sediments, were more efficient in TeRed than strains isolated from Aljustrel or Jales sediments. The strains with the highest rate of TeRed were *B. altitudinis* 3W19, *B. safensis* 10W7 and *B. mycoides* ALJ98a. The relation between Te^r phenotype and the existence of genetic determinants for Te^r was visible in the *Bacillus* genera in mining isolates. Five *Bacillus* strains exibited *ter* gene systems, with two possible genetic organizations. All strains possessed multiple copies of genes encoding proteins of the TerD family and one gene encoding a protein of the TerC family.

In this study we presentd, in **Chapter IV,** significant improvements on the knowledge of cellular and metabolic response to Te (IV) by highly resistant *Bacillus* as *Paenibacillus* strains. The metabolic response to Te (IV), in highly resistant *Paenibacillus* and *Bacillus* strains, was demonstrated for the first time. Each organism was impacted by growth in the presence of Te (IV), with varying levels of ROS increase and general metabolic decrease. Nonetheless, both strains were able to reduce intracellular ROS levels over time.

Analysis of the genomes of *B. altitudinis* 3W19 and *P. pabuli* ALJ109b highlighted differences in specific Te^r potential by each strain. In comparison to *P. pabuli* ALJ109b, in *B. altitudinis* 3W19 were detected more Te (IV) related genes for putative metalloid transporte or for Te^r.

Te (IV) showed to induce ROS generation that the strain solved by expressing specific proteins and by activating some metabolic pathways. Proteins related to oxidative stress response, particularly associated with cell wall or cell envelope were over-represented. The phage shock protein PspA, a marker protein for stress response, was among the highest over-expressed proteins in both *B. altitudinis* 3W19 and *P. pabuli* ALJ109b. Each strain was unique in its metabolic response, with few common proteins over or down regulated, and with apparent Te (IV) different specific resistance responses. The specific Te (IV) response observed for *B. altitudinis* 3W19 is clear, with the over-expression of the three *terD* paralogs, from the *ter* gene cluster. This result is demonstrated by LC-MS/MS proteomic and validated by q RT-PCR. The overall over/down representation of metabolic pathways was specific to each organism with the metabolic pathways of translation, cellular motility, metabolism of aminoacids and cell growth and death over-represented, and transcription down-represented in *B. altitudinis* 3W19. In *P. pabuli* ALJ109b the metabolic pathways of folding, sorting and degradation and biosynthesis of secondary metabolites were over-represented and only xenobiotic biodegradation was found with decreased representation. The representation of the metabolic pathways is in accordance with the response to other stress conditions, namely metals, as seen in previous studies. This work demonstrated the importance of high throughput technologies in determination of cell response to a metalloid with increasing importance in human activity.

The focused characterization of a highly Te (IV) resistant *Paenibacillus* strain, in **Chapter V**, revealed a highly efficient TeNP production method. This strain can produce monodisperse TeNPs, with a high Re and Rr. The physical characterization of the nanoparticles formed revealed the existence of Te containing crystalline structures, with less than 100 nm in, at least, one axis and with no distinct emission peack in the UV-Visible range. The genomic and high throughput proteomics analyses did not identify any previously demonstrated TeRed mechanisms. Nevertheless, *P. pabuli* ALJ109b was able to eliminate the toxic Te (IV) through TeRed. We demonstrated that *P. pabuli* ALJ109b overexpressed flagellin, FlaA, in the presence of Te (IV) and that this protein had a high Te (0) formation activity at room temperature and pH of 9. The flagellin purified from *P. pabuli* ALJ109b was an effective Te (IV) reducer with potential in nanoparticle fabrication.

The production of extracellular monodisperse NPs is a highly desired process for many applications but is rarely observed. The biological production of monodisperse, extracellular NPs was always a limitation in this biomanufacturing technology. The nanoparticles produced by *P. pabuli* ALJ109b appear monodisperse, a single shape is observed, and extracellular considering the use of flagellin, a protein from an extracellular component, as a biotemplate for TeNPs production. Therefore, this Thesis presents a major inovation in a bottleneck process for biological NP formation.

Future perspectives

During this work, the strains with demonstrated ability for Te (IV) resistance were tested for the presence of known Te (IV) resistance determinants. This resulted in the selection of a *Bacillus altitudinis* strain 3W19 with an unique genetic arrangement of the Te^r genes, from the *ter* gene cluster, for the species. Proteomic and transcription analysis revealed the increased expression of the three *terD* paralog genes in response to Te (IV), but little considerations were given to the regulation of the expression of such genes. It is of interest to explore in greater detail the genome of *B. altitudinis* 3W19 for the existence of a *terW* element or homologue regulation elements. In addition, targeted mutagenesis could be used to reveal or confirm regulatory elements of the *ter* gene cluster. This thesis opens the possibility for a new TeNP production methodology that needed to be explored. Considering the possibility of using flagellin from *Paenibacillus pabuli* ALJ109b for a commercial application of TeNP production, further characterization is needed to determine the characteristics of the nanoparticles formed, such as dynamic light scattering and ζ-potential. The importance of these new studies will determine the range of application the TeNPs produced. Furthermore, with this work, some advancements were made in determining on environmental bacteria their ability for high Te (IV) resistance. A selection of resistant strains will provide candidates for future studies such as the bioleaching of Te from mineral or industrial residues. By determining the molecules that are responsible for Te leaching considerations can be made to improve the cell function and increase Te mobilization from solid substrates.

Final remarks

Tellurium is one of the most versatile metalloids and its potential in human activity is, in my opinion, not still fully discovered. As such, there will be, in the foreseeable future a continued demand for research in Te related research. I consider that this work marked a difference in the research of a metalloid that has been elusive to the overall biochemistry of the planet, when compared to other metals and metalloids studied in the field of microbiology. In this work, a bottom- up aproach was used to select organisms with optimal properties to the objectives outlined. This resulted in the utilization of a broad range of methodologies that complemented each other and enriched the work and its discussion. Several conclusions presented are the result of double confirmations by complementary methodologies which weighs in the validity of the present study. The current study, comprising the description of the state of the art, and the research performed, gather considerable evidence that demonstrate the interaction of several bacteria with Te. Many gaps remain to be filled, from the participation of microorganisms in tgeformation of natural Te containing solid structures, to the utilization of Te from ores and other substrates by bacteria and other organisms, or from the specific molecular targets of the Te (IV) induced toxicity to the resistance mechanisms regulation and specificity in most bacteria. These and other fascinating questions will be the responsibility of researchers to come, willing to accept the challenges of these tasks. I wish them the best of luck.

References

Alavi, S; Amoozegar, M. A; & Khajeh, K (2014). Enzyme(s) responsible for tellurite reducing activity in a moderately halophilic bacterium, *Salinicoccus iranensis* strain QW6. *Extremophiles*, *18*(6), 953–961. https://doi.org/10.1007/s00792-014-0665-6

Anantharaman, V; Iyer, L. M; & Aravind, L (2014). Ter-dependent stress response systems: novel pathways related to metal sensing, production of a nucleoside-like metabolite, and DNA-processing. *Molecular Biosystem*, *8*(12), 3142–3165. https://doi.org/10.1039/c2mb25239b.Ter-dependent

Anderson, C. S (2021). *Mineral Commodity Summaries: TELLURIUM*.

Andreae, M. O (1984). Determination of inorganic tellurium species in natural waters. *Analytical Chemistry*, *56*(12), 2064–2066. https://doi.org/10.1021/ac00276a019

Arenas-Salinas, M; Vargas-Pérez, J. I; Morales, W; Pinto, C; Muñoz-Díaz, P; Cornejo, F. A; Pugin, B; Sandoval, J. M; Díaz-Vásquez, W. A; Muñoz-Villagrán, C; Rodríguez-Rojas, F; Morales, E. H; Vásquez, C. C; & Arenas, F. A (2016). Flavoprotein-mediated tellurite reduction: Structural basis and applications to the synthesis of tellurium-containing nanostructures. *Frontiers in Microbiology*, *7*(JUL), 1–14. https://doi.org/10.3389/fmicb.2016.01160

Arenas, F. A; Leal, C. A; Pinto, C. A; Arenas-Salinas, M. A; Morales, W. A; Cornejo, F. A; Díaz-Vásquez, W. A; & Vásquez, C. C (2014). On the mechanism underlying tellurite reduction by *Aeromonas caviae* ST dihydrolipoamide dehydrogenase. *Biochimie*, *102*(1), 174–182. https://doi.org/10.1016/j.biochi.2014.03.008

A**renas, F. A; Pugin, B; Henrı, N. A; Arenas-salinas, M. A; D, W. A; Pe, M; Chasteen, T. G; Mun, C. M; & Va, C. C** (2014). Isolation, identification and characterization of highly tellurite- resistant, tellurite-reducing bacteria from Antarctica. *Polar Science*, *8*, 40–52. https://doi.org/10.1016/j.polar.2014.01.001

Avazéri, C; Turner, R. J; Pommier, J; Weiner, J. H; Giordano, G; & Verméglio, A (1997). Tellurite reductase activity of nitrate reductase is responsible for the basal resistance of *Escherichia coli* to tellurite. *Microbiology*, *143*(4), 1181–1189. https://doi.org/10.1099/00221287-143-4-1181

Aziz, R. K; Bartels, D; Best, A. a, DeJongh, M; Disz, T; Edwards, R. a, Formsma, K; Gerdes, S; Glass, E. M; Kubal, M; Meyer, F; Olsen, G. J; Olson, R; Osterman, A. L; Overbeek, R. a, McNeil, L. K; Paarmann, D; Paczian, T; Parrello, B; & Zagnitko, O (2008). The RAST Server: rapid annotations using subsystems technology. *BMC Genomics*, *9*, 75. https://doi.org/10.1186/1471-2164-9-75

Ba, L. A; Mandy, D; Jamier, V; & Jacob, C (2010). Tellurium: an element with great biological potency and potential. *Organic & Biomolecular Chemistry*, *8*, 4203–4216. https://doi.org/10.1039/c0Ob00086h

Baesman, S. M; Bullen, T. D; Dewald, J; Zhang, D; Curran, S; Islam, F. S; Beveridge, T. J; & Oremland, R. S (2007). Formation of tellurium nanocrystals during anaerobic growth of bacteria that use Te oxyanions as respiratory electron acceptors. *Applied and Environmental Microbiology*, *73*(7), 2135–2143. https://doi.org/10.1128/AEM.02558-06

Belzile, N; & Chen, Y. W (2015). Tellurium in the environment: A critical review focused on natural waters, soils, sediments and airborne particles. *Applied Geochemistry*, *63*, 83–92. https://doi.org/10.1016/j.apgeochem.2015.07.002

Blake, D. P; Hillman, K; Fenlon, D. R; & Low, J. C (2003). Transfer of antibiotic resistance between commensal and pathogenic members of the Enterobacteriaceae under ileal conditions. *Journal of Applied Microbiology*, *95*(3), 428–436. https://doi.org/10.1046/j.1365-2672.2003.01988.x

Borghese, R; Baccolini, C; Francia, F; Sabatino, P; Turner, R. J; & Zannoni, D (2014). Reduction of chalcogen oxyanions and generation of nanoprecipitates by the photosynthetic bacterium *Rhodobacter capsulatus*. *Journal of Hazardous Materials*, *269*, 24–30. https://doi.org/10.1016/j.jhazmat.2013.12.028

Borghese, R; Brucale, M; Fortunato, G; Lanzi, M; Mezzi, A; Valle, F; Cavallini, M; & Zannoni, D (2017). Reprint of "Extracellular production of tellurium nanoparticles by the photosynthetic bacterium *Rhodobacter capsulatus*." *Journal of Hazardous Materials*, *324*, 31–38. https://doi.org/10.1016/j.jhazmat.2016.11.002

Borghese, R; Malferrari, M; Brucale, M; Ortolani, L; Franchini, M; Rapino, S; Borsetti, F; & Zannoni, D (2020). Structural and electrochemical characterization of lawsone-dependent production of tellurium-metal nanoprecipitates by photosynthetic cells of *Rhodobacter capsulatus*. *Bioelectrochemistry*, *133*, 107456. https://doi.org/10.1016/j.bioelechem.2020.107456

Borghese, R; Marchetti, D; & Zannoni, D (2008). The highly toxic oxyanion tellurite (TeO_3^{2-}) enters the phototrophic bacterium *Rhodobacter capsulatus* via an as yet uncharacterized monocarboxylate transport system. *Archives of Microbiology*, *189*(2), 93–100. https://doi.org/10.1007/s00203-007-0297-7

Borghese, R; & Zannoni, D (2010). Acetate permease (ActP) is responsible for tellurite (TeO_3^{2-}) uptake and resistance in cells of the facultative phototroph *Rhodobacter capsulatus*. *Applied and Environmental Microbiology*, *76*(3), 942–944. https://doi.org/10.1128/AEM.02765-09

Borsetti, F; Toninello, A; & Zannoni, D (2003). Tellurite uptake by cells of the facultative phototroph *Rhodobacter capsulatus* is a ΔpH-dependent process. *FEBS Letters*, *554*(3), 315–318. https://doi.org/10.1016/S0014-5793(03)01180-3

Bradford, M (1976). A rapid and sensitive method for the quantitation of microgram quantities of protein utilizing the principle of protein-dye binding. *Analytical Biochemistry*, *72*(1–2), 248–254. https://doi.org/10.1006/abio.1976.9999

Brettin, T; Davis, J. J; Disz, T; Edwards, R. A; Gerdes, S; Olsen, G. J; Olson, R; Overbeek, R; Parrello, B; Pusch, G. D; Shukla, M; Thomason, J. A; Stevens, R; Vonstein, V; Wattam, A. R; & Xia, F (2015). RASTtk: A modular and extensible implementation of the RAST algorithm for building custom annotation pipelines and annotating batches of genomes. *Scientific Reports*, *5*(1), 8365. https://doi.org/10.1038/srep08365

Burian, J; Tu, N; Kl'učár, L; Guller, L; Lloyd-Jones, G; Stuchlík, S; Fejdi, P; Siekel, P; & Turňa, J (1998). *In vivo* and *in vitro* cloning and phenotype characterization of tellurite resistance determinant conferred by plasmid pTE53 of a clinical isolate of *Escherichia coli*. *Folia Microbiologica*, *43*(6), 589–599. https://doi.org/10.1007/BF02816374

Byrappa, K; & Adschiri, T (2007). Hydrothermal technology for nanotechnology. *Progress in Crystal Growth and Characterization of Materials*, *53*(2), 117–166. https://doi.org/10.1016/j.pcrysgrow.2007.04.001

Caldeira, J. B; Morais, P. V; & Branco, R (2020). Exploiting the biological response of two *Serratia fonticola* strains to the critical metals, gallium and indium. *Scientific Reports*, *10*(1), 20348. https://doi.org/10.1038/s41598-020-77447-7

Calderón, I. L; Arenas, F. A; Pérez, J. M; Fuentes, D. E; Araya, M. A; Saavedra, C. P; Tantaleán, J. C; Pichuantes, S. E; Youderian, P. A; & Vásquez, C. C (2006). Catalases are NAD(P)H-dependent tellurite reductases. *PLoS ONE*, *1*(1), e70. https://doi.org/10.1371/journal.pone.0000070

Cao, G. S; Juan Zhang, X; Su, L; & Yang Ruan, Y (2011). Hydrothermal synthesis of selenium and tellurium nanorods. *Journal of Experimental Nanoscience*, *6*(2), 121–126. https://doi.org/10.1080/17458081003774677

Cash, P (2009). Proteomics in the study of the molecular taxonomy and epidemiology of bacterial pathogens. *Electrophoresis*, *30*(S1), S133–S141. https://doi.org/10.1002/elps.200900059

Chasteen, T; Fuentes, D; Tantalean, J; & Vásquez, C (2009). Tellurite: history, oxitative stress, and molecular mechanisms of resistance. *FEMS Microbiol Rev*, *33*, 820–832. https://doi.org/10.1111/j.1574-6976.2009.00177.x

Chen, B; Fang, L; Yan, X; Zhang, A; Chen, P; Luan, T; Hu, L; & Jiang, G (2019). A unique Pb-binding flagellin as an effective remediation tool for Pb contamination in aquatic environment. *Journal of Hazardous Materials*, *363*(September 2018), 34–40. https://doi.org/10.1016/j.jhazmat.2018.10.004

Cheng, Z; Wei, Y. Y. C; Sung, W. W. L; Glick, B. R; & McConkey, B. J (2009). Proteomic analysis of the response of the plant growth-promoting bacterium *Pseudomonas putida* UW4 to nickel stress. *Proteome Science*, *7*, 1–8. https://doi.org/10.1186/1477-5956-7-18

Chien, C.C; & Han, C.T (2009). Tellurite resistance and reduction by a *Paenibacillus* sp. isolated from heavy metal-contaminated sediment. *Environmental Toxicology and Chemistry / SETAC*, *28*(8), 1627–1632. https://doi.org/10.1897/08-521.1

Chien, C. C; Jiang, M. H; Tsai, M. R; & Chien, C. C (2011). Isolation and characterization of an environmental cadmium- and tellurite-resistant *Pseudomonas* strain. *Environmental Toxicology and Chemistry*, *30*(10), 2202–2207. https://doi.org/10.1002/etc.620

Choi, N. C; Cho, K. H; Kim, B. J; Lee, S; & Park, C. Y (2018). Enhancement of Au–Ag–Te contents in tellurium-bearing ore minerals via bioleaching. *International Journal of Minerals, Metallurgy and Materials*, *25*(3), 262–270. https://doi.org/10.1007/s12613-018-1569-8

Choudhury, H. G; Cameron, A. D; Iwata, S; & Beis, K (2011). Structure and mechanism of the chalcogen-detoxifying protein TehB from *Escherichia coli*. *Biochemical Journal*, *435*(1), 85–91. https://doi.org/10.1042/BJ20102014

Chourey, K; Thompson, M. R; Morrell-Falvey, J; VerBerkmoes, N. C; Brown, S. D; Shah, M; Zhou, J; Doktycz, M; Hettich, R. L; & Thompson, D. K (2006). Global molecular and morphological effects of 24-hour chromium(VI) exposure on *Shewanella oneidensis* MR-1. *Applied and Environmental Microbiology*, *72*(9), 6331–6344. https://doi.org/10.1128/AEM.00813-06

Christy, A. G; Mills, S. J; & Kampf, A. R (2016). A review of the structural architecture of tellurium oxycompounds. *Mineralogical Magazine*, *80*(3), 415–545. https://doi.org/10.1180/minmag.2016.080.093

Chung, A. P; Coimbra, C; Farias, P; Francisco, R; Branco, R; Simão, F. V; Gomes, E; Pereira, A; Vila, M. C; Fiúza, A; Mortensen, M. S; Sørensen, S. J; & Morais, P. V (2019). Tailings microbial community profile and prediction of its functionality in basins of tungsten mine. *Scientific Reports*, *9*(1), 19596. https://doi.org/10.1038/s41598-019-55706-6

Climo, M; Watling, H. R; & Van Bronswijk, W (2000). Biooxidation as pre-treatment for a telluride-rich refractory gold concentrate. *Minerals Engineering*, *13*(12), 1219–1229. https://doi.org/10.1016/s0892-6875(00)00106-0

Contreras, F; Vargas, E; Jiménez, K; Muñoz-Villagrán, C; Figueroa, M; Vásquez, C; & Arenas, F (2018). Reduction of gold (III) and tellurium (IV) by *Enterobacter cloacae* MF01 results in nanostructure formation both in aerobic and anaerobic conditions. *Frontiers in Microbiology*, 9(December), 1–15. https://doi.org/10.3389/fmicb.2018.03118

Cox, J; Hein, M. Y; Luber, C. A; Paron, I; Nagaraj, N; & Mann, M (2014). Accurate proteome-wide label-free quantification by delayed normalization and maximal peptide ratio extraction, termed MaxLFQ. *Molecular & Cellular Proteomics*, *13*(9), 2513–2526. https://doi.org/10.1074/mcp.M113.031591

Cox, J; Neuhauser, N; Michalski, A; Scheltema, R. A; Olsen, J. V; & Mann, M (2011). Andromeda: A Peptide search engine integrated into the MaxQuant environment. *Journal of Proteome Research*, *10*(4), 1794–1805. https://doi.org/10.1021/pr101065j

Csotonyi, J. T; Stackebrandt, E; & Yurkov, V (2006). Anaerobic respiration on tellurate and other metalloids in bacteria from hydrothermal vent fields in the Eastern Pacific Ocean. *Applied and Environmental Microbiology*, *72*(7), 4950–4956. https://doi.org/10.1128/AEM.00223-06

Decorosi, F; Tatti, E; Mini, A; Giovannetti, L; & Viti, C (2009). Characterization of two genes involved in chromate resistance in a Cr(VI)-hyper-resistant bacterium. *Extremophiles*, *13*(6), 917–923. https://doi.org/10.1007/s00792-009-0279-6

Demergasso, C. S; Galleguillos P; P. A; Escudero G; L. V; Zepeda A; V. J; Castillo, D; & Casamayor, E. O (2005). Molecular characterization of microbial populations in a low-grade copper ore bioleaching test heap. *Hydrometallurgy*, *80*(4), 241–253. https://doi.org/10.1016/j.hydromet.2005.07.013

Díaz-Vásquez, W. A; Abarca-Lagunas, M. J; Cornejo, F. A; Pinto, C. A; Arenas, F. A; & Vásquez, C. C (2015). Tellurite-mediated damage to the *Escherichia coli* NDH-dehydrogenases and terminal oxidases in aerobic conditions. *Archives of Biochemistry and Biophysics*, *566*, 67–75. https://doi.org/10.1016/j.abb.2014.10.011

Dittmer, D. C (2003). Tellurium. *Chemical & Engineering News*, *81*(36), 128.

Djoko, K. Y; Phan, M. D; Peters, K. M; Walker, M. J; Schembri, M. A; & McEwan, A. G (2017). Interplay between tolerance mechanisms to copper and acid stress in *Escherichia coli*. *Proceedings of the National Academy of Sciences of the United States of America*, *114*(26), 6818–6823. https://doi.org/10.1073/pnas.1620232114

Dodson, J. R; Parker, H. L; García, A. M; Hicken, A; Asemave, K; Farmer, T. J; He, H; Clark, J. H; & Hunt, A. J (2015). Bio-derived materials as a green route for precious & critical metal recovery and re-use. *Green Chemistry*, *17*(4), 1951–1965. https://doi.org/10.1039/c4gc02483d

Dong, Y; Liu, Y; Lin, H; & Lin, C (2019). Improving vanadium extraction from stone coal via combination of blank roasting and bioleaching by ARTP-mutated *Bacillus mucilaginosus*. *Transactions of Nonferrous Metals Society of China (English Edition)*, *29*(4), 849–858. https://doi.org/10.1016/S1003-6326(19)64995-2

Du, J; Duan, S; Miao, J; Zhai, M; & Cao, Y (2021). Purification and characterization of chitinase from *Paenibacillus* sp. *Biotechnology and Applied Biochemistry*, *68*(1), 30–40. https://doi.org/10.1002/bab.1889

Dyllick-Brenzinger, M; Liu, M; Winstone, T. L; Taylor, D. E; & Turner, R. J (2000). The role of cysteine residues in tellurite resistance mediated by the TehAB determinant. *Biochemical and Biophysical Research Communications*, *277*(2), 394–400. https://doi.org/10.1006/bbrc.2000.3686

Elías, A; Díaz-Vásquez, W; Abarca-Lagunas, M. J; Chasteen, T. G; Arenas, F; & Vásquez, C. C (2015). The ActP acetate transporter acts prior to the PitA phosphate carrier in tellurite uptake by *Escherichia coli*. *Microbiological Research*, *177*, 15–21. https://doi.org/10.1016/j.micres.2015.04.010

Elias, M; Wellner, A; Goldin-Azulay, K; Chabriere, E; Vorholt, J. A; Erb, T. J; & Tawfik, D. S (2012). The molecular basis of phosphate discrimination in arsenate-rich environments. *Nature*, *491*(7422), 134–137. https://doi.org/10.1038/nature11517

Etezad, S. M; Khajeh, K; Soudi, M; Ghazvini, P. T. M; & Dabirmanesh, B (2009). Evidence on the presence of two distinct enzymes responsible for the reduction of selenate and tellurite in *Bacillus* sp. STG-83. *Enzyme and Microbial Technology*, *45*(1), 1–6. https://doi.org/10.1016/j.enzmictec.2009.04.004

Faraldo-Gómez, J. D; & Sansom, M. S. P (2003). Acquisition of siderophores in Gram-negative bacteria. *Nature Reviews Molecular Cell Biology*, *4*(2), 105–116. https://doi.org/10.1038/nrm1015

Feldmann, J; & Hirner, A. V (1995). Occurrence of volatile metal and metalloid species in landfill and sewage gases. *International Journal of Environmental Analytical Chemistry*, *60*(2–4), 339–359. https://doi.org/10.1080/03067319508042888

Feng, D; Aldrich, C; & Tan, H (2000). Treatment of acid mine water by use of heavy metal precipitation and ion exchange. *Minerals Engineering*, *13*(6), 623–642. https://doi.org/10.1016/S0892-6875(00)00045-5

Figueroa, M; Fernandez, V; Arenas-Salinas, M; Ahumada, D; Muñoz-Villagrán, C; Cornejo, F; Vargas, E; Latorre, M; Morales, E; Vásquez, C; & Arenas, F (2018). Synthesis and antibacterial activity of metal(loid) nanostructures by environmental multi-metal(loid) resistant bacteria and metal(loid)-reducing flavoproteins. *Frontiers in Microbiology*, *9*:959. https://doi.org/10.3389/fmicb.2018.00959

Filella, M; Reimann, C; Biver, M; Rodushkin, I; & Rodushkina, K (2019). Tellurium in the environment: Current knowledge and identification of gaps. *Environmental Chemistry*, *16*(4), 215–228. https://doi.org/10.1071/EN18229

Fischer, W (2001). A second note on the term "Chalcogen." *Journal of Chemical Education*, *78*(10), 1333. https://doi.org/10.1021/ed078p1333.1

Forootanfar, H; Amirpour-Rostami, S; Jafari, M; Forootanfar, A; Yousefizadeh, Z; & Shakibaie, M (2015). Microbial-assisted synthesis and evaluation the cytotoxic effect of tellurium nanorods. *Materials Science and Engineering C*, *49*, 183–189. https://doi.org/10.1016/j.msec.2014.12.078

F**ranks, S. E; Ebrahimi, C; Hollands, A; Okumura, C. Y; Aroian, R. V; Nizet, V; & McGillivray, S. M** (2014). Novel role for the *yceGH* tellurite resistance genes in the pathogenesis of *Bacillus anthracis*. *Infection and Immunity*, *82*(3), 1132–1140. https://doi.org/10.1128/IAI.01614-13

Fränzle, S; & Markert, B (2000). The Biological System of the Elements (BSE). Part II: a theoretical model for establishing the essentiality of chemical elements. The application of stoichiometric network analysis to the biological system of the elements. *Science of The Total Environment*, *249*(1–3), 223–241. https://doi.org/10.1016/S0048-9697(99)00520-3

Freitas, E. V; & Nascimento, C (2017). Degradability of natural and synthetic chelating agents applied to a lead-contaminated soil. *Journal of Soils and Sediments*, *17*(5), 1272–1278. https://doi.org/10.1007/s11368-015-1350-9

Gharieb, M. M; Kierans, M; & Gadd, G. M (1999). Transformation and tolerance of tellurite by filamentous fungi: accumulation, reduction, and volatilization. *Mycological Research*, *103*(3), 299–305. https://doi.org/10.1017/S0953756298007102

Giese, E. C; Carpen, H. L; Bertolino, L. C; & Schneider, C. L (2019). Characterization and bioleaching of nickel laterite ore using *Bacillus subtilis* strain. *Biotechnology Progress*, *35*(6). https://doi.org/10.1002/btpr.2860

Godfarb, R. J; Berger, B. R; George, M. W; & Seal II, R. R (2017). Tellurium. In *Critical Mineral Resources of the United States—Economic and Environmental Geology and Prospects for Future Supply*. https://doi.org/10.1016/B978-0-12-386454-3.00936-2

Goff, J; & Yee, N (2017). Tellurate enters *Escherichia coli* K-12 cells via the SulT-type sulfate transporter CysPUWA. *FEMS Microbiology Letters*, *364*(24), 1–5. https://doi.org/10.1093/femsle/fnx241

Gómez-Gómez, B; Pérez-Corona, T; Mozzi, F; Pescuma, M; & Madrid, Y (2019). Silac-based quantitative proteomic analysis of *Lactobacillus reuteri* CRL 1101 response to the presence of selenite and selenium nanoparticles. *Journal of Proteomics*, *195*, 53–65. https://doi.org/10.1016/j.jprot.2018.12.025

Goncharoff, P; Saadi, S; Chang, C. H; Saltman, L. H; & Figurski, D. H (1991). Structural, molecular, and genetic analysis of the *kilA* operon of broad-host-range plasmid RK2. *Journal of Bacteriology*, *173*(11), 3463–3477. https://doi.org/10.1128/jb.173.11.3463-3477.1991

Gopinathan, P; Ashok, A. M; & Selvakumar, R (2013). Bacterial flagella as biotemplate for the synthesis of silver nanoparticle impregnated bionanomaterial. *Applied Surface Science*, *276*, 717–722. https://doi.org/10.1016/j.apsusc.2013.03.159

Goris, J; Konstantinidis, K. T; Klappenbach, J. A; Coenye, T; Vandamme, P; & Tiedje, J. M (2007). DNA–DNA hybridization values and their relationship to whole-genome sequence similarities. *International Journal of Systematic and Evolutionary Microbiology*, *57*(1), 81–91. https://doi.org/10.1099/ijs.0.64483-0

Govett, G. J. S (1983). Rock Geochemistry in Mineral Exploration; Handbook of Exploration Geochemistry (Volume 3). Elsevier.

Grangeia, C; Ávila, P; Matias, M; & da Silva, E. F (2011). Mine tailings integrated investigations: The case of Rio tailings (Panasqueira Mine, Central Portugal). *Engineering Geology*, *123*(4), 359–372. https://doi.org/10.1016/j.enggeo.2011.10.001

Guo, Y; Deng, T; Zhang, N; & Liao, M (2012). Tellurium extraction from the unique independent tellurium ores in China by bioleaching. *Advanced Materials Research*, *343–344*, 625–630. https://doi.org/10.4028/www.scientific.net/AMR.343-344.625

Guo, Y. F; Zhang, N; Li, D. C; Tang, F. M; & Deng, T. L (2012). Tellurium recovery from the unique tellurium ores. *Advanced Materials Research*, *549*, 1060–1063. https://doi.org/10.4028/www.scientific.net/AMR.549.1060

Guzzo, J; & Dubow, M. S (2000). A novel selenite- and tellurite-inducible gene in *Escherichia coli*. *Applied and Environmental Microbiology*, *66*(11), 4972–4978. https://doi.org/10.1128/AEM.66.11.4972-4978.2000

He, S; Guo, Z; Zhang, Y; Zhang, S; Wang, J; & Gu, N (2007). Biosynthesis of gold nanoparticles using the bacteria *Rhodopseudomonas capsulata*. *Materials Letters*, *61*(18), 3984–3987. https://doi.org/10.1016/j.matlet.2007.01.018

Hein, J. R; Koschinsky, A; & Halliday, A. N (2003). Global occurrence of tellurium-rich ferromanganese crusts and a model for the enrichment of tellurium. *Geochimica et Cosmochimica Acta*, *67*(6), 1117–1127. https://doi.org/10.1016/S0016-7037(00)01279-6

Herschend, J; Damholt, Z. B. V; Marquard, A. M; Svensson, B; Sørensen, S. J; Hägglund, P; & Burmølle, M (2017). A meta-proteomics approach to study the interspecies interactions affecting microbial biofilm development in a model community. *Scientific Reports*, *7*(1), 1–13. https://doi.org/10.1038/s41598-017-16633-6

Hill, S. M; Jobling, M. G; Lloyd, B. H; Strike, P; & Ritchie, D. A (1993). Functional expression of the tellurite resistance determinant from the IncHI-2 plasmid pMER610. *MGG Molecular & General Genetics*, *241*(1–2), 203–212. https://doi.org/10.1007/BF00280218

Hirner, A. ; Krupp, E; Schulz, F; Koziol, M; & Hofmeister, W (1998). Organometal(loid) species in geochemical exploration: preliminary qualitative results. *Journal of Geochemical Exploration*, *64*(1–3), 133–139. https://doi.org/10.1016/S0375-6742(98)00026-0

Izrael-Živković, L; Rikalović, M; Gojgić-Cvijović, G; Kazazić, S; Vrvić, M; Brčeski, I; Beškoski, V; Lončarević, B; Gopčević, K; & Karadžić, I (2018). Cadmium specific proteomic responses of a highly resistant: *Pseudomonas aeruginosa san ai*. *RSC Advances*, *8*(19), 10549–10560. https://doi.org/10.1039/c8ra00371h

Jakubowski, W (2000). 2,7-dichlorofluorescein oxidation and reactive oxigen species: What does it measure? *Cell Biology International*, *24*(10), 757–760. https://doi.org/10.1006/cbir.2000.0556

Jimoh, A. A; & Lin, J (2019). Enhancement of *Paenibacillus* sp. D9 lipopeptide biosurfactant production through the optimization of medium composition and its application for biodegradation of hydrophobic pollutants. *Applied Biochemistry and Biotechnology*, *187*(3), 724–743. https://doi.org/10.1007/s12010-018-2847-7

J**olley, K. A; Bliss, C. M; Bennett, J. S; Bratcher, H. B; Brehony, C; Colles, F. M; Wimalarathna, H; Harrison, O. B; Sheppard, S. K; Cody, A. J; & Maiden, M. C. J** (2012). Ribosomal multilocus sequence typing: universal characterization of bacteria from domain to strain. *Microbiology*, *158*(4), 1005–1015. https://doi.org/10.1099/mic.0.055459-0

Kabiri, M; Amoozegar, M. A; Tabebordbar, M; Gilany, K; & Salekdeh, G. H (2009). Effects of selenite and tellurite on growth, physiology, and proteome of a moderately halophilic bacterium. *Journal of Proteome Research*, *8*(6), 3098–3108. https://doi.org/10.1021/pr900005h

Kanehisa, M; Sato, Y; & Morishima, K (2016). BlastKOALA and GhostKOALA: KEGG Tools for functional characterization of genome and metagenome sequences. *Journal of Molecular Biology*, *428*(4), 726–731. https://doi.org/10.1016/j.jmb.2015.11.006

Kanz, C; Aldebert, P; Althorpe, N; Baker, W; Baldwin, A; Bates, K; Browne, P; van den Broek, A; Castro, M; Cochrane, G; Duggan, K; Eberhardt, R; Faruque, N; Gamble, J; Diez, F. G; Harte, N; Kulikova, T; Lin, Q; Lombard, V; & Apweiler, R (2005). The EMBL Nucleotide Sequence Database. *Nucleic Acids Res*, *33*(Database issue), D29-33. https://doi.org/10.1093/nar/gki098

Kellogg, D. K; & Wende, R. D (1946). Use of a potassium tellurite medium in the detection of *Corynebacterium diphtheriae*. *American Journal of Public Health and the Nation's Health*, *36*(7), 739–745. http://www.ncbi.nlm.nih.gov/pubmed/18016380

Kelstrup, C. D; Young, C; Lavallee, R; Nielsen, M. L; & Olsen, J. V (2012). Optimized fast and sensitive acquisition methods for shotgun proteomics on a quadrupole orbitrap mass spectrometer. *Journal of Proteome Research*, *11*(6), 3487–3497. https://doi.org/10.1021/pr3000249

Kim, D. H; Kanaly, R. A; & Hur, H. G (2012). Biological accumulation of tellurium nanorod structures via reduction of tellurite by *Shewanella oneidensis* MR-1. *Bioresource Technology*, *125*, 127–131. https://doi.org/10.1016/j.biortech.2012.08.129

Kim, D. H; Kim, M. G; Jiang, S; Lee, J. H; & Hur, H. G (2013). Promoted reduction of tellurite and formation of extracellular tellurium nanorods by concerted reaction between iron and *Shewanella oneidensis* MR-1. *Environmental Science and Technology*, *47*(15), 8709–8715. https://doi.org/10.1021/es401302w

Kim, M. G; Kim, D; Kim, T; Park, S; Kwon, G; Kim, M. S; Shin, T. J; Ahn, H; & Hur, H (2015). Unusual Li-ion storage through anionic redox processes of bacteria-driven tellurium nanorods. *Journal of Materials Chemistry A*, *3*, 16978–16987. https://doi.org/10.1039/C5TA04038H

Klonowska, A; & Heulin, T (2005). Selenite and tellurite reduction by *Shewanella oneidensis*. *Applied and Environmental Microbiology 71*(9), 5607–5609. https://doi.org/10.1128/AEM.71.9.5607

Knuutinen, J; Bomberg, M; Kemell, M; & Lusa, M (2019). Ni(II) Interactions in boreal *Paenibacillus* sp; *Methylobacterium* sp; *Paraburkholderia* sp; and *Pseudomonas* sp. strains isolated from an acidic, ombrotrophic bog. *Frontiers in Microbiology*, *10*:2677, 1–21. https://doi.org/10.3389/fmicb.2019.02677

Kormutakova, R; Klucar, L; & Turna, J (2000). DNA sequence analysis of the tellurite-resistance determinant from clinical strain of *Escherichia coli* and identification of essential genes. *BioMetals*, *13*(2), 135–139. https://doi.org/10.1023/A:1009272122989

Kösters, J; Diaz-Bone, R. ; Planer-Friedrich, B; Rothweiler, B; & Hirner, A (2003). Identification of organic arsenic, tin, antimony and tellurium compounds in environmental samples by GC-MS. *Journal of Molecular Structure*, *661–662*, 347–356. https://doi.org/10.1016/j.molstruc.2003.09.005

Krupp, E. M; Grümping, R; Furchtbar, U. R. R; & Hirner, A. V (1996). Speciation of metals and metalloids in sediments with LTGC/ICP-MS. *Analytical and Bioanalytical Chemistry*, *354*(5–6), 546–549. https://doi.org/10.1007/s0021663540546

Kumano, M; Tamakoshi, A; & Yamane, K (1997). A 32 kb nucleotide sequence from the region of the lincomycin-resistance gene (22°-25°) of the *Bacillus subtilis* chromosome and identification of the site of the *lin*-2 mutation. *Microbiology*, *143*(8), 2775–2782. https://doi.org/10.1099/00221287-143-8-2775

Kumara, M. T; Tripp, B. C; & Muralidharan, S (2007). Self-assembly of metal nanoparticles and nanotubes on bioengineered flagella scaffolds. *Chemistry of Materials*, *19*(8), 2056–2064. https://doi.org/10.1021/cm062178b

Kumari, M; & Thakur, I. S (2018). Biochemical and proteomic characterization of *Paenibacillus* sp. ISTP10 for its role in plant growth promotion and in rhizostabilization of cadmium. *Bioresource Technology Reports*, *3*(May), 59–66. https://doi.org/10.1016/j.biteb.2018.06.001

Kuzyk, S. B; Hughes, E; & Yurkov, V (2021). Discovery of siderophore and metallophore production in the aerobic anoxygenic phototrophs. *Microorganisms*, *9*(5), 959. https://doi.org/10.3390/microorganisms9050959

Kyle, J. H; Breuer, P. L; Bunney, K. G; Pleysier, R; & May, P. M (2011). Review of trace toxic elements (Pb, Cd, Hg, As, Sb, Bi, Se, Te) and their deportment in gold processing. Part 1: Mineralogy, aqueous chemistry and toxicity. *Hydrometallurgy*, *107*(3–4), 91–100. https://doi.org/10.1016/j.hydromet.2011.01.010

Levinson, A. A (1974). *Introduction to exploration geochemistry* (1st ed.). Applied Publishing.

Liu, B; Su, G; Yang, Y; Yao, Y; Huang, Y; Hu, L; Zhong, H; & He, Z (2019). Vertical distribution of microbial communities in chromium-contaminated soil and isolation of Cr(VI)-Reducing strains. *Ecotoxicology and Environmental Safety*, *180*(February), 242–251. https://doi.org/10.1016/j.ecoenv.2019.05.023

Liu, Jingjing, Liu, W; Zhang, Y; Chen, C; Wu, W; & Zhang, T. C (2021). Microbial communities in rare earth mining soil after in-situ leaching mining. *Science of the Total Environment*, *755*, 142521. https://doi.org/10.1016/j.scitotenv.2020.142521

Liu, Jun, Hua, Z. S; Chen, L. X; Kuang, J. L; Li, S. J; Shu, W. S; & Huang, L. N (2014). Correlating microbial diversity patterns with geochemistry in an extreme and heterogeneous environment of mine tailings. *Applied and Environmental Microbiology*, *80*(12), 3677–3686. https://doi.org/10.1128/AEM.00294-14

Liu, M; Turner, R. J; Winstone, T. L; Saetre, A; Dyllick-Brenzinger, M; Jickling, G; Tari, L. W; Weiner, J. H; & Taylor, D. E (2000). *Escherichia coli* TehB requires S-adenosylmethionine as a cofactor to mediate tellurite resistance. *Journal of Bacteriology*, *182*(22), 6509–6513. https://doi.org/10.1128/JB.182.22.6509-6513.2000

Lloyd, J. R; Mabbett, A. N; Williams, D. R; & Macaskie, L. E (2001). Metal reduction by sulphate-reducing bacteria: physiological diversity and metal specificity. *Hydrometallurgy*, *59*(2–3), 327–337. https://doi.org/10.1016/S0304-386X(00)00175-4

Lopes, A. R; Madureira, D; Diaz, A; Santos, S; Vila, M. C; & Nunes, O. C (2020). Characterisation of bacterial communities from an active mining site and assessment of its potential metal solubilising activity. *Journal of Environmental Chemical Engineering*, *8*(6), 104495. https://doi.org/10.1016/j.jece.2020.104495

Lv, Y; Li, J; Ye, H; Du, D; Sun, P; Ma, M; & Zhang, T. C (2020). Bioleaching of silicon in electrolytic manganese residue (EMR) by *Paenibacillus mucilaginosus*: Impact of silicate mineral structures. *Chemosphere*, *256*, 127043. https://doi.org/10.1016/j.chemosphere.2020.127043

Maltman, C; Piercey-Normore, M. D; & Yurkov, V (2015). Tellurite-, tellurate-, and selenite-based anaerobic respiration by strain CM-3 isolated from gold mine tailings. *Extremophiles*, *19*(5), 1013–1019. https://doi.org/10.1007/s00792-015-0776-8

Maltman, C; & Yurkov, V (2019). Extreme environments and high-level bacterial tellurite resistance. *Microorganisms*, *7*(12), 1–24. https://doi.org/10.3390/microorganisms7120601

Manso, M. A; Léonil, J; Jan, G; & Gagnaire, V (2005). Application of proteomics to the characterisation of milk and dairy products. *International Dairy Journal*, *15*(6–9), 845–855. https://doi.org/10.1016/j.idairyj.2004.07.021

Martins, S; Couto, H; & Ferraz, P (2019, June 20). Auriferous mineralization of Jales and Gralheira (northern Portugal): A contribution to the understanding of mineral paragenesis. *International Multidisciplinary Scientific GeoConference : SGEM*. https://doi.org/10.5593/sgem2019/1.1/S01.007

Mayers, B; & Xia, Y (2002). Formation of tellurium nanotubes through concentration depletion at the surfaces of seeds. *Advanced Materials*, *14*(4), 279–282. https://doi.org/10.1002/1521-4095(20020219)14:4<279::AID-ADMA279>3.0.CO;2-2

Michel, A; Agerer, F; Hauck, C. R; Herrmann, M; Ullrich, J; Hacker, J; & Ohlsen, K (2006). Global regulatory impact of ClpP protease of *Staphylococcus aureus* on regulons involved in virulence, oxidative stress response, autolysis, and DNA repair. *Journal of Bacteriology*, *188*(16), 5783–5796. https://doi.org/10.1128/JB.00074-06

Miranda, A. T; González, M. V; González, G; Vargas, E; Campos-García, J; & Cervantes, C (2005). Involvement of DNA helicases in chromate resistance by *Pseudomonas aeruginosa* PAO1. *Mutation Research/Fundamental and Molecular Mechanisms of Mutagenesis*, *578*(1–2), 202–209. https://doi.org/10.1016/j.mrfmmm.2005.05.018

Mirjani, R; Faramarzi, M. A; Sharifzadeh, M; Setayesh, N; Khoshayand, M. R; & Shahverdi, A. R (2015). Biosynthesis of tellurium nanoparticles by *Lactobacillus plantarum* and the effect of nanoparticle-enriched probiotics on the lipid profiles of mice. *IET Nanobiotechnology*, *9*(5), 300–305. https://doi.org/10.1049/iet-nbt.2014.0057

Moazzam, P; Boroumand, Y; Rabiei, P; Baghbaderani, S. S; Mokarian, P; Mohagheghian, F; Mohammed, L. J; & Razmjou, A (2021). Lithium bioleaching: An emerging approach for the recovery of Li from spent lithium ion batteries. *Chemosphere*, *277*, 130196. https://doi.org/10.1016/j.chemosphere.2021.130196

Mohanty, A; Kathawala, M. H; Zhang, J; Chen, W. N; Loo, J. S. C; Kjelleberg, S; Yang, L; & Cao, B (2014). Biogenic tellurium nanorods as a novel antivirulence agent inhibiting pyoverdine production in *Pseudomonas aeruginosa*. *Biotechnology and Bioengineering*, *111*(5), 858–865. https://doi.org/10.1002/bit.25147

Moore, M. D; & Kaplan, S (1992). Identification of intrinsic high-level resistance to rare-earth oxides and oxyanions in members of the class Proteobacteria: characterization of tellurite, selenite, and rhodium sesquioxide reduction in *Rhodobacter sphaeroides*. *Journal of Bacteriology*, *174*(5), 1505–1514. https://doi.org/10.1128/jb.174.5.1505-1514.1992

Moore, M. S; & Parsons, E. I (1958). A study of a modified Tinsdale's medium for the primary isolation of *Corynebacterium diphtheriae*. *Journal of Infectious Diseases*, *102*(1), 88–93. https://doi.org/10.1093/infdis/102.1.88

Morais, P. V; Branco, R; & Francisco, R (2011). Chromium resistance strategies and toxicity: what makes *Ochrobactrum tritici* 5bvl1 a strain highly resistant. *Biometals : An International Journal on the Role of Metal Ions in Biology, Biochemistry, and Medicine*, *24*(3), 401–410. https://doi.org/10.1007/s10534-011-9446-1

Moreno, R; & Rojo, F (2013). The contribution of proteomics to the unveiling of the survival strategies used by *Pseudomonas putida* in changing and hostile environments. *Proteomics*, *13*(18–19), 2822–2830. https://doi.org/10.1002/pmic.201200503

Muñoz-Villagrán, C. M; Mendez, K. N; Cornejo, F; Figueroa, M; Undabarrena, A; Morales, E. H; Arenas-Salinas, M; Arenas, F. A; Castro-Nallar, E; & Vásquez, C. C (2018). Comparative genomic analysis of a new tellurite-resistant *Psychrobacter* strain isolated from the Antarctic Peninsula. *PeerJ*, *2018*(2), 1–23. https://doi.org/10.7717/peerj.4402

Nandakumar, R; Espirito Santo, C; Madayiputhiya, N; & Grass, G (2011). Quantitative proteomic profiling of the *Escherichia coli* response to metallic copper surfaces. *BioMetals*, *24*(3), 429–444. https://doi.org/10.1007/s10534-011-9434-5

Narayanan, K. B; & Sakthivel, N (2010). Biological synthesis of metal nanoparticles by microbes. *Advances in Colloid and Interface Science*, *156*(1–2), 1–13. https://doi.org/10.1016/j.cis.2010.02.001

Naseri, T; Bahaloo-Horeh, N; & Mousavi, S. M (2019). Environmentally friendly recovery of valuable metals from spent coin cells through two-step bioleaching using *Acidithiobacillus thiooxidans*. *Journal of Environmental Management*, *235*(1), 357–367. https://doi.org/10.1016/j.jenvman.2019.01.086

Nayak, R. R; Pradhan, N; Behera, D; Pradhan, K. M; Mishra, S; Sukla, L. B; & Mishra, B. K (2011). Green synthesis of silver nanoparticle by *Penicillium purpurogenum* NPMF: The process and optimization. *Journal of Nanoparticle Research*, *13*(8), 3129–3137. https://doi.org/10.1007/s11051-010-0208-8

Nguyen, T. T. H; Kikuchi, T; Tokunaga, T; Iyoda, S; & Iguchi, A (2021). Diversity of the tellurite resistance gene operon in *Escherichia coli*. *Frontiers in Microbiology*, *12*(May), 1–13. https://doi.org/10.3389/fmicb.2021.681175

Nielsen, P; Fritze, D; & Priest, F. G (1995). Phenetic diversity of alkaliphilic *Bacillus* strains: Proposal for nine new species. *Microbiology*, *141*(7), 1745–1761. https://doi.org/10.1099/13500872-141-7-1745

Ningfei, L; & Hongguan, X (2011). Bioleaching of low grade tellurium sulfide mineral. *Energy Procedia*, *16*(PART B), 946–951. https://doi.org/10.1016/j.egypro.2012.01.151

Nogueira, C. W; Zeni, G; & Rocha, J. B. T (2004). Organoselenium and organotellurium compounds: toxicology and pharmacology. *Chemical Reviews*, *104*(12), 6255–6286. https://doi.org/10.1021/cr0406559

Nuss, P (2019). Losses and environmental aspects of a byproduct metal: Tellurium. *Environmental Chemistry*, *16*(4), 243–250. https://doi.org/10.1071/EN18282

O'Gara, J. P; Gomelsky, M; & Kaplan, S (1997). Identification and molecular genetic analysis of multiple loci contributing to high-level tellurite resistance in *Rhodobacter sphaeroides* 2.4.1. *Applied and Environmental Microbiology*, *63*(12), 4713–4720.

Ogunyemi, S. O; Zhang, M; Abdallah, Y; Ahmed, T; Qiu, W; Ali, M. A; Yan, C; Yang, Y; Chen, J; & Li, B (2020). The bio-synthesis of three metal oxide nanoparticles (ZnO, MnO_2, and MgO) and their antibacterial activity against the bacterial leaf blight pathogen. *Frontiers in Microbiology*, *11*(December), 1–14. https://doi.org/10.3389/fmicb.2020.588326

Ollivier, P. R. L; Bahrou, A. S; Church, T. M; & Hanson, T. E (2011). Aeration controls the reduction and methylation of tellurium by the aerobic, tellurite-resistant marine yeast *Rhodotorula mucilaginosa*. *Applied and Environmental Microbiology*, *77*(13), 4610–4617. https://doi.org/10.1128/AEM.00351-11

Ollivier, P. R. L; Bahrou, A. S; Marcus, S; Cox, T; Church, T. M; & Hanson, T. E (2008). Volatilization and precipitation of tellurium by aerobic, tellurite-resistant marine microbes. *Applied and Environmental Microbiology*, *74*(23), 7163–7173. https://doi.org/10.1128/AEM.00733-08

Orth, D; Grif, K; Dierich, M. P; & Würzner, R (2007). Variability in tellurite resistance and the ter gene cluster among Shiga toxin-producing *Escherichia coli* isolated from humans, animals and food. *Research in Microbiology*, *158*(2), 105–111. https://doi.org/10.1016/j.resmic.2006.10.007

Oves, M; Khan, M. S; & Zaidi, A (2013). Biosorption of heavy metals by B*acillus thuringiensis* strain OSM29 originating from industrial effluent contaminated north Indian soil. *Saudi Journal of Biological Sciences*, *20*(2), 121–129. https://doi.org/10.1016/j.sjbs.2012.11.006

Pal, C; Bengtsson-Palme, J; Rensing, C; Kristiansson, E; & Larsson, D. G. J (2014). BacMet: antibacterial biocide and metal resistance genes database. *Nucleic Acids Research*, *42*(D1), D737–D743. https://doi.org/10.1093/nar/gkt1252

Pfaffl, M. W (2001). A new mathematical model for relative quantification in real-time RT-PCR. *Nucleic Acids Research*, *29*(9), 45e – 45. https://doi.org/10.1093/nar/29.9.e45

Piacenza, E; Presentato, A; Zonaro, E; Lampis, S; Vallini, G; & Turner, R. J (2018). Selenium and tellurium nanomaterials. *Physical Sciences Reviews*, *3*(5). https://doi.org/10.1515/psr-2017-0100

Plaza, D. O; Gallardo, C; Straub, Y. D; Bravo, D; & Pérez-Donoso, J. M (2016). Biological synthesis of fluorescent nanoparticles by cadmium and tellurite resistant Antarctic bacteria: exploring novel natural nanofactories. *Microbial Cell Factories*, *15*(1), 76. https://doi.org/10.1186/s12934-016-0477-8

Ponnusamy, D; Hartson, S. D; & Clinkenbeard, K. D (2011). Intracellular *Yersinia pestis* expresses general stress response and tellurite resistance proteins in mouse macrophages. *Veterinary Microbiology*, *150*(1–2), 146–151. https://doi.org/10.1016/j.vetmic.2010.12.025

Pontieri, P; De Stefano, M; Massardo, D. R; Gunge, N; Miyakawa, I; Sando, N; Pignone, D; Pizzolante, G; Romano, R; Alifano, P; & Del Giudice, L (2015). Tellurium as a valuable tool for studying the prokaryotic origins of mitochondria. *Gene*, *559*(2), 177–183. https://doi.org/10.1016/j.gene.2015.01.060

Prado Acosta, M; Valdman, E; Leite, S. G. F; Battaglini, F; & Ruzal, S. M (2005). Biosorption of copper by *Paenibacillus polymyxa* cells and their exopolysaccharide. *World Journal of Microbiology and Biotechnology*, *21*(6–7), 1157–1163. https://doi.org/10.1007/s11274-005-0381-6

Presentato, A; Piacenza, E; Anikovskiy, M; Cappelletti, M; Zannoni, D; & Turner, R. J (2016). *Rhodococcus aetherivorans* BCP1 as cell factory for the production of intracellular tellurium nanorods under aerobic conditions. *Microbial Cell Factories*, *15*(1), 1–14. https://doi.org/10.1186/s12934-016-0602-8

Presentato, A; Piacenza, E; Darbandi, A; Anikovskiy, M; Cappelletti, M; Zannoni, D; & Turner, R. J (2018). Assembly, growth and conductive properties of tellurium nanorods produced by *Rhodococcus aetherivorans* BCP1. *Scientific Reports*, *8*(1), 2–11. https://doi.org/10.1038/s41598-018-22320-x

Presentato, A; Turner, R. J; Vásquez, C. C; Yurkov, V; & Zannoni, D (2019). Tellurite-dependent blackening of bacteria emerges from the dark ages. *Environmental Chemistry*, *16*(4), 266–288. https://doi.org/10.1071/EN18238

Pugin, B; Cornejo, F. A; Muñoz-Díaz, P; Muñoz-Villagrán, C. M; Vargas-Pérez, J. I; Arenas, F. A; & Vásquez, C. C (2014). Glutathione reductase-mediated synthesis of tellurium-containing nanostructures exhibiting antibacterial properties. *Applied and Environmental Microbiology*, *80*(22), 7061–7070. https://doi.org/10.1128/AEM.02207-14

Rainey, F. A; Ward-Rainey, N; Kroppenstedt, R. M; & Stackebrandt, E (1996). The genus *Nocardiopsis* represents a phylogenetically coherent taxon and a distinct actinomycete lineage: proposal of *Nocardiopsaceae* fam. nov. *Int J Syst Bacteriol*, *46*(4), 1088–1092.

Ramadan, S. E; Razak, A. A; Ragab, A. M; & El-Meleigy, M (1989). Incorporation of tellurium into amino acids and proteins in a tellurium-tolerant fungi. *Biological Trace Element Research*, *20*(3), 225–232. https://doi.org/10.1007/BF02917437

Ramírez, V; Baez, A; López, P; Bustillos, R; Villalobos, M. Á; Carreño, R; Contreras, J. L; Muñoz-Rojas, J; Fuentes, L. E; Martínez, J; & Munive, J. A (2019). Chromium hyper-tolerant *Bacillus* sp. MH778713 assists phytoremediation of heavy metals by mesquite trees (*Prosopis laevigata*). *Frontiers in Microbiology*, *10*. https://doi.org/10.3389/fmicb.2019.01833

Ramos-Ruiz, A; Wilkening, J. V; Field, J. A; & Sierra-Alvarez, R (2017). Leaching of cadmium and tellurium from cadmium telluride (CdTe) thin-film solar panels under simulated landfill conditions. *Journal of Hazardous Materials*, *336*, 57–64. https://doi.org/10.1016/j.jhazmat.2017.04.052

Rangannan, V; & Bansal, M (2010). High-quality annotation of promoter regions for 913 bacterial genomes. *Bioinformatics*, *26*(24), 3043–3050. https://doi.org/10.1093/bioinformatics/btq577

Rappsilber, J; Mann, M; & Ishihama, Y (2007). Protocol for micro-purification, enrichment, pre-fractionation and storage of peptides for proteomics using StageTips. *Nature Protocols*, *2*(8), 1896–1906. https://doi.org/10.1038/nprot.2007.261

Rasoulnia, P; Barthen, R; & Lakaniemi, A. M (2021). A critical review of bioleaching of rare earth elements: The mechanisms and effect of process parameters. *Critical Reviews in Environmental Science and Technology*, *51*(4), 378–427. https://doi.org/10.1080/10643389.2020.1727718

Reinoso, C. A; Appanna, V. D; & Vásquez, C. C (2013). α-ketoglutarate accumulation is not dependent on isocitrate dehydrogenase activity during tellurite detoxification in *Escherichia coli*. *BioMed Research International*, *2013*. https://doi.org/10.1155/2013/784190

Rouxel, O; Fouquet, Y; & Ludden, J. N (2004). Subsurface processes at the lucky strike hydrothermal field, Mid-Atlantic ridge: evidence from sulfur, selenium, and iron isotopes. *Geochimica et Cosmochimica Acta*, *68*(10), 2295–2311. https://doi.org/10.1016/j.gca.2003.11.029

Rutherford, K; Parkhill, J; Crook, J; Horsnell, T; Rice, P; Rajandream, M. A; & Barrell, B (2000). Artemis: sequence visualization and annotation. *Bioinformatics*, *16*(10), 944–945. http://www.ncbi.nlm.nih.gov/pubmed/11120685

Sabaty, M; Avazeri, C; Pignol, D; & Vermeglio, A (2001). Characterization of the reduction of selenate and tellurite by nitrate reductases. *Applied and Environmental Microbiology*, *67*(3–12), 5122–5126. https://doi.org/10.1128/AEM.67.11.5122-5126.2001

Sandoval, J. M; Arenas, F. A; García, J. A; Díaz-Vásquez, W. A; Valdivia-González, M; Sabotier, M; & Vásquez, C. C (2015). *Escherichia coli* 6-phosphogluconate dehydrogenase aids in tellurite resistance by reducing the toxicant in a NADPH-dependent manner. *Microbiological Research*, *177*, 22–27. https://doi.org/10.1016/j.micres.2015.05.002

Sansinenea, E (Ed.) (2012). *Bacillus thuringiensis Biotechnology*. Springer Netherlands. https://doi.org/10.1007/978-94-007-3021-2

Sanssouci, É; Lerat, S; Grondin, G; Shareck, F; & Beaulieu, C (2011). *tdd8*: a TerD domain-encoding gene involved in *Streptomyces coelicolor* differentiation. *Antonie van Leeuwenhoek*, *100*(3), 385–398. https://doi.org/10.1007/s10482-011-9593-y

Segata, N; Börnigen, D; Morgan, X. C; & Huttenhower, C (2013). PhyloPhlAn is a new method for improved phylogenetic and taxonomic placement of microbes. *Nature Communications*, *4*(1), 2304. https://doi.org/10.1038/ncomms3304

Sen, S; Sharma, M; Kumar, V; Muthe, K; Satyam, P; Bhatta, U; Roy, M; Gaur, N; Gupta, S; & Yakhmi, J (2009). Chlorine gas sensors using one-dimensional tellurium nanostructures. *Talanta*, *77*(5), 1567–1572. https://doi.org/10.1016/j.talanta.2008.09.055

Sibanda, T; Selvarajan, R; Msagati, T; Venkatachalam, S; & Meddows-Taylor, S (2019). Defunct gold mine tailings are natural reservoir for unique bacterial communities revealed by high-throughput sequencing analysis. *Science of the Total Environment*, *650*, 2199–2209. https://doi.org/10.1016/j.scitotenv.2018.09.380

Silva, T. P; Matos, J. X; De Oliveira, D; Veiga, J. P; Morais, I; Gonçalves, P; & Albardeiro, L (2020). Mineral Inventory of the Algares 30-Level Adit, Aljustrel Mine, Iberian Pyrite Belt, Portugal. *Minerals*, *10*(10), 853. https://doi.org/10.3390/min10100853

Singh, R; Shedbalkar, U. U; Wadhwani, S. A; & Chopade, B. A (2015). Bacteriagenic silver nanoparticles: synthesis, mechanism, and applications. *Applied Microbiology and Biotechnology*, *99*(11), 4579–4593. https://doi.org/10.1007/s00253-015-6622-1

Solovyev, V; & Salamov, A (2010). Automatic annotation of microbial genomes and metagenomic sequences. In *Metagenomics and its Applications in Agriculture, Biomedicine and Environmental Studies* (pp. 61–78). Nova Science Publishers.

Sredni, B; Geffen-Aricha, R; Duan, W; Albeck, M; Shalit, F; Lander, H. M; Kinor, N; Sagi, O; Albeck, A; Yosef, S; Brodsky, M; Sredni-Kenigsbuch, D; Sonino, T; Longo, D. L; Mattson, M. P; & Yadid, G (2007). Multifunctional tellurium molecule protects and restores dopaminergic neurons in Parkinson's disease models. *The FASEB Journal*, *21*(8), 1870–1883. https://doi.org/10.1096/fj.06-7500com

Srivastava, P; Nikhil, E. V. R; Bragança, J. M; & Kowshik, M (2015). Anti-bacterial TeNPs biosynthesized by haloarcheaon *Halococcus salifodinae* BK3. *Extremophiles : Life under Extreme Conditions*, *19*(4), 875–884. https://doi.org/10.1007/s00792-015-0767-9

Storey, J. D (2002). A direct approach to false discovery rates. *Journal of the Royal Statistical Society: Series B (Statistical Methodology)*, *64*(3), 479–498. https://doi.org/10.1111/1467-9868.00346

Suntharalingam, P; Senadheera, M. D; Mair, R. W; Lévesque, C. M; & Cvitkovitch, D. G (2009). The LiaFSR system regulates the cell envelope stress response in *Streptococcus* mutans. *Journal of Bacteriology*, *191*(9), 2973–2984. https://doi.org/10.1128/JB.01563-08

Suzina, N. E; Duda, V. I; Anisimova, L. A; Dmitriev, V. V; & Boronin, A. M (1995). Cytological aspects of resistance to potassium tellurite conferred on *Pseudomonas* cells by plasmids. *Archives of Microbiology*, *163*(4), 282–285. https://doi.org/10.1007/BF00393381

Tamura, K; Dudley, J; Nei, M; & Kumar, S (2007). MEGA4: Molecular Evolutionary Genetics Analysis (MEGA) software version 4.0. *Mol Biol Evol*, *24*(8), 1596–1599. https://doi.org/10.1093/molbev/msm092

Tanaka, M; Arakaki, A; Staniland, S. S; & Matsunaga, T (2010). Simultaneously discrete biomineralization of magnetite and tellurium nanocrystals in magnetotactic bacteria. *Applied and Environmental Microbiology*, *76*(16), 5526–5532. https://doi.org/10.1128/AEM.00589-10

Taylor, D. E (1999). Bacterial tellurite resistance. *Trends in Microbiology*, *7*(3), 111–115. https://doi.org/10.1016/S0966-842X(99)01454-7

Taylor, D. E; Rooker, M; Keelan, M; Ng, L.-K; Martin, I; Perna, N. T; Burland, N. T. V; & Blattner, F. R (2002). Genomic variability of O islands encoding tellurite resistance in enterohemorrhagic *Escherichia coli* O157:H7 Isolates. *Journal of Bacteriology*, *184*(17), 4690–4698. https://doi.org/10.1128/JB.184.17.4690-4698.2002

Theisen, J; Zylstra, G. J; & Yee, N (2013). Genetic evidence for a molybdopterin-containing tellurate reductase. *Applied and Environmental Microbiology*, *79*(10), 3171–3175. https://doi.org/10.1128/AEM.03996-12

Tomás, J. M; & Kay, W. W (1986). Tellurite susceptibility and non-plasmid-mediated resistance in *Escherichia coli*. *Antimicrobial Agents and Chemotherapy*, *30*(1), 127–131. https://doi.org/10.1128/AAC.30.1.127

Toptchieva, A; Sisson, G; Bryden, L. J; Taylor, D. E; & Hoffman, P. S (2003). An inducible tellurite-resistance operon in *Proteus mirabilis*. *Microbiology*, *149*(5), 1285–1295. https://doi.org/10.1099/mic.0.25981-0

Tsai, W. C; Kuo, T. Y; Lin, C. Y; Lin, J. C; & Chen, W. J (2015). *Photobacterium damselae* subsp. *piscicida* responds to antimicrobial peptides through phage-shock-protein A (PspA)-related extracytoplasmic stress response system. *Journal of Applied Microbiology*, *118*(1), 27–38. https://doi.org/10.1111/jam.12672

Tugarova, A. V; & Kamnev, A. A (2017). Proteins in microbial synthesis of selenium nanoparticles. *Talanta*, *174*, 539–547. https://doi.org/10.1016/j.talanta.2017.06.013

Turner, R. J; Hou, Y; Weiner, J. H; & Taylor, D. E (1992). The arsenical ATPase efflux pump mediates tellurite resistance. *Journal of Bacteriology*, *174*(9), 3092–3094. https://doi.org/10.1128/jb.174.9.3092-3094.1992

Turner, R. J, Weiner, J. H; & Taylor, D. E (1992). Use of diethyldithiocarbamate for quantitative determination of tellurite uptake by bacteria. *Analytical Biochemistry*, *204*(2), 292–295. http://www.ncbi.nlm.nih.gov/pubmed/1332532

Turner, R. J, Weiner, J. H; & Taylor, D. E (1994). In vivo complementation and site-specific mutagenesis of the tellurite resistance determinant *kilAtelAB* from IncPα plasmid RK2Te(r). *Microbiology*, *140*(6), 1319–1326. https://doi.org/10.1099/00221287-140-6-1319

Turner, R. J, Borghese, R; & Zannoni, D (2012). Microbial processing of tellurium as a tool in biotechnology. *Biotechnology Advances*, *30*(5), 954–963. https://doi.org/10.1016/j.biotechadv.2011.08.018

Turner, R J, Weiner, J. H; & Taylor, D. E (1995). The tellurite-resistance determinants t*ehAtehI3* and *k*/*aAk*/*aBte*/*B* have different biochemical requirements. *Microbiology*, *3*, 3133–3140.

Vaigankar, D. C; Dubey, S. K; Mujawar, S. Y; D'Costa, A; & Shyama, S. K (2018). Tellurite biotransformation and detoxification by *Shewanella baltica* with simultaneous synthesis of tellurium nanorods exhibiting photo-catalytic and anti-biofilm activity. *Ecotoxicology and Environmental Safety*, *165*(May), 516–526. https://doi.org/10.1016/j.ecoenv.2018.08.111

Valdivia-González, M. A; Díaz-Vásquez, W. A; Ruiz-León, D; Becerra, A. A; Aguayo, D. R; Pérez-Donoso, J. M; & Vásquez, C. C (2018). A comparative analysis of tellurite detoxification by members of the genus *Shewanella*. *Archives of Microbiology*, *200*(2), 267–273. https://doi.org/10.1007/s00203-017-1438-2

Valkovicova, L; Valkova, D; Vavrova, S; Alekhina, O; Hoang, V. P; Jezna, M; & Turna, J (2011). The role of TerW protein in the tellurite resistance of uropathogenic *Escherichia coli*. *Biologia*, *66*(4), 565–573. https://doi.org/10.2478/s11756-011-0075-5

Vert, M; Doi, Y; Hellwich, K. H; Hess, M; Hodge, P; Kubisa, P; Rinaudo, M; & Schué, F (2012). Terminology for biorelated polymers and applications (IUPAC Recommendations 2012). *Pure and Applied Chemistry*, *84*(2), 377–410. https://doi.org/10.1351/PAC-REC-10-12-04

Voigt, B; & Bradley, J (2020). *Boliden Summary Report Resources and Reserves 2020* Kankberg – Åkulla Östra. https://www.boliden.com/globalassets/operations/exploration/mineral-resources-and-mineral-reserves-pdf/2020/resources-and-reserves-kankberg-2020-12-31.pdf

Walter, E. G; Thomas, C. M; Ibbotson, J. P; & Taylor, D. E (1991). Transcriptional analysis, translational analysis, and sequence of the *kilA*-tellurite resistance region of plasmid RK2Te(r). *Journal of Bacteriology*, *173*(3), 1111–1119. https://doi.org/10.1128/jb.173.3.1111-1119.1991

Walter, E G, & Taylor, D. E (1989). Comparison of tellurite resistance determinants from the IncP alpha plasmid RP4Ter and the IncHII plasmid pHH1508a. *Journal of Bacteriology*, *171*(4), 2160–2165. https://doi.org/10.1128/jb.171.4.2160-2165.1989

Walter, Emily G; Weiner, J. H; & Taylor, D. E (1991). Nucleotide sequence and overexpression of the tellurite-resistance determinant from the IncHII plasmid pHH1508a. *Gene*, *101*(1), 1–7. https://doi.org/10.1016/0378-1119(91)90217-Y

Wang, R; Sens, D. A; Garrett, S; Somjii, S; Sens, M. A; & Lu, X (2007). The resistance of metallothionein to proteolytic digestion: An LC-MS/MS analysis. *Electrophoresis*, *28*(16), 2942–2952. https://doi.org/10.1002/elps.200600835

Wang, Zaicong, & Becker, H (2014). Abundances of sulfur, selenium, tellurium, rhenium and platinum-group elements in eighteen reference materials by isotope dilution sector-field ICP-MS and negative TIMS. *Geostandards and Geoanalytical Research*, n/a-n/a. https://doi.org/10.1111/j.1751-908X.2013.00258.x

Wang, Z; Bu, Y; Zhao, Y; Zhang, Z; Liu, L; & Zhou, H (2018). Morphology-tunable tellurium nanomaterials produced by the tellurite-reducing bacterium *Lysinibacillus* sp. ZYM-1. *Environmental Science and Pollution Research*, *25*(21), 20756–20768. https://doi.org/10.1007/s11356-018-2257-y

Wenzel, M; Kohl, B; Münch, D; Raatschen, N; Albada, H. B; Hamoen, L; Metzler-Nolte, N; Sahl, H. G; & Bandow, J. E (2012). Proteomic response of *Bacillus subtilis* to lantibiotics reflects differences in interaction with the cytoplasmic membrane. *Antimicrobial Agents and Chemotherapy*, *56*(11), 5749–5757. https://doi.org/10.1128/AAC.01380-12

Whelan, K. F; Colleran, E; & Taylor, D. E (1995). Phage inhibition, colicin resistance, and tellurite resistance are encoded by a single cluster of genes on the IncHI2 plasmid R478. *Journal of Bacteriology*, *177*(17), 5016–5027. https://doi.org/10.1128/jb.177.17.5016-5027.1995

Whiteley, J. D; & Murray, F (2005). Determination of platinum group elements (PGE) in environmental samples by ICP-MS: a critical assessment of matrix separation for the mitigation of interferences. *Geochemistry: Exploration, Environment, Analysis*, *5*(1), 3–10. https://doi.org/10.1144/1467-7873/03-035

Yarema, M. C (2005). Acute tellurium toxicity from ingestion of metal-oxidizing solutions. *Pediatrics*, *116*(2), e319–321. https://doi.org/10.1542/peds.2005-0172

Zare, B; Faramarzi, M. A; Sepehrizadeh, Z; Shakibaie, M; Rezaie, S; & Shahverdi, A. R (2012). Biosynthesis and recovery of rod-shaped tellurium nanoparticles and their bactericidal activities. *Materials Research Bulletin*, *47*(11), 3719–3725. https://doi.org/10.1016/j.materresbull.2012.06.034

Zhai, Q; Xiao, Y; Zhao, J; Tian, F; Zhang, H; Narbad, A; & Chen, W (2017). Identification of key proteins and pathways in cadmium tolerance of *Lactobacillus plantarum* strains by proteomic analysis. *Scientific Reports*, *7*(1), 1–17. https://doi.org/10.1038/s41598-017-01180-x1

Zhang, J; Zhang, Y; Richmond, W; & Wang, H (2010). Processing technologies for gold-telluride ores. *Internationa Journal of Minerals, Metallurgy and Materials*, *17*(1), 1–10. https://doi.org/10.1007/s12613-010-0101-6

Zhao, J; & Pring, A (2019). Mineral transformations in Gold–(Silver) tellurides in the presence of fluids: Nature and experiment. *Minerals*, *9*(3). https://doi.org/10.3390/min9030167

Zonaro, E; Piacenza, E; Presentato, A; Monti, F; Anna, R. D; Lampis, S; & Vallini, G (2017). *Ochrobactrum* sp. MPV1 from a dump of roasted pyrites can be exploited as bacterial catalyst for the biogenesis of selenium and tellurium nanoparticles. *Microbial Cell Factories*, 1–17. https://doi.org/10.1186/s12934-017-0826-2

Appendix 1:

Deposited data in public databases. Deposit of strains of relevance to this thesis in culture collection.

Data availability

Strains used in this study were identified and the 16S rRNA sequence were deposited in NCBI – GenBank database, under accession numbers (OK644207-OK644280). Sequences of genetic determinants, from *ter* gene cluster, were deposited in NCBI – GenBank database, under accession numbers (OL344531-OL344548).

Draft genome of strain ALJ109b was deposited at DDBJ/ENA/GenBank under the BioProject number PRJNA606039, BioSample number SAMN14083445, and accession number PRJNA606039. Raw sequences have been deposited in the Sequence Read Archive (SRA) database under the accession number SRR11096018.

Draft genome of strain B1S54.2 3W19 was deposited at DDBJ/ENA/GenBank under the BioProject number PRJNA606037, BioSample number SAMN14083405, and accession number PRJNA606037. Raw sequences have been deposited in the Sequence Read Archive (SRA) database under the accession number SRR11095950.

Strains of interest, used in this study, were deposited in the UCCCB culture collection under the identifiers: *Cellulomonas marina* B2S222 5W10 (UCCCB86), *Bacillus altitudinis* B1S542 3W19 (UCCCB87), *Paenibacillus pabuli* ALJ109b (UCCCB89), *Bacillus safensis* B1S542 10W7 (UCCCB133), *Bacilus mycoides* ALJ98a (UCCCB134), *Mesorhizobium qingshengii* Jales Te58 (UCCCB135), *Mesorhizobium qingshengii* Jales Te59 (UCCCB136), *Bacillus zhangouensis* B2S222 5W24 (UCCCB137) and *Paenibacillus tundrae* ALJ98b (UCCCB138).

The mass spectrometry proteomics raw data and results from analysis by MaxQuant have been deposited to the ProteomeXchange Consortium via the PRIDE partner repository with the dataset identifier PXD017546.

Appendix 2:

Screennig for tellurite resistance, mininmal inhibitory concentration and resistance genes.

Supplementary Table 1. Minimal Inhibitory Concentrations in solid and liquid R2A media, for identified bacterial isolates originating from three mining sites. Symbols: +growth; ± weak growth; - no growth, always compared to control.

Mine	Sample	Strain	Species	Solid media				Liquid media		
				Te (IV) mM				Te (IV) mM		
				0	0.5	1	3	0	0.5	3
Panasqueira mine	Basin 1 core sediments	B1.S5.4.2 5W23	*Bacillus zhangzhouensis*	+	+	+	+	+	-	-
		B1.S4.2.2 10W10	*Paenibacillus etheri*	+	+	+	+	+	-	-
		B1.S5.4.2 5W30	*Paenibacillus lupini*	+	+	+	-	+	-	-
		B1.S5.3.2 10W1	*Bacillus zhangzhouensis*	+	+	+	+	-	-	-
		B1.S5.4.2 10W27	*Bacillus aryabhattai*	+	+	+	-	+	-	-
		B1.S5.4.2 5W4	*Bacillus toyonensis*	+	+	±	-	+	-	-
		B1.S5.4.2 10W15	*Paenibacillus amylolyticus*	+	+	+	±	+	-	-
		B1.S5.4.2 10W28	*Paenibacillus xylanexedens*	+	+	+	+	+	-	-
		B1.S5.4.2 5W10	*Cellulomonas fimi*	+	+	+	+	+	-	-
		B1.S4.2.2 2As4	*Cellulomonas cellasea*	+	±	±	±	+	+	-
		B1.S5.4.2 10W16	*Bacillus simplex*	+	+	±	-	+	-	-
		B1.S5.4.2 5W6	*Fictibacillus enclensis*	+	+	±	-	-	-	-
		B1.S5.4.2 10W32	*Fontibacillus aquaticus*	+	+	±	-	-	-	-
		B1.S5.4.2 5W29	*Paenibacillus xylanexedens*	+	+	+	+	-	-	-
		B1.S5.2.2 10W5	*Paenibacillus xinjiangensis*	+	+	+	-	+	-	-
		B1.S4.2.2 3W7	*Paenibacillus etheri*	+	±	±	-	+	-	-
		B1.S5.4.2 5W33	*Paenibacillus sp.*	+	±	±	±	+	-	-
		B1.S5.4.2 3W20	*Bacillus altitudinis*	+	+	+	-	+	-	-
		B1.S5.3.2 10W7	*Paenibacillus sp.*	+	+	+	+	+	+	-
		B1.S5.3.2 10W12	*Micrococcus aloeverae*	+	+	+	±	+	-	-
		B1.S5.2.2 3W6	*Paenibacillus xinjiangensis*	+	+	+	-	+	-	-
		B1.S4.2.2 3W5	*Paenibacillus etheri*	+	+	+	-	+	-	-
		B1.S5.4.2 10W7	*Bacillus safensis*	+	+	+	+	+	+	+
		B1.S5.4.2 3W19	*Bacillus altitudinis*	+	+	+	+	+	+	+

Supplementary Table 1. (continuation)

Mine	Sample	Strain	Species	Solid media				Liquid media		
				Te (IV) mM				Te (IV) mM		
				0	0.5	1	3	0	0.5	3
Panasqueira mine	Basin 2 core sediments	B2.S2.2.2 5W24	*Bacillus zhangzhouensis*	+	+	+	+	+	+	-
		B2.S2.3.2 10W3	*Actinotalea ferrariae*	+	+	+	+	+	-	-
		B2.S3.2.2 10W11	*Cellulomonas cellasea*	+	±	±	±	+	-	-
		B2.S2.2.2 10W19	*Mesorhizobium qingshengii*	+	+	+	+	+	-	-
		B2.S2.2.2 2As20	*Cellulomonas cellasea*	+	±	±	±	+	-	-
		B2.S2.2.2 5W10	*Cellulomonas marina*	+	±	±	-	+	+	-
		B2.S2.2.2 5W23	*Cellulomonas cellasea*	+	±	±	-	+	-	-
		B2.S3.2.2 2As13	*Cellulomonas cellasea*	+	±	±	±	+	-	-
		B2.S2.4.2 3W3	*Mesorhizobium qingshengii*	+	±	±	±	+	-	-
		B2.S2.3.2 3W12	*Rhodococcus corynebacterioides*	+	+	+	±	+	-	-
		B2.S3.4.2 5W12	*Dermacoccus nishinomiyaensis*	+	±	±	-	+	-	-
		B2.S2.3.2 Ga14	*Staphylococcus warneri*	+	±	+	-	+	-	-
		B2.S3.3.2 5W3	*Actinotalea ferrariae*	+	±	±	-	-	-	-
		B2.S2.2.2 2As1	*Cellulomonas cellasea*	+	+	+	±	+	+	-
		B2.S3.2.2 3W16	*Actinotalea ferrariae*	+	±	±	-	+	-	-
		B2.S3.4.2 2As5	*Bacillus altitudinis*	+	+	+	+	+	+	-
		B2.S2.3.2 10W11	*Psychrobacillus psychrodurans*	+	±	±	-	+	-	-
		B2.S3.4.2 10W7	*Tessaracoccus lapidicaptus*	+	±	±	-	+	-	-
		B2.S3.2.2 2As8	*Flavihumibacter stibioxidans*	+	±	-	-	+	+	-
		B2.S3.3.2 3W8	*Nocardioides pakistanensis*	+	±	±	±	+	-	-
		B2.S3.2.2 2As7	*Cellulomonas cellasea*	+	-	±	±	-	-	-
		B2.S2.3.2 10W1	*Bacillus simplex*	+	+	+	-	+	-	-
		B2.S3.2.2 3W3	*Bacillus zhangzhouensis*	+	+	+	+	-	-	-
		B2.S2.2.2 2As2	*Rhizobium selenitireducens*	+	±	±	±	+	-	-
		B2.S3.2.2 5W2	*Cellulomonas cellasea*	+	±	±	±	+	+	-
		B2.S3.2.2 3W14	*Cellulomonas cellasea*	+	±	±	±	+	-	-
	Water	B2.A1 In2	*Rhodanobacter glycinis*	+	±	+	±	+	-	-
		B2.A2 W2	*Diaphorobacter polyhydroxybutyrativorans*	+	+	+	-	+	+	-
		B2.A1 Ga1	*Serratia glossinae*	+	+	+	±	+	-	-
		B2.A2 0.5Te1	*Tsukamurella strandjordii*	+	+	+	+	+	-	-

Supplementary Table 1. (continuation)

Mine	Sample	Strain	Species	Solid media				Liquid media		
				Te (IV) mM				Te (IV) mM		
				0	0.5	1	3	0	0.5	3
Aljustrel mine	Sediments	ALJ98a	*Bacillus mycoides*	+	+	+	+	+	+	+
		ALJ98b	*Paenibacillus tundrae*	+	+	+	+	+	+	+
		ALJ109b	*Paenibacillus sp.*	+	+	+	+	+	+	+
Jales galery	Sediments	Jales Ga15	*Mesorhizobium qingshengii*	+	+	+	±	+	+	-
		Jales 19	*Mesorhizobium qingshengii*	+	+	+	±	+	-	-
		Jales 26	*Sphingomonas alpina*	+	-	+	-	+	-	-
		Jales W30	*Mesorhizobium qingshengii*	+	±	±	-	-	-	-
		Jales As33	*Mycobacterium montmartrense*	+	+	±	-	+	-	-
		Jales As34	*Mycobacterium montmartrense*	+	+	+	±	+	-	-
		Jales 37	*Sphingomonas oligophenolica*	+	+	+	-	+	-	-
		Jales As35	*Mycobacterium montmartrense*	+	+	±	±	+	-	-
		Jales As7	*Paenibacillus borealis*	+	+	±	-	-	-	-
		Jales W10	*Curtobacterium flaccumfaciens*	+	+	-	±	+	+	-
		Jales W48	*Mycobacterium gilvum*	+	+	±	±	+	-	-
		Jales 20	*Mesorhizobium qingshengii*	+	+	±	±	+	-	-
		Jales 27	*Mesorhizobium qingshengii*	+	+	±	±	+	-	-
		Jales 17	*Mesorhizobium qingshengii*	+	+	±	-	+	-	-
		Jales As13	*Curtobacterium flaccumfaciens*	+	+	-	±	+	-	-
		Jales As8	*Sphingobium aromaticiconvertens*	+	±	±	±	+	-	-
		Jales As46	*Mesorhizobium qingshengii*	+	+	±	-	+	-	-
		Jales Te58	*Mesorhizobium qingshengii*	+	+	+	-	+	+	-
		Jales 44	*Okibacterium fritillariae*	+	±	±	±	+	-	-
		Jales Ga42	*Mycobacterium peregrinum*	+	+	+	-	+	-	-
		Jales As52	*Mesorhizobium qingshengii*	+	+	+	-	+	-	-
		Jales 40	*Mycobacterium sp.*	+	+	±	-	+	-	-
		Jales 54	*Mesorhizobium huakuii*	+	+	±	±	+	-	-
		Jales 51	*Hydrotalea flava*	+	±	±	-	+	-	-
		Jales 62	*Sphingobium sp.*	+	+	+	±	+	-	-
		Jales 50	*Mesorhizobium qingshengii*	+	+	±	-	-	-	-
		Jales 21	*Mycobacterium fortuitum*	+	+	+	±	+	-	-
		Jales Ga6	*Curtobacterium flaccumfaciens*	+	±	-	±	+	+	-
		Jales Te55	*Mesorhizobium qingshengii*	+	+	±	±	+	+	+
		Jales 28	*Mesorhizobium qingshengii*	+	+	±	-	+	-	-
		Jales W3	*Bradyrhizobium cajani*	+	+	±	±	+	-	-
		Jales Te59	*Mesorhizobium qingshengii*	+	+	+	-	+	+	-

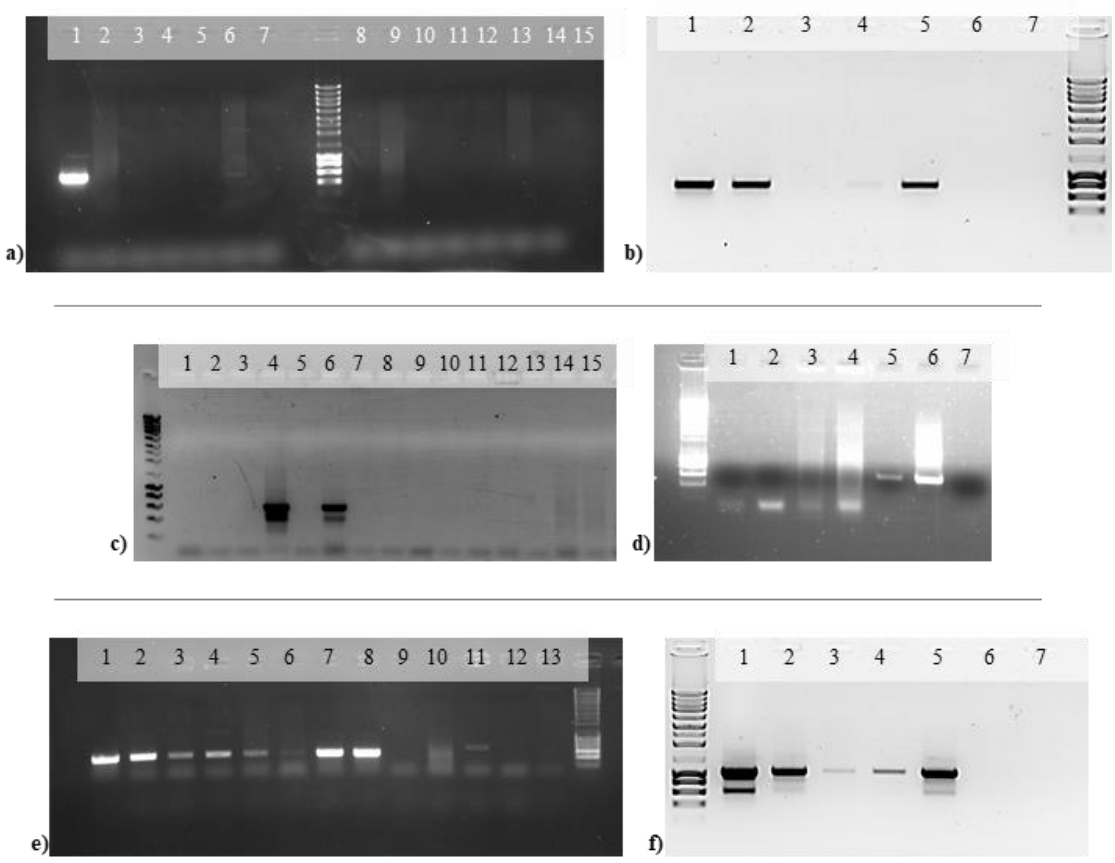

Supplementary Figure 1. Screening for Te^r genes in environmental isolates. PCR for **a)** *terB* gene in isolates: 1 – *Bacillus aerophilus* 3W19; 2 – *Bacillus safensis* 10W7; 3 – *Paenibacillus pumilus* ALJ109b; 4 – *Flavihumibacter stibioxidans* 2As8; 5 – *Bacillus zhangzhouensis* 5W24; 6 – *Diaphorobacter polyhydroxybutyrativorans* B2A2W2; 7 – *Fictibacillus enclensis* 5W6; 8 – *Tsukamurella strandjordii* 0.5Te1; 9 – *Thermomonas brevis* B2A3W6; 10 – *Cellulomonas marina* 5W10; 11 – *Mesorhizobium qingshengii* Jales Te55; 12 – *M. qingshengii* Jales Te59; 13 – *Bacillus mycoides* ALJ98a; 14 – *Paenibacillus taichungensis* ALJ98b; 15 – Negative control. PCR for **b)** *terC* gene in isolates: 1 – *B. aerophilus* 3W19; 2 – *B. safensis* 10W7; 3 – *P. pumilus* ALJ109b; 4 – *F. stibioxidans* 2As8; 5 – *B. zhangzhouensis* 5W24; 6 – *D. polyhydroxybutyrativorans* B2A2W2; 7 – Negative control. PCR for **c)** *terD* gene in isolates: 1 – *T. strandjordii* 0.5Te1; 2 – *T. brevis* B2A3W6; 3 – *D. polyhydroxybutyrativorans* B2A2W2; 4 – *B. mycoides* ALJ98a; 5 – *P. taichungensis* ALJ98b; 6 – *P. pumilus* ALJ109b; 7 – *B. safensis* 10W7; 8 – *B. aerophilus* 3W19; 9 – *F. enclensis* 5W6; 10 – *Bacillus aryabhattai* 10W27b; 11 – *C. marina* 5W10; 12 – *B. zhangzhouensis* 5W24; 13 – *M. qingshengii* Jales Te55; 14 – *M. qingshengii* Jales Te59; 15 – Negative control. PCR for **d)** *terD* gene in isolates:

1 – *F. stibioxidans* 2As8; 2 – *T. brevis* B2A3W6; 3 – *D. polyhydroxybutyrativorans* B2A2W2; 4 – *B. mycoide* ALJ98a; 5 – *B. aerophilus* 3W19; 6 – *P. pumilus* ALJ109b (positive control); 7 – Negative control. PCR for **e)** *terZ* gene: 1 – *B. aerophilus* 3W19; 2 – *B. safensis* 10W7; 3 – *P. pumilus* ALJ109b; 4 – *B. mycoide* ALJ98a; 5 – *M. qingshengii* Jales Te55; 6 – *C. marina* 5W10; 7 – *F. stibioxidans* 2As8; 8 – *B. zhangzhouensis* 5W24; 9 – *D. polyhydroxybutyrativorans* B2A2W2; 10 – *T. strandjordii* 0.5Te1; 11 – *F. enclensis* 5W6; 12 – *B. zhangzhouensis* 5W24; 13 – Negative control. PCR for **f)** *telA* gene in isolates: 1 – *B. aerophilus* 3W19; 2 – *B. safensis* 10W7; 3 – *P. pumilus* ALJ109b; 4 – *F. stibioxidans* 2As8; 5 – *B. zhangzhouensis* 5W24; 6 – *D. polyhydroxybutyrativorans* B2A2W2; 7 – Negative control.

Appendix 3:

Integration of genome and proteomic data for *Paenibacillus pabuli* ALJ109b and *Bacillus altitudinis* 3W19

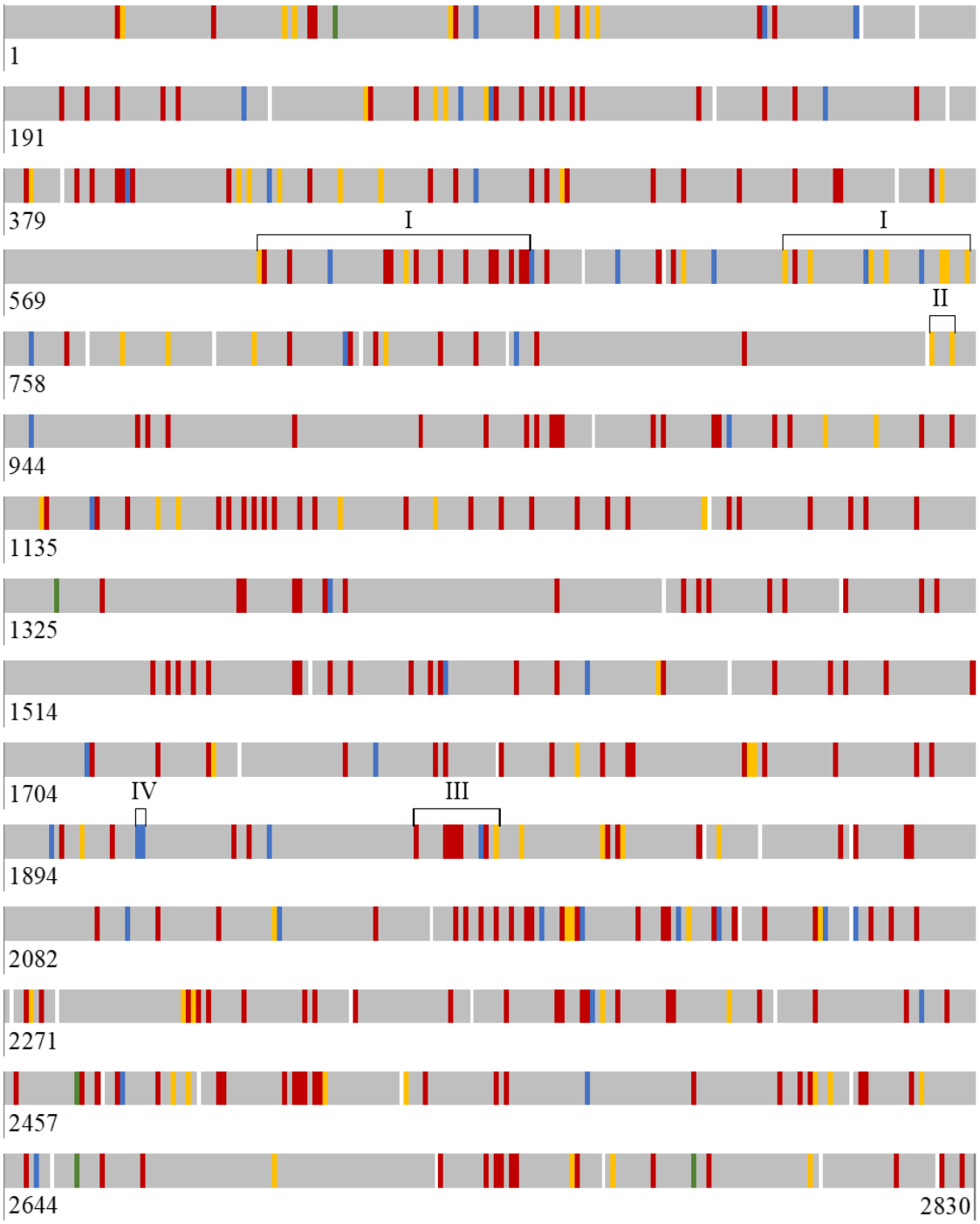

Supplementary Figure 2. Integration of proteomic information in genomic arrangement of *Bacillus altitudinis* 3W19. Genes/ RNA sequences are represented by merged vertical bars, grey – with unaltered expression, with or without Te (IV), blue – over-expressed CDS in the presence of Te (IV), green – exclusively expressed in the presence of Te (IV), yellow – over-expressed CDS in the absence of Te (IV), red – completely inhibited in the presence of Te (IV). Vertical white bars represent end of contig. Functional groups, I – V, were highlighted based on functionally linked genes according to a metabolic function, with increased or decreased overall expression in the presence of Te (IV) (RAST analyses), within a contig. Highlighted features of contiguous and over expressed pathways are detailed in the associated table bellow.

Supplementary Figure 2. Continuation

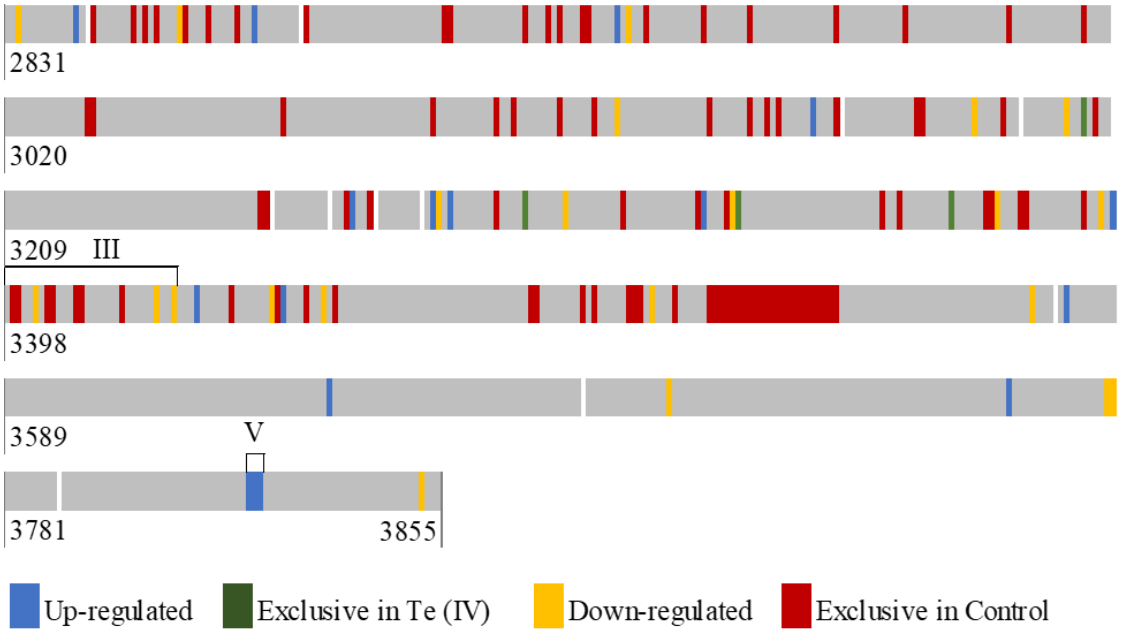

ID	CDS	Description
I	-	DNA processing and Translation
II	Ba_CDS_935 - 939	Oligopeptide transport system - *opp*
III	Ba_CDS_2955-2957	Flagella construction
IV	Ba_CDS_1920-1921	Unknown function
V	Ba_CDS_3822-3824	Te (IV) resistance system

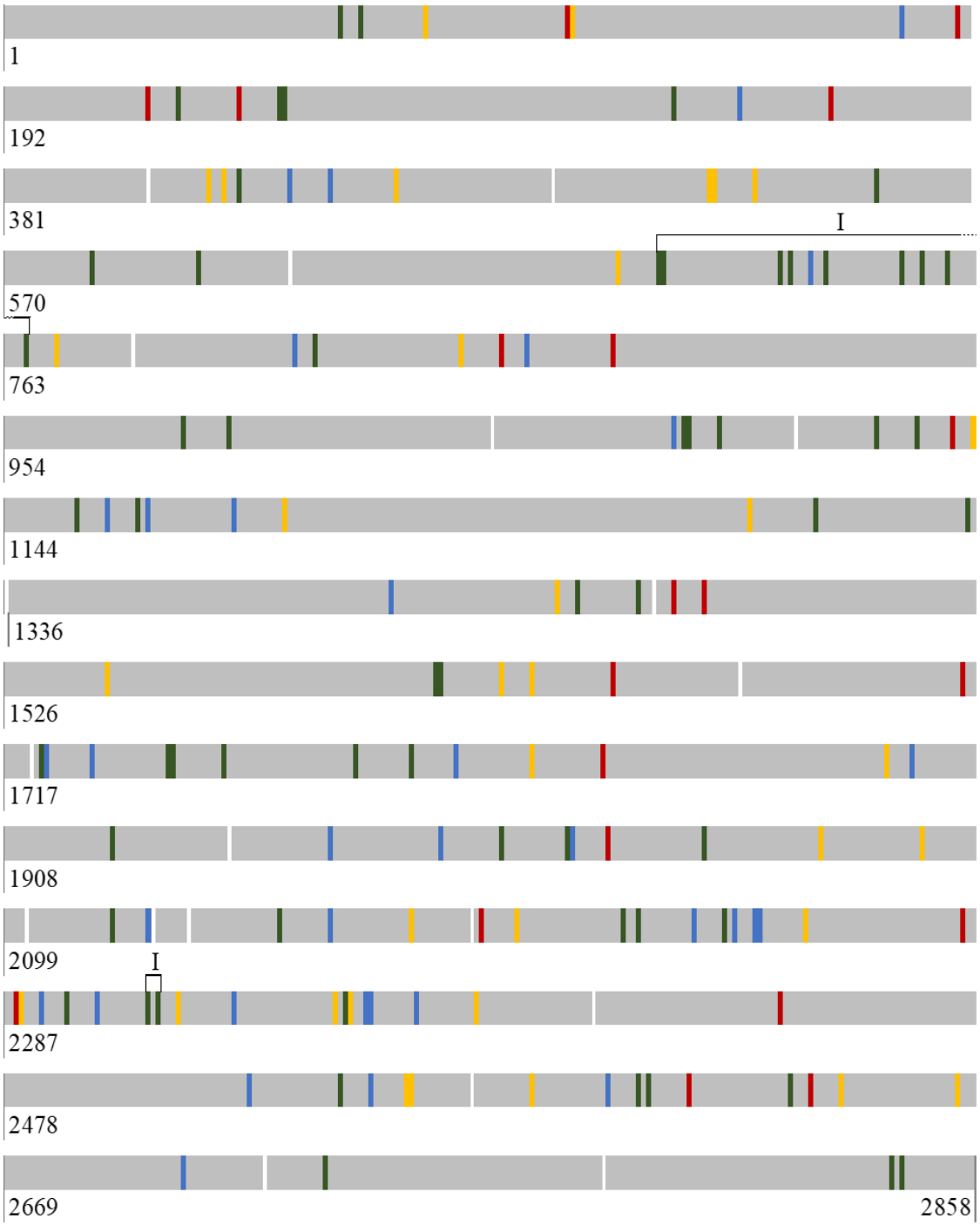

Supplementary Figure 3. Integration of proteomic information in genomic arrangement of *Paenibacillus pabuli* ALJ109b. Genes/ RNA sequences are represented by merged vertical bars, grey – with unaltered expression, with or without Te (IV), blue – over-expressed CDS in the presence of Te (IV), green – exclusively expressed in the presence of Te (IV), yellow – over-expressed CDS in the absence of Te (IV), red – completely inhibited in the presence of Te (IV). Vertical white bars represent end of contig. Functional groups, I – V, were highlighted based on functionally linked genes according to a metabolic function, with increased or decreased overall expression in the presence of Te (IV) (RAST analyses), within a contig. Highlighted features of contiguous and over expressed pathways are detailed in the associated table bellow.

Supplementary Figure 3. Continuation

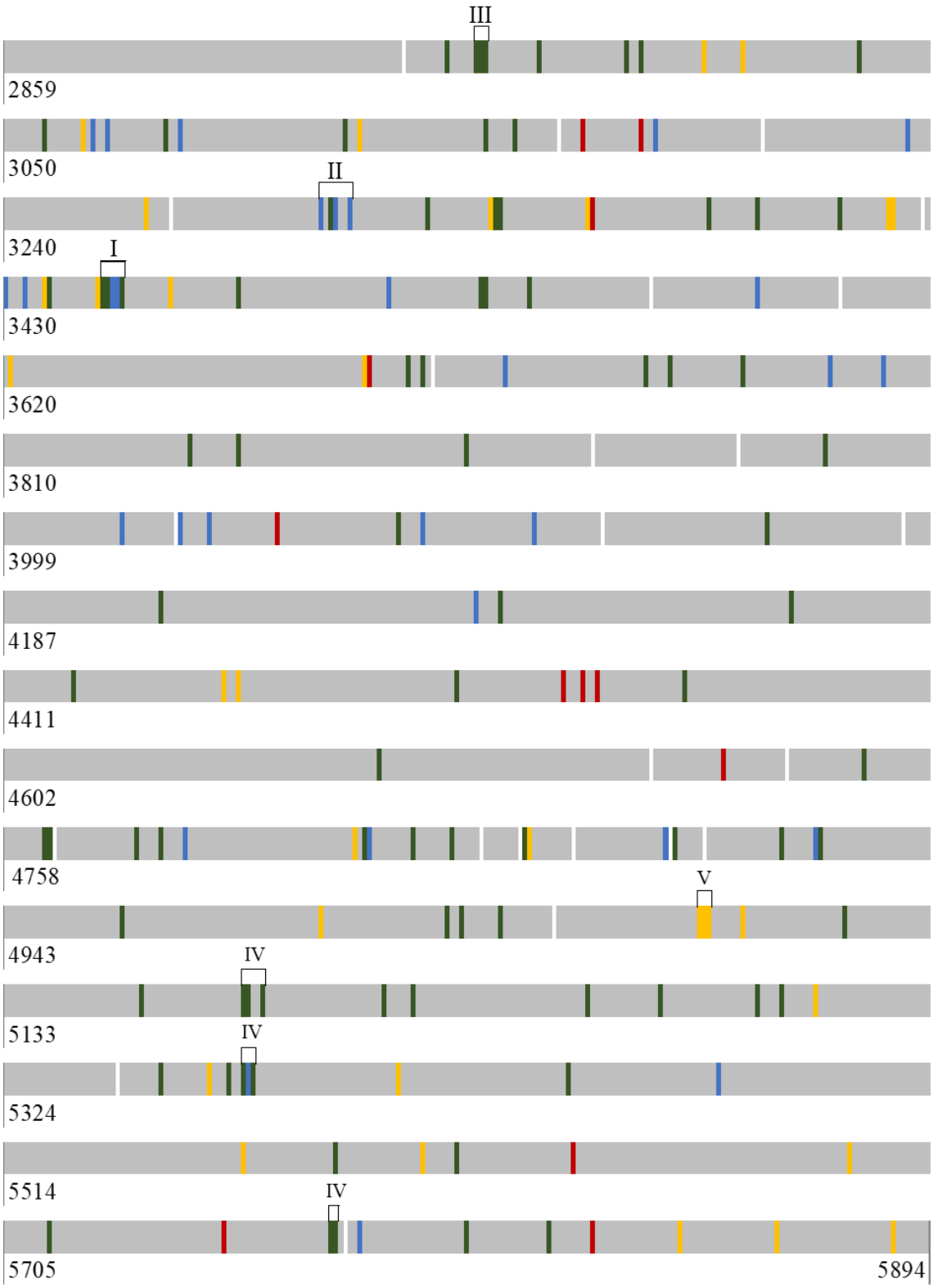

Supplementary Figure 3. Continuation

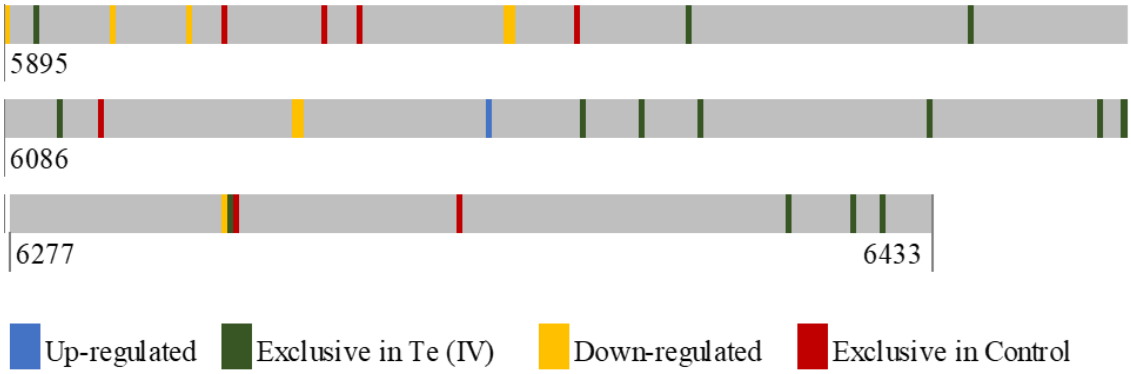

ID	CDS	Description
I		AminoAcid Synthesis
	Pp_CDS 700 701/ 724/ 726/ 730; Pp_CDS 2315/ 2316; Pp_CDS 3451-3453	Lysine biosynthesis; Methionine salvage and synthesis; Threonine and homoserine synthesis
II	Pp_ 3304-3310	*lia* operon
III	Pp_2955-2957	*ars* operon
IV	-	Unknown function

Appendix 4:

Proteomic data generated by LC-MS/MS analysis for *Paenibacillus pabuli* ALJ109b and *Bacillus altitudinis* 3W19.

Supplementary Table 2. *Bacillus altitudinis* 3W19 annotated CDS with significant variation between tested conditions: Control – without Te (IV), Te (IV) – with 5×10^{-4} M Te (IV).

PRT-ID	KO	Definition	Difference log_2	Significance (q-welsh t-test)
Ba_CDS_939	K15580	*oppA*; oligopeptide transport system substrate-binding protein	-5.3	0.000
Ba_CDS_3377	K03106	SRP54; signal recognition particle subunit SRP54 [EC:3.6.5.4]	-4.0	0.000
Ba_CDS_2533	K15973	*mhqR*; MarR family transcriptional regulator. 2-MHQ and catechol-resistance regulon repressor	-3.6	0.000
Ba_CDS_1219	K00925	*ackA*; acetate kinase [EC:2.7.2.1]	-3.4	0.000
Ba_CDS_1996	K07692	*degU*; two-component system. NarL family. response regulator DegU	-3.4	0.000
Ba_CDS_3453	K00962	*pnp*; polyribonucleotide nucleotidyltransferase [EC:2.7.7.8]	-3.3	0.000
Ba_CDS_720	K03043	*rpoB*; DNA-directed RNA polymerase subunit beta [EC:2.7.7.6]	-3.0	0.000
Ba_CDS_3186	K04564	SOD2; superoxide dismutase. Fe-Mn family [EC:1.15.1.1]	-2.8	0.000
Ba_CDS_1115	K00053	*ilvC*; ketol-acid reductoisomerase [EC:1.1.1.86]	-2.8	0.000
Ba_CDS_2833	K01679	E4.2.1.2B; fumC; fumarate hydratase. class II [EC:4.2.1.2]	-2.8	0.000
Ba_CDS_1815	K01744	*aspA*; aspartate ammonia-lyase [EC:4.3.1.1]	-2.5	0.000
Ba_CDS_444	K02945	RP-S1; small subunit ribosomal protein S1	-2.5	0.000
Ba_CDS_1745	K00658	DLST; 2-oxoglutarate dehydrogenase E2 component (dihydrolipoamide succinyltransferase) [EC:2.3.1.61]	-2.4	0.000
Ba_CDS_562	K00004	BDH; (R.R)-butanediol dehydrogenase / meso-butanediol dehydrogenase / diacetyl reductase [EC:1.1.1.4 1.1.1.- 1.1.1.303]	-2.3	0.000
Ba_CDS_2518	K01810	GPI; glucose-6-phosphate isomerase [EC:5.3.1.9]	-2.3	0.000
Ba_CDS_2135	K00615	E2.2.1.1; tktA; transketolase [EC:2.2.1.1]	-2.3	0.000
Ba_CDS_2192	K06412	*spoVG*; stage V sporulation protein G	-2.2	0.003
Ba_CDS_118	K02112	ATPF1B; F-type H+/Na+-transporting ATPase subunit beta [EC:7.1.2.2 7.2.2.1]	-2.2	0.000
Ba_CDS_285	K03885	*ndh*; NADH dehydrogenase [EC:1.6.99.3]	-2.1	0.000
Ba_CDS_700	K03696	*clpC*; ATP-dependent Clp protease ATP-binding subunit ClpC	-2.1	0.000
Ba_CDS_935	K10823	*oppF*; oligopeptide transport system ATP-binding protein	-2.0	0.000
Ba_CDS_3331	K01956	*carA*; carbamoyl-phosphate synthase small subunit [EC:6.3.5.5]	-2.0	0.000
Ba_CDS_3395	K03667	*hslU*; ATP-dependent HslUV protease ATP-binding subunit HslU	-1.9	0.000
Ba_CDS_618	K07015	uncharacterized protein	-1.9	0.001
Ba_CDS_752	K02518	*infA*; translation initiation factor IF-1	-1.8	0.003
Ba_CDS_2193	K04042	*glmU*; bifunctional UDP-N-acetylglucosamine pyrophosphorylase / Glucosamine-1-phosphate N-acetyltransferase [EC:2.7.7.23 2.3.1.157]	-1.8	0.001
Ba_CDS_488	K03768	PPIB; peptidyl-prolyl cis-trans isomerase B (cyclophilin B) [EC:5.2.1.8]	-1.8	0.001
Ba_CDS_277	K00259	*ald*; alanine dehydrogenase [EC:1.4.1.1]	-1.8	0.003
Ba_CDS_116	K02111	ATPF1A; F-type H+/Na+-transporting ATPase subunit alpha [EC:7.1.2.2 7.2.2.1]	-1.7	0.005
Ba_CDS_1850	K00927	PGK; phosphoglycerate kinase [EC:2.7.2.3]	-1.7	0.001
Ba_CDS_737	K02904	RP-L29; large subunit ribosomal protein L29	-1.7	0.005
Ba_CDS_2275	K02818	PTS-Tre-EIIB; PTS system. trehalose-specific IIB component [EC:2.7.1.201]	-1.7	0.004

Ba_CDS_3302	K03531	*ftsZ*; cell division protein FtsZ	-1.7	0.005
Ba_CDS_1272	K13853	*aroG*; 3-deoxy-7-phosphoheptulonate synthase / chorismate mutase [EC:2.5.1.54 5.4.99.5]	-1.7	0.003
Ba_CDS_3126	K02939	RP-L9; large subunit ribosomal protein L9	-1.6	0.005
Ba_CDS_424	K01736	*aroC*; chorismate synthase [EC:4.2.3.5]	-1.6	0.025
Ba_CDS_3852	K01916	*nadE*; NAD+ synthase [EC:6.3.1.5]	-1.6	0.002
Ba_CDS_1909	K00090	*ghrB*; glyoxylate/hydroxypyruvate/2-ketogluconate reductase [EC:1.1.1.79 1.1.1.81 1.1.1.215]	-1.6	0.030
Ba_CDS_725	K02355	*fusA*; elongation factor G	-1.5	0.003
Ba_CDS_756	K03040	*rpoA*; DNA-directed RNA polymerase subunit alpha [EC:2.7.7.6]	-1.5	0.005
Ba_CDS_3427	K02405	*fliA*; RNA polymerase sigma factor for flagellar operon FliA	-1.4	0.005
Ba_CDS_384	K02503	HINT1; histidine triad (HIT) family protein	-1.4	0.005
Ba_CDS_3575	K05937	uncharacterized protein	-1.3	0.006
Ba_CDS_2409	K03624	*greA*; transcription elongation factor GreA	-1.3	0.006
Ba_CDS_89	K00616	E2.2.1.2; transaldolase [EC:2.2.1.2]	-1.3	0.009
Ba_CDS_2489	K06215	*pdxS*; pyridoxal 5'-phosphate synthase pdxS subunit [EC:4.3.3.6]	-1.3	0.006
Ba_CDS_2033	K06207	*typA*; GTP-binding protein	-1.3	0.009
Ba_CDS_2492	K00088	IMPDH; IMP dehydrogenase [EC:1.1.1.205]	-1.3	0.006
Ba_CDS_1164	K01889	FARSA; phenylalanyl-tRNA synthetase alpha chain [EC:6.1.1.20]	-1.3	0.025
Ba_CDS_2633	K00655	*plsC*; 1-acyl-sn-glycerol-3-phosphate acyltransferase [EC:2.3.1.51]	-1.3	0.009
Ba_CDS_740	K02895	RP-L24; large subunit ribosomal protein L24	-1.2	0.008
Ba_CDS_56	K01821	*praC*; 4-oxalocrotonate tautomerase [EC:5.3.2.6]	-1.2	0.010
Ba_CDS_1849	K01803	TPI; triosephosphate isomerase (TIM) [EC:5.3.1.1]	-1.2	0.015
Ba_CDS_2860	K11189	PTS-HPR; phosphocarrier protein	-1.2	0.044
Ba_CDS_2016	K01791	*wecB*; UDP-N-acetylglucosamine 2-epimerase (non-hydrolysing) [EC:5.1.3.14]	-1.2	0.012
Ba_CDS_1142	K00240	*sdhB*; succinate dehydrogenase / fumarate reductase. iron-sulfur subunit [EC:1.3.5.1 1.3.5.4]	-1.2	0.035
Ba_CDS_780	K01661	*menB*; naphthoate synthase [EC:4.1.3.36]	-1.2	0.009
Ba_CDS_452	K00260	*gudB*; glutamate dehydrogenase [EC:1.4.1.2]	-1.2	0.009
Ba_CDS_3509	K06416	*spoVS*; stage V sporulation protein S	-1.2	0.045
Ba_CDS_2304	K00605	*gcvT*; aminomethyltransferase [EC:2.1.2.10]	-1.2	0.015
Ba_CDS_2384	K17472	*cymR*; Rrf2 family transcriptional regulator. cysteine metabolism repressor	-1.2	0.013
Ba_CDS_24	K00625	E2.3.1.8; phosphate acetyltransferase [EC:2.3.1.8]	-1.2	0.012
Ba_CDS_2616	K00055	E1.1.1.90; aryl-alcohol dehydrogenase [EC:1.1.1.90]	-1.2	0.024
Ba_CDS_2241	K02433	*gatA*; aspartyl-tRNA(Asn)/glutamyl-tRNA(Gln) amidotransferase subunit A [EC:6.3.5.6 6.3.5.7]	-1.1	0.017
Ba_CDS_2761	K00627	DLAT; pyruvate dehydrogenase E2 component (dihydrolipoamide acetyltransferase) [EC:2.3.1.12]	-1.1	0.007
Ba_CDS_2216	K01738	*cysK*; cysteine synthase [EC:2.5.1.47]	-1.1	0.010
Ba_CDS_2613	K02406	*fliC*; flagellin	-1.1	0.022
Ba_CDS_1642	K00789	*metK*; S-adenosylmethionine synthetase [EC:2.5.1.6]	-1.1	0.014
Ba_CDS_110	K00761	*upp*; uracil phosphoribosyltransferase [EC:2.4.2.9]	-1.1	0.025
Ba_CDS_2754	K01258	*pepT*; tripeptide aminopeptidase [EC:3.4.11.4]	-1.1	0.046

Ba_CDS_3424	K03408	*cheW*; purine-binding chemotaxis protein CheW	-1.0	0.034
Ba_CDS_3403	K02412	*fliI*; flagellum-specific ATP synthase [EC:3.6.3.50]	-1.0	0.032
Ba_CDS_3280	K02911	RP-L32; large subunit ribosomal protein L32	-1.0	0.018
Ba_CDS_2306	K00283	*gcvPB*; glycine dehydrogenase subunit 2 [EC:1.4.4.2]	-1.0	0.033
Ba_CDS_432	K03530	*hupB*; DNA-binding protein HU-beta	-1.0	0.042
Ba_CDS_647	K09117	uncharacterized protein	-1.0	0.043
Ba_CDS_751	K01265	*map*; methionyl aminopeptidase [EC:3.4.11.18]	-1.0	0.032
Ba_CDS_426	K00940	*ndk*; nucleoside-diphosphate kinase [EC:2.7.4.6]	-1.0	0.037
Ba_CDS_1105	K03978	*engB*; GTP-binding protein	-1.0	0.031
Ba_CDS_2012	K01448	*amiABC*; N-acetylmuramoyl-L-alanine amidase [EC:3.5.1.28]	-1.0	0.033
Ba_CDS_789	K01673	*cynT*; carbonic anhydrase [EC:4.2.1.1]	-1.0	0.030
Ba_CDS_805	K03799	*htpX*; heat shock protein HtpX [EC:3.4.24.-]	-0.9	0.032
Ba_CDS_3703	K03431	*glmM*; phosphoglucosamine mutase [EC:5.4.2.10]	-0.9	0.025
Ba_CDS_3444	K02600	*nusA*; N utilization substance protein A	-0.9	0.045
Ba_CDS_1200	K00873	PK; pyruvate kinase [EC:2.7.1.40]	-0.9	0.033
Ba_CDS_3397	K02387	*flgB*; flagellar basal-body rod protein FlgB	0.9	0.038
Ba_CDS_1903	K01358	*clpP*; ATP-dependent Clp protease. protease subunit [EC:3.4.21.92]	0.9	0.048
Ba_CDS_94	K02909	RP-L31; large subunit ribosomal protein L31	0.9	0.044
Ba_CDS_632	K02968	RP-S20; small subunit ribosomal protein S20	1.0	0.036
Ba_CDS_3580	K05520	*pfpI*; protease I [EC:3.5.1.124]	1.0	0.041
Ba_CDS_238	K10010	*tcyC*; L-cystine transport system ATP-binding protein [EC:7.4.2.1]	1.0	0.025
Ba_CDS_430	K06285	*mtrB*; transcription attenuation protein (tryptophan RNA-binding attenuator protein)	1.1	0.023
Ba_CDS_2195	K02897	RP-L25; large subunit ribosomal protein L25	1.1	0.033
Ba_CDS_2242	K02435	*gatC*; aspartyl-tRNA(Asn)/glutamyl-tRNA(Gln) amidotransferase subunit C [EC:6.3.5.6 6.3.5.7]	1.1	0.045
Ba_CDS_823	K15973	*mhqR*; MarR family transcriptional regulator. 2-MHQ and catechol-resistance regulon repressor	1.1	0.022
Ba_CDS_3279	K07040	uncharacterized protein	1.1	0.030
Ba_CDS_1920	K00384	*trxB*; thioredoxin reductase (NADPH) [EC:1.8.1.9]	1.1	0.044
Ba_CDS_1628	K16920	*ytrE*; acetoin utilization transport system ATP-binding protein	1.1	0.048
Ba_CDS_1600	K06183	*rsuA*; 16S rRNA pseudouridine516 synthase [EC:5.4.99.19]	1.1	0.009
Ba_CDS_1776	K03216	*trmL*; tRNA (cytidine/uridine-2'-O-)-methyltransferase [EC:2.1.1.207]	1.1	0.022
Ba_CDS_3824	K05795	*terD*; tellurium resistance protein TerD	1.2	0.008
Ba_CDS_286	K21567	*fnr*; ferredoxin/flavodoxin---NADP+ reductase [EC:1.18.1.2 1.19.1.1]	1.2	0.006
Ba_CDS_3160	K02338	*dnaN*; DNA polymerase III subunit beta [EC:2.7.7.7]	1.2	0.030
Ba_CDS_2873	K09457	*queF*; 7-cyano-7-deazaguanine reductase [EC:1.7.1.13]	1.2	0.008
Ba_CDS_3326	K02825	*pyrR*; pyrimidine operon attenuation protein / uracil phosphoribosyltransferase [EC:2.4.2.9]	1.2	0.011
Ba_CDS_280	K01255	CARP; leucyl aminopeptidase [EC:3.4.11.1]	1.3	0.007
Ba_CDS_949	K09458	*fabF*; 3-oxoacyl-[acyl-carrier-protein] synthase II [EC:2.3.1.179]	1.3	0.007

Ba_CDS_688	K00537	*arsC1*; arsenate reductase (glutaredoxin) [EC:1.20.4.1]	1.3	0.011
Ba_CDS_1086	K06287	*maf*; septum formation protein	1.3	0.033
Ba_CDS_1720	K03784	*deoD*; purine-nucleoside phosphorylase [EC:2.4.2.1]	1.4	0.011
Ba_CDS_2382	K22132	*tcdA*; tRNA threonylcarbamoyladenosine dehydratase	1.4	0.039
Ba_CDS_3431	K09903	*pyrH*; uridylate kinase [EC:2.7.4.22]	1.4	0.025
Ba_CDS_2934	K01497	*ribA*; GTP cyclohydrolase II [EC:3.5.4.25]	1.4	0.010
Ba_CDS_763	K02996	RP-S9; small subunit ribosomal protein S9	1.4	0.007
Ba_CDS_672	K03527	*ispH*; 4-hydroxy-3-methylbut-2-en-1-yl diphosphate reductase [EC:1.17.7.4]	1.5	0.006
Ba_CDS_471	K06178	*rluB*; 23S rRNA pseudouridine2605 synthase [EC:5.4.99.22]	1.5	0.003
Ba_CDS_2222	K00950	*folK*; 2-amino-4-hydroxy-6-hydroxymethyldihydropteridine diphosphokinase [EC:2.7.6.3]	1.6	0.005
Ba_CDS_2650	K00864	*glpK*; glycerol kinase [EC:2.7.1.30]	1.7	0.004
Ba_CDS_402	K00215	*dapB*; 4-hydroxy-tetrahydrodipicolinate reductase [EC:1.17.1.8]	1.8	0.001
Ba_CDS_747	K02907	RP-L30; large subunit ribosomal protein L30	1.9	0.016
Ba_CDS_1988	K02396	*flgK*; flagellar hook-associated protein 1 FlgK	1.9	0.001
Ba_CDS_350	K19285	*nfrA1*; FMN reductase (NADPH) [EC:1.5.1.38]	1.9	0.000
Ba_CDS_706	K09698	*gltX*; nondiscriminating glutamyl-tRNA synthetase [EC:6.1.1.24]	1.9	0.001
Ba_CDS_151	K02392	*flgG*; flagellar basal-body rod protein FlgG	2.0	0.001
Ba_CDS_2479	K09747	YbaB/EbfC fam; Nucleoid-associated protein	2.0	0.000
Ba_CDS_3267	K06726	*rbsD*; D-ribose pyranase [EC:5.4.99.62]	2.1	0.003
Ba_CDS_736	K02878	RP-L16; large subunit ribosomal protein L16	2.2	0.004
Ba_CDS_2214	K04083	*hslO*; molecular chaperone Hsp33	2.2	0.001
Ba_CDS_2843	K03969	*pspA*; phage shock protein A	2.3	0.000
Ba_CDS_1152	K03521	*fixA*; electron transfer flavoprotein beta subunit	2.4	0.000
Ba_CDS_1389	K04757	*rsbW*; serine/threonine-protein kinase RsbW [EC:2.7.11.1]	2.5	0.000
Ba_CDS_3823	K05795	*terD*; tellurium resistance protein TerD	2.9	0.000
Ba_CDS_2106	K03741	*arsC2*; arsenate reductase (thioredoxin) [EC:1.20.4.4]	3.0	0.000
Additional 16 unidentified and unassigned (KO) proteins have significant change in abundance, five with over regulation in the presence of Te (IV) 5×10^{-4} M and 11 down regulated in the presence of Te (IV) 5×10^{-4} M				

Supplementary Table 3. *Bacillus altitudinis* 3W19 annotated CDS exclusive in either tested condition: Control – without Te (IV), Te (IV) – with 5×10^{-4} M Te (IV).

PRT-ID	KO	Definition	Test
Ba_CDS_2657	K16509	*spxA*; regulatory protein spx	Te (IV)
Ba_CDS_2777	K03569	*mreB*; rod shape-determining protein MreB and related proteins	Te (IV)
Ba_CDS_3204	K22109	*gbsR*; HTH-type transcriptional regulator, glycine betaine synthesis regulator	Te (IV)
Ba_CDS_3295	K02563	*murG*; UDP-N-acetylglucosamine--N-acetylmuramyl-(pentapeptide) pyrophosphoryl-undecaprenol N-acetylglucosamine transferase [EC:2.4.1.227]	Te (IV)
Ba_CDS_3332	K01955	*carB*; carbamoyl-phosphate synthase large subunit [EC:6.3.5.5]	Te (IV)
Ba_CDS_3369	K03621	*plsX*; phosphate acyltransferase [EC:2.3.1.274]	Te (IV)
Ba_CDS_23	K00435	*hemQ*; Fe-coproporphyrin III decarboxylase [EC:1.11.1.-]	Control
Ba_CDS_61	K00797	*speE*; spermidine synthase [EC:2.5.1.16]	Control
Ba_CDS_62	K01480	*speB*; agmatinase [EC:3.5.3.11]	Control
Ba_CDS_90	K00790	*murA*; UDP-N-acetylglucosamine 1-carboxyvinyltransferase [EC:2.5.1.7]	Control
Ba_CDS_114	K02109	ATPF0B; F-type H+-transporting ATPase subunit b	Control
Ba_CDS_150	K02392	*flgG*; flagellar basal-body rod protein FlgG	Control
Ba_CDS_153	K02372	*fabZ*; 3-hydroxyacyl-[acyl-carrier-protein] dehydratase [EC:4.2.1.59]	Control
Ba_CDS_202	K00318	PRODH; proline dehydrogenase [EC:1.5.-.-]	Control
Ba_CDS_207	K02424	*fliY*; L-cystine transport system substrate-binding protein	Control
Ba_CDS_213	K03406	*mcp*; methyl-accepting chemotaxis protein	Control
Ba_CDS_291	K13628	*iscA*; iron-sulfur cluster assembly protein	Control
Ba_CDS_295	K03885	*ndh*; NADH dehydrogenase [EC:1.6.99.3]	Control
Ba_CDS_301	K01733	*thrC*; threonine synthase [EC:4.2.3.1]	Control
Ba_CDS_303	K00015	*gyaR*; glyoxylate reductase [EC:1.1.1.26]	Control
Ba_CDS_326	K02016	ABC.FEV.S; iron complex transport system substrate-binding protein	Control
Ba_CDS_344	K02826	*qoxA*; cytochrome aa3-600 menaquinol oxidase subunit II [EC:7.1.1.5]	Control
Ba_CDS_383	K00831	*serC*; phosphoserine aminotransferase [EC:2.6.1.52]	Control
Ba_CDS_395	K01918	*panC*; pantoate--beta-alanine ligase [EC:6.3.2.1]	Control
Ba_CDS_400	K01463	*bshB1*; N-acetylglucosamine malate deacetylase 1 [EC:3.5.1.-]	Control
Ba_CDS_401	K01734	*mgsA*; methylglyoxal synthase [EC:4.2.3.3]	Control
Ba_CDS_422	K06208	*aroH*; chorismate mutase [EC:5.4.99.5]	Control
Ba_CDS_438	K03977	*engA*; GTPase	Control
Ba_CDS_462	K00058	*serA*; D-3-phosphoglycerate dehydrogenase / 2-oxoglutarate reductase [EC:1.1.1.95 1.1.1.399]	Control
Ba_CDS_467	K07775	*resD*; two-component system, OmpR family, response regulator ResD	Control
Ba_CDS_482	K14652	*ribBA*; 3,4-dihydroxy 2-butanone 4-phosphate synthase / GTP cyclohydrolase II [EC:4.1.99.12 3.5.4.25]	Control
Ba_CDS_506	K03711	*fur*; Fur family transcriptional regulator, ferric uptake regulator	Control
Ba_CDS_512	K01515	*nudF*; ADP-ribose pyrophosphatase [EC:3.6.1.13]	Control
Ba_CDS_534	K00286	*proC*; pyrroline-5-carboxylate reductase [EC:1.5.1.2]	Control
Ba_CDS_543	K00784	*rnz*; ribonuclease Z [EC:3.1.26.11]	Control
Ba_CDS_619	K06948	*yqeH*; 30S ribosome assembly GTPase	Control
Ba_CDS_624	K09710	*ybeB*; ribosome-associated protein	Control
Ba_CDS_643	K09761	*rsmE*; 16S rRNA (uracil1498-N3)-methyltransferase [EC:2.1.1.193]	Control

Ba_CDS_644	K18707	*mtaB*; threonylcarbamoyladenosine tRNA methylthiotransferase MtaB [EC:2.8.4.5]	Control
Ba_CDS_654	K06217	*phoH*; phosphate starvation-inducible protein PhoH and related proteins	Control
Ba_CDS_659	K03595	*era*; GTPase	Control
Ba_CDS_665	K09773	*ppsR*; [pyruvate, water dikinase]-phosphate phosphotransferase / [pyruvate, water dikinase] kinase [EC:2.7.4.28 2.7.11.33]	Control
Ba_CDS_668	K03086	*rpoD*; RNA polymerase primary sigma factor	Control
Ba_CDS_670	K06967	*trmK*; tRNA (adenine22-N1)-methyltransferase [EC:2.1.1.217]	Control
Ba_CDS_675	K01151	*nfo*; deoxyribonuclease IV [EC:3.1.21.2]	Control
Ba_CDS_696	K02073	*metQ*; D-methionine transport system substrate-binding protein	Control
Ba_CDS_698	K19411	*mcsA*; protein arginine kinase activator	Control
Ba_CDS_722	K07590	RP-L7A; large subunit ribosomal protein L7A	Control
Ba_CDS_770	K03593	*mrp*; ATP-binding protein involved in chromosome partitioning	Control
Ba_CDS_812	K00567	*ogt*; methylated-DNA-[protein]-cysteine S-methyltransferase [EC:2.1.1.63]	Control
Ba_CDS_824	K02557	*motB*; chemotaxis protein MotB	Control
Ba_CDS_899	K00266	*gltD*; glutamate synthase (NADPH) small chain [EC:1.4.1.13]	Control
Ba_CDS_970	K21064	*ycsE*; 5-amino-6-(5-phospho-D-ribitylamino)uracil phosphatase [EC:3.1.3.104]	Control
Ba_CDS_1026	K02016	ABC.FEV.S; iron complex transport system substrate-binding protein	Control
Ba_CDS_1039	K06595	*hemAT*; heam-based aerotactic trancducer	Control
Ba_CDS_1052	K00231	PPOX; protoporphyrinogen/coproporphyrinogen III oxidase [EC:1.3.3.4 1.3.3.15]	Control
Ba_CDS_1053	K01772	*hemH*; protoporphyrin/coproporphyrin ferrochelatase [EC:4.99.1.1 4.99.1.9]	Control
Ba_CDS_1054	K01599	*hemE*; uroporphyrinogen decarboxylase [EC:4.1.1.37]	Control
Ba_CDS_1071	K04518	*pheA2*; prephenate dehydratase [EC:4.2.1.51]	Control
Ba_CDS_1073	K03979	*obgE*; GTPase [EC:3.6.5.-]	Control
Ba_CDS_1083	K03570	*mreC*; rod shape-determining protein MreC	Control
Ba_CDS_1084	K03569	*mreB*; rod shape-determining protein MreB and related proteins	Control
Ba_CDS_1095	K01845	*hemL*; glutamate-1-semialdehyde 2,1-aminomutase [EC:5.4.3.8]	Control
Ba_CDS_1098	K01749	*hemC*; hydroxymethylbilane synthase [EC:2.5.1.61]	Control
Ba_CDS_1124	K03367	*dltA*; D-alanine--poly(phosphoribitol) ligase subunit 1 [EC:6.1.1.13]	Control
Ba_CDS_1130	K07095	uncharacterized protein	Control
Ba_CDS_1143	K00239	*sdhA*; succinate dehydrogenase / fumarate reductase, flavoprotein subunit [EC:1.3.5.1 1.3.5.4]	Control
Ba_CDS_1153	K13767	*fadB*; enoyl-CoA hydratase [EC:4.2.1.17]	Control
Ba_CDS_1158	K07456	*mutS2*; DNA mismatch repair protein MutS2	Control
Ba_CDS_1176	K07025	putative hydrolase of the HAD superfamily	Control
Ba_CDS_1178	K01868	TARS; threonyl-tRNA synthetase [EC:6.1.1.3]	Control
Ba_CDS_1181	K11144	*dnaI*; primosomal protein DnaI	Control
Ba_CDS_1183	K07738	*nrdR*; transcriptional repressor NrdR	Control
Ba_CDS_1185	K01611	*speD*; S-adenosylmethionine decarboxylase [EC:4.1.1.50]	Control
Ba_CDS_1187	K00859	*coaE*; dephospho-CoA kinase [EC:2.7.1.24]	Control
Ba_CDS_1192	K07658	*phoB1*; two-component system, OmpR family, alkaline phosphatase synthesis response regulator PhoP	Control
Ba_CDS_1195	K01647	CS; citrate synthase [EC:2.3.3.1]	Control
Ba_CDS_1226	K00858	*ppnK*; NAD+ kinase [EC:2.7.1.23]	Control
Ba_CDS_1232	K02016	ABC.FEV.S; iron complex transport system substrate-binding protein	Control

Ba_CDS_1238	K11632	*bceB*; bacitracin transport system permease protein	Control
Ba_CDS_1247	K01895	ACSS; acetyl-CoA synthetase [EC:6.2.1.1]	Control
Ba_CDS_1253	K06286	*ezrA*; septation ring formation regulator	Control
Ba_CDS_1257	K08968	*msrC*; L-methionine (R)-S-oxide reductase [EC:1.8.4.14]	Control
Ba_CDS_1278	K16961	*yxeM*; putative S-methylcysteine transport system substrate-binding protein	Control
Ba_CDS_1303	K02798	PTS-Mtl-EIIA; PTS system, mannitol-specific IIA component [EC:2.7.1.197]	Control
Ba_CDS_1344	K03169	*topB*; DNA topoisomerase III [EC:5.99.1.2]	Control
Ba_CDS_1371	K01921	*ddl*; D-alanine-D-alanine ligase [EC:6.3.2.4]	Control
Ba_CDS_1372	K01929	*murF*; UDP-N-acetylmuramoyl-tripeptide--D-alanyl-D-alanine ligase [EC:6.3.2.10]	Control
Ba_CDS_1382	K07723	*ndoAI*; CopG family transcriptional regulator / antitoxin EndoAI	Control
Ba_CDS_1383	K07171	*mazF*; mRNA interferase MazF [EC:3.1.-.-]	Control
Ba_CDS_1388	K04749	*rsbV*; anti-sigma B factor antagonist	Control
Ba_CDS_1392	K06959	*tex*; protein Tex	Control
Ba_CDS_1460	K10112	*msmX*; multiple sugar transport system ATP-binding protein	Control
Ba_CDS_1477	K03698	*cbf*; 3'-5' exoribonuclease [EC:3.1.-.-]	Control
Ba_CDS_1488	K00946	*thiL*; thiamine-monophosphate kinase [EC:2.7.4.16]	Control
Ba_CDS_1506	K07260	*vanY*; zinc D-Ala-D-Ala carboxypeptidase [EC:3.4.17.14]	Control
Ba_CDS_1543	K01588	*purE*; 5-(carboxyamino)imidazole ribonucleotide mutase [EC:5.4.99.18]	Control
Ba_CDS_1546	K01923	*purC*; phosphoribosylaminoimidazole-succinocarboxamide synthase [EC:6.3.2.6]	Control
Ba_CDS_1548	K01952	*purL*; phosphoribosylformylglycinamidine synthase [EC:6.3.5.3]	Control
Ba_CDS_1551	K01933	*purM*; phosphoribosylformylglycinamidine cyclo-ligase [EC:6.3.3.1]	Control
Ba_CDS_1554	K01945	*purD*; phosphoribosylamine---glycine ligase [EC:6.3.4.13]	Control
Ba_CDS_1571	K01972	E6.5.1.2; DNA ligase (NAD+) [EC:6.5.1.2]	Control
Ba_CDS_1577	K01924	*murC*; UDP-N-acetylmuramate--alanine ligase [EC:6.3.2.8]	Control
Ba_CDS_1597	K01439	*dapE*; succinyl-diaminopimelate desuccinylase [EC:3.5.1.18]	Control
Ba_CDS_1622	K01869	LARS; leucyl-tRNA synthetase [EC:6.1.1.4]	Control
Ba_CDS_1643	K01610	E4.1.1.49; phosphoenolpyruvate carboxykinase (ATP) [EC:4.1.1.49]	Control
Ba_CDS_1678	K01938	*fhs*; formate--tetrahydrofolate ligase [EC:6.3.4.3]	Control
Ba_CDS_1703	K12267	*msrAB*; peptide methionine sulfoxide reductase msrA/msrB [EC:1.8.4.11 1.8.4.12]	Control
Ba_CDS_1721	K07260	*vanY*; zinc D-Ala-D-Ala carboxypeptidase [EC:3.4.17.14]	Control
Ba_CDS_1744	K00164	OGDH; 2-oxoglutarate dehydrogenase E1 component [EC:1.2.4.2]	Control
Ba_CDS_1770	K03809	*wrbA*; NAD(P)H dehydrogenase (quinone) [EC:1.6.5.2]	Control
Ba_CDS_1788	K01740	*metY*; O-acetylhomoserine (thiol)-lyase [EC:2.5.1.49]	Control
Ba_CDS_1790	K19005	*ltaS*; lipoteichoic acid synthase [EC:2.7.8.20]	Control
Ba_CDS_1810	K19975	*mntC*; manganese/zinc transport system substrate-binding protein	Control
Ba_CDS_1820	K21600	*csoR*; CsoR family transcriptional regulator, copper-sensing transcriptional repressor	Control
Ba_CDS_1825	K03664	*smpB*; SsrA-binding protein	Control
Ba_CDS_1826	K12573	*rnr*; ribonuclease R [EC:3.1.-.-]	Control
Ba_CDS_1848	K15633	*gpmI*; 2,3-bisphosphoglycerate-independent phosphoglycerate mutase [EC:5.4.2.12]	Control
Ba_CDS_1852	K05311	*cggR*; central glycolytic genes regulator	Control
Ba_CDS_1866	K15584	*nikA*; nickel transport system substrate-binding protein	Control
Ba_CDS_1882	K02016	ABC.FEV.S; iron complex transport system substrate-binding protein	Control

Ba_CDS_1885	K22278	*pdgA*; peptidoglycan-N-acetylglucosamine deacetylase [EC:3.5.1.104]	Control
Ba_CDS_1915	K11184	*chr*; catabolite repression HPr-like protein	Control
Ba_CDS_1939	K06023	*hprK*; HPr kinase/phosphorylase [EC:2.7.11.- 2.7.4.-]	Control
Ba_CDS_1942	K03710	GntR family transcriptional regulator	Control
Ba_CDS_1975	K02836	*prfB*; peptide chain release factor 2	Control
Ba_CDS_1981	K02422	*fliS*; flagellar protein FliS	Control
Ba_CDS_1982	K02407	*fliD*; flagellar hook-associated protein 2	Control
Ba_CDS_1983	K06603	*flaG*; flagellar protein FlaG	Control
Ba_CDS_1984	K03563	*csrA*; carbon storage regulator	Control
Ba_CDS_2030	K01227	E3.2.1.96; mannosyl-glycoprotein endo-beta-N-acetylglucosaminidase [EC:3.2.1.96]	Control
Ba_CDS_2056	K01809	*manA*; mannose-6-phosphate isomerase [EC:5.3.1.8]	Control
Ba_CDS_2058	K00381	*cysI*; sulfite reductase (NADPH) hemoprotein beta-component [EC:1.8.1.2]	Control
Ba_CDS_2069	K08302	*gatY-kbaY*; tagatose 1,6-diphosphate aldolase GatY/KbaY [EC:4.1.2.40]	Control
Ba_CDS_2112	K02621	*parC*; topoisomerase IV subunit A [EC:5.99.1.-]	Control
Ba_CDS_2124	K01681	ACO; aconitate hydratase [EC:4.2.1.3]	Control
Ba_CDS_2155	K19267	*qorB*; NAD(P)H dehydrogenase (quinone) [EC:1.6.5.2]	Control
Ba_CDS_2170	K00943	*tmk*; dTMP kinase [EC:2.7.4.9]	Control
Ba_CDS_2172	K09770	uncharacterized protein	Control
Ba_CDS_2178	K07056	*rsmI*; 16S rRNA (cytidine1402-2'-O)-methyltransferase [EC:2.1.1.198]	Control
Ba_CDS_2181	K01874	MARS; methionyl-tRNA synthetase [EC:6.1.1.10]	Control
Ba_CDS_2184	K05985	*rnmV*; ribonuclease M5 [EC:3.1.26.8]	Control
Ba_CDS_2185	K02528	*ksgA*; 16S rRNA (adenine1518-N6/adenine1519-N6)-dimethyltransferase [EC:2.1.1.182]	Control
Ba_CDS_2191	K09022	*ridA*; 2-iminobutanoate/2-iminopropanoate deaminase [EC:3.5.99.10]	Control
Ba_CDS_2194	K00948	PRPS; ribose-phosphate pyrophosphokinase [EC:2.7.6.1]	Control
Ba_CDS_2206	K07571	S1 RNA binding domain protein	Control
Ba_CDS_2211	K00760	*hprT*; hypoxanthine phosphoribosyltransferase [EC:2.4.2.8]	Control
Ba_CDS_2212	K03798	*ftsH*; cell division protease FtsH [EC:3.4.24.-]	Control
Ba_CDS_2221	K01633	*folB*; 7,8-dihydroneopterin aldolase/epimerase/oxygenase [EC:4.1.2.25 5.1.99.8 1.13.11.81]	Control
Ba_CDS_2225	K04567	KARS; lysyl-tRNA synthetase, class II [EC:6.1.1.6]	Control
Ba_CDS_2240	K02434	*gatB*; aspartyl-tRNA(Asn)/glutamyl-tRNA(Gln) amidotransferase subunit B [EC:6.3.5.6 6.3.5.7]	Control
Ba_CDS_2250	K05823	*dapL*; N-acetyldiaminopimelate deacetylase [EC:3.5.1.47]	Control
Ba_CDS_2254	K03839	*fldA*; flavodoxin I	Control
Ba_CDS_2274	K01226	*treC*; trehalose-6-phosphate hydrolase [EC:3.2.1.93]	Control
Ba_CDS_2277	K03406	*mcp*; methyl-accepting chemotaxis protein	Control
Ba_CDS_2305	K00282	*gcvPA*; glycine dehydrogenase subunit 1 [EC:1.4.4.2]	Control
Ba_CDS_2315	K01262	*pepP*; Xaa-Pro aminopeptidase [EC:3.4.11.9]	Control
Ba_CDS_2327	K01961	*accC*; acetyl-CoA carboxylase, biotin carboxylase subunit [EC:6.4.1.2 6.3.4.14]	Control
Ba_CDS_2329	K03625	*nusB*; N utilization substance protein B	Control
Ba_CDS_2336	K01299	E3.4.17.19; carboxypeptidase Taq [EC:3.4.17.19]	Control
Ba_CDS_2355	K05366	*mrcA*; penicillin-binding protein 1A [EC:2.4.1.129 3.4.16.4]	Control
Ba_CDS_2365	K00773	*tgt*; queuine tRNA-ribosyltransferase [EC:2.4.2.29]	Control
Ba_CDS_2375	K00759	APRT; adenine phosphoribosyltransferase [EC:2.4.2.7]	Control

Ba_CDS_2376	K00951	*relA*; GTP pyrophosphokinase [EC:2.7.6.5]	Control
Ba_CDS_2380	K01892	HARS; histidyl-tRNA synthetase [EC:6.1.1.21]	Control
Ba_CDS_2381	K01876	*aspS*; aspartyl-tRNA synthetase [EC:6.1.1.12]	Control
Ba_CDS_2397	K01872	AARS; alanyl-tRNA synthetase [EC:6.1.1.7]	Control
Ba_CDS_2415	K17216	*mccA*; cystathionine beta-synthase (O-acetyl-L-serine) [EC:2.5.1.134]	Control
Ba_CDS_2425	K01512	*acyP*; acylphosphatase [EC:3.6.1.7]	Control
Ba_CDS_2451	K15738	*uup*; ABC transport system ATP-binding/permease protein	Control
Ba_CDS_2459	K21467	*pbpC*; penicillin-binding protein 3	Control
Ba_CDS_2475	K01222	E3.2.1.86A; 6-phospho-beta-glucosidase [EC:3.2.1.86]	Control
Ba_CDS_2478	K06187	*recR*; recombination protein RecR	Control
Ba_CDS_2497	K02056	ABC.SS.A; simple sugar transport system ATP-binding protein [EC:3.6.3.17]	Control
Ba_CDS_2498	K07335	*bmpA*; basic membrane protein A and related proteins	Control
Ba_CDS_2513	K10907	aminotransferase [EC:2.6.1.-]	Control
Ba_CDS_2514	K07570	GSP13; general stress protein 13	Control
Ba_CDS_2516	K19955	*adh2*; alcohol dehydrogenase [EC:1.1.1.-]	Control
Ba_CDS_2517	K19955	*adh2*; alcohol dehydrogenase [EC:1.1.1.-]	Control
Ba_CDS_2551	K00549	*metE*; 5-methyltetrahydropteroyltriglutamate--homocysteine methyltransferase [EC:2.1.1.14]	Control
Ba_CDS_2590	K21417	*acoB*; acetoin:2,6-dichlorophenolindophenol oxidoreductase subunit beta [EC:1.1.1.-]	Control
Ba_CDS_2612	K02406	*fliC*; flagellin	Control
Ba_CDS_2621	K00824	*dat*; D-alanine transaminase [EC:2.6.1.21]	Control
Ba_CDS_2631	K11923	*cueR*; MerR family transcriptional regulator, copper efflux regulator	Control
Ba_CDS_2648	K01835	*pgm*; phosphoglucomutase [EC:5.4.2.2]	Control
Ba_CDS_2662	K08602	*pepF*; oligoendopeptidase F [EC:3.4.24.-]	Control
Ba_CDS_2670	K00858	*ppnK*; NAD+ kinase [EC:2.7.1.23]	Control
Ba_CDS_2728	K03402	*argR*; transcriptional regulator of arginine metabolism	Control
Ba_CDS_2737	K00634	*ptb*; phosphate butyryltransferase [EC:2.3.1.19]	Control
Ba_CDS_2739	K00929	*buk*; butyrate kinase [EC:2.7.2.7]	Control
Ba_CDS_2740	K00382	DLD; dihydrolipoamide dehydrogenase [EC:1.8.1.4]	Control
Ba_CDS_2742	K00167	BCKDHB; 2-oxoisovalerate dehydrogenase E1 component beta subunit [EC:1.2.4.4]	Control
Ba_CDS_2743	K09699	DBT; 2-oxoisovalerate dehydrogenase E2 component (dihydrolipoyl transacylase) [EC:2.3.1.168]	Control
Ba_CDS_2755	K03408	*cheW*; purine-binding chemotaxis protein CheW	Control
Ba_CDS_2816	K02016	ABC.FEV.S; iron complex transport system substrate-binding protein	Control
Ba_CDS_2828	K04771	*degP*; serine protease Do [EC:3.4.21.107]	Control
Ba_CDS_2845	K03415	*cheV*; two-component system, chemotaxis family, chemotaxis protein CheV	Control
Ba_CDS_2852	K21465	*pbpA*; penicillin-binding protein A	Control
Ba_CDS_2854	K00020	*mmsB*; 3-hydroxyisobutyrate dehydrogenase [EC:1.1.1.31]	Control
Ba_CDS_2856	K03406	*mcp*; methyl-accepting chemotaxis protein	Control
Ba_CDS_2861	K20116	PTS-Glc1-EIIA; PTS system, glucose-specific IIA component [EC:2.7.1.199]	Control
Ba_CDS_2881	K00788	*thiE*; thiamine-phosphate pyrophosphorylase [EC:2.5.1.3]	Control
Ba_CDS_2904	K01222	E3.2.1.86A; 6-phospho-beta-glucosidase [EC:3.2.1.86]	Control
Ba_CDS_2905	K02759	PTS-Cel-EIIA; PTS system, cellobiose-specific IIA component [EC:2.7.1.196 2.7.1.205]	Control
Ba_CDS_2918	K16012	*cydC*; ATP-binding cassette, subfamily C, bacterial CydC	Control

Ba_CDS_2922	K02013	ABC.FEV.A; iron complex transport system ATP-binding protein [EC:3.6.3.34]	Control
Ba_CDS_2924	K02016	ABC.FEV.S; iron complex transport system substrate-binding protein	Control
Ba_CDS_2928	K02016	ABC.FEV.S; iron complex transport system substrate-binding protein	Control
Ba_CDS_2939	K02760	PTS-Cel-EIIB; PTS system, cellobiose-specific IIB component [EC:2.7.1.196 2.7.1.205]	Control
Ba_CDS_2949	K01744	*aspA*; aspartate ammonia-lyase [EC:4.3.1.1]	Control
Ba_CDS_2957	K01258	*pepT*; tripeptide aminopeptidase [EC:3.4.11.4]	Control
Ba_CDS_3034	K06193	*phnA*; protein PhnA	Control
Ba_CDS_3035	K00865	*glxK*; glycerate 2-kinase [EC:2.7.1.165]	Control
Ba_CDS_3105	K01939	*purA*; adenylosuccinate synthase [EC:6.3.4.4]	Control
Ba_CDS_3116	K02361	*entC*; isochorismate synthase [EC:5.4.4.2]	Control
Ba_CDS_3122	K02016	ABC.FEV.S; iron complex transport system substrate-binding protein	Control
Ba_CDS_3142	K06942	*ychF*; ribosome-binding ATPase	Control
Ba_CDS_3149	K03497	*parB*; chromosome partitioning protein, ParB family	Control
Ba_CDS_3152	K03497	*parB*; chromosome partitioning protein, ParB family	Control
Ba_CDS_3154	K03495	*gidA*; tRNA uridine 5-carboxymethylaminomethyl modification enzyme	Control
Ba_CDS_3164	K02470	*gyrB*; DNA gyrase subunit B [EC:5.99.1.3]	Control
Ba_CDS_3191	K03526	*gcpE*; (E)-4-hydroxy-3-methylbut-2-enyl-diphosphate synthase [EC:1.17.7.1 1.17.7.3]	Control
Ba_CDS_3253	K05520	*pfpI*; protease I [EC:3.5.1.124]	Control
Ba_CDS_3254	K03406	*mcp*; methyl-accepting chemotaxis protein	Control
Ba_CDS_3266	K00852	*rbsK*; ribokinase [EC:2.7.1.15]	Control
Ba_CDS_3270	K10439	*rbsB*; ribose transport system substrate-binding protein	Control
Ba_CDS_3290	K01928	*murE*; UDP-N-acetylmuramoyl-L-alanyl-D-glutamate--2,6-diaminopimelate ligase [EC:6.3.2.13]	Control
Ba_CDS_3312	K02782	PTS-Gut-EIIB; PTS system, glucitol/sorbitol-specific IIB component [EC:2.7.1.198]	Control
Ba_CDS_3325	K06180	*rluD*; 23S rRNA pseudouridine1911/1915/1917 synthase [EC:5.4.99.23]	Control
Ba_CDS_3330	K01465	URA4; dihydroorotase [EC:3.5.2.3]	Control
Ba_CDS_3357	K20074	*prpC*; PPM family protein phosphatase [EC:3.1.3.16]	Control
Ba_CDS_3360	K01783	*rpe*; ribulose-phosphate 3-epimerase [EC:5.1.3.1]	Control
Ba_CDS_3375	K03110	*ftsY*; fused signal recognition particle receptor	Control
Ba_CDS_3376	K09787	uncharacterized protein	Control
Ba_CDS_3381	K02860	*rimM*; 16S rRNA processing protein RimM	Control
Ba_CDS_3382	K00554	*trmD*; tRNA (guanine37-N1)-methyltransferase [EC:2.1.1.228]	Control
Ba_CDS_3392	K04094	*trmFO*; methylenetetrahydrofolate--tRNA-(uracil-5-)-methyltransferase [EC:2.1.1.74]	Control
Ba_CDS_3399	K02408	*fliE*; flagellar hook-basal body complex protein FliE	Control
Ba_CDS_3400	K02409	*fliF*; flagellar M-ring protein FliF	Control
Ba_CDS_3411	K02416	*fliM*; flagellar motor switch protein FliM	Control
Ba_CDS_3418	K02401	*flhB*; flagellar biosynthetic protein FlhB	Control
Ba_CDS_3437	K01881	PARS; prolyl-tRNA synthetase [EC:6.1.1.15]	Control
Ba_CDS_3445	K07742	*ylxR*; uncharacterized protein	Control
Ba_CDS_3450	K03177	*truB*; tRNA pseudouridine55 synthase [EC:5.4.99.25]	Control
Ba_CDS_3488	K01714	*dapA*; 4-hydroxy-tetrahydrodipicolinate synthase [EC:4.3.3.7]	Control
Ba_CDS_3489	K12574	*rnj*; ribonuclease J [EC:3.1.-.-]	Control
Ba_CDS_3499	K06994	putative drug exporter of the RND superfamily	Control

Ba_CDS_3505	K03742	*pncC*; nicotinamide-nucleotide amidase [EC:3.5.1.42]	Control
Ba_CDS_3506	K03553	*recA*; recombination protein RecA	Control
Ba_CDS_3507	K18682	*rny*; ribonucrease Y [EC:3.1.-.-]	Control
Ba_CDS_3513	K00639	*kbl*; glycine C-acetyltransferase [EC:2.3.1.29]	Control
Ba_CDS_3523	K07736	*carD*; CarD family transcriptional regulator	Control
Ba_CDS_3526	K17734	*aprX*; serine protease AprX [EC:3.4.21.-]	Control
Ba_CDS_3529	K03297	*emrE*; small multidrug resistance pump	Control
Ba_CDS_3530	K03297	*emrE*; small multidrug resistance pump	Control
Ba_CDS_3534	K00791	*miaA*; tRNA dimethylallyltransferase [EC:2.5.1.75]	Control
Ba_CDS_3535	K03666	*hfq*; host factor-I protein	Control
Ba_CDS_3538	K03647	*nrdI*; protein involved in ribonucleotide reduction	Control
Ba_CDS_3539	K00525	E1.17.4.1A; ribonucleoside-diphosphate reductase alpha chain [EC:1.17.4.1]	Control
Ba_CDS_3540	K00526	E1.17.4.1B; ribonucleoside-diphosphate reductase beta chain [EC:1.17.4.1]	Control
Additional 87 unidentified and unassigned (KO) proteins are found exclusive in either the control test condition (24) or in the Te (IV) 5×10^{-4} test condition (63)			

Supplementary Table 4. *Paenibacillus pabuli* ALJ109b annotated CDS with significant variation between tested conditions

PRT-ID	KO	Definition	Difference log_2	Significance (q-welsh t-test)
Pp_CDS_5086	K00656	E2.3.1.54; pflD; formate C-acetyltransferase [EC:2.3.1.54]	-2.8	0.007
Pp_CDS_5085	K04069	*pflA*; pyruvate formate lyase activating enzyme [EC:1.97.1.4]	-2.5	0.001
Pp_CDS_773	K03839	*fldA*; flavodoxin I	-2.3	0.007
Pp_CDS_5087	K04072	*adhE*; acetaldehyde dehydrogenase / alcohol dehydrogenase [EC:1.2.1.10 1.1.1.1]	-2.3	0.021
Pp_CDS_3694	K00363	*nirD*; nitrite reductase (NADH) small subunit [EC:1.7.1.15]	-2.0	0.003
Pp_CDS_518	K15777	DOPA; 4,5-DOPA dioxygenase extradiol [EC:1.13.11.-]	-1.9	0.000
Pp_CDS_6135	K07069	uncharacterized protein	-1.9	0.005
Pp_CDS_3066	K06416	*spoVS*; stage V sporulation protein S	-1.7	0.004
Pp_CDS_3359	K11710	*troB*; manganese/zinc/iron transport system ATP- binding protein	-1.7	0.000
Pp_CDS_3422	K00240	*sdhB*; succinate dehydrogenase / fumarate reductase, iron-sulfur subunit [EC:1.3.5.1 1.3.5.4]	-1.6	0.001
Pp_CDS_5895	K00294	E1.2.1.88; 1-pyrroline-5-carboxylate dehydrogenase [EC:1.2.1.88]	-1.5	0.030
Pp_CDS_5008	K11991	*tadA*; tRNA(adenine34) deaminase [EC:3.5.4.33]	-1.5	0.001
Pp_CDS_5365	K01489	*cdd*; cytidine deaminase [EC:3.5.4.5]	-1.4	0.001
Pp_CDS_2290	K06284	*abrB*; transcriptional pleiotropic regulator of transition state genes	-1.3	0.008
Pp_CDS_3449	K00826	E2.6.1.42; branched-chain amino acid aminotransferase [EC:2.6.1.42]	-1.3	0.034
Pp_CDS_1444	K09807	uncharacterized protein	-1.3	0.006
Pp_CDS_457	K02874	RP-L14; large subunit ribosomal protein L14	-1.2	0.027
Pp_CDS_2665	K00027	ME2; malate dehydrogenase (oxaloacetate-decarboxylating) [EC:1.1.1.38]	-1.2	0.034
Pp_CDS_692	K03886	MQCRA; menaquinol-cytochrome c reductase iron-sulfur subunit [EC:1.10.2.-]	-1.1	0.035
Pp_CDS_5887	K00259	*ald*; alanine dehydrogenase [EC:1.4.1.1]	-1.1	0.047
Pp_CDS_852	K00874	*kdgK*; 2-dehydro-3-deoxygluconokinase [EC:2.7.1.45]	-1.1	0.035
Pp_CDS_2642	K01807	*rpiA*; ribose 5-phosphate isomerase A [EC:5.3.1.6]	-1.1	0.023
Pp_CDS_1546	K00020	*mmsB*; 3-hydroxyisobutyrate dehydrogenase [EC:1.1.1.31]	-1.1	0.026
Pp_CDS_4459	K01619	*deoC*; deoxyribose-phosphate aldolase [EC:4.1.2.4]	-1.1	0.031
Pp_CDS_2581	K01104	E3.1.3.48; protein-tyrosine phosphatase [EC:3.1.3.48]	-1.0	0.025
Pp_CDS_2253	K00860	*cysC*; adenylylsulfate kinase [EC:2.7.1.25]	-1.0	0.041
Pp_CDS_4456	K03784	*deoD*; purine-nucleoside phosphorylase [EC:2.4.2.1]	-1.0	0.027
Pp_CDS_113	K00661	*maa*; maltose O-acetyltransferase [EC:2.3.1.79]	-1.0	0.030
Pp_CDS_423	K01770	*ispF*; 2-C-methyl-D-erythritol 2,4-cyclodiphosphate synthase [EC:4.6.1.12]	-1.0	0.031
Pp_CDS_3464	K03610	*minC*; septum site-determining protein MinC	-1.0	0.039
Pp_CDS_3421	K00239	*sdhA*; succinate dehydrogenase / fumarate reductase, flavoprotein subunit [EC:1.3.5.1 1.3.5.4]	-1.0	0.039
Pp_CDS_1143	K02406	*fliC*; flagellin	-1.0	0.036
Pp_CDS_3002	K07095	uncharacterized protein	-0.9	0.047
Pp_CDS_4829	K03711	fur; Fur family transcriptional regulator, ferric uptake regulator	-0.9	0.040
Pp_CDS_1630	K00005	*gldA*; glycerol dehydrogenase [EC:1.1.1.6]	-0.9	0.043
Pp_CDS_5300	K05810	*yfiH*; polyphenol oxidase [EC:1.10.3.-]	-0.9	0.046
Pp_CDS_2088	K00850	*pfkA*; 6-phosphofructokinase 1 [EC:2.7.1.11]	-0.9	0.045
Pp_CDS_1624	K03829	*yedL*; putative acetyltransferase [EC:2.3.1.-]	-0.9	0.038
Pp_CDS_5600	K03624	*greA*; transcription elongation factor GreA	-0.9	0.038

Pp_CDS_4863	K03602	*xseB*; exodeoxyribonuclease VII small subunit [EC:3.1.11.6]	-0.8	0.046
Pp_CDS_3123	K03411	*cheD*; chemotaxis protein CheD [EC:3.5.1.44]	-0.8	0.050
Pp_CDS_444	K02358	*tuf*; elongation factor Tu	0.8	0.046
Pp_CDS_436	K02935	RP-L7; large subunit ribosomal protein L7/L12	0.8	0.046
Pp_CDS_3800	K00384	*trxB*; thioredoxin reductase (NADPH) [EC:1.8.1.9]	0.8	0.043
Pp_CDS_5777	K02990	RP-S6; small subunit ribosomal protein S6	0.8	0.047
Pp_CDS_2160	K00973	E2.7.7.24; glucose-1-phosphate thymidylyltransferase [EC:2.7.7.24]	0.8	0.038
Pp_CDS_1971	K01962	*accA*; acetyl-CoA carboxylase carboxyl transferase subunit alpha [EC:6.4.1.2 2.1.3.15]	0.9	0.036
Pp_CDS_2358	K01653	E2.2.1.6S; acetolactate synthase I/III small subunit [EC:2.2.1.6]	0.9	0.047
Pp_CDS_2596	K00648	*fabH*; 3-oxoacyl-[acyl-carrier-protein] synthase III [EC:2.3.1.180]	0.9	0.036
Pp_CDS_1189	K02113	ATPF1D; F-type H+-transporting ATPase subunit delta	0.9	0.040
Pp_CDS_3086	K12574	*rnj*; ribonuclease J [EC:3.1.-.-]	0.9	0.048
Pp_CDS_819	K22132	*tcdA*; tRNA threonylcarbamoyladenosine dehydratase	0.9	0.035
Pp_CDS_3071	K03553	*recA*; recombination protein RecA	0.9	0.032
Pp_CDS_178	K00133	*asd*; aspartate-semialdehyde dehydrogenase [EC:1.2.1.11]	0.9	0.040
Pp_CDS_2243	K00899	*mtnK*; 5-methylthioribose kinase [EC:2.7.1.100]	0.9	0.044
Pp_CDS_2526	K03665	*hflX*; GTPase	0.9	0.043
Pp_CDS_3068	K18682	*rny*; ribonucrease Y [EC:3.1.-.-]	0.9	0.033
Pp_CDS_1993	K00859	*coaE*; dephospho-CoA kinase [EC:2.7.1.24]	1.0	0.035
Pp_CDS_730	K08969	*mtnE*; aminotransferase [EC:2.6.1.-]	1.0	0.039
Pp_CDS_2231	K21142	*moaX*; MoaE-MoaD fusion protein [EC:2.8.1.12]	1.0	0.033
Pp_CDS_3584	K01595	*ppc*; phosphoenolpyruvate carboxylase [EC:4.1.1.31]	1.0	0.039
Pp_CDS_2550	K08967	*mtnD*; 1,2-dihydroxy-3-keto-5-methylthiopentene dioxygenase [EC:1.13.11.53 1.13.11.54]	1.0	0.034
Pp_CDS_6168	K02035	ABC.PE.S; peptide/nickel transport system substrate-binding protein	1.0	0.046
Pp_CDS_4107	K01092	E3.1.3.25; myo-inositol-1(or 4)-monophosphatase [EC:3.1.3.25]	1.0	0.025
Pp_CDS_4890	K01756	*purB*; adenylosuccinate lyase [EC:4.3.2.2]	1.0	0.027
Pp_CDS_4919	K01756	*purB*; adenylosuccinate lyase [EC:4.3.2.2]	1.0	0.027
Pp_CDS_335	K01226	*treC*; trehalose-6-phosphate hydrolase [EC:3.2.1.93]	1.1	0.035
Pp_CDS_2019	K02768	PTS-Fru-EIIA; PTS system, fructose-specific IIA component [EC:2.7.1.202]	1.1	0.032
Pp_CDS_1895	K01265	*map*; methionyl aminopeptidase [EC:3.4.11.18]	1.1	0.033
Pp_CDS_4034	K07571	S1 RNA binding domain protein	1.1	0.021
Pp_CDS_1733	K07258	*dacC*; serine-type D-Ala-D-Ala carboxypeptidase (penicillin-binding protein 5/6) [EC:3.4.16.4]	1.1	0.031
Pp_CDS_4832	K01515	*nudF*; ADP-ribose pyrophosphatase [EC:3.6.1.13]	1.1	0.020
Pp_CDS_2294	K03856	AROA2; 3-deoxy-7-phosphoheptulonate synthase [EC:2.5.1.54]	1.1	0.023
Pp_CDS_4023	K07533	*prsA*; foldase protein PrsA [EC:5.2.1.8]	1.1	0.027
Pp_CDS_2305	K01868	TARS; threonyl-tRNA synthetase [EC:6.1.1.3]	1.1	0.027
Pp_CDS_1805	K03816	*xpt*; xanthine phosphoribosyltransferase [EC:2.4.2.22]	1.1	0.028
Pp_CDS_4794	K07335	*bmpA*; basic membrane protein A and related proteins	1.1	0.034
Pp_CDS_2359	K01652	E2.2.1.6L; acetolactate synthase I/II/III large subunit [EC:2.2.1.6]	1.2	0.025
Pp_CDS_2239	K09013	*sufC*; Fe-S cluster assembly ATP-binding protein	1.2	0.007
Pp_CDS_1172	K02372	*fabZ*; 3-hydroxyacyl-[acyl-carrier-protein] dehydratase [EC:4.2.1.59]	1.2	0.022
Pp_CDS_4040	K03798	*ftsH*; cell division protease FtsH [EC:3.4.24.-]	1.2	0.043
Pp_CDS_3310	K11618	*liaR*; two-component system, NarL family, response regulator LiaR	1.3	0.003

Pp_CDS_3453	K00003	*hom*; homoserine dehydrogenase [EC:1.1.1.3]	1.3	0.007
Pp_CDS_2244	K08963	*mtnA*; methylthioribose-1-phosphate isomerase [EC:5.3.1.23]	1.3	0.020
Pp_CDS_5470	K01989	ABC.X4.S; putative ABC transport system substrate-binding protein	1.4	0.000
Pp_CDS_3234	K01448	*amiABC*; N-acetylmuramoyl-L-alanine amidase [EC:3.5.1.28]	1.5	0.003
Pp_CDS_2368	K02887	RP-L20; large subunit ribosomal protein L20	1.5	0.005
Pp_CDS_3183	K03529	*smc*; chromosome segregation protein	1.6	0.001
Pp_CDS_3452	K01733	*thrC*; threonine synthase [EC:4.2.3.1]	1.9	0.005
Pp_CDS_1085	K03969	*pspA*; phage shock protein A	1.9	0.000
Pp_CDS_865	K07192	*FLOT*; flotillin	2.8	0.000
Pp_CDS_3307	K03969	*liaH*; similar to phage shock protein A	4.1	0.000
Pp_CDS_3304	K03969	*pspA*; phage shock protein A	4.2	0.000
Additional 48 unidentified and/or unassigned (KO) proteins have significant change in abundance, 14 with over regulation in the presence of Te (IV) 5×10^{-4} M and 34 down regulated in the presence of Te (IV) 5×10^{-4} M				

Supplementary Table 5. *Paenibacillus pabuli* ALJ109b annotated CDS exclusive in both tested conditions

ID	KO	Definition	Test
Pp_CDS_112	K00661	*maa*; maltose O-acetyltransferase [EC:2.3.1.79]	Control
Pp_CDS_1466	K00765	*hisG*; ATP phosphoribosyltransferase [EC:2.4.2.17]	Control
Pp_CDS_1472	K06023	*hprK*; HPr kinase/phosphorylase [EC:2.7.11.- 2.7.4.-]	Control
Pp_CDS_2284	K17318	*lplA*; putative aldouronate transport system substrate-binding protein	Control
Pp_CDS_2612	K10188	*lacE*; lactose/L-arabinose transport system substrate-binding protein	Control
Pp_CDS_3168	K03470	*rnhB*; ribonuclease HII [EC:3.1.26.4]	Control
Pp_CDS_3180	K09787	uncharacterized protein	Control
Pp_CDS_3360	K11708	*troC*; manganese/zinc/iron transport system permease protein	Control
Pp_CDS_353	K13954	*yiaY*; alcohol dehydrogenase [EC:1.1.1.1]	Control
Pp_CDS_3695	K00362	*nirB*; nitrite reductase (NADH) large subunit [EC:1.7.1.15]	Control
Pp_CDS_5750	K04771	*degP*; serine protease Do [EC:3.4.21.107]	Control
Pp_CDS_5825	K10542	*mglA*; methyl-galactoside transport system ATP-binding protein [EC:3.6.3.17]	Control
Pp_CDS_5955	K01737	*queD*; 6-pyruvoyltetrahydropterin/6-carboxytetrahydropterin synthase [EC:4.2.3.12 4.1.2.50]	Control
Pp_CDS_6102	K07171	*mazF*; mRNA interferase MazF [EC:3.1.-.-]	Control
Pp_CDS_860	K01784	*galE*; UDP-glucose 4-epimerase [EC:5.1.3.2]	Control
Pp_CDS_1124	K00145	*argC*; N-acetyl-gamma-glutamyl-phosphate reductase [EC:1.2.1.38]	Te (IV)
Pp_CDS_1304	K06911	uncharacterized protein	Te (IV)
Pp_CDS_1334	K11069	*potD*; spermidine/putrescine transport system substrate-binding protein	Te (IV)
Pp_CDS_1448	K06958	*rapZ*; RNase adapter protein RapZ	Te (IV)
Pp_CDS_1460	K11755	*hisIE*; phosphoribosyl-ATP pyrophosphohydrolase / phosphoribosyl-AMP cyclohydrolase [EC:3.6.1.31 3.5.4.19]	Te (IV)
Pp_CDS_1612	K07114	*yfbK*; Ca-activated chloride channel homolog	Te (IV)
Pp_CDS_1723	K03790	*rimJ*; [ribosomal protein S5]-alanine N-acetyltransferase [EC:2.3.1.267]	Te (IV)
Pp_CDS_1748	K01534	*zntA*; Cd2+/Zn2+-exporting ATPase [EC:3.6.3.3 3.6.3.5]	Te (IV)
Pp_CDS_1749	K21903	*cadC*; ArsR family transcriptional regulator, lead/cadmium/zinc/bismuth-responsive transcriptional repressor	Te (IV)
Pp_CDS_1785	K01990	ABC-2.A; ABC-2 type transport system ATP-binding protein	Te (IV)
Pp_CDS_1796	K02275	*coxB*; cytochrome c oxidase subunit II [EC:1.9.3.1]	Te (IV)
Pp_CDS_2018	K00882	*fruK*; 1-phosphofructokinase [EC:2.7.1.56]	Te (IV)
Pp_CDS_2045	K01776	*murI*; glutamate racemase [EC:5.1.1.3]	Te (IV)
Pp_CDS_2119	K06183	*rsuA*; 16S rRNA pseudouridine516 synthase [EC:5.4.99.19]	Te (IV)
Pp_CDS_2150	K01972	E6.5.1.2; DNA ligase (NAD+) [EC:6.5.1.2]	Te (IV)
Pp_CDS_2220	K01652	E2.2.1.6L; acetolactate synthase I/II/III large subunit [EC:2.2.1.6]	Te (IV)
Pp_CDS_2237	K11717	*sufS*; cysteine desulfurase / selenocysteine lyase [EC:2.8.1.7 4.4.1.16]	Te (IV)
Pp_CDS_226	K00381	*cysI*; sulfite reductase (NADPH) hemoprotein beta-component [EC:1.8.1.2]	Te (IV)
Pp_CDS_2299	K11618	*liaR*; two-component system, NarL family, response regulator LiaR	Te (IV)
Pp_CDS_2315	K01760	*metC*; cysteine-S-conjugate beta-lyase [EC:4.4.1.13]	Te (IV)
Pp_CDS_2317	K00651	*metA*; homoserine O-succinyltransferase/O-acetyltransferase [EC:2.3.1.46 2.3.1.31]	Te (IV)
Pp_CDS_2354	K00052	*leuB*; 3-isopropylmalate dehydrogenase [EC:1.1.1.85]	Te (IV)
Pp_CDS_246	K19689	*ampS*; aminopeptidase [EC:3.4.11.-]	Te (IV)
Pp_CDS_247	K01895	ACSS; acetyl-CoA synthetase [EC:6.2.1.1]	Te (IV)

Pp_CDS_2602	K07177	Lon-like protease	Te (IV)
Pp_CDS_2604	K00954	E2.7.7.3A; pantetheine-phosphate adenylyltransferase [EC:2.7.7.3]	Te (IV)
Pp_CDS_2632	K06994	putative drug exporter of the RND superfamily	Te (IV)
Pp_CDS_2842	K02529	*lacI*; LacI family transcriptional regulator	Te (IV)
Pp_CDS_2844	K06726	*rbsD*; D-ribose pyranase [EC:5.4.99.62]	Te (IV)
Pp_CDS_2949	K03484	*scrR*; LacI family transcriptional regulator, sucrose operon repressor	Te (IV)
Pp_CDS_2957	K03892	*arsR*; ArsR family transcriptional regulator, arsenate/arsenite/antimonite-responsive transcriptional repressor	Te (IV)
Pp_CDS_2986	K01834	PGAM; 2,3-bisphosphoglycerate-dependent phosphoglycerate mutase [EC:5.4.2.11]	Te (IV)
Pp_CDS_3058	K00763	*pncB*; nicotinate phosphoribosyltransferase [EC:6.3.4.21]	Te (IV)
Pp_CDS_3083	K03466	*ftsK*; DNA segregation ATPase FtsK/SpoIIIE, S-DNA-T family	Te (IV)
Pp_CDS_3120	K09749	uncharacterized protein	Te (IV)
Pp_CDS_3149	K02410	*fliG*; flagellar motor switch protein FliG	Te (IV)
Pp_CDS_3155	K01419	*hslV*; ATP-dependent HslUV protease, peptidase subunit HslV [EC:3.4.25.2]	Te (IV)
Pp_CDS_322	K07816	E2.7.6.5X; putative GTP pyrophosphokinase [EC:2.7.6.5]	Te (IV)
Pp_CDS_3394	K00435	*hemQ*; Fe-coproporphyrin III decarboxylase [EC:1.11.1.-]	Te (IV)
Pp_CDS_3411	K11144	*dnaI*; primosomal protein DnaI	Te (IV)
Pp_CDS_3439	K01613	*psd*; phosphatidylserine decarboxylase [EC:4.1.1.65]	Te (IV)
Pp_CDS_3450	K04518	*pheA2*; prephenate dehydratase [EC:4.2.1.51]	Te (IV)
Pp_CDS_3451	K00872	*thrB1*; homoserine kinase [EC:2.7.1.39]	Te (IV)
Pp_CDS_3454	K06209	*pheB*; chorismate mutase [EC:5.4.99.5]	Te (IV)
Pp_CDS_3478	K01698	*hemB*; porphobilinogen synthase [EC:4.2.1.24]	Te (IV)
Pp_CDS_3528	K01443	*nagA*; N-acetylglucosamine-6-phosphate deacetylase [EC:3.5.1.25]	Te (IV)
Pp_CDS_3529	K02564	*nagB*; glucosamine-6-phosphate deaminase [EC:3.5.99.6]	Te (IV)
Pp_CDS_3538	K01990	ABC-2.A; ABC-2 type transport system ATP-binding protein	Te (IV)
Pp_CDS_3703	K03924	*moxR*; MoxR-like ATPase [EC:3.6.3.-]	Te (IV)
Pp_CDS_3706	K07015	uncharacterized protein	Te (IV)
Pp_CDS_3848	K02016	ABC.FEV.S; iron complex transport system substrate-binding protein	Te (IV)
Pp_CDS_3858	K00262	E1.4.1.4; glutamate dehydrogenase (NADP+) [EC:1.4.1.4]	Te (IV)
Pp_CDS_3905	K01759	GLO1; lactoylglutathione lyase [EC:4.4.1.5]	Te (IV)
Pp_CDS_4079	K18979	*queG*; epoxyqueuosine reductase [EC:1.17.99.6]	Te (IV)
Pp_CDS_4154	K02424	*fliY*; L-cystine transport system substrate-binding protein	Te (IV)
Pp_CDS_4219	K02503	HINT1; histidine triad (HIT) family protein	Te (IV)
Pp_CDS_426	K01883	CARS; cysteinyl-tRNA synthetase [EC:6.1.1.16]	Te (IV)
Pp_CDS_4504	K19689	*ampS*; aminopeptidase [EC:3.4.11.-]	Te (IV)
Pp_CDS_4551	K06878	tRNA-binding protein	Te (IV)
Pp_CDS_4766	K09705	uncharacterized protein	Te (IV)
Pp_CDS_4841	K00382	DLD; dihydrolipoamide dehydrogenase [EC:1.8.1.4]	Te (IV)
Pp_CDS_4849	K21567	*fnr*; ferredoxin/flavodoxin---NADP+ reductase [EC:1.18.1.2 1.19.1.1]	Te (IV)
Pp_CDS_4862	K13789	GGPS; geranylgeranyl diphosphate synthase, type II [EC:2.5.1.1 2.5.1.10 2.5.1.29]	Te (IV)
Pp_CDS_4891	K01589	*purK*; 5-(carboxyamino)imidazole ribonucleotide synthase [EC:6.3.4.18]	Te (IV)
Pp_CDS_4912	K03705	*hrcA*; heat-inducible transcriptional repressor	Te (IV)
Pp_CDS_4920	K01589	*purK*; 5-(carboxyamino)imidazole ribonucleotide synthase [EC:6.3.4.18]	Te (IV)
Pp_CDS_5037	K06377	*spo0M*; sporulation-control protein	Te (IV)

Pp_CDS_5045	K16216	*yueD*; benzil reductase ((S)-benzoin forming) [EC:1.1.1.320]	Te (IV)
Pp_CDS_5161	K12132	*prkC*; eukaryotic-like serine/threonine-protein kinase [EC:2.7.11.1]	Te (IV)
Pp_CDS_5211	K00800	*aroA*; 3-phosphoshikimate 1-carboxyvinyltransferase [EC:2.5.1.19]	Te (IV)
Pp_CDS_5217	K01585	*speA*; arginine decarboxylase [EC:4.1.1.19]	Te (IV)
Pp_CDS_5253	K06972	PITRM1; presequence protease [EC:3.4.24.-]	Te (IV)
Pp_CDS_5268	K02027	ABC.MS.S; multiple sugar transport system substrate-binding protein	Te (IV)
Pp_CDS_5288	K06180	*rluD*; 23S rRNA pseudouridine1911/1915/1917 synthase [EC:5.4.99.23]	Te (IV)
Pp_CDS_5293	K01870	IARS; isoleucyl-tRNA synthetase [EC:6.1.1.5]	Te (IV)
Pp_CDS_5369	K06217	*phoH*; phosphate starvation-inducible protein PhoH and related proteins	Te (IV)
Pp_CDS_5374	K07403	*nfeD*; membrane-bound serine protease (ClpP class)	Te (IV)
Pp_CDS_5439	K00851	E2.7.1.12; gluconokinase [EC:2.7.1.12]	Te (IV)
Pp_CDS_5607	K04780	*dhbF*; nonribosomal peptide synthetase DhbF	Te (IV)
Pp_CDS_5714	K00662	*aacC*; aminoglycoside 3-N-acetyltransferase [EC:2.3.1.81]	Te (IV)
Pp_CDS_5773	K02031	ABC.PE.A; peptide/nickel transport system ATP-binding protein	Te (IV)
Pp_CDS_5799	K02313	*dnaA*; chromosomal replication initiator protein	Te (IV)
Pp_CDS_5816	K03530	*hupB*; DNA-binding protein HU-beta	Te (IV)
Pp_CDS_6011	K01421	*yhgE*; putative membrane protein	Te (IV)
Pp_CDS_6059	K06158	ABCF3; ATP-binding cassette, subfamily F, member 3	Te (IV)
Pp_CDS_6184	K03800	*lplA*; lipoate---protein ligase [EC:6.3.1.20]	Te (IV)
Pp_CDS_6194	K00768	E2.4.2.21; nicotinate-nucleotide--dimethylbenzimidazole phosphoribosyltransferase [EC:2.4.2.21]	Te (IV)
Pp_CDS_6425	K07032	uncharacterized protein	Te (IV)
Pp_CDS_700	K00215	*dapB*; 4-hydroxy-tetrahydrodipicolinate reductase [EC:1.17.1.8]	Te (IV)
Pp_CDS_701	K01734	*mgsA*; methylglyoxal synthase [EC:4.2.3.3]	Te (IV)
Pp_CDS_71	K09702	uncharacterized protein	Te (IV)
Pp_CDS_724	K08964	*mtnB*; methylthioribulose-1-phosphate dehydratase [EC:4.2.1.109]	Te (IV)
Pp_CDS_726	K08965	*mtnW*; 2,3-diketo-5-methylthiopentyl-1-phosphate enolase [EC:5.3.2.5]	Te (IV)
Pp_CDS_733	K13566	NIT2; omega-amidase [EC:3.5.1.3]	Te (IV)
Pp_CDS_767	K06180	*rluD*; 23S rRNA pseudouridine1911/1915/1917 synthase [EC:5.4.99.23]	Te (IV)
Pp_CDS_823	K03657	*uvrD*; DNA helicase II / ATP-dependent DNA helicase PcrA [EC:3.6.4.12]	Te (IV)
Pp_CDS_998	K00134	GAPDH; glyceraldehyde 3-phosphate dehydrogenase [EC:1.2.1.12]	Te (IV)
Additional 87 unidentified and unassigned (KO) proteins are found exclusive in either the control test condition (24) or in the Te (IV) 5×10^{-4} M test condition (63)			